Delft University of Technology

Fix(at)ing the Spine

Exploration of Novel Anchors and Steerable Bone Drills for Spinal Fusion Surgery

de Kater, E.P.

Important note
To cite this publication, please use the final published version (if applicable).
Please check the document version above.

Fix(at)ing the Spine

Exploration of Novel Anchors and Steerable Bone Drills for Spinal Fusion Surgery

The spine serves as our literal backbone, providing support and facilitating movement, but spinal issues can greatly impact daily life. Spinal fusion surgery addresses severe problems by fusing adjacent vertebrae using pedicle screws and rods. However, traditional f xation methods like these encounter challenges such as screw loosening, particularly in weaker bone. This thesis presents an exploratory study delving into alternative bone anchor designs to enhance the f xation strength. Additionally, this thesis explores the use of steerable bone drills to enable alternative anchor trajectories, aiming to further enhance the f xation. This thesis also examines additional functionalities, such as tissue removal, to improve medical procedures. Through these investigations, the thesis aims to advance spinal fusion surgery techniques, ultimately enhancing patient outcomes and quality of life.
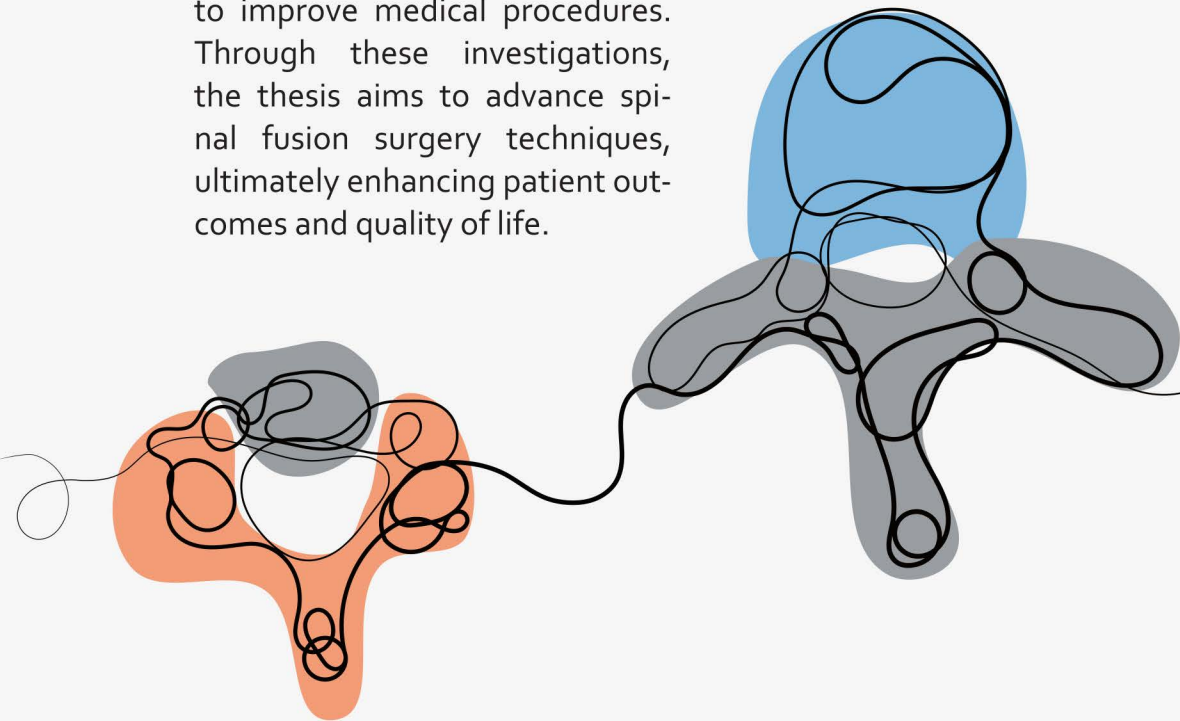
Fix(at)ing the Spine

Exploration of Novel Anchors and Steerable Bone Drills for Spinal Fusion Surgery
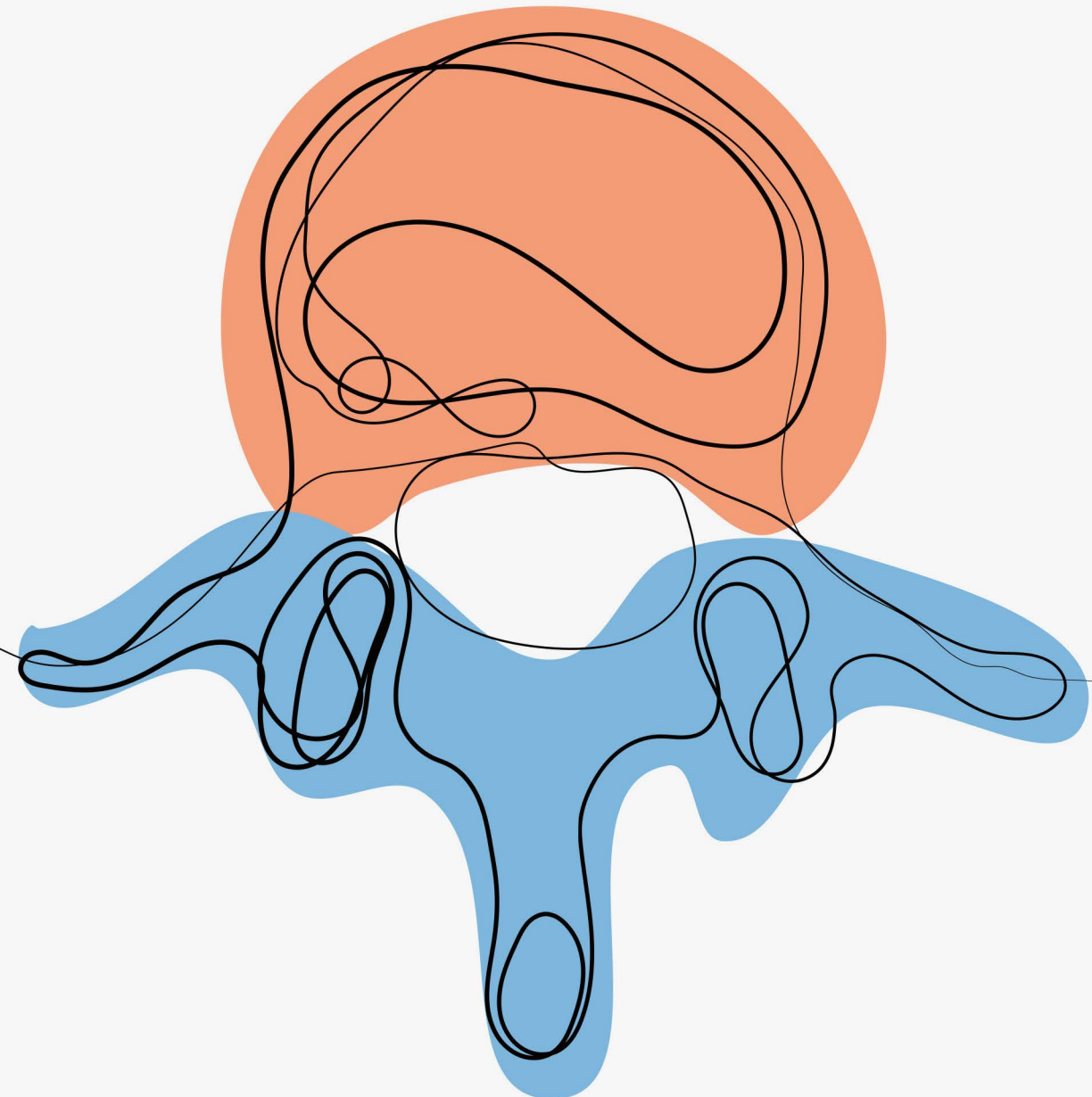
Esther Paula de Kater

Esther Paula de Kater

Propositions belonging to the thesis

Fix(at)ing the Spine

Exploration of Novel Anchors and Steerable Bone Drills for Spinal Fusion Surgery

Esther Paula de Kater

1. Steerable screws either don't steer or don't screw. (This thesis)

2. Pull-out testing of pedicle screws is a bad golden standard. (This thesis)

3. An independent researcher should be a collaborator.

4. The core business of a university is primarily provided by temporary employees.

5. Striving for gender diversity is an empty promise if a student is only referred to as 'he'.
   (Onderwijs- en ExamenRegeling (OER), bachelor mechanical engineering 2023-2024, TU Delft).

6. Teaching is a skill that must be taught.

7. The absence of deadlines on the work floor elevates stress rather than alleviate it.

8. Listening skills should be educated, not only presentation skills.

9. Unwritten rules are difficult to rewrite.

10. Co-housing communities can ease the housing problem, the climate problem, and loneliness all at once.

These propositions are regarded as opposable and defendable, and have been approved as such by the supervisors Prof.dr.ir. Paul Breedveld and Dr.ir. Aimée Sakes

FIX(AT)ING THE SPINE

EXPLORATION OF NOVEL ANCHORS AND STEERABLE BONE DRILLS FOR SPINAL FUSION SURGERY

FIX(AT)ING THE SPINE

EXPLORATION OF NOVEL ANCHORS AND STEERABLE BONE DRILLS FOR SPINAL FUSION SURGERY

Dissertation

for the purpose of obtaining the degree of doctor
at Delft University of Technology
by the authority of the Rector Magnificus,
Prof.dr.ir. T.H.J.J. van der Hagen,
chair of the Board for Doctorates
to be defended publicly on
Thursday 12 December 2024 at 10:00 o'clock

by

Esther Paula DE KATER

Master of Science in Mechanical Engineering and Biomedical Engineering
Delft University of Technology, the Netherlands.

CONTENTS

SUMMARY

The human spine plays a crucial role in providing the necessary support and facilitating movements, such as bending and twisting. However, spinal problems, including degeneration, herniated disks, or deformation, can lead to significant problems such as pain and discomfort for patients. In more severe cases, spinal fusion surgery can be considered. This surgical procedure involves fusing adjacent vertebrae by inserting pedicle screws through the pedicle into the vertebral body and connecting them to rods that run along the spine. This correction creates a rigid construct, preventing all motion between the vertebrae facilitating their fusion into one bony mass. Despite its generally high success rate, screw loosening is a relatively common complication, especially in patients suffering from osteoporosis. The decrease in bone density characterising osteoporosis, compromises the fixation strength of the pedicle screw, resulting is screw loosening and may even necessitate revision surgery. Screw loosening is often characterised by toggling, a pivoting motion of the pedicle screw that compresses the surrounding cancellous bone, compromising the fixation strength of the screw.

The objective of this PhD Thesis was to explore alternative solutions aimed at preventing pedicle screw loosening during and after spinal fusion surgery. This thesis is organised into three parts: **Part I: Anchor Design**, centres on the development of novel spinal bone anchors with the primary goal of enhancing their fixation strength. **Part II: Anchor Placement**, delves into the placement of spinal bone anchors, giving particular attention to the development of steerable bone drills. These drills facilitate the creation of alternative pilot holes for a more optimal placement of spinal bone anchors to enhance the fixation strength. **Part III: Additional Functionalities**, outlines potential supplementary functionalities mainly focused on taking biopsies of bone or soft tissue.

Part I: Anchor Design begins with **Chapter 2**, providing an overview of spinal bone anchors as potential alternatives to the conventional pedicle screw, as described in patent literature. The chapter identifies five distinct methods for generating fixation strength between the spinal bone anchor and the vertebra: 1) anchors utilising threading, 2) anchors employing a curved path, 3) anchors that (party) expand, 4) anchors incorporating cement, and 5) anchors designed to initiate bone ingrowth. These methods are discussed in terms of their potential to increase fixation strength and their safety considerations, surrounding both placement and removal of the anchor. **Chapter 3** describes the development and validation of a novel spinal bone anchor employing a curved path to enhance the fixation strength by incorporating an elastic pre-bend nitinol anchor. This pre-curved anchor can be advanced through a cannulated pedicle screw to generate improved fixation within the vertebral body, resulting in an increase in pull-out resistance when used in combination with the conventional pedicle screw. In **Chapter 4**, an alternative anchor is explored to enhance the toggling resistance by integrating an expandable section that conforms to the hourglass shape of the pedicle. This results in a

larger contact area with the strong cortical bone layer of the pedicle, preventing the undesirable toggling motion. The designed anchor successfully expanded and conformed to the pedicle in osteoporotic bone phantom material. **Chapter 5** introduces the use of an L-shaped anchor to create a macro-shape lock with the cortical bone layer of the vertebral body. Utilising this macro-shape lock in conjunction with the conventional pedicle screw could enhance the fixation strength of spinal bone anchors. Besides the fixation strength, this chapter investigates the damage to the vertebra after complete pull-out of the anchor.

Part II: Anchor Placement commences with **Chapter 6**, providing an overview of steerable bone drills described in scientific and patent literature. The steering methods utilised in the presented drill designs are categorised as: 1) device-defined, 2) environment-defined, or 3) user-defined. Drills utilising a device-defined drilling method are often steered by using a rigid guide and lack the ability for path adaptation during the procedure. In contrast, with the environment-defined steering method, the drill path is determined during the procedure based on the tissue interaction forces. However, the user cannot influence the path during the procedure, a capacity only possible when using the user-defined steering method. In **Chapter 7**, the presented flexible bone drill features a flexible fluid-filled shaft with a hammer tip which can be used in combination with a guide resulting in a device-defined steering method. The drill successfully transferred the hydraulic pressure wave generated in the handle to the drill tip, with the flexible shaft in straight, 45° curve or 90° curve orientation. This adaptability allows the drill to access more complicated entry point without damaging surrounding tissue. **Chapter 8** introduces a bone drill inspired by the tsetse fly which can steer using a environment-defined steering method. The drill was successfully drilled through osteoporotic and healthy bone phantom material. Additionally, for insertion angles up to 15°, the drill effectively deflected upon contact with the strong cortical bone layer, passively steering to drill along the cortical bone layer. Interestingly, this drill can be utilised to create tunnels with a non-round cross-section, offering potential advantages in placing bone anchors with a non-round cross-section such as the one described in Chapter 4. **Chapter 9** describes the development of a drill utilising replaceable pre-bend cores allowing the user to drill a multi-curved tunnel. The drill is designed to incorporate Diffuse Reflectance Spectroscopy (DRS) to provide cortical breach detection during drilling. The drill could successfully drill a multi-curved tunnel comprising a straight section followed by a curved section.

Part III: Additional Functionalities begins with **Chapter 10**, offering an overview of the various mechanisms incorporated in bone biopsy needles: 1) to sample the biopsy, 2) to sever the biopsy and 3) to harvest the bone biopsy, as descried in patent literature. In **Chapter 11**, the design of a flexible tissue transporter inspired by the ovipositor of the parasitic wasp is presented that can be used to harvest soft tissue samples. This instrument was able to successfully transport soft tissue phantoms through its central lumen without risking clogging with the flexible shaft in various orientations. **Chapter 12** introduces a gripper integrated into the soft tissue transporter of Chapter 11. This enables the gripping of soft tissue, allowing for subsequent transportation through the

central lumen. The presented gripper successfully gripped tissue with various shapes and effectively transported them.

This thesis describes the challenges associated with spinal fusion surgery, specifically targeting the enhancement of fixation strength in spinal bone anchors to address the problem of screw loosening. The designs presented in this thesis include alternative spinal bone anchor designs and designs for steerable bone drills aimed at optimising the placement of alternative anchor, with the ultimate goal of enhancing the fixation strength. This thesis provides an exploratory overview of potential directions for mitigating screw loosening in spinal fusion surgery, marking a foundational step towards overcoming fixation challenges in spinal fusion surgery procedures.

SAMENVATTING

De wervelkolom geeft stabiliteit aan het menselijk lichaam, maar maakt tegelijker tijd bewegingen, zoals buigen en draaien, mogelijk. Problemen aan de wervelkolom, bijvoorbeeld door degeneratie, hernia's of misvormingen, kunnen leiden tot veel ongemak en pijn bij patiënten. In ernstigere gevallen kan het dan nodig zijn om deze problemen chirurgisch te verhelpen, bijvoorbeeld door spondylodese. Tijdens deze operatie worden aangrenzende wervels gefixeerd door het plaatsen van pedikelschroeven in de wervels die bevestigd worden aan twee staven die langs de ruggengraat worden aangebracht. Op deze manier wordt alle beweging tussen de wervels voorkomen, zodat de wervels over tijd vergroeien tot één botmassa. Over het algemeen is spondylodese een succesvolle ingreep, maar soms raken de geplaatste pedikelschroeven los. Dit is voornamelijk een probleem bij patiënten die lijden aan osteoporose, aangezien de afname van de botdichtheid de fixatiesterkte van de pedikelschroef vermindert. Dit kan lijden tot het losraken van de schroeven waardoor een revisieoperatie nodig kan zijn.

Het doel van dit proefschrift is om alternatieve methoden te onderzoeken die gericht zijn op het verbeteren van de fixatiesterkte in vergelijking met de huidige pedikelschroeven die gebruikt worden tijdens spondylodese. Dit proefschrift is opgedeeld in drie delen. **Deel I: Anchor Design (Anker Ontwerp)** richt zich op de ontwikkeling van nieuwe spinale botankers met als primaire doel hun fixatiesterkte te verbeteren. **Deel II: Anchor Placement (Anker Plaatsing)** focust op de plaatsing van spinale botankers, voornamelijk doormiddel van het ontwikkelen van stuurbaar botboren. Deze boren vergemakkelijken het maken van alternatieve tunnels voor een meer optimale plaatsing van spinale botankers om op deze manier de fixatiesterkte te verbeteren. **Deel III: Additional Functionalities (Aanvullende functionaliteiten)** schetst potentiële aanvullende functionaliteiten die voornamelijk gericht zijn op het nemen van biopsieën van zowel botweefsel en zacht weefsel.

Deel I: Anchor Design (Anker Ontwerp) begint met **Hoofdstuk 2**, waarin een overzicht wordt gegeven van spinale botankers, beschreven in de patentliteratuur, die als alternatieven voor de conventionele pedikelschroef gebruikt kunnen worden. Er worden vijf verschillende methoden beschreven om fixatiesterkte van de spinale botankers en de wervel te creëren: 1) doormiddel van schroefdraad, 2) door gebruik van kromme ankers, 3) door ankers die (gedeeltelijk)uitzetten, 4) door het gebruik van cement, en 5) door ankers die botgroei in het anker stimuleren. Deze methoden worden vergeleken op de potentiële toename in fixatiesterkte en de veiligheid in gebruik, zowel bij het plaatsen als het verwijderen van het anker. **Hoofdstuk 3** beschrijft de ontwikkeling en validatie van een nieuw botanker dat een gebogen pad gebruikt om de fixatiesterkte van een pedikelschroef te verbeteren. Hiervoor wordt een elastisch voorgebogen nitinol anker door een holle pedikelschroef gevoerd, om op deze manier een verbeterde fixatie binnenin het wervellichaam te genereren. Deze toegevoegde verankering resulterent in een toename

van de fixatiesterkte vergeleken met een pedikelschroef zonder deze extra verankeringsmethode. In **Hoofdstuk 4** wordt een alternatief anker onderzocht om het wiebelen van een spinaal botanker te verminderen door middel van een uitvouwbaar gedeelte in het anker dat zich aanpast naar de zandloper vorm van de pedikel. Dit resulteert in een groter contactoppervlak met de sterke corticale botlaag in de pedikel, waardoor het ongewenste wiebelen van het anker wordt voorkomen. Het ontworpen anker kon zich succesvol uitvouwen en vormen naar de pedikel in osteoporotisch botfantoommateriaal. **Hoofdstuk 5** introduceert het gebruik van een L-vormig anker om een vormfixatie te creëren met de corticale botlaag van het wervellichaam. Het toevoegen van deze vormfixatie aan de conventionele pedikelschroef kan de fixatiesterkte van spinale botankers verbeteren. Naast het onderzoek naar de fixatiesterkte van dit bontanker ontwerp, is ook de schade aan de wervel onderzocht dat ontstaat als het anker volledig uit de wervel wordt getrokken.

Deel II: Anchor Placement (Anker Plaatsing) begint met **Hoofdstuk 6**, waarin een overzicht wordt gegeven van stuurbaar botboren zoals beschreven in wetenschappelijke- en patentliteratuur. De stuurmethoden die worden gebruikt in de gepresenteerde boorontwerpen worden gecategoriseerd in drie groepen: 1) apparaat-gedefinieerd sturen, 2) omgeving-gedefinieerd sturen, of 3) gebruiker-gedefinieerd sturen. Boren die een apparaat-gedefinieerde stuurmethode gebruiken, worden vaak gestuurd in combinatie met een rigide geleider en missen het vermogen tot aanpassing van het boorpad tijdens de procedure. In tegenstelling wordt bij de omgeving-gedefinieerde stuurmethode het boorpad tijdens de procedure bepaald op basis van de weefselinteractiekrachten. Echter, de gebruiker kan het pad tijdens de procedure niet beïnvloeden, dit kan alleen bij de boren die een gebruiker-gedefinieerde stuurmethode gebruiken. **Hoofdstuk 7** presenteert een botboor met een flexibele vloeistofgevulde schacht en een hamertip die kan worden gebruikt in combinatie met een geleiding, resulterend in een apparaat-gedefinieerde stuurmethode. De boor kon succesvol de in het handvat gegenereerde hydraulische drukgolf overbrengen naar de hamertip, met de flexibele schacht in een rechte positie en in een 45° of 90° kromming. Deze flexibiliteit maakt het mogelijk om toegang te krijgen tot meer gecompliceerde gebieden zonder het omliggende weefsel te beschadigen. **Hoofdstuk 8** introduceert een botboor geïnspireerd op de tseetseevlieg die kan sturen met een omgeving-gedefinieerde stuurmethode. De boor kon succesvol boren door osteoporotisch en gezond botfantoommateriaal. Bovendien werd de boor effectief afgebogen bij contact met het corticale botfantoommateriaal voor insertiehoeken tot 15°. Een ander interessant punt is dat deze boor kan worden gebruikt om tunnels te creëren met een niet-ronde doorsnede, wat mogelijke voordelen biedt bij het plaatsen van botankers met een niet-ronde doorsnede, zoals beschreven in Hoofdstuk 4. **Hoofdstuk 9** beschrijft de ontwikkeling van een boor met vervangbare voorgebogen kernen waarmee de gebruiker een tunnel kan boren met meerdere gekromde secties. De boor is ontworpen zodat Diffuse ReflectieSpectroscopie (DRS) technologie kan worden geïntegreerd om corticale breuken tijdens het boren te voorkomen. De boor kon met succes een tunnel boren, bestaande uit een recht gedeelte gevolgd door een gekromd gedeelte.

Deel III: Additional Functionalities (Aanvullende functionaliteiten) begint met **Hoofd-**

stuk 10, waarin een overzicht wordt gegeven van de verschillende mechanismen in bot-biopsienaalden om: 1) de biopsie te omvatten, 2) om de biopsie af te snijden en 3) om de biopsie uit te nemen, zoals beschreven in patentliteratuur. In **Hoofdstuk 11** wordt het ontwerp van een flexibele weefseltransporteur gepresenteerd, die kan worden gebruikt om zachte weefselmonsters te transporteren, geïnspireerd door de legboor van de parasitaire wesp. Met dit instrument kan zacht fantoomweefsel succesvol worden getransporteerd door de schacht, zonder verstopping te riskeren met de flexibele schacht in verschillende oriëntaties. **Hoofdstuk 12** introduceert een grijper, geïntegreerd op de tip van de weefseltransporteur uit Hoofdstuk 11. Deze grijper maakt het mogelijk om zacht weefsel vast te grijpen, waarna het kan worden getransporteerd door de schacht. De gepresenteerde grijper kon succesvol verschillend gevormde stukjes fantoomweefsel vastgrijpen en transporteerde deze effectief.

Dit proefschrift behandelt de uitdagingen die gepaard gaan met wervelkolomfusiechirurgie, waarbij specifiek wordt gericht op de verbetering van de fixatiesterkte van spinale botankers om het probleem van losse pedikelschroeven aan te pakken. De ontwerpen die in dit proefschrift worden gepresenteerd, omvatten alternatieve ontwerpen van spinale botankers en ontwerpen van stuurbaar botboren gericht op het optimaliseren van de plaatsing van alternatieve ankers, met als uiteindelijk doel het verbeteren van de fixatiesterkte. Dit proefschrift biedt een verkennend overzicht van mogelijke richtingen voor het verminderen van loskomende pedikelschroeven bij wervelkolomfusiechirurgie, en markeert daarmee een fundamentele stap naar het overwinnen van fixatie-uitdagingen in procedures voor wervelkolomfusiechirurgie.

1

INTRODUCTION

1.1. THE HUMAN SPINE

The spine serves as our literal backbone, providing essential support for sitting, standing upright, walking and accommodating movements such as bending and twisting. Given this crucial role, issues related to the spine can significantly impact a person's daily life. Spinal problems can range from lower back pain caused by herniated disks to complex spine deformities like scoliosis. These spinal problems can lead to discomfort, pain and reduced mobility and may require surgical intervention to resolve.

The spinal column consists of vertebrae separated by intervertebral discs and the spinal cord that runs through this structure. The human spine comprises seven cervical vertebrae in the neck, twelve thoracic vertebrae in the upper back, and five lumbar vertebrae in the lower back (Figure 1.1). Each type of vertebra serves a distinct purpose: cervical vertebrae support the head and allow for extensive movements, thoracic vertebrae hold the ribcage, and lumbar vertebrae support the body's weight.

Although these different types of vertebrae exhibit variations in shape and size, they share a common anatomical structure. Every vertebra comprises two primary components: 1) the oval-shaped vertebra body structured for bearing loads and 2) the vertebral arch which is connected to the vertebral body via the pedicles and protects the spinal cord. This arch also incorporates the facet joints that facilitate movement between adjacent vertebrae and the transverse processes that serve as attachment points for ligaments.

The load bearing capabilities of the vertebrae come mainly from the outer layer composed of dense cortical bone, encapsulating the more porous cancellous bone within making the vertebra more light weight (Figure 1.2). The cortical bone exhibits a significantly higher elastic modulus and a greater yield strength, enabling it to withstand greater forces as compared to the porous cancellous bone.

1.2. SPINAL FUSION SURGERY

Spinal fusion surgery is a necessary treatment to address severe spinal deformities, alleviate pain, or to treat spinal instability [11]. In this procedure, two or more adjacent vertebrae of the spine are surgically "fused" to eliminate all movement between them. While various methods have been developed to achieve this vertebral fusion, the golden
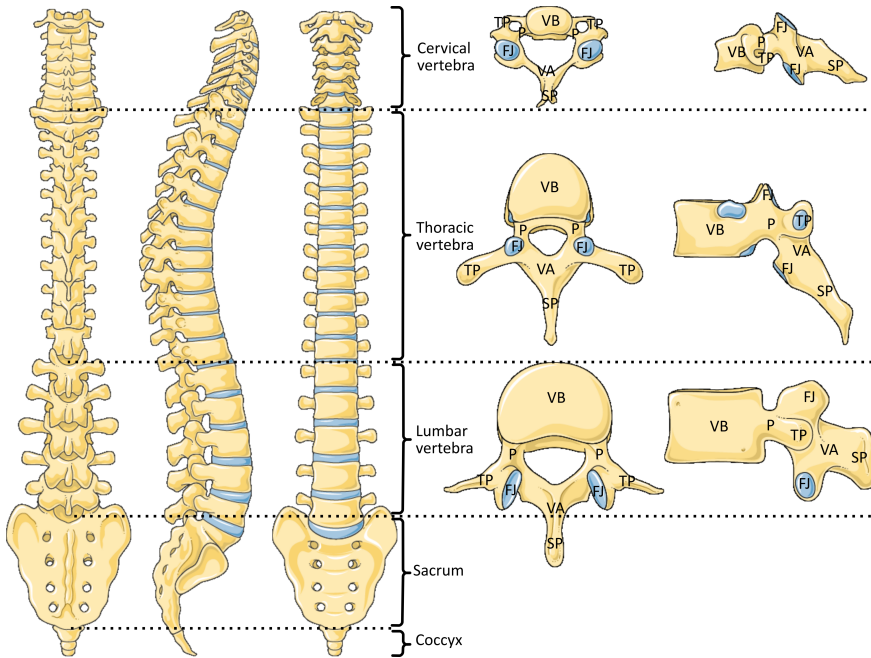
Figure 1.1: Human spine anatomy. The human spine comprises seven cervical vertebra, 12 thoracic vertebra and five lumbar vertebra. Each of these vertebrae consist of a vertebral body (VB) and a vertebral arch (VA) connected to the vertebral body via the pedicles (P). The vertrebral arch includes the spinous process (SP), the transverse process (TP) and the facet joints (FJ). Illustration adapted from Servier Medical Art by Servier, licensed under a Creative Commons Attribution 3.0 Unported License.

standard involves the use of pedicle screws inserted through the pedicle into the vertebral body [4]. These pedicle screws are interconnected by rods to immobilise the vertebrae, ensuring complete fusion through the assistance of bone grafts (Figure 1.3a).

Pedicle screws are commonly placed using the free-hand technique, where the pedicle screws are placed without the use of real-time imaging techniques for guidance. The steps for placing a pedicle screw via the free-hand technique are depicted in Figure 1.3b. The procedure starts in Step 1 with locating the entry point for the pedicle screw using anatomical landmarks and pre-operative imaging. At the located entry point, the cortical bone layer is removed using a burr, rongeur or awl. During Step 2, the cancellous bone within the pedicle is pushed aside using a slightly curved, blunt pedicle probe. The probe is initially introduced with a lateral curve for the first 15-20 mm and then rotated medially. This technique minimises the risk of breaching the medial side of the pedicle, which could potentially damage the spinal cord [7]. In Step 3, a ball-tip probe is utilised to palpate the pedicle walls, determining the appropriate screw size and identifying any cortical breaches. Finally in Step 4, the screw is inserted either as a self-tapping screw or after tapping the screw thread in the hole with a separate tap.
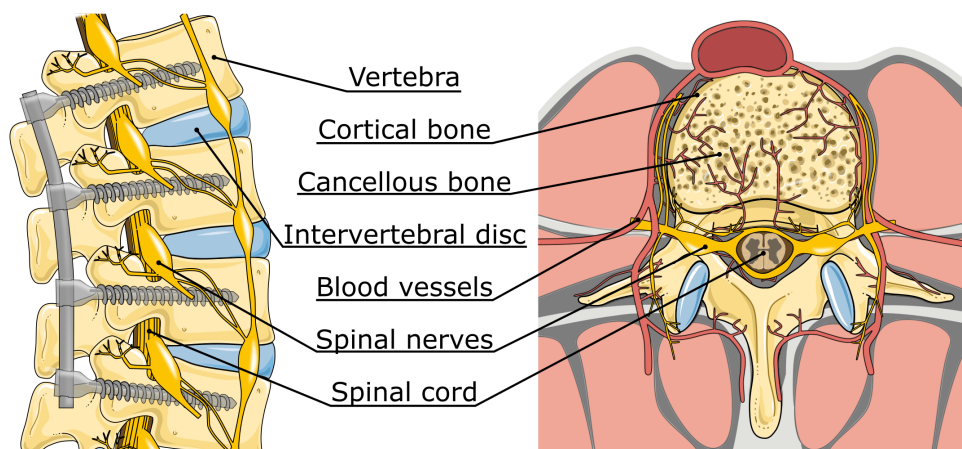
Figure 1.2: Vertebra with an outer layer of dense cortical bone encapsulating the porous cancellous bone. The vertebra is surrounded by blood vessels, nerves, and the spinal cord. Illustration adapted from Servier Medical Art by Servier, licensed under a Creative Commons Attribution 3.0 Unported License.

1.3. CHALLENGES IN SPINAL FUSION SURGERY

1.3.1. SCREW FIXATION

Inadequate screw fixation within the vertebra lowers the success rate of spinal fusion surgery. While pedicle screw fixation is considered the golden standard in spinal fusion surgery due to their superior fixation strength, screw loosening remains a prevalent issue. In the clinical study performed by Wu *et al.* [14] among 658 placed screws, 4.7% experienced loosening and 0.46% broke within three and a half years after placement. In cases involving patients suffering from compromised bone quality, such as osteoporosis, the fixation strength of pedicle screws is further weakened, increasing the risk of screw loosening [1]. Screw loosening can impede the desired fusion and result in the need for revision surgery. After pedicle screw placement, a major portion of the screw resides within the porous cancellous bone, with only a small section of the screw that is positioned in the pedicle actually making contact with the compact cortical bone. Lateral forces acting on the screw can lead to toggling of the screw around the point where the screw is in contact with the cortical bone (Figure 1.4a). The toggling action compresses the surrounding cancellous bone, undermining the screw's fixation strength and potentially causing it to pull-out (Figure 1.4b).

Current advancements in spinal fusion instrumentation primarily revolve around optimising the conventional pedicle screw by altering thread depth, pitch, and shape [5]. Nonetheless, the dimensions of the pedicle screws are constrained by the size and shape of the vertebra, ensuring the screw does no breach the cortical bone layer as this may lead to severe damage to surrounding tissue, such as vascular and nervous tissue [13, 9]. The screw diameter is confined to the minor diameter of the pedicle, and screw length is restricted by the size of the vertebral body.

As an alternative for standard pedicle screws, additional fixation methods, such as cement augmented screws, have been introduced. These screws exhibit higher pull-out
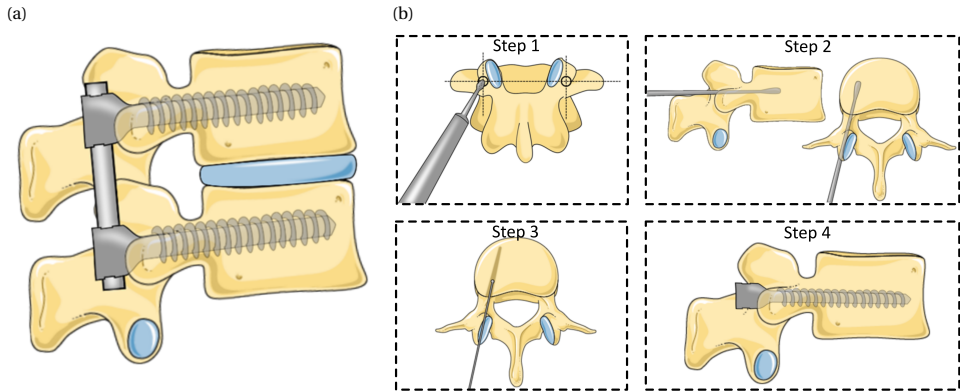
Figure 1.3: Spinal fusion surgery. (a) Surgically fused vertebrae with pedicle screws and rods. (b) Steps followed when placing pedicle screws using the free-hand technique. Illustration adapted from Servier Medical Art by Servier, licensed under a Creative Commons Attribution 3.0 Unported License.

forces, yet their removal in case of for instance infection proves challenging [2]. Consequently, an alternative anchoring approach must be identified to enhance the bone anchor's ability to withstand both lateral and axial forces acting upon spinal bone anchors. Given that cortical bone possesses greater resistance to forces as compared to the cancellous bone, anchoring along the cortical bone layer of the vertebra holds the potential for improved fixation.

1.3.2. SCREW PLACEMENT

Drilling the pilot hole for a pedicle screw presents a significant challenge, as even minor deviations from the intended path can result in severe damage to surrounding vital structures like vascular and nervous tissue [13, 9]. Moreover, improper positioning of pedicle screws can substantially compromise the fixation strength. A screw is considered mispositioned if it breaches the cortical layer and protrudes from the vertebra. While screw misplacement occurs in around 7.8% of screws inserted in the lumbar thoracic area, clinical consequences only arise in 0.5% of instances [3]. In cases where mispositioning leads to clinical issues, corrective surgery may be necessary to mitigate harm to neurological, visceral and vascular structures.

In order to address potential positioning challenges during pedicle screw placement, various guidance techniques have been proposed. Fluoroscopy provides improved accuracy but raises concerns about heightened radiation exposure for both the clinicians and the patient [7]. An alternative approach is Diffuse Reflectance Spectroscopy (DRS), which distinguishes between cortical and cancellous bone without subjecting individuals to harmful radiation [10].

While these guiding techniques offer alerts to avoid cortical breaches, the current probe employed for creating the pilot hole is rigid and lacks flexibility for trajectory adjustments. A steerable bone drill equipped with sensors would not only indicate cortical

(a)

Toggling

Cortical bone
Cancellous bone
Screw

(b)

Pull-out
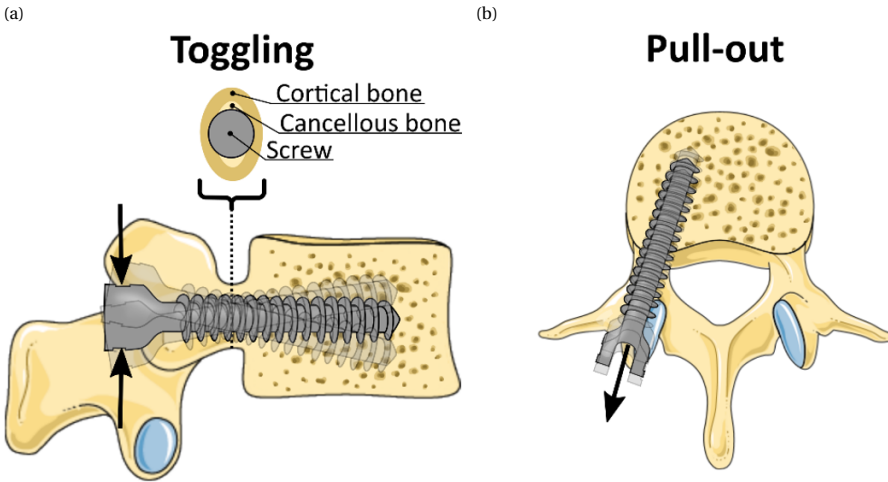
Figure 1.4: Schematic representation of screw loosening. (a) Toggling of pedicle screws can result in loosening of the screw due to the compression of the surrounding cancellous bone. (b) Loosening of the screws can hamper the desired fusion and may even result in pull-out of the screw. Illustration adapted from Servier Medical Art by Servier, licensed under a Creative Commons Attribution 3.0 Unported License.

layer penetration but also enable real-time trajectory adjustments to prevent breaches or follow the cortical bone layer to increase anchor fixation. The patent review of Sendrow-icz *et al.* [8] provides an overview of the state-of-the-art of steerable bone drills. Amongst the forty identified drill designs, only six were commercially available. Remarkably, none of these drill designs allow the surgeon control over the drill trajectory during insertion, indicating that the field of steerable bone drilling is still in its early development.

1.4. AIM OF THIS THESIS

Conventional pedicle screws exhibit an average pull-out strength of approximately 1000 N [15] and demonstrate significant displacements when subjected to lateral forces as low as 200 N [6]. The aim of this thesis is to investigate alternative fixation methods with the potential to enhance the fixation strength of conventional spinal bone anchors. To achieve this, the thesis will focus on anchor designs that increase the contact area between the anchor and the cortical bone layer of the vertebra. The exploration involves the examination of innovative designs for spinal bone anchoring and the exploration of alternative drilling techniques that offer adaptability in trajectory while passing through the vertebra. To avoid disruption to surrounding anatomy, drill designs are constrained to a maximum outer diameter of 4 mm and a minimum radius of curvature of 15-20 mm for lumbar vertebrae [12]. Within the scope of this thesis, various designs and proto-types for alternative spinal bone anchors and steerable bone drills are presented all with the overarching goal to enhance the efficacy of spinal fusion surgery by increasing the success rate through these advancements.

1
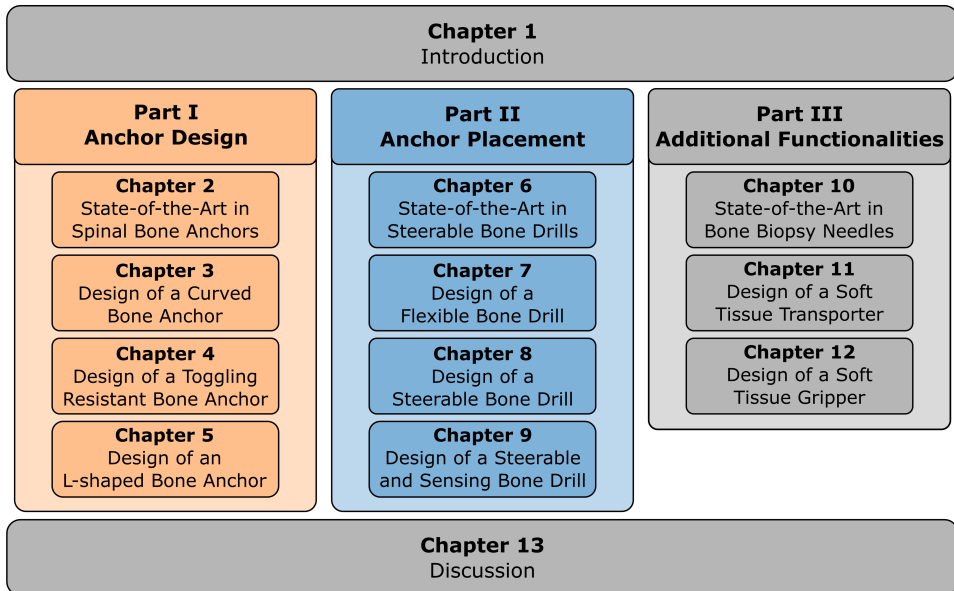
Figure 1.5: Visual layout of this thesis.

1.5. OUTLINE OF THIS THESIS

This thesis is organised in three parts, each addressing key aspects of improved fixation of spinal bone anchors for spinal fusion surgery. **Part I: Anchor Design** investigates alternative spinal bone anchors with the primary objective of increasing fixation strength. **Part II: Anchor Placement** details innovative designs of steerable bone drills aimed at facilitating the placement of novel spinal bone anchors. **Part III: Additional Functionalities** outlines potential supplementary features that could be integrated in both spinal bone anchors and bone drills, enhancing their overall functionality.

A common structure is followed across all three parts, starting with a state-of-the-art review to offer a comprehensive overview of potential design directions. Subsequent chapters in each part provide detailed descriptions of different designs that have been developed and validated. The schematic overview in Figure 1.5 visually represents the organised flow of the thesis, starting with **Chapter 1**, which serves as the introduction to the entire body of work.

Part I: Anchor Design
Chapter 2 offers a state-of-the-art review of spinal bone anchors as documented in patent literature. **Chapter 3** delves into the use of a pre-bend nitinol anchor combined with the pedicle screw, validating the potential for enhanced fixation. Following this, **Chapter 4** outlines the design and validation process of a toggling-resistant bone anchor, achieved through shaping to the pedicle with an integrated expandable section. **Chapter 5** discussed the utilisation of an L-shaped anchor, designed to create a macro-shape lock with the cortical bone layer, thereby improving pull-out resistance.

1

Part II: Anchor Placement
Chapter 6 provides a state-of-the-art review of steerable bone drills described in both scientific and patent literature. **Chapter 7** introduces a flexible bone drill that utilises a hydraulic pressure wave to hammer through bone. Moving forward, **Chapter 8** presents a steerable bone drill inspired by the tsetse fly, capable of passively steering along the cortical bone layer. **Chapter 9** describes the design and validation of a steerable bone drill with a cortical breach detecting sensor incorporated in the drill tip.

Part III: Additional Functionalities
Chapter 10 provides a state-of-the-art review of bone biopsy needles, documented in patent literature. **Chapter 11** describes the design and validation of a flexible soft tissue transporter, drawing inspiration from the ovipositor of parasitic wasps. **Chapter 12** further extends the functionality of the soft tissue transporter by incorporating a gripper to facilitate tissue gripping and subsequent transportation.

The thesis concludes with **Chapter 13**, where a comprehensive discussion and conclusion are provided, summarising the main findings and contributions of each chapter.

BIBLIOGRAPHY

[1]   Daniel J. Burval et al. "Primary Pedicle Screw Augmentation in Osteoporotic Lumbar Vertebrae: Biomechanical Analysis of Pedicle Fixation Strength". In: *Spine* 32.10 (May 1, 2007), pp. 1077–1083. (Visited on 06/04/2021).

[2]   Bruce M. Frankel, Sabino D'Agostino, and Chiang Wang. "A biomechanical cadaveric analysis of polymethylmethacrylate-augmented pedicle screw fixation". In: *Journal of Neurosurgery: Spine* 7.1 (2007). Publisher: American Association of Neurological Surgeons, pp. 47–53.

[3]   Oliver P. Gautschi et al. "Clinically relevant complications related to pedicle screw placement in thoracolumbar surgery and their management: a literature review of 35,630 pedicle screws". In: *Neurosurgical focus* 31.4 (2011). Publisher: American Association of Neurological Surgeons, E8.

[4]   E. Ladd Jones et al. "Cervical Pedicle Screws Versus Lateral Mass Screws: Anatomic Feasibility and Biomechanical Comparison". In: *Spine* 22.9 (May 1, 1997), pp. 977–982. (Visited on 02/25/2021).

[5]   Luigi La Barbera. "Chapter 17 - Fixation and Fusion". In: *Biomechanics of the Spine*. Ed. by Fabio Galbusera and Hans-Joachim Wilke. Academic Press, Jan. 1, 2018, pp. 301–327. ISBN: 978-0-12-812851-0. (Visited on 02/25/2021).

[6]   M Law, A F Tencer, and P A Anderson. "Caudo-cephalad loading of pedicle screws: mechanisms of loosening and methods of augmentation". In: *Spine* 18.16 (Dec. 1, 1993), pp. 2438–2443. (Visited on 12/14/2021).

[7]   Varun Puvanesarajah et al. "Techniques and accuracy of thoracolumbar pedicle screw placement". In: *World journal of orthopedics* 5.2 (2014), p. 112.

[8]   Alexander Sendrowicz et al. "Surgical drilling of curved holes in bone–a patent review". In: *Expert review of medical devices* 16.4 (2019). Publisher: Taylor & Francis, pp. 287–298.

[9]   Se-Il Suk et al. "Thoracic Pedicle Screw Fixation in Spinal Deformities: Are They Really Safe?" In: *Spine* 26.18 (Sept. 15, 2001), pp. 2049–2057. (Visited on 12/09/2021).

[10] Akash Swamy et al. "Diffuse reflectance spectroscopy, a potential optical sensing technology for the detection of cortical breaches during spinal screw placement". In: *Journal of biomedical optics* 24.1 (2019). Publisher: International Society for Optics and Photonics, p. 017002.

1

[11] Venkata Ramakrishna Tukkapuram, Abumi Kuniyoshi, and Manabu Ito. "A Review of the Historical Evolution, Biomechanical Advantage, Clinical Applications, and Safe Insertion Techniques of Cervical Pedicle Screw Fixation". In: *Spine Surgery and Related Research* 3.2 (Apr. 27, 2019), pp. 126–135. (Visited on 02/09/2021).

[12] Eric Philippus Hendricus Adrianus Verdult. "Drilling back: design & development of a directional drilling device, New Spinal Anchoring Technique". In: (1998).

[13] Bernd Wegener et al. "Delayed perforation of the aorta by a thoracic pedicle screw". In: *European Spine Journal* 17.2 (Sept. 1, 2008), pp. 351–354. (Visited on 12/09/2021).

[14] Jau-Ching Wu et al. "Pedicle screw loosening in dynamic stabilization: incidence, risk, and outcome in 126 patients". In: *Neurosurgical Focus* 31.4 (Oct. 2011), E9.

[15] M R Zindrick et al. "A biomechanical study of intrapeduncular screw fixation in the lumbosacral spine". In: *Clinical orthopaedics and related research* 203 (Feb. 1, 1986), pp. 99–112.

I

ANCHOR DESIGN

2
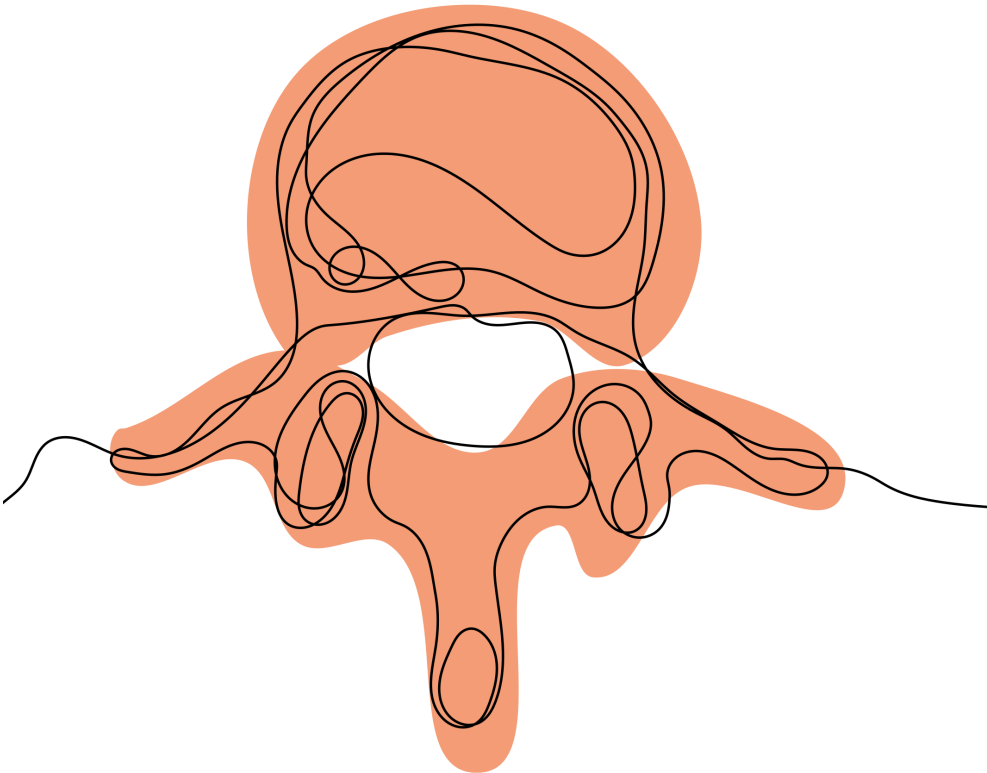
STATE-OF-THE-ART IN SPINAL BONE ANCHORS

This review provides an overview of the patent literature on posteriorly placed intrapedicular bone anchors. Conventional pedicle screws are the gold standard to create a fixation in the vertebra for spinal fusion surgery but may lack fixation strength, especially in osteoporotic bone. The ageing population demands new bone anchors that have an increased fixation strength, that can be placed safely, and, if necessary, can be removed without damaging the surrounding tissue. The patent search was conducted using a classification search in the Espacenet patent database. Only patents with a Cooperative Patent Classification of A61B17/70 or A61B17/7001 concerning spinal positioners and stabilisers were eligible for inclusion. The search query resulted in the identification of 731 patents. Based on preset inclusion criteria, a total of 56 unique patents on different anchoring methods were included, reviewed and categorised in this study. Five unique fixation methods were identified; (1) anchors that use threading, (2) anchors that utilise a curved path through the vertebra, (3) anchors that (partly) expand, (4) anchors that use cement and (5) anchors that are designed to initiate bone in growth. Of the anchor designs included in this study, eight had a corresponding commercial product, six of which were evaluated in clinical trials. This review provides insights into worldwide patented intrapedicular bone anchors that aim to increase the fixation strength compared to the conventional pedicle screw. The identified anchoring methods and their working principles can be used for clinical decision-making and as a source of inspiration when designing novel bone anchors.

2.1. Introduction

2.1.1. Background of Spinal Fusion Surgery

Spinal fusion surgery is performed to stabilise the spine in cases of spine degeneration, deformity, fractures, intervertebral disc disease, or after tumour removal [124]. Data from 2018 show that the most frequently performed spinal fusion procedure is interbody fusion with more than 350.000 procedures performed annually in the USA alone [103]. The number of performed spinal fusion surgeries is expected to grow. This growing trend is thought to be the result of an ageing population with increasing degenerative disorders and the ongoing advances in medical technology such as improved imaging technologies and anaesthesia, which allow more patients to be considered for spinal fusion surgery [34, 36, 77, 122]. In line with this, the number of performed fusion surgeries in patients aged 65 and older in the USA increased by 239% between 1998 and 2008 [102]. Factors such as new fixation devices, new bone grafting materials and the increased availability of minimally invasive surgery, are thought to play a role in this rapid increase.

During spinal fusion surgery, two or more adjacent vertebrae are interlocked or fixed to each other to prevent all motion between them. Fixation induces subsequent bony overgrowth and fusion, which will ensure the mechanical stability in the long term. In posterior approaches for spinal fusion surgery, the vertebrae are fixed to each other using screws and rods. Pedicle screws are placed bilaterally through the pedicles of each vertebra included in the construct. The screws are connected to each other by using rods, see Figure 2.1a. The effectiveness of the spinal fixation, before bony fusion has occurred, depends on the anchoring strength of the pedicle screw [136] .

The vertebrae consist of a cortical shell that is very dense and encloses the porous cancellous bone. Due to its porosity, the cancellous bone is more elastic and has a lower compressive strength than the cortical bone. Placing the screw through the small tubular shaped pedicle increases the contact between the screw and the cortical bone resulting in greatly improved fixation strength.

2.1.2. History of the Pedicle Screw

The discovery of X-rays, by Roentgen in 1885 gave a better understanding of the anatomy and biomechanics of the spine and allowed for the development of surgical spine interventions. The first procedure in which a spine was partly fused in order to regain stability was described by Hibbs in 1912 [64]. This spinal fusion was achieved by partly fracturing the spinal processes in order to generate contact between the bones of adjacent vertebrae. This approach required long-term immobilisation of the patient as even minor motion at the bony interface could prevent fusion. To achieve immediate fixation, the use of screws through adjacent facet joints were proposed by King in 1944 [76]. As an alternative solution, Boucher (1959) presented the use of screws through the pedicles [21], while Harrington (1962) presented the use of rods connected with hooks around the bone (lamina) to achieve scoliosis correction [60]. In 1976 Roy Camille described the use of pedicle screws in combination with plates allowing fixation to multiple pedicle screws, which distributes the force acting on the screw [104]. Currently, the pedicle screw is the gold standard for fixation of the spine and can be used to form a construct

(a)

(b)

Anterior

Vertebra body

Pedicle

Facet joint

Lamina

Spinous pocess

Transverse process

Posterior

2
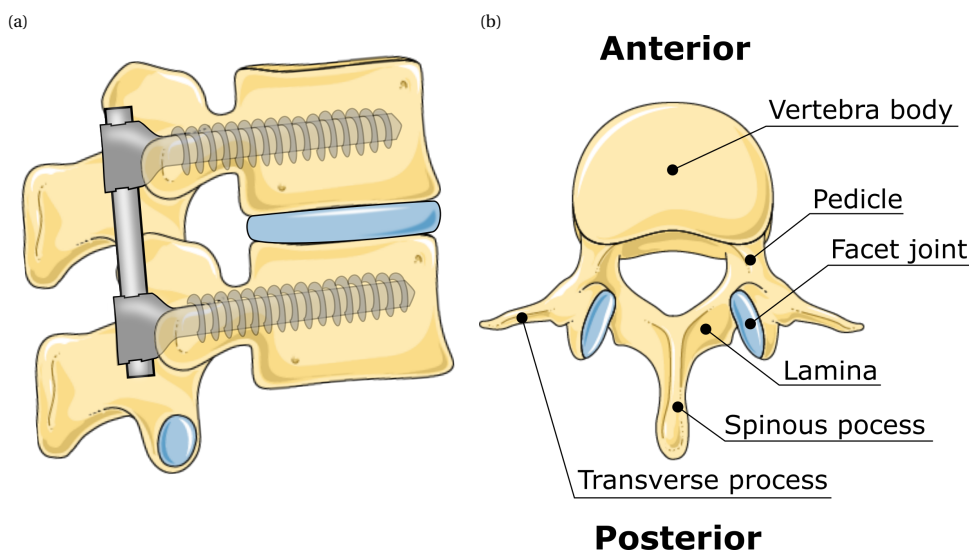
Figure 2.1: (a) Schematic representation of a fixation of the adjacent vertebrae with help of pedicle screws and rods. (b) Schematic representation of the anatomy of a lumbar vertebra. Illustration adapted from Servier Medical Art by Servier, licensed under a Creative Commons Attribution 3.0 Unported License.

with plates, rods and wires.

2.1.3. CHALLENGES WHEN USING PEDICLE SCREWS

The current pedicle screws are placed via a posterior approach through the pedicle into the vertebral body. In open surgery a large incision is made along the midline of the spine over the spinous processes. The muscles are then detached from the bone and pushed aside with retractors to expose the posterior aspects of the vertebrae: the spinous processes, lamina, facet joints and transverse processes (Figure 2.1b). Minimally invasive procedures aim to reduce the soft tissue damage by performing the surgery through small incisions in line with the entry points for the pedicle screws, at the drawback of the surgeon having less direct visual feedback to position the screws safely. Incorrectly placed screws may damage vascular and nervous tissue or result in poor fixation strength of the construct [118, 128]. To achieve safe placement of pedicle screws, image guidance, either via 2D fluoroscopy or 3D navigation, has become an essential part of spinal fusion surgery [66]. However, fluoroscopy has the drawbacks of exposing the patient and staff in the operating room to radiation while only providing 2D-imaging in one plane at a time. In contrast, intraoperative computed tomography (CT)-based 3D navigation uses intraoperative references to track and match the patient position as to provide highly accurate positional feedback based on the patient's own 3D imaging information [66].

During fixation, especially when deformities are corrected, large axial and lateral forces are exerted on the pedicle screw. The resistance to axial pull-out is mainly determined by the holding strength of the screw in the cortical bone of the pedicle [65].

Larger screws may increase the fixation strength but are also more challenging to place without breaching the cortical bone [22]. The lateral forces are mainly absorbed by the cancellous bone [83, 136]. In order to achieve successful fusion, the screw must prevent motion between the adjacent vertebrae even when large forces are applied.

Inadequate screw fixation can cause complications such as screw loosening or breaking of the screw. In a study by Wu *et al.* [129], 4.7% of 658 placed screws had loosened and 0.46% had broken within three and a half years after placement. A lower bone density is correlated with decreased fixation strength of a screw, which may result in screw loosening and pull-out [25]. This is especially a problem in elderly as they often suffer from osteoporosis [136]. With an ageing population and an increasing need for spinal fusion surgery, improvements in the current concept of pedicle screw fixation are in demand.

2.1.4. Goal

Pedicle screws have several advantages over other means of fixation in the spine, but the design of the screw has virtually not changed since its introduction. Insufficient fixation strength remains an issue, especially in the osteoporotic bone of elderly patients. The goal of this review is to provide a systematic overview of patented intrapedicular bone anchors. The included bone anchor designs are compared based on the design, placement, fixation and pull-out strength as well as the removal strategy. This review could provide insights into the future direction of spine fixation and could be a source of inspiration for the design of new anchors and aid clinical decision-making.

2.2. Materials and Methods

2.2.1. Patent Search Method

The patent search was conducted using the Espacenet patent database, which contains a large number of patents and supports extensive search queries. A classification search was conducted in which only patents with a Cooperative Patent Classification (CPC) of A61B17/70 or A61B17/7001 were included. Class A61B17/70 includes spinal positioners and stabilizers. Subcategories were not included as the patents in these subcategories focus on spinal positioners such as plates or the tools used to place these spinal positioners, which falls outside the scope of this review. As an exception, subclass A61B17/7001 was included, as this subclass includes screws or hooks combined with longitudinal elements which do not contact the vertebrae. This is the class in which the regular pedicle screw is listed. Subclasses were again not considered, as these focus on other devices used during spinal fusion surgery, such as the connection rods used between the screws and the longitudinal elements. The search query was enriched by a title search using key words, ensuring that only patents focused on anchoring were included. This resulted in the following final search query: *(cpc = "A61B17/70" OR cpc = "A61B17/7001") AND (ti any "anchor*" OR ti any "screw*" OR ti any "fast*")*

2.2.2. Eligiblity Critera

The scope of this study is to provide an overview of bone anchors that are placed through the pedicle, intending to replace the use of conventional pedicle screws. The identified bone anchors should allow for the connection by rods to achieve bone fusion between

(a)   (b)   (c)   (d)   (e)

Threaded   Curved   Expandable   Cement   Bone
Anchors   Anchors   Anchors   Augmented   Ingrowth
                                                Anchors   Anchors

[37, 133, 10, 70, 39, 63,   [2, 13, 44, 51, 90, 93,   [9, 17, 28, 30, 45, 47,   [79, 84, 88, 134, 135]   [84, 67, 72, 78, 4, 8, 49,
23, 101, 41, 134, 33, 71,   108]   50, 53, 59, 62, 74, 75,   87, 81, 26, 14, 120, 1,
3, 27, 16]   89, 92, 97, 127]   43, 94]
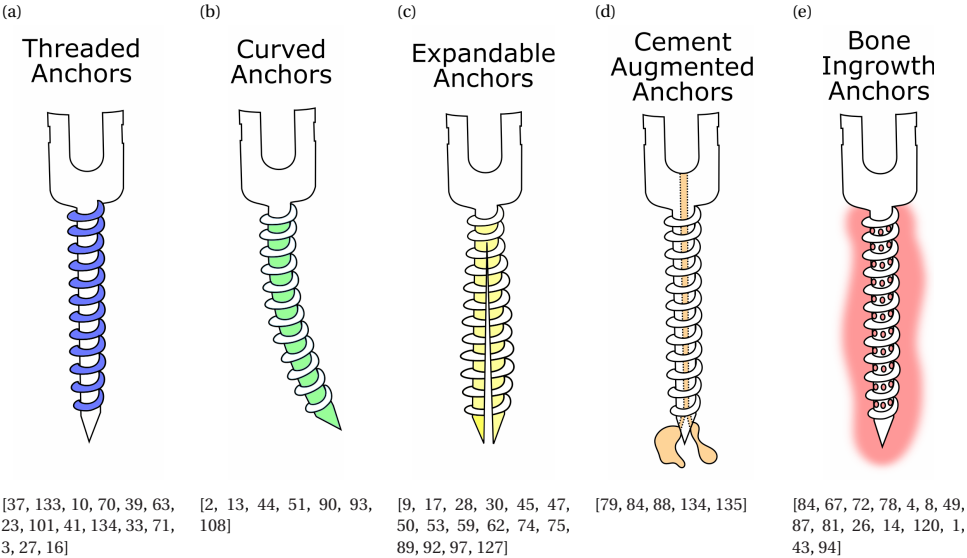
Figure 2.2: Schematic representation of the five identified methods to increase the fixation of bone anchors: (a) anchors that use threading, (b) anchors that utilise a curved path through the vertebra, (c) anchors that (partly) expand, (d) anchors that use cement and (e) anchors that are designed to initiate bone ingrowth.

multiple vertebrae. Patents focusing only on the screw head or tools used during the placement of pedicle screws were not included in this review.

2.2.3. General Results

The listed search query resulted in the identification of 731 patents (February 2022). These patents were included or excluded based on the set eligibility criteria. The titles, abstracts and drawings of the patents were screened to determine if the eligibility criteria were met. When there was uncertainty as to whether a patent should be included, the description was read. Patents with the same inventors and describing the same anchoring method were indicated as duplicates although these patents might not be duplicates in the legal sense. In these cases, only the most recent patent was included in this review. This resulted in 56 unique patents that were included in this review.

2.3. Results

2.3.1. Overview

The patents were categorised based on the anchoring method used to ensure a good fixation between the screw and the surrounding bone. Five unique fixation methods were identified: (1) anchors that use threading, (2) anchors that utilise a curved path through the vertebra, (3) anchors that (partly) expand, (4) anchors that use cement and (5) anchors that are designed to initiate bone in growth. The five fixation methods are schematically represented in Figure 2.2.

2
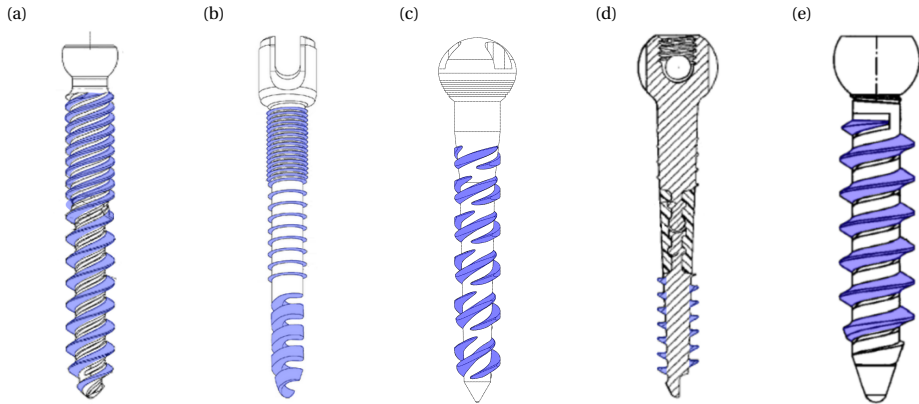
Figure 2.3: Anchors relying on thread (blue) in order to create a fixation with the surrounding bone. (a) Anchor with a smaller pitched thread at the proximal end of the anchor. Figure adapted from Yoon and Lee [133]. (b) Anchor with a changing pith and thread depth along the length of the anchor. Figure adapted from Jung *et al.* [71]. (c) Anchor with an interrupted threaded section to increase the fixation in the cancellous bone. Figure adapted from Alon [3]. (d) Anchor with a threaded section as well as a flexible section. Figure adapted from Casutt [27]. (e) Anchor with a flexible connection between the screw thread and the screw. Figure adapted from Biedermann *et al.* [16]

2.3.2. THREADED ANCHORS

Threaded anchors were found in fifteen patents [37, 133, 10, 70, 39, 63, 23, 101, 41, 134, 33, 71, 3, 27, 16], which all describe methods to ensure fixation of the bone anchor by using one or multiple threaded sections. The fixation strength of a threaded anchor depends on the shape, material and surface properties of the threaded section in contact with the surrounding bone. Screws designed for fixation in cortical bone are often characterised by threads with a small pitch, in order to increase the number of threads in contact with the thin layer of cortical bone. Screws that are designed for fixation within cancellous bone are characterised by a larger pitch and larger thread depth to increase the contact area with the cancellous bone.

The anchors described are intended for placement via a posterior approach. After placement, the distal section of the anchor is located in the vertebral body surrounded by cancellous bone, while the proximal section of the anchor is located in the pedicle and will have contact with the cortical bone. The bone anchor described by Crook *et al.* [37] uses a triple lead screw that allows for a quick insertion while increasing the fixation in the cortical bone due to the smaller pitch. Yoon and Lee [133] described an anchor with a quadruple threads in the proximal section of which two threads continue in the distal section while the other two threads are carved out of the distal section. This results in a distal section with a pitch that is twice as large as the proximal section as well as a larger thread depth (Figure 2.3a). Threaded anchors in which the threads differs over the length of the anchor to optimise it for fixation within the surrounding type of bone were found in eight other patents [10, 23, 39, 41, 63, 70, 101, 134]. The threads can be optimised by using a multi-threaded proximal section or by decreasing the minor diameter of the screw while keeping the major diameter constant to make the thread depth deeper in

the distal section. The anchor described by Cole [33] does the opposite and consists of a single-threaded proximal section with a constant cross section and a tapered distal tip, which is double threaded.

Jung *et al.* [71] described an anchor that has a shaft in which three sections can be identified (Figure 2.3b). The proximal portion is intended for fixation within the cortical bone layer and has a constant diameter that is threaded with a small pitch. The middle section has the same diameter as the proximal portion will be located in the cancellous bone and is equipped with threads with a larger pitch. The third, and most distal section, is shaped like a corkscrew, and the cancellous bone is retained inside this screw section. Alon [3] described an anchor with interrupted threaded sections that only compresses the cancellous bone without chipping the bone and thus weakening the fixation (Figure 2.3c).

The anchor described by Casutt [27] employs a different way of improving fixation strength. The described anchor has a flexible zone between the more rigid upper and lower shaft regions allowing the anchor to bend along with the bone (Figure 2.3d). High strains on the surrounding bone and high stresses in the shaft of the anchor are thus avoided. The placement and the design of the flexible zone can be matched with the vertebra characteristics. Biedermann *et al.* [16] described an anchor with incorporated flexibility as well, but in this case the screw threads and the core are connected by a ridge that allows small motions between the two (Figure 2.3e).

2.3.3. CURVED ANCHORS

This group includes anchors that improve the fixation strength of the anchors by placing them along a curved path to employ a shape lock principle. Seven of the included patents [2, 13, 44, 51, 90, 93, 108] belong in this category. The included anchors may be pre-curved, or include one or more flexible sections that allow for bending of the anchor.

Ben-Arye *et al.* [13] and Matityahu *et al.* [90] both described anchors that are pre curved. The curve is thought to increase the fixation as the anchor cannot be pulled out with an axial pull force. To further improve the fixation, the distal tips of the anchors that meet within the vertebral body can be connected by tightening a cable that runs through both anchors as described by Ben-Arye *et al.* [13] (Figure 2.4a). When the anchor must be removed, for instance to treat an infection, the cable can be untightened and, subsequently, the individual anchors can be pulled out.

Aghayev *et al.* [2], Glerum *et al.* [51] and Meek *et al.* [93] described anchors that can be introduced into a vertebra via the pedicle after which the anchor bends superior and can enter the adjacent vertebra via the vertebral endplate. Aghayev *et al.* [2] and Glerum *et al.* [51] described a bendable section that is created by interconnected (compliant) segments (Figure 2.4b). Meek *et al.* [93] described an anchor that has a flexible section made out of a tube that has a helical shape with interlocking teeth similar to the flexible section in the anchor described by Errico *et al.* [44] (Figure 2.4c). The interlocking teeth allow for flexibility while being able to transfer longitudinal rotation. Saidha and White [108] described a flexible anchor that has a bendable corkscrew structure, which allows placing the anchor in a curved pathway.

2
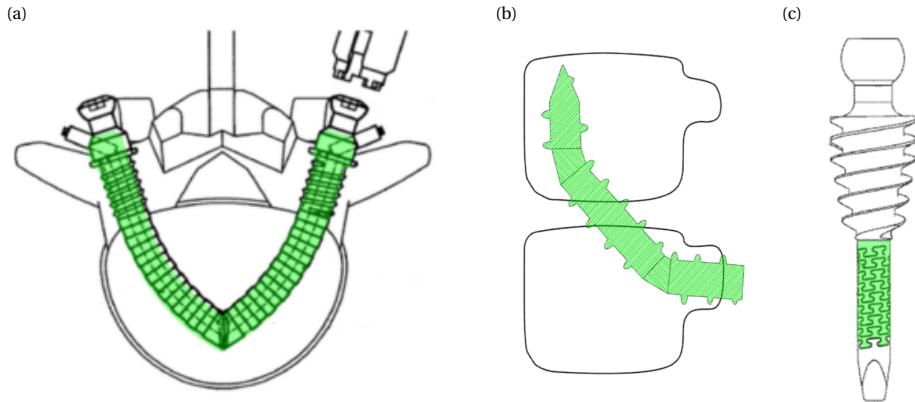
Figure 2.4: Anchors implanted in a curved path (green) to create an improved fixation. (a) Pre curved bone anchor consisting of two parts that are connected at the distal tip by a flexible wire rope that runs through the anchor. Figure adapted from Ben-Arye *et al.* [13]. (b) Bone anchors with a joint that allows bending of the anchor. Figure adapted from Aghayev *et al.* [2]. (c) Partly threaded anchor with a flexible section. Figure adapted from Errico *et al.* [44]

2.3.4. Expandable Anchors

Expandable anchors were found in sixteen patents [9, 17, 28, 30, 45, 47, 50, 53, 59, 62, 74, 75, 89, 92, 97, 127]. All of them describe bone anchors with one or more structures that can be expanded after placement in order to increase the fixation strength of the anchor. A proposed use of expansion is a secondary structure that acts similar to a wall plug [9, 30, 59, 75]. In these anchors, the plug is first inserted into a pre-made cavity, after which a screw is placed leading to radial expansion of the plug. The plug shapes to the cavity increasing the pull-out strength and preventing micro-motion of the anchor.

Other patents also describe anchors that use radial expansion in order to improve the fixation, but without the use of a secondary structure [53, 62, 89]. Gooch [53] described an anchor that expands partly in the pedicle, Hawkins *et al.* [62] and Maestretti *et al.* [89] described anchors in which the expansion will take place inside the vertebral body, resulting in the anchor expanding inside the cancellous bone. Hawkins *et al.* [62] described a bone anchor consisting of two curved blades each having a barbed side at the inside of the curve meant for bone engagement (Figure 2.5a). Both blades are introduced into the premade cavity where the bone engaging sides of the blades oppose each other and are in contact with the cavity's surface. The two blades can be connected at the proximal side resulting in an expansion of the distal tips. This ensures the fixation of the anchor within the surrounding bone.

2.3.5. Cement Augmented Anchors

Five anchors that use cement to increase the fixation strength of the anchor were included [79, 84, 88, 134, 135]. In all the identified anchors in this group, a hollow section is present, to allow a fluid to run through it [79, 84, 88, 134, 135]. These anchors can be
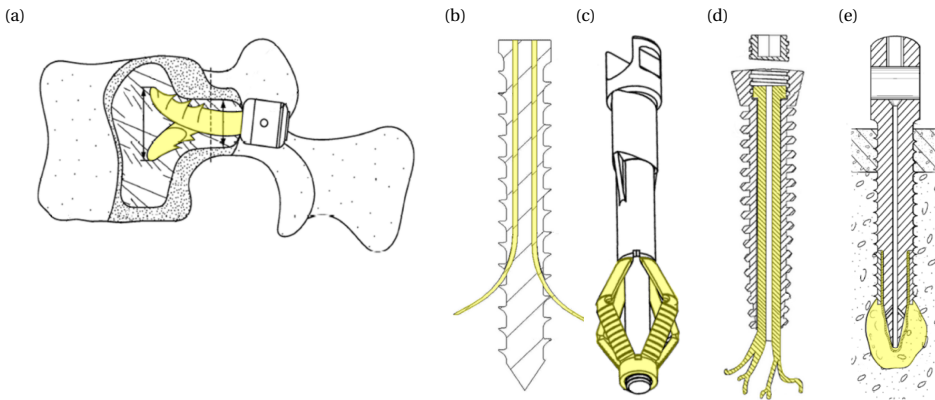
Figure 2.5: Anchors that have an expanding structure (yellow) to achieve a fixation with the surrounding bone. (a) Anchor consisting out of two pre curved parts that engage in the bone. Figure adapted from Hawkins *et al.* [62]. (b) Anchor with to laterally expanding blades. Figure adapted from Feng *et al.* [45]. (c) Anchor with multiple laterally expanding blades Mcdonald and Thornes [92]. (d) Anchor with root-like shaped struts. Figure adapted from Gregory and Ghobial [50]. (e) Anchor with a part that expands in a predrilled cavity by filling the expanding section with bone cement. Figure adapted from Froehlich [47]

used in combination with bone cement, for example PolyMethyl MethAcrylate (PMMA). The bone cement is pushed through the central channel and exits through one of the side channels and is pressed into the pores of the cancellous bone (Figure 2.6a). As the cement hardens, a rigid construct between the screw and the porous bone is achieved. Thus, the screw is thought to have a higher pull-out force. Kohm and Ferdinand [79] propose to use such a hollow screw and place it in pre-made linked cavities, which are filled with cement in order to increase the fixation strength (Figure 2.6b).

2.3.6. BONE INGROWTH ANCHORS

The group bone ingrowth supporting anchors includes fifteen patents [84, 67, 72, 78, 4, 8, 49, 87, 81, 26, 14, 120, 1, 43, 94]. Bone integration in the anchors can be achieved by a smart design of the shape of the anchor, as described by Huwais [67] and Juszczyk [72]. The two (partly) threaded anchors described in these patents have a non-circular cross section. Huwais [67] described an anchor with ridges that stress the bone upon implementation (Figure 2.6c). The applied stresses on the bone should be between the yield point and the ultimate tensile strength, and aims to induce bone growth. Juszczyk [72] described an anchor with an elliptical cross section that has a similar working principle.

Kohketsu and Ojima and Andersson *et al.* described the use of artificial bone in order to obtain a firm fixation of a bone anchor [78, 4]. A plug made of artificial bone such as hardened calcium phosphate can be used. Introduction of a screw into the plug breaks it, however, the chips of the plug material ensure the fixation of the screw as they are absorbed by the bone to promote bone growth (Figure 2.6d) [78].

A number of anchors increase their fixation strength by enhancing the outer surface of the anchor with a bone ingrowth-promoting layer. One option is to roughen the

2
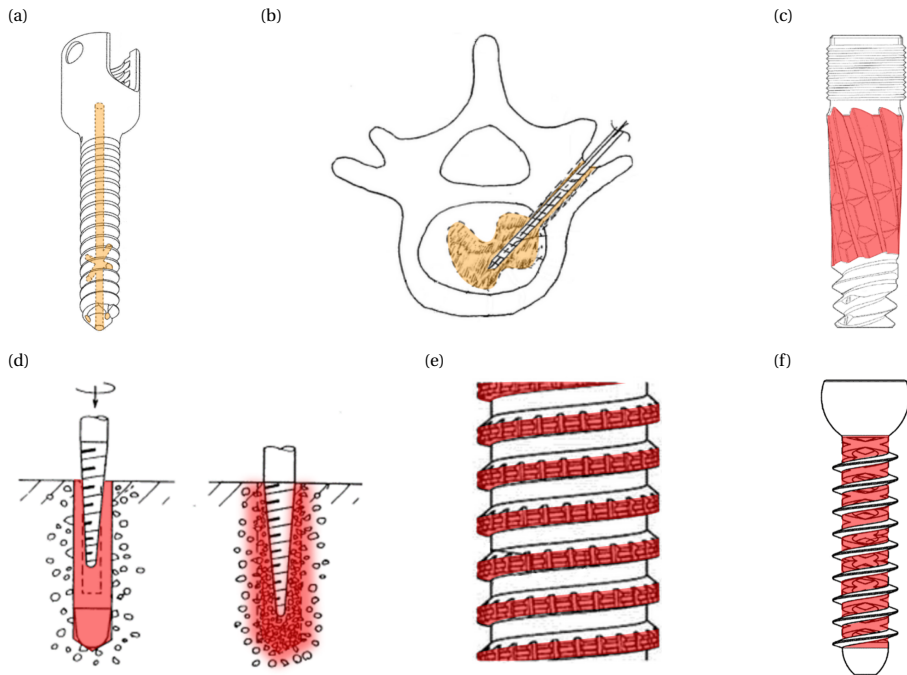
Figure 2.6: Anchors that use cement (orange), or aim to initiate bone ingrowth (red). (a) A threaded anchor with a channel through which the bone cement can be fed. Figure adapted from Zhou [135]. (b) Anchor fixed in the bone by utilizing two interlinked cavities filled with cement. Figure adapted from Kohm and Ferdinand [79]. (c) The ridges on the anchor surface cause elastic deformation of the surrounding bone during introduction, resulting in bone growth. Figure adapted from Huwais [67]. d The use of a plug that breaks upon introduction of the screw. The plug chips encourage bone ingrowth. Figure adapted from Kohketsu and Ojima [78]. (e) A porous structure on the threaded bone anchor that allows for bone ingrowth. Figure adapted from Liu and Yang [87]. (f) A threaded bone anchor with holes that allow for bone ingrowth. Figure adapted from Kyle and Patel [81]

2

outer surface of the bone anchor as to create a bone-implant interface [8]. Additionally, a porous structure that allows bone ingrowth can be used to increase the fixation strength of a bone anchor. In the device described by Arnin [8], for instance, the proximal section of the bone anchor is coated with a porous hydroxyl apatite layer to promote bone ingrowth [49]. Another option is to use a porous threaded section (Figure 2.6e) [87]. Li *et al.* [84] proposed a porous distal section that does not only allow for bone ingrowth, but also lowers the local stress to the distal tip due to the increased flexibility of this section. This anchor can also be enhanced by a channel for the application of bone cement. Finally, another option is to increase the pore diameter to allow and stimulate bone ingrowth (Figure 2.6f) [14, 26, 81]. These holes can also be used for drug delivery and the application of fillers. In addition, non-threaded anchor sections can be enhanced with holes and materials that promote bone growth [1, 43]. Mehl and Mesiwala [94], for example, proposed an anchor that during insertion, accumulates bone chips in the holes and ridges that run along the anchor in order to achieve fast bone ingrowth.

2.4. FROM PATENT TO COMMERCIALISATION

To get more insight in the commercialisation of the designs presented in the included patents, a list of commercial product corresponding to the designs included in this study was made. These products were identified through a review of the products of the companies to which the patents were assigned and comparing the resemblance between the patents and the products. This was done for each patent filed by a company. Approximately 74% of the patents included in this study are filed by a company, 10% by an academic institution and 16% by independent inventors. From this, it can be deduced that this field of research is primarily industry-driven. A list of commercial products corresponding to the bone anchors included in this study is presented in Table 2.1. Most of the identified products focus on bone ingrowth, but are not (yet) used as bone anchors for application in spinal fusion surgery. Some are in the trial phase for use as a medical product, while others are clinically used but not as a substitute for pedicle screws but for hip fractures or sacroiliac (SI)-joint fusion.

2.5. DISCUSSION

2.5.1. COMPARATIVE ANALYSIS

Of the patents included in this study, 27% are in the category of 'expandable anchors'. This is remarkable since this method is not used to increase the fixation strength in commercially available intrapedicular bone anchors. Expandable structures inside the vertebral body are, however, used in vertebroplasty. During this type of surgery, a collapsed vertebra is reinforced using an expandable structure in combination with bone cement. A possible explanation for the high number of expandable anchors may be the versatile design of such anchors. There are many ways to achieve expansion, and each can be patented individually. The category 'cement augmented anchors' only account for 6% of the included patents, and the designs described in these patents are much more straightforward as they all contain a central channel through which the cement is transported. The other categories 'threaded anchors', 'curved anchors' and 'bone ingrowth anchors' account for 26%, 14% and 27%, respectively. Figure 2.7 shows the temporal distribution

Table 2.1: Overview of the commercial availability of the bone anchors described by the included patents.

Commercial product	Company	Reference	(Clinical) studies	Method / Group	patent reference
QuattroTM	Mantiz Logitech Inc., Republic of Korea	[91]	[11]	Threaded	[133]
VertLift Intended for vertebroplasty	SpineAlign Medical, Inc., United States	[119]	[7]	Expandable	[28]
X-Bolt ®	X-Bolt Orthopaedics, Ireland	[131]	[58, 57, 52, 73, 32, 54, 46] [56, 55, 99, 35]	Expandable	[92]
Fiber AnchorTM	Theracell Inc., United States	[121]	[126]	Bone ingrowth	[4]
ProMISTM	Premia Spine USA, United States	[114]	[111]	Bone ingrowth	[8]
SIrosTM Intended for SI-joint fusion	Genesyspine® United States	[82]	-	Bone ingrowth	[14]
iFuse Intended for SI-joint fusion	SI-BONE, inc., United States	[68]	[15, 6, 5, 98, 38, 123, 69] [85, 20, 117, 19, 18, 40] [106, 86, 29, 110, 85, 48, 107] [105, 95, 42]	Bone ingrowth	[43]
SImpact® Intended for SI-joint fusion	Life Spine, United States	[113]	-	Bone ingrowth	[94]

of the included patents classified per fixation method. There is an overall increase in the number of patents published over time especially when taking into account that only patents published till February 2022 are included in this review. There is no clear trend towards one of the five identified fixation methods but in the last six years, there has been a clear increase in patents that describe anchors that initiate bone ingrowth.

2.5.2. COMPARISON ANCHOR PLACEMENT

Safe anchor placement is an important issue when designing spinal bone anchors to avoid damage to the vertebra itself and the surrounding anatomical structures such as nerve roots, blood vessels and the spinal cord during anchor placement. When using threaded anchors, the aim is to achieve maximal cortical bone purchase during the placement. The highest fixation strength is achieved by anchors that have a maximum outer diameter and length that can be placed without the occurrence of cortical breach [31]. The trade-off between maximal bone purchase and avoiding damage has led to the recommendation to use a screw diameter that is 80% of the pedicle width [115]. This re-
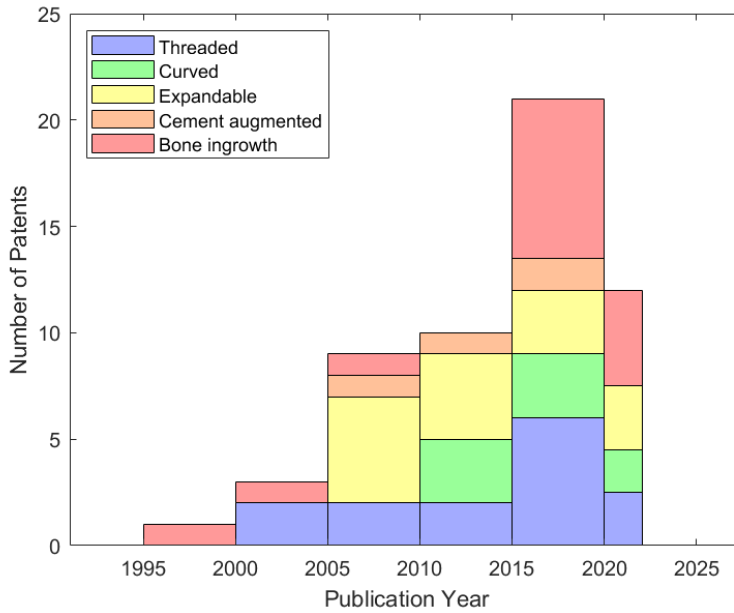
Figure 2.7: Temporal distribution of relevant patents categories based on the fixation method (threaded, curved, expandable, cement augmented, or bone ingrowth) until February 2022

sults in a placement accuracy that ranges from 60 to 97.5% in the lumbar spine, and from 27.6 to 96.5% in the thoracic spine using conventional pedicle screws with the free-hand method [80].

Bone anchors that are cement augmented or that have a coating to induce bone ingrowth have a similar placement strategy as the conventional pedicle screw. Although no literature could be found on the placement accuracy with such anchors, it is likely that their placement accuracy is similar to conventional pedicle screws. Additional risks that arise during placement of cement augmented bone anchors are thermal and chemical bone necrosis due to the polymerisation of the bone cement [116] and cement leakage out of the vertebral body via veins or cortical defects [132]. Although cement leakage can result in serious complications such as pulmonary embolisms, the risks of clinically relevant complications are slim: in a study of 98 patients with 474 cement augmented pedicle screws, leakage occurred in 93.6% of the patients but all cases were asymptomatic [96].

For curved or expandable bone anchors, placement is more critical as the placement of these anchors is more difficult to predict and to could potentially cause more harm. We think that real-time feedback of the anchor location within the vertebra is a necessity to prevent injury to surrounding structures when using curved or expandable anchors. 3D navigation or other systems such as electrical conductivity or diffuse reflectance spectroscopy (DRS) should be used to reliably detect cortical breaches [24].

2.5.3. Comparison anchor fixation

The fixation strength of bone anchors is often measured by the pull-out force; the force required to axially pull the anchor out of the vertebra. In this section we will give an indication for the fixation strength for each of the five identified fixation methods. These findings should be taken as a rough estimate for the fixation strength as differences in design, while using the same anchoring method, could result in significant differences in fixations strength.

The use of double threaded screws significantly increases the pull-out strength with 20% as compared to conventional single-threaded screws [112]. To our knowledge there is no data available on the fixation strength of curved anchors. Yet, placing the screw along a well-selected curved path as compared to the straight path of a conventional pedicle screw is likely to increase the fixation strength. Bi-cortical fixation, where the distal tip of a straight screw engages in the opposite cortex improves the pull-out force to 120% compared to conventional screw placement [136]. Similar effects might be reached when using curved intrapedicular bone anchors. Anchors with a hydroxyapatite-coating that promotes bone ingrowth can increase the pull-out strength 1.5 times as compared to the pull-out strength of conventional screws [61]. It takes, however, days to weeks for the bone to grow and increase the fixation strength. Cement augmented anchors improve the fixation even more, as the load is transferred to the vertebral body via the cement [12]. The pull-out strength of cement augmented screws can almost double the pull-out strength compared to the conventional pedicle screws that are not cement augmented [136]. Lastly, expandable bone anchors can also improve the pull-out strength compared to conventional pedicle screws [125]. The study of Wu *et al.* [130] shows that the used anchors became loose in 4.1% of the cases while with conventional pedicle screws, loosening occurred in 12.9% of the cases, showing clearly the advantage of the expandable anchors in terms of loosening. However, the same study showed that 0.4% of the expandable anchors broke while none of the conventional pedicle screws broke, which is a clear drawback of expandable anchors. A possible explanation is that expandable bone anchors consist of multiple moving parts that makes them more fragile.

2.5.4. Comparison Anchor Removal

Causes for implant removal are pain, discomfort or deep infection, which makes removal of bone anchors a necessity. However, the screws must be fixated well such that fusion of the vertebrae can take place. It was found that 15% of the pedicle screws are not functional anymore within one year, for instance, due to loosening [100]. In the study of Sandén *et al.* [109] it was found that threaded anchors were already loose after 10–22 months or could be removed by a maximum torque of only 25 Ncm. It must be noted that the fusion of the vertebra is expected to take place within the first six months after surgery. During these six months, good fixation of the screws is a necessity to allow for the desired fusion, as even minor motions between the vertebrae can prevent fusion, but afterwards, the screws are redundant. Removal of expandable anchors can be challenging depending on the design, as bone ingrowth can occur within the open spaces of the expanded anchor. This could prevent folding of the anchor into the original state and subsequently damage the pedicle during the removal of the anchor [130]. The removal of cement augmented anchors with a screw thread is also a challenge as the cement cre-

ates a firm fixation by flowing into the pores of the cancellous bone. The anchor can be removed similarly to a threaded anchor by rotating it out, but the removal of the remaining cement may cause damage to the vertebral body or the pedicle [136]. Removal of anchors with a hydroxyapatite-coating is also challenging. The study of Sandén *et al.* showed that the required torque to remove a hydroxyapatite-coated anchor could exceed 600 Ncm [109].

2.5.5. LIMITATIONS AND FUTURE RESEARCH

This review provides an overview of the bone anchors found in patent literature. Even though patents merely describe novel ideas without giving many details about suitability for surgical practice, we have included this information in this review to the best of our knowledge. The patent search was carried out within two patent classes: A61B17/70 and A61B17/7001, which both focus on anchors for spinal stabilisation. It would be interesting to expand this study with a patent review on bone anchors for other anatomical sites as these may also be applicable in the spine. Furthermore, only patent literature was included in this review to provide insights into the development of future intrapedicular bone anchors. Including anchor designs presented in scientific literature could also be interesting for future research.

This study provides an overview of the currently patented means to improve the fixation strength of intrapedicular bone anchors. The overview can provide insights into the future direction of technologies for spine fixation and could serve as a source of inspiration for the design of new anchors that allow for safe placement and removal while increasing the fixation strength of the anchor in the vertebra.

2.6. CONCLUSION

Due to ageing of the population, an increase in spinal fusion surgeries will be performed in osteoporotic bone. To achieve reliable fixation in this weaker bone, alternatives to the conventional pedicle screw, which is now the gold standard for spine fixation, are desirable. A patent search has been performed to map what lies beyond the pedicle screw. Five means to increase the fixation of a bone anchor have been identified: (1) anchors that use threading, (2) anchors that utilise a curved path through the vertebra, (3) anchors that (partly) expand, (4) anchors that use cement and (5) anchors that are designed to initiate bone ingrowth. This overview provides insights into worldwide patented creative ideas by which the fixation strength of bone anchors that run through the pedicle can be improved, which may also serve to improve fixation strength of bone anchors in general.

BIBLIOGRAPHY

[1] Max Aebi. "Self-cutting hollow cylindrical bone anchoring element". Pat. AU736471B2. Synthes Ag. July 26, 2001.

[2] Kamran Aghayev et al. "Transdiscal screw". U.S. pat. 10314631B2. H Lee Moffitt Cancer Ct & Res. June 11, 2019.

[3] Guy Alon. "Orthopedic fastener and associated systems and methods". U.S. pat. 11000326B1. Alon Guy. May 11, 2021.

[4] Gunnar Andersson et al. "Demineralized Bone Fiber Composition for Augmentation of Fixation". Pat. WO2019033082A1. Theracell Inc. Feb. 14, 2019.

[5] Bernardo de Andrada Pereira et al. "Biomechanical effects of a novel posteriorly placed sacroiliac joint fusion device integrated with traditional lumbopelvic long-construct instrumentation". In: *Journal of Neurosurgery. Spine* (June 18, 2021), pp. 1–10.

[6] Bernardo de Andrada Pereira et al. "Biomechanics of a laterally placed sacroiliac joint fusion device supplemental to S2 alar-iliac fixation in a long-segment adult spinal deformity construct: a cadaveric study of stability and strain distribution". In: *Journal of Neurosurgery. Spine* (Sept. 17, 2021), pp. 1–11.

[7] Giovanni Carlo Anselmetti et al. "Vertebral augmentation with nitinol endoprosthesis: clinical experience in 40 patients with 1-year follow-up". In: *Cardiovascular and interventional radiology* 37.1 (Feb. 2014), pp. 193–202.

[8] Uri Arnin. "Pedicle Screw Surface Treatment for Improving Bone-Implant Interface". Pat. WO2008059505A2. Arnin Uri; Impliant Ltd. May 22, 2008.

[9] Ezzine Banouskou and Jean-François Oglaza. "Universal Anchor for Bone Fixation". U.S. pat. 2015045841A1. Vexim. Feb. 12, 2015.

[10] Yossef Bar et al. "Double Threaded Orthopedic Screw". Pat. CA2746032A1. Mazor Robotics Ltd. June 17, 2010.

[11] F. Alan Barber and Morley A. Herbert. "Cyclic Loading Biomechanical Analysis of the Pullout Strengths of Rotator Cuff and Glenoid Anchors: 2013 Update". In: *Arthroscopy: The Journal of Arthroscopic & Related Surgery* 29.5 (May 1, 2013), pp. 832–844. (Visited on 12/09/2021).

[12] S. Becker et al. "Assessment of different screw augmentation techniques and screw designs in osteoporotic spines". In: *European Spine Journal* 17.11 (Nov. 1, 2008), pp. 1462–1469. (Visited on 05/04/2021).

[13] Asaf Ben-Arye, Arnon Epstein, and Yuval Shezifi. "Bone Anchoring System". U.S. pat. 2010305700A1. Ben-Arye Asaf; Epstein Arnon; Scorpion Surgical Technologies Ltd; Shezifi Yuval. Dec. 2, 2010.

[14] Brian Bergeron et al. "Material Directing Orthopedic Anchor". Pat. WO2019152737A1. Genesys Spine. Aug. 8, 2019.

[15] Connor Berlin et al. "Robotic Sacroiliac Fixation Technique for Triangular Titanium Implant in Adult Degenerative Scoliosis Surgery: 2-Dimensional Operative Video". In: *Operative Neurosurgery (Hagerstown, Md.)* 21.6 (Nov. 15, 2021), E555–E556.

[16] Lutz Biedermann, Bernd Fischer, and Wilfried Matthis. "Bone Screw and Method for Providing Bone Screw". Pat. JP2015073905A. Biedermann Technologies Gmbh. Apr. 20, 2015.

[17] Lutz Biedermann, Wilfried Matthis, and Helmar Rapp. "Bone Anchoring Element". U.S. pat. 2016361104A1. Biedermann Technologies Gmbh. Dec. 15, 2016.

[18] R. Bornemann et al. "Clinical Trial to Test the iFuse Implant System® in Patients with Sacroiliac Joint Syndrome: One Year Results". In: *Zeitschrift Fur Orthopadie Und Unfallchirurgie* 154.6 (Dec. 2016), pp. 601–605.

[19] Rahel Bornemann et al. "Diagnosis of Patients with Painful Sacroiliac Joint Syndrome". In: *Zeitschrift Fur Orthopadie Und Unfallchirurgie* 155.3 (June 2017), pp. 281–287.

[20] Rahel Bornemann et al. "Two-year clinical results of patients with sacroiliac joint syndrome treated by arthrodesis using a triangular implant system". In: *Technology and Health Care: Official Journal of the European Society for Engineering and Medicine* 25.2 (2017), pp. 319–325.

[21] H. H. Boucher. "A method of spinal fusion". In: *The Journal of Bone and Joint Surgery. British volume* 41-B.2 (May 1, 1959), pp. 248–259. (Visited on 02/10/2021).

[22] A. G. Brantley et al. "The effects of pedicle screw fit. An in vitro study." In: *Spine* 19.15 (1994), pp. 1752–1758.

[23] Ian Burgess and Alistair Ashley Thompson. "Improvements in and Relating to Bone Fixins". Pat. WO0015128A1. Burgess Ian; Depuy Int Ltd; Thompson Alistair Ashley. Mar. 23, 2000.

[24] Gustav Burström et al. "Diffuse reflectance spectroscopy accurately identifies the pre-cortical zone to avoid impending pedicle screw breach in spinal fixation surgery". In: *Biomedical Optics Express* 10.11 (Oct. 24, 2019), pp. 5905–5920. (Visited on 09/16/2021).

[25] Daniel J. Burval et al. "Primary Pedicle Screw Augmentation in Osteoporotic Lumbar Vertebrae: Biomechanical Analysis of Pedicle Fixation Strength". In: *Spine* 32.10 (May 1, 2007), pp. 1077–1083. (Visited on 06/04/2021).

[26] Frank Castro. "Surgical Fastener". Pat. WO2020040862A1. Blue Sky Tech Llc. Feb. 27, 2020.

[27] Simon Casutt. "Pedicle Screw". European pat. 1865862A1. Zimmer Gmbh. Dec. 19, 2007.

[28] Benny M. Chan, Paul E. Chirico, and Sean R. Pakbaz. "Devices for Stabiliz-
      ing Bone Compatible for Use with Bone Screws". European pat. 2173268A1.
      Spinealign Medical Inc. Apr. 14, 2010.

[29] Daniel J. Cher, W. Carlton Reckling, and Robyn A. Capobianco. "Implant survivor-
      ship analysis after minimally invasive sacroiliac joint fusion using the iFuse Im-
      plant System(®)". In: *Medical Devices (Auckland, N.Z.)* 8 (2015), pp. 485–492.

[30] Kyu Jung Cho, Min Sik Shin, and Jin Soon Kim. "A Spinal Screw Module". Pat.
      WO2008146981A1. Gs Medical Co Ltd; Cho Kyu Jung; Shin Min Sik; Kim Jin Soon.
      Dec. 4, 2008.

[31] W. Cho, S. K. Cho, and C. Wu. "The biomechanics of pedicle screw-based instru-
      mentation". In: *The Journal of Bone and Joint Surgery. British volume* 92-B.8 (Aug.
      2010). Publisher: The British Editorial Society of Bone & Joint Surgery, pp. 1061–
      1065. (Visited on 03/16/2022).

[32] A. D. Clarke, J. B. T. Herron, and J. L. McVie. "X-Bolt unforeseen placement com-
      plication: case report". In: *The Annals of The Royal College of Surgeons of England*
      99.8 (Nov. 2017), e227–e229.

[33] Chad Cole. "Spinal Fixation Device". U.S. pat. 2018368889A1. K2m Inc. Dec. 27,
      2018.

[34] Paolo A. Cortesi et al. "Epidemiologic and Economic Burden Attributable to First
      Spinal Fusion Surgery: Analysis From an Italian Administrative Database". In:
      Spine 42.18 (Sept. 15, 2017), pp. 1398–1404. (Visited on 12/01/2021).

[35] Matthew L. Costa et al. "Intramedullary nail fixation versus locking plate fixation
      for adults with a fracture of the distal tibia: the UK FixDT RCT". In: *Health Tech-
      nology Assessment (Winchester, England)* 22.25 (May 2018), pp. 1–148.

[36] John A. Cowan Jr. et al. "Changes in utilization of spinal fusion in the united
      states". In: *Neurosurgery* 59.1 (July 1, 2006), pp. 15–20. (Visited on 04/23/2021).

[37] David Crook, Peter Harris, and Chester Sharps. "Triple Lead Bone Screw". U.S.
      pat. 2011152948A1. U S Spine Inc; Crook David; Harris Peter; Sharps Chester.
      June 23, 2011.

[38] Megan Dale et al. "iFuse Implant System for Treating Chronic Sacroiliac Joint
      Pain: A NICE Medical Technology Guidance". In: *Applied Health Economics and
      Health Policy* 18.3 (June 2020), pp. 363–373.

[39] Xiangjun Deng, Zhiwei Song, and Jianjun Yang. "Pedicle screw". Pat.
      CN109620382A. Beautech Medical Instr Jiangsu Co Ltd. Apr. 16, 2019.

[40] Julius Dengler et al. "Referred leg pain originating from the sacroiliac joint: 6-
      month outcomes from the prospective randomized controlled iMIA trial". In:
      Acta Neurochirurgica 158.11 (Nov. 2016), pp. 2219–2224.

[41] Francis Denis et al. "Multi-Thread Bone Screw". Pat. WO2007095447A1. Warsaw
      Orthopedic Inc; Denis Francis; Transfeldt Ensor E; Garvey Timothy a; Schwender
      James D; Perra Joseph H; Pinto Manuel R; Veldman Michael S; Rezach William A.
      Aug. 23, 2007.

[42] Bradley S. Duhon et al. "Safety and 6-month effectiveness of minimally invasive sacroiliac joint fusion: a prospective study". In: *Medical Devices (Auckland, N.Z.)* 6 (2013), pp. 219–229.

[43] Robert Eastlack et al. "Implants for Spinal Fixation and or Fusion". Pat. WO2020168269A1. Si-Bone Inc. Aug. 20, 2020.

[44] Thomas Errico et al. "Fixation Device and Method of Using the Same". Pat. WO2018183837A1. K2m Inc. Oct. 4, 2018.

[45] Yafei Feng et al. "Medical anchor type vertebral pedicle screw". Pat. CN103860251A. Fourth Military Medical Univ. June 18, 2014.

[46] M. A. Fernandez et al. "The tip-apex distance in the X-Bolt dynamic plating system". In: *Bone & Joint Research* 6.4 (Apr. 1, 2017), pp. 204–207. (Visited on 12/09/2021).

[47] Markus Froehlich. "Bone Anchor System". U.S. pat. 2009099609A1. Zimmer Gmbh. Apr. 16, 2009.

[48] P. Gaetani et al. "Percutaneous arthrodesis of sacro-iliac joint: a pilot study". In: *Journal of Neurosurgical Sciences* 57.4 (Dec. 2013), pp. 297–301.

[49] Yajun Gao et al. "Pedicle screw". Pat. CN104398297A. Shandong Weigao Orthopedic Device Company Ltd. Mar. 11, 2015.

[50] Bassem Georgy and Eman K. R. Ghobial. "Device and Method for Orthopedic Fracture Fixation". Pat. WO2009086024A1. Georgy Bassem; Ghobial Eman K R. July 9, 2009.

[51] Chad Glerum et al. "Pedicle-Based Intradiscal Fixation Devices and Methods". U.S. pat. 2021307924A1. Globus Medical Inc. Oct. 7, 2021.

[52] En Lin Goh et al. "Complications following hip fracture: Results from the World Hip Trauma Evaluation cohort study". In: *Injury* 51.6 (June 1, 2020), pp. 1331–1336. (Visited on 12/09/2021).

[53] Hubert L. Gooch. "Anchor for Augmentation of Screw Purchase and Improvement of Screw Safety in Pedicle Screw Fixation and Bone Fracture Fixation Systems". U.S. pat. 2007118131A1. May 24, 2007.

[54] J. D. Gosiewski, T. P. Holsgrove, and H. S. Gill. "The efficacy of rotational control designs in promoting torsional stability of hip fracture fixation". In: *Bone & Joint Research* 6.5 (May 1, 2017), pp. 270–276. (Visited on 12/09/2021).

[55] X. L. Griffin et al. "The Warwick Hip Trauma Evaluation One – an abridged protocol for the WHiTE One Study". In: *Bone & Joint Research* 2.10 (Oct. 1, 2013), pp. 206–209. (Visited on 12/09/2021).

[56] X. L. Griffin et al. "The Warwick Hip Trauma Evaluation One: a randomised pilot trial comparing the X-Bolt Dynamic Hip Plating System with sliding hip screw fixation in complex extracapsular hip fractures: WHiTE (One)". In: *The Bone & Joint Journal* 98-B.5 (May 2016), pp. 686–689.

[57]   Xavier L. Griffin et al. "Effect on health-related quality of life of the X-Bolt dy-
       namic plating system versus the sliding hip screw for the fixation of trochanteric
       fractures of the hip in adults: the WHiTE Four randomized clinical trial". In: *The
       Bone & Joint Journal* 103-B.2 (Feb. 1, 2021), pp. 256–263. (Visited on 12/09/2021).

[58]   Xavier L. Griffin et al. "Randomised controlled trial of the sliding hip screw ver-
       sus X-Bolt Dynamic Hip Plating System for the fixation of trochanteric fractures
       of the hip in adults: a protocol study for WHiTE 4 (WHiTE4)". In: *BMJ Open* 8.1
       (Jan. 1, 2018). Publisher: British Medical Journal Publishing Group Section: Emer-
       gency medicine, e019944. (Visited on 10/21/2021).

[59]   Bryan Griffiths et al. "Expandable Fixation Assemblies". European pat.
       2451373A1. Synthes Gmbh. May 16, 2012.

[60]   P. R. Harrington. "Treatment of scoliosis. Correction and internal fixation by spine
       instrumentation". In: *The Journal of Bone and Joint Surgery. American Volume* 44-
       A (June 1962), pp. 591–610.

[61]   Toru Hasegawa et al. "Hydroxyapatite-coating of pedicle screws improves resis-
       tance against pull-out force in the osteoporotic canine lumbar spine model: a
       pilot study". In: *The Spine Journal* 5.3 (May 1, 2005), pp. 239–243. (Visited on
       04/26/2021).

[62]   John Riley Hawkins, Alexander Grinberg, and Michael Michielli. "Revisable Or-
       thopedic Anchor and Methods of Use". U.S. pat. 2016008033A1. Depuy Synthes
       Products Inc. Jan. 14, 2016.

[63]   Martin Hess and Fridolin J. Schlaepfer. "Screw". Pat. WO0032125A1. Hess Martin;
       Schlaepfer Fridolin J; Synthes Ag; Synthes Usa. June 8, 2000.

[64]   Rusell A. Hibbs. "An operation for Pott's disease of the spine". In: *Journal of
       the American Medical Association* 59.6 (Aug. 10, 1912), pp. 433–436. (Visited on
       03/16/2022).

[65]   Toru Hirano et al. "Structural characteristics of the pedicle and its role in screw
       stability". In: *Spine* 22.21 (1997), pp. 2504–2510.

[66]   Ibrahim Hussain et al. "Evolving Navigation, Robotics, and Augmented Reality in
       Minimally Invasive Spine Surgery". In: *Global Spine Journal* 10.2 (Apr. 1, 2020),
       22S–33S. (Visited on 12/01/2021).

[67]   Salah Huwais. "Implant/Anchor for Cellular and Visco-Elastic Materials". U.S.
       pat. 2015297275A1. Huwais Ip Holding Llc. Oct. 22, 2015.

[68]   *iFuse: The Triangle-Shaped Implant Designed Specifically for the SI Joint*. SI-
       BONE. (Visited on 10/20/2021).

[69]   Je Hoon Jeong, Jeremi M. Leasure, and Jon Park. "Assessment of Biomechanical
       Changes After Sacroiliac Joint Fusion by Application of the 3-Dimensional Mo-
       tion Analysis Technique". In: *World Neurosurgery* 117 (Sept. 2018), e538–e543.

[70]   Myoung Lae Jo et al. "Implant for Spine Fixation". Pat. KR20150066158A. Cg Bio
       Co Ltd; Univ Hallym Iacf. June 16, 2015.

2

[71]   Eun Mi Jung et al. "Pedicle Screw". Pat. KR101731421B1. Imi Co Ltd; Jung Eun Mi. May 4, 2017.

[72]   Mateusz Juszczyk, Alfons Kelnberger, and Heinrich Wecker. "Screw with an Elliptical Longitudinal and/or Cross Section". Pat. CA2923088A1. Ceramtec Gmbh. Mar. 12, 2015.

[73]   Steven Kahane et al. "Biomechanical Study Comparing Cut-out Resistance of the X-Bolt® and Dynamic Hip Screw at Various Tip-Apex Distances". In: *Surgical technology international* 35 (Nov. 1, 2019), pp. 395–401.

[74]   Kyoung Tae Kim. "Screw Anchor Assembly". European pat. 3254633A1. Kyungpook National Univ Industry-Academic Cooperation Foundation. Dec. 13, 2017.

[75]   Min Seok Kim. "Screw for Fixing Vertebra". Pat. WO2011025098A1. Kim Min Seok; L & K Biomed Co Ltd. Mar. 3, 2011.

[76]   Don King. "Internal fixation for lumbosacral fusion". In: *The American Journal of Surgery* 66.3 (Dec. 1, 1944), pp. 357–361. (Visited on 03/16/2022).

[77]   Kazuyoshi Kobayashi et al. "Epidemiological trends in spine surgery over 10 years in a multicenter database". In: *European Spine Journal* 27.8 (Aug. 1, 2018), pp. 1698–1703. (Visited on 12/01/2021).

[78]   Masahiro Kohketsu and Satoshi Ojima. "Anchor for fixing a screw in bone". British pat. 2301535A. Asahi Optical Co Ltd. Dec. 11, 1996.

[79]   Andrew C. Kohm and Arthur E. Ferdinand. "Apparatuses and Methods for Bone Screw Augmentation". Pat. WO2008121608A2. Kyphon Sarl; Kohm Andrew C; Ferdinand Arthur E. Oct. 9, 2008.

[80]   Victor Kosmopoulos and Constantin Schizas. "Pedicle Screw Placement Accuracy: A Meta-analysis". In: *Spine* 32.3 (Feb. 1, 2007), E111. (Visited on 09/16/2021).

[81]   Kuntz Kyle and Shyam Patel. "Implants for Tissue Fixation and Fusion". Pat. CA3063504A1. Cutting Edge Spine Llc. Nov. 15, 2018.

[82]   *Lateral Sacroiliac Joint Fusion - SIros™ 3D Printed*. (Visited on 10/20/2021).

[83]   M Law, A F Tencer, and P A Anderson. "Caudo-cephalad loading of pedicle screws: mechanisms of loosening and methods of augmentation". In: *Spine* 18.16 (Dec. 1, 1993), pp. 2438–2443. (Visited on 12/14/2021).

[84]   Bo Li et al. "Porous screw". Pat. CN109124748A. Beijing Xingmeng Information Tech Co Ltd. Jan. 4, 2019.

[85]   Derek P. Lindsey et al. "Evaluation of a minimally invasive procedure for sacroiliac joint fusion - an in vitro biomechanical analysis of initial and cycled properties". In: *Medical Devices (Auckland, N.Z.)* 7 (2014), pp. 131–137.

[86]   Derek P. Lindsey et al. "Sacroiliac Joint Fusion Minimally Affects Adjacent Lumbar Segment Motion: A Finite Element Study". In: *International Journal of Spine Surgery* 9 (2015), p. 64.

[87] Yun Liu and Dacheng Yang. "Spine screw". Pat. CN104840243A. Naton Medical Group; Tianjin Jinxingda Ind Co Ltd; Tianjin Zhengtian Medical Appliance Co Ltd. Aug. 19, 2015.

[88] Zongping Luo et al. "Combined-Type Perfusable Pedicle Screw System". Pat. WO2017197868A1. Wang Zhirong. Nov. 23, 2017.

[89] Gianluca Maestretti, Yves-Alain Ratron, and Jean-Francois Oglaza. "Expansible intravertebral implant system with posterior pedicle fixation". U.S. pat. 10603080B2. Vexim. Mar. 31, 2020.

[90] Amir M. Matityahu, Robert Trigg Mcclellan, and William H. Dillin. "Posterior Spinal Fastener". European pat. 2299921A1. Total Connect Spine Llc. Mar. 30, 2011.

[91] Matiz. *Mantiz: QUATTRO.* (accessed: 19.10.2021).

[92] Ross Mcdonald and Brian Thornes. "A Bolt Apparatus for Vertebral Fixation". Pat. WO2020178409A1. Sota Orthopaedics Ltd. Sept. 10, 2020.

[93] Robert N. Meek, Carly Anderson Thaler, and Steven Charles Dimmer. "Bone-Fixation Device and System". Pat. WO2020077457A1. Univ British Columbia. Apr. 23, 2020.

[94] David T. Mehl and Ali H. Mesiwala. "Bone screw implant for sacroiliac joint fusion". U.S. pat. 11045238B2. Life Spine Inc. June 29, 2021.

[95] Larry E. Miller, W. Carlton Reckling, and Jon E. Block. "Analysis of postmarket complaints database for the iFuse SI Joint Fusion System®: a minimally invasive treatment for degenerative sacroiliitis and sacroiliac joint disruption". In: *Medical Devices (Auckland, N.Z.)* 6 (2013), pp. 77–84.

[96] Jan U. Mueller et al. "Cement leakage in pedicle screw augmentation: a prospective analysis of 98 patients and 474 augmented pedicle screws". In: *Journal of Neurosurgery: Spine* 25.1 (July 2016), pp. 103–109.

[97] Gert Nijenbanning. "Medical Device for Treating Broken Bones or Fixing Stabilising Elements to Bone Parts". European pat. 1937172A1. Corpus Liberum B V; Baat Holding B V. July 2, 2008.

[98] V. Novák et al. "Minimally Invasive Sacroiliac Joint Stabilization". In: *Acta Chirurgiae Orthopaedicae Et Traumatologiae Cechoslovaca* 88.1 (Jan. 2021), pp. 35–38.

[99] F. O'Neill et al. "Influence of implant design on the method of failure for three implants designed for use in the treatment of intertrochanteric fractures: the dynamic hip screw (DHS), DHS blade and X-BOLT". In: *European Journal of Trauma and Emergency Surgery* 39.3 (June 1, 2013), pp. 249–255. (Visited on 12/09/2021).

[100] Acke Ohlin et al. "Complications after transpedicular stabilization of the spine. A survivorship analysis of 163 cases." In: *Spine* 19.24 (Dec. 1994), pp. 2774–2779.

[101] Jianqing Qian and Bing Zhou. "Pedicle screw capable of preventing angle loss". Pat. CN112043369A. Jiangsu Shuangyang Medical Instr Co Ltd. Dec. 8, 2020.

[102] Sean S. Rajaee et al. "Spinal Fusion in the United States: Analysis of Trends From 1998 to 2008". In: *Spine* 37.1 (Jan. 1, 2012), pp. 67–76. (Visited on 02/09/2021).

[103]   iData Research. *How Many Spinal Fusions are Performed Each Year in the United States?* iData Research. May 25, 2018. (Visited on 09/24/2021).

[104]   R. Roy-Camille et al. "Osteosynthesis of thoraco-lumbar spine fractures with metal plates screwed through the vertebral pedicles". In: *Reconstruction Surgery and Traumatology* 15 (1976), pp. 2–16.

[105]   Leonard Rudolf. "MIS Fusion of the SI Joint: Does Prior Lumbar Spinal Fusion Affect Patient Outcomes?" In: *The Open Orthopaedics Journal* 7 (2013), pp. 163–168.

[106]   Josh D. Saavoss, Lane Koenig, and Daniel J. Cher. "Productivity benefits of minimally invasive surgery in patients with chronic sacroiliac joint dysfunction". In: *ClinicoEconomics and outcomes research: CEOR* 8 (2016), pp. 77–85.

[107]   Donald Sachs and Robyn Capobianco. "Minimally invasive sacroiliac joint fusion: one-year outcomes in 40 patients". In: *Advances in Orthopedics* 2013 (2013), p. 536128.

[108]   Sean Saidha and Michael White. "Flexible Helical Fixation Device". Pat. WO2012121705A1. Synthes Usa Llc; Synthes Gmbh; Saidha Sean; White Michael. Sept. 13, 2012.

[109]   Bengt Sandén et al. "Improved extraction torque of hydroxyapatite-coated pedicle screws". In: *European spine journal* 9.6 (Dec. 2000), pp. 534–537.

[110]   Josh E. Schroeder et al. "Early results of sacro-iliac joint fixation following long fusion to the sacrum in adult spine deformity". In: *HSS journal: the musculoskeletal journal of Hospital for Special Surgery* 10.1 (Feb. 2014), pp. 30–35.

[111]   Zvi Schwartz et al. "Effect of Micrometer-Scale Roughness of the Surface of Ti6Al4V Pedicle Screws in Vitro and in Vivo". In: *The Journal of Bone and Joint Surgery. American volume.* 90.11 (Nov. 1, 2008), pp. 2485–2498. (Visited on 10/19/2021).

[112]   Wei Ren Daniel Seng et al. "Pedicle Screw Designs in Spinal Surgery: Is There a Difference? A Biomechanical Study on Primary and Revision Pull-Out Strength". In: *Spine* 44.3 (Feb. 1, 2019), E144. (Visited on 01/21/2022).

[113]   *SImpact®*. Life Spine. (Visited on 10/21/2021).

[114]   *Solid Screw Fixation by Pedicle Screw-Based ProMIS™ System Implants*. (Visited on 10/19/2021).

[115]   Giovanni F. Solitro et al. "Currently Adopted Criteria for Pedicle Screw Diameter Selection". In: *International Journal of Spine Surgery* 13.2 (Apr. 1, 2019), pp. 132–145. (Visited on 09/16/2021).

[116]   M. Stańczyk and B. van Rietbergen. "Thermal analysis of bone cement polymerisation at the cement–bone interface". In: *Journal of Biomechanics* 37.12 (Dec. 1, 2004), pp. 1803–1810. (Visited on 05/07/2021).

[117] Bengt Sturesson et al. "Six-month outcomes from a randomized controlled trial of minimally invasive SI joint fusion with triangular titanium implants vs conservative management". In: *European Spine Journal: Official Publication of the European Spine Society, the European Spinal Deformity Society, and the European Section of the Cervical Spine Research Society* 26.3 (Mar. 2017), pp. 708–719.

[118] Se-II Suk et al. "Thoracic Pedicle Screw Fixation in Spinal Deformities: Are They Really Safe?" In: *Spine* 26.18 (Sept. 15, 2001), pp. 2049–2057. (Visited on 12/09/2021).

[119] *Technology - SpineAlign Medical*. (Visited on 10/19/2021).

[120] Dale a Tempco et al. "Bone screw and method of manufacture". U.S. pat. 10993753B2. Warsaw Orthopedic Inc. May 4, 2021.

[121] *TheraCell: Technologies - Fiber Matrix Technology™ - Fiber Anchor™*. (Visited on 10/19/2021).

[122] Caroline P. Thirukumaran et al. "National Trends in the Surgical Management of Adult Lumbar Isthmic Spondylolisthesis: 1998 to 2011". In: *Spine* 41.6 (Mar. 15, 2016), pp. 490–501. (Visited on 12/01/2021).

[123] Zung Vu Tran, Anna Ivashchenko, and Logan Brooks. "Sacroiliac Joint Fusion Methodology - Minimally Invasive Compared to Screw-Type Surgeries: A Systematic Review and Meta-Analysis". In: *Pain Physician* 22.1 (Jan. 2019), pp. 29–40.

[124] Venkata Ramakrishna Tukkapuram, Abumi Kuniyoshi, and Manabu Ito. "A Review of the Historical Evolution, Biomechanical Advantage, Clinical Applications, and Safe Insertion Techniques of Cervical Pedicle Screw Fixation". In: *Spine Surgery and Related Research* 3.2 (Apr. 27, 2019), pp. 126–135. (Visited on 02/09/2021).

[125] Srilakshmi Vishnubhotla et al. "A titanium expandable pedicle screw improves initial pullout strength as compared with standard pedicle screws". In: *The Spine Journal* 11.8 (Aug. 1, 2011), pp. 777–781. (Visited on 05/18/2021).

[126] William Robert Walsh et al. "Critical Size Bone Defect Healing Using Collagen–Calcium Phosphate Bone Graft Materials". In: *PLOS ONE* 12.1 (Jan. 3, 2017), e0168883. (Visited on 12/09/2021).

[127] Haiqiang Wang et al. "Telescopic Double-Threaded Pull-Out Resistant Pedicle Screw Assembly for Medical Use". Pat. WO2016054951A1. Fourth Military Medical Univ. Apr. 14, 2016.

[128] Bernd Wegener et al. "Delayed perforation of the aorta by a thoracic pedicle screw". In: *European Spine Journal* 17.2 (Sept. 1, 2008), pp. 351–354. (Visited on 12/09/2021).

[129] Jau-Ching Wu et al. "Pedicle screw loosening in dynamic stabilization: incidence, risk, and outcome in 126 patients". In: *Neurosurgical Focus* 31.4 (Oct. 2011), E9.

[130] Zi-xiang Wu et al. "A comparative study on screw loosening in osteoporotic lumbar spine fusion between expandable and conventional pedicle screws". In: *Archives of Orthopaedic and Trauma Surgery* 132.4 (Apr. 1, 2012), pp. 471–476. (Visited on 05/06/2021).

[131] *X-Bolt | SPINE*. (Visited on 10/19/2021).

[132] Jin Sup Yeom et al. "Leakage of cement in percutaneous transpedicular vertebroplasty for painful osteoporotic compression fractures". In: *The Journal of bone and joint surgery. British volume* 85.1 (Jan. 2003), pp. 83–89.

[133] Hong Won Yoon and Kwang Hoon Lee. "Pedicle screw with quadruple screw thread". U.S. pat. 10512494B2. Mantiz Logtech Co Ltd. Dec. 24, 2019.

[134] Songyuan Zheng et al. "Spinal screw". Pat. CN112220545A. Tianjin Walkman Biomaterial Co Ltd. Jan. 15, 2021.

[135] Jianming Zhou. "Minimally-invasive hollow multi-side-pore pedicle screw". Pat. CN103815956A. Zhejiang Kangci Medical Technology Co Ltd. May 28, 2014.

[136] M R Zindrick et al. "A biomechanical study of intrapeduncular screw fixation in the lumbosacral spine". In: *Clinical orthopaedics and related research* 203 (Feb. 1, 1986), pp. 99–112.

2

3

DESIGN OF A CURVED BONE ANCHOR

Pedicle screws have long been established as the gold standard for spinal bone fixation. However, their fixation strength can be compromised in cases of low bone density, particularly in osteoporotic bone, due to the reliance on a micro-shape lock between the screw thread and the surrounding bone. To address this challenge, we propose augmenting conventional pedicles screws with a curved compliant anchor. This anchor integrates a curved super-elastic nitinol rod that is advanced through a cannulated pedicle screw, forming a macro-shape lock within the vertebral body to aid the fixation strength. Both placement safety and fixation strength of this novel spinal bone anchor were validated on tissue phantoms (Sawbones). The radius of the curved compliant anchor's path demonstrates high precision while exhibiting strong dependence on the bone density in which the anchor is placed. When the curved compliant anchor is combined with a conventional pedicle screw, the mean maximum pull-out force elevated to 290 N, marking a 14% enhancement in pull-out resistance compared to using a pedicle screw alone. Further augmentation with multiple curved compliant anchors holds promise for even greater fixation. The application of a curved compliant spinal bone anchor offers a promising means of increasing the fixation strength of pedicles screws, which is especially relevant in challenging clinical scenarios such a patient suffering from osteoporosis.

3.1. Introduction

3.1.1. Bone anchoring

Back issues, including conditions like herniated discs, spinal deformities, and spinal instability, often necessitate spinal fusion surgery. This orthopaedic intervention involves the fusion of multiple adjacent vertebrae into a single bony mass. Interbody fusion stands out as the most frequently performed type of spinal fusion surgery, with an annual occurrence of over 352.000 performed cases in the United States alone [25]. This number is expected to rise in the foreseeable future, as the prevalence of degenerative disorders rises due to an ageing population and advances in medical technology, which expand the number of eligible patients [18, 8, 14, 7, 28]. In line with these trends, the number of lumbar fusions for patients aged over 65 increased with 138% between 2004 and 2015 in the United States [18]. During spinal fusion surgery, the objective is to correct spinal deformities and to generate stability of the spine. In order to achieve this, a connection between adjacent vertebrae is constructed by introducing pedicle screws into the vertebrae and linking them with rods that traverse alongside the vertebrae (Figure 3.1). This rigid construct intends to eliminate any movement between the adjacent vertebrae, facilitating their fusion with the assistance of bone graft material. The success of spinal fusion surgery is highly dependent on the anchoring strength of the pedicle screw within the vertebra, as even minor movement between the vertebrae can hinder the desired fusion [33].

3.1.2. Problem Definition

While pedicle screws are considered the gold standard in spinal fusion surgery, their fixation may lack, leading to complications such as screw loosening, unsuccessful fusion, and the need for revision surgery. Understanding the vertebral anatomy is of importance in this context. Vertebrae comprise a dense and strong outer layer of cortical bone encasing porous cancellous bone. The main part of a positioned pedicle screw is surrounded by the porous cancellous bone. Only the small section of the screw within the pedicle engage with the cortical bone. Sometimes the distal tip of the screw is engaged in the anterior cortex of the vertebral body to enhance the contact area with the cortical bone. These two relatively small sections accounts for up to 85% of the screw's pull-out resistance, while the main part of the screw that is surrounded with the cancellous bone contributes only 15-20% of the pull-out resistance [30].

Pedicle screw loosening is a clinically relevant complication. Several studies have reported the prevalence, risk factors, and outcomes associated with screw loosening in spinal fusion surgery [9, 4, 24, 31]. These complications are of particular concern in patients with poor bone quality or challenging anatomical conditions, where traditional fixation methods may be insufficient. Screw loosening is more prevalent in patient suffering from osteoporosis [33, 6]. Osteoporosis is characterised by reduced bone density due to the degeneration of cancellous bone and thinning of the cortical bone layer within the pedicle [11]. Wu *et al.* [31] reported a 4.7% incidence of screw loosening in non-osteoporotic vertebra, while the meta-analysis conducted by Rometsch *et al.* [26] revealed a significantly higher average screw loosening incidence of 22.5% in osteoporotic vertebra.
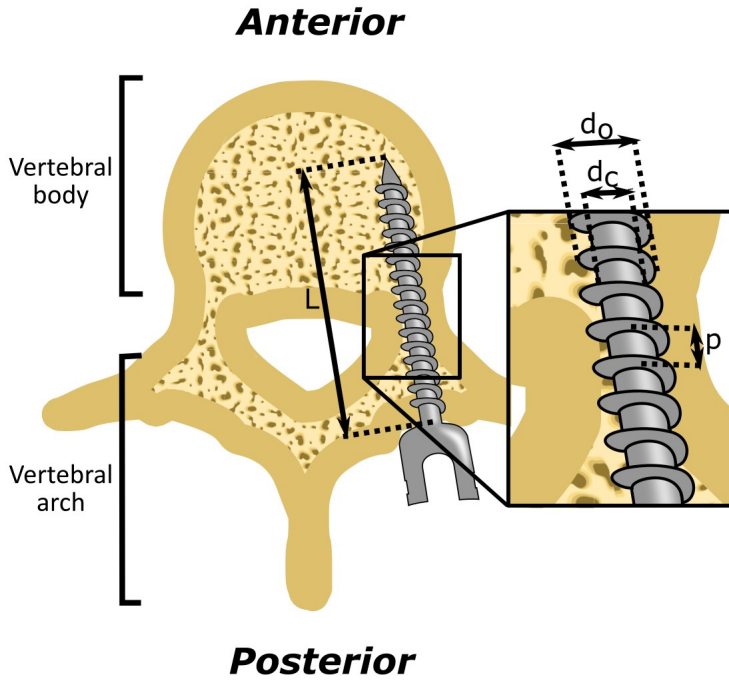
Figure 3.1: Vertebral fixation. The current golden standard uses pedicle screws with screw thread to create a fixation using micro shape-lock.

An important indicator of screw fixation strength within a homogeneous material is the Flank Overlap Area (FOA) [mm^2], representing the area of material captured by the screw thread. The FOA represents the area of interaction between the screw thread and the bone, which is critical for determining the anchoring strength of the screw. The FOA can be calculated using Equation 3.1 [15], with d_o the outer diameter of the screw [mm], d_c the core diameter of the screw [mm], L the shaft length of the screw [mm], and p the pitch of the screw thread [mm] (Figure 3.1).

$$FOA = \frac{1}{4}\pi(d_o{}^2 - d_c{}^2)\frac{L}{p} \tag{3.1}$$

The magnitude of the FOA is primarily influenced by the distance between the outer diameter of the screw and the core diameter of the screw. This distance determines the area of interface between the bone and the screw thread, thereby directly impacting the anchoring effectiveness of the screw. In spinal fusion surgery, the optimisation of the FOA is limited by the vertebra's size. Pedicle screws must conform to specific dimensions of the vertebra, including the pedicle and the vertebral body, to ensure proper placement. For instance, the screw should pass through the pedicle without breaching the cortical bone layer, limiting the outer diameter, and the screw length should be selected to avoid penetrating the anterior cortical wall. While reducing the screw's inner diameter has the potential to increase the FOA, it would come at the cost of weakening the

screw itself. Similarly, reducing the screw thread pitch may enhance the FOA for screws in a homogeneous material, but this principle does not apply to pedicle screws used in porous, non-homogeneous bone. A pitch smaller than the pore size of cancellous bone would hinder effective bone material capture between the threads, compromising screw fixation strength.

While the screw thread's micro-fixation mechanism performs well in homogeneous material such as dense cortical bone, it is not ideally suited for reliable fixation within porous cancellous bone. Achieving fixation in cancellous bone, particularly in patients suffering from osteoporosis, presents a considerable challenge due to the compromised bone quality, reducing the fixation strength of pedicle screws. This underscores the need to explore methods to establish secure fixation within cancellous bone.

3.1.3. STATE-OF-THE-ART: ANCHORING IN CANCELLOUS BONE

To increase the fixation strength of pedicle screws within the cancellous bone, ongoing research explores alternative anchoring methods [12]. Cement-augmented pedicle screws are frequently employed to enhance fixation strength in osteoporotic bone. These screws feature a central lumen through which cement, such as PolyMethylMethAcrylate (PMMA), is injected. The cement exits the screw via side channels at the distal tip, flowing into cancellous bone pores to create a firm shape lock. Consequently, load on the screw transfers to the vertebral bone via the cement, nearly doubling the pull-out strength as compared to conventional pedicle screws [33]. However, there are challenges associated with the use of cement-augmented screws. Heat generated during cement hardening can result in bone necrosis [27]. Additionally, cement leakage from the vertebra via cortical defects or veins may occur, and although this rarely results in clinical complications such as Pulmonary Embolisms (PE), the occurrence of asymptomatic cement leakage is high [22, 19, 32]. While the rates of asymptomatic cement leakage and asymptomatic PE are relatively high, it is important to note that the occurrence of clinical consequences is rare. This distinction underscores the generally low clinical risk associated with these findings despite their frequency. In the study of Mueller *et al.* [22], asymptomatic perivertebral cement leakage was observed in 93.6% of patients (88 patients) and 73.3% of augmented vertebrae (165 vertebrae), most frequently occurring in the perivertebral venous system, while clinically asymptomatic pulmonary cement embolism was noted in 4.1% of patients (4 patients). Martín-Fernández *et al.* [19] found that cement leakage was seen in 62.3% of vertebrae (650 vertebrae) with no major clinical complications, though 0.6% of patients (2 patients) experienced radicular pain, and 4.1% of patients (13 patients) developed deep infections requiring surgical debridement. However, it is important to note that the removal of screws, whether for the management of infection or for revision procedures (such as in cases of pseudarthrosis or adjacent segment disease), can be significantly complicated by the presence of cement augmentation. The cement's integration with the bone and its role in providing additional stability make these procedures more challenging and may increase the risk of damage to the surrounding bone and tissue [33, 19].

Another alternative anchoring method, outlined in patent literature but not yet clinically implemented, involves the utilization of curved anchors [13], see Figure 3.2. The curved path of such an anchor could enhance fixation strength by employing a macro

Rigid Curved Anchors

(a)   (b)

3

Multi-Segmented Anchors

(c)   (d)   (e)
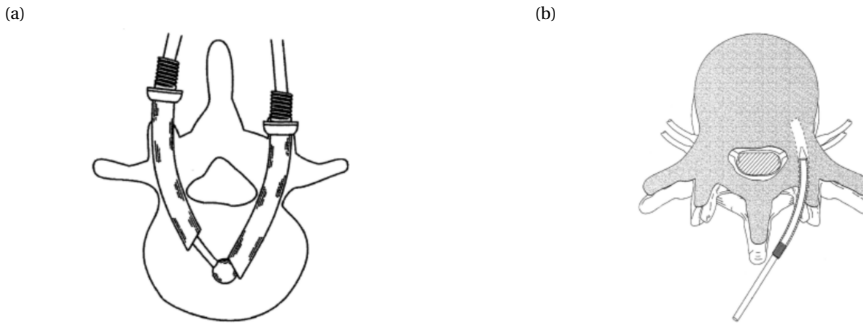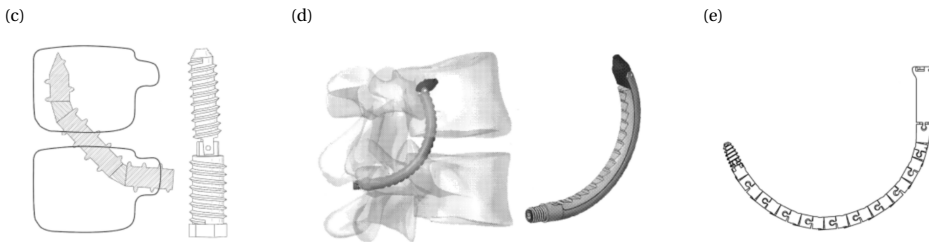
Figure 3.2: Alternative Anchoring Methods. Curved anchors are proposed in the patent literature. Rigid curved anchors consist of rigid pre-bend elements and are proposed by (a) Ben-Arye *et al.* [2] and (b) Matityahu *et al.* [20]. Multi-segmented anchors contain multiple segments that can move with respect to each other and are proposed by (c) Aghayev *et al.* [1], (d) Glerum *et al.* [10] and (e) Meek *et al.* [21]

shape-lock between the spinal bone anchor and the cancellous bone in the vertebral body. Rigid curved anchors, described by Ben-Arye *et al.* [2] and Matityahu *et al.* [20], can be placed in a pre-drilled curved tunnel. Unlike conventional pedicle screws, these anchors rely solely on macro-fixation within the vertebral body, omitting screw thread and thus the associated fixation strength. The patents by Aghayev *et al.* [1], Glerum *et al.* [10] and Meek *et al.* [21] propose anchors composed of separate segments capable of bending with respect to each other to create a curved macro-shape fixation. Utilising conventional joints or helical shapes with interlocking teeth facilitates the desired compliance of the anchor while maintaining segment connection. These compliant anchors assist in placement within the vertebra, and potentially enable the use of a macro-shape fixation in combination with the conventional pedicle screws. However, the use of joints weakens the anchor structure, posing a risk of implant failure under high loads acting on the bone anchors.

3.1.4. GOAL OF THIS STUDY
The objective of this study is to develop and evaluate a novel curved compliant bone anchor, intended as an additional means of fixation, that supplements the conventional
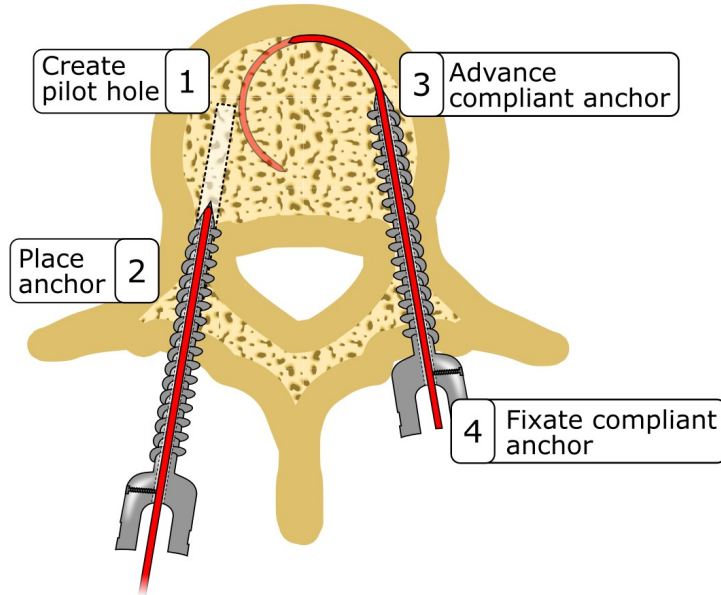
Figure 3.3: The curved compliant anchor combined with the currently used pedicle screws is placed in four steps: 1) Create the pilot hole, 2) place the anchor, 3) advance the curved compliant anchor and 4) fixate the curved compliant anchor.

pedicle screw and enhances fixation strength by establishing a macro-shape lock within the vertebral body. Our aim is to achieve this macro-shape lock using a compliant structure as to avoid the use of joints that may weaken the anchor.

3.2. Anchor Development

3.2.1. Proposed Solution

To enhance the fixation strength of conventional pedicle screws, we propose the incorporation of a curved compliant anchor that can be advanced through a cannulated pedicle screw, providing and additional mode of fixation alongside the conventional screw threads. Utilising an elastic material for the curved compliant anchor eliminates the need for intricate joints or structures, ensuring smooth advancement of the curved compliant anchor through the straight lumen of the cannulated pedicle screw (Figure 3.3). The curved compliant anchor features a sharp tip and is curved into a precise circular arch, facilitating its insertion through the cancellous bone.

The placement of our proposed curved compliant anchor similar to conventional pedicle screws, with two additional steps after pedicle screw placement. Initially, the entry point is determined, and a cortical wall opening is created. Subsequently, a straight tunnel is formed through the pedicle into the vertebral body. The cannulated pedicle screw containing the curved compliant anchor is screwed into the straight tunnel similarly to the placement of a conventional pedicle screw. Subsequently, the curved com-
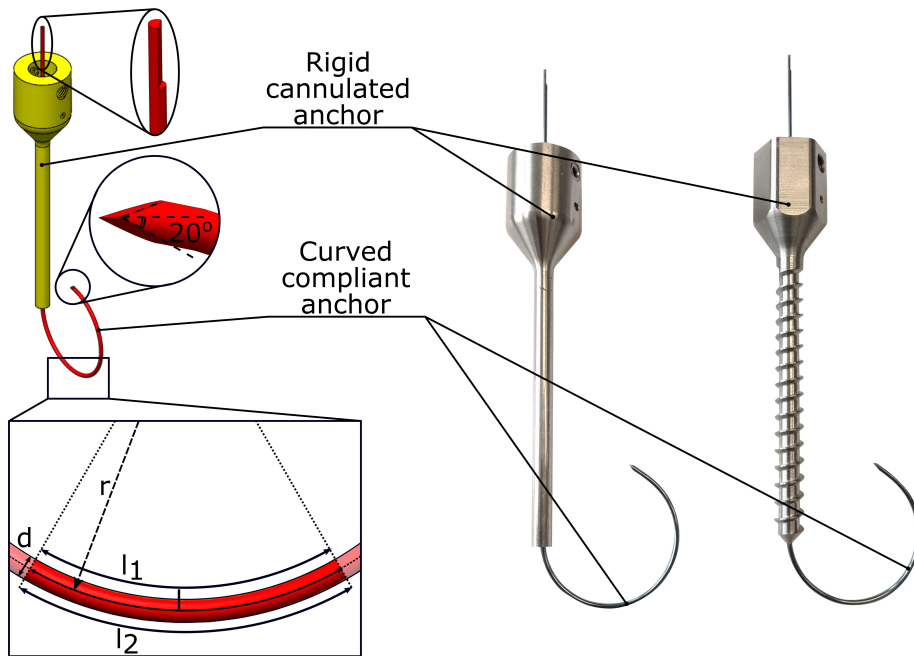
Figure 3.4: The curved compliant anchor combined with the currently used pedicle screws is placed in four steps: 1) Create the pilot hole, 2) place the anchor, 3) advance the curved compliant anchor and 4) fixate the curved compliant anchor.

pliant anchor is advanced through cannulated screw into the vertebral body, assuming its curved shape when exiting the cannulated pedicle screw. Once fully inserted into the vertebral body, the curved compliant anchor is secured to the pedicle screw using a bolt. This ensures that pulling forces exerted on the anchor are transferred to the bone through both the screw thread and the compliant anchor.

3.2.2. ANCHOR DESIGN
The curved compliant anchor is intended to complement currently clinically available pedicle screws. Therefore, the placement and fixation strength of the curved compliant anchor will be evaluated without and with considering the fixation strength of the pedicle screw thread. For this purpose, two rigid cannulated anchors were developed: one anchor without a screw thread, and one with a screw thread, both containing a central lumen ($\varnothing$ 1.5 mm) for the insertion of the curved compliant anchor (Figure 3.4). Given that advancing the curved complaint anchor through the straight lumen of the rigid cannulated anchor requires significant deformation of the curved compliant anchor, it demands the use of an elastic material to prevent plastic deformation.

Nitinol is renowned for its high elastic elongation of up to 8% without undergoing plastic deformation [29]. Additionally, nitinol is biocompatible which makes it suitable to use for long-term implementation, which is required for spinal fusion surgery. Therefore, nitinol presents an ideal material choice for the curved compliant anchor, allowing

for the necessary large deformations without compromising its integrity.

The minimal radius of the nitinol rod that can be straightened without experiencing plastic deformation can be computed using Equation 3.2, with R [mm] the minimal bending radius, d [mm] the diameter of the nitinol rod and ϵ [-] the allowable strain of the nitinol rod [29].

$$R = \frac{d}{2\epsilon} + \frac{d}{2} \tag{3.2}$$

Given that cannulated pedicle screws typically accommodate Kirschner-wires (K-wires) with a diameter of up to 1.5 mm, the curved compliant anchor is designed with a similar diameter of 1.25 mm. Utilising a super elastic nitinol rod with a diameter of 1.25 mm and an allowable strain of 0.08, yields in a minimal bending radius of approximately 8.5 mm. It was decided to use a nitinol rod with a pre-curved radius of 15 mm as this not only prevents plastic deformation but also reduces the force required to straighten the rod, while ensuring the curve fits within the vertebral body.

3.2.3. ANCHOR PROTOTYPING

The rigid cannulated anchors were manufactured from stainless steel using conventional machining techniques. The curved compliant anchor was made of a super elastic nitinol rod (Nitinol Device and Components, 1.25 mm, mechanically polished). To achieve the desired curvature, the nitinol rod was placed in a mold to ensure the desired curvature and, subsequently heated for a minimum of 20 minutes at $500^o C$. To facilitate smooth advancement of the curved compliant anchor through bone, the nitinol tip was sharpened with a bevel angle of 20°, similar to the tips of currently used K-wires [17, 16]. At the opposite end of the curved compliant anchor a flattened section was incorporated to enable the connection to a linear stage for controlled placement and alignment of the curvature of the compliant anchor within the vertebra.

The curved compliant anchor can, after advancement through the rigid cannulated anchor, be secured to the rigid cannulated anchor using a small bolt. The design of the rigid cannulated anchor is such that it can be effortlessly connected with two bolts to a pull-out testing machine especially designed to validate the fixation strength of the anchor.

3.3. ANCHOR PLACEMENT EXPERIMENT

3.3.1. EXPERIMENTAL GOAL

Accurate placement of a spinal bone anchor is crucial to prevent damage to surrounding anatomy. The compliant nature of the curved compliant anchor makes that the interaction forces between the cancellous bone and the curved compliant anchor could influence the anchor path during insertion. A higher bone density increases these interaction forces during advancement of the curved compliant anchor. Consequently, these forces may result in a deviation from the intended path. The aim of the Anchor Placement Experiment was therefore to investigate whether and how bone density affects the accuracy of placement of the curved compliant anchor.

3.3.2. EXPERIMENTAL VARIABLES

The independent variable in this experiment was the bone density. The effect of bone density on the placement accuracy of the curved compliant anchor was investigated by inserting the curved compliant anchor into three types of bone phantoms (SawBones) with compressive strengths of 5, 10 and 15 Pounds per Cubic Food (PCF), representing severe osteoporotic, osteoporotic and healthy bone, respectively [23].

The dependent variable was the anchor path radius. The radius of the circular path followed by the curved compliant anchor was measured and compared with the radius of the curved compliant anchor in free space (15 mm). The controlled variables in the experiment were the introduction velocity (1 mm/s) of the curved compliant anchor and the radius and length of the curved compliant anchor in free space (radius: 15 mm, length: 70 mm), which remain constant. Only the anchor without screw thread was tested in this experiment.

3.3.3. EXPERIMENTAL FACILITY

The experimental facility is depicted in Figure 3.5. The curved compliant anchor (red, nitinol), housed within the non-threaded rigid cannulated anchor (yellow, stainless steel), is connected to the linear stage using a connector (orange, brass). The connector anchor ensures accurate placement of the curved compliant anchor within the bone phantom (10 mm x 70 mm x 70 mm). To prevent buckling of the curved compliant anchor during advancement through the bone phantom, a rigid guide (green) and a spring (blue, Verenfabriek De Spiraal, $\varnothing_{outer}$ = 2 mm, $\varnothing_{wire}$ = 0.2 mm) were positioned around the proximal part of the curved compliant anchor.

3.3.4. EXPERIMENTAL PROTOCOL

Bone phantoms were prepared with a bandsaw, after which a cylindrical hole ($\varnothing$ 3 mm, length: 30 mm) was created using a drill press. The curved compliant anchor was inserted into the rigid cannulated anchor without screw thread, ensuring alignment of the distal tips of the concentric anchors. Subsequently, the concentric anchors were placed into the pre-made hole of the bone phantom. The spring was then positioned around the curved compliant anchor and the compliant anchor was attached to the linear stage via the connector. Subsequently, the rigid guide was pushed over the connector, the compliant anchor, and the spring.

At this stage, the linear stage was employed to advance the curved compliant anchor through the bone at a velocity of 1 mm/s over a distance of 70 mm, corresponding to the length of the curved section of the anchor (70 mm). Upon completion of the anchor placement, the bone phantom was filed down until the curved compliant anchor became visible. Subsequently, the curved compliant anchor was removed, leaving the tunnel through which the anchor passed visible for analysis. This test was performed three times in each bone density (5 PCF, 10 PCF and 15 PCF).

3.3.5. DATA ANALYSIS

After removal of the curved compliant anchors, the bone phantoms were scanned using a document scanner. Subsequently the scanned images were analysed using Matlab R2019b. Initially, a reference measurement was taken to establish the scale of the image
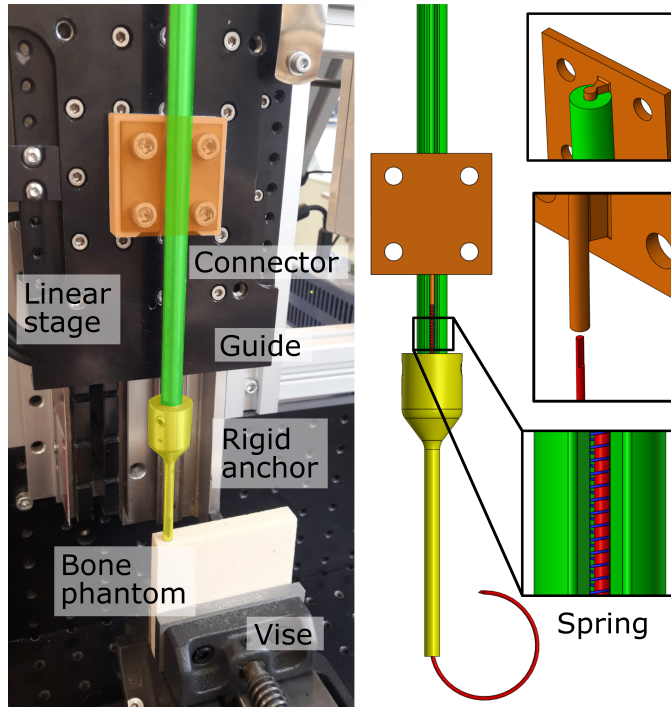
Figure 3.5: Experimental facility Placement Validation. A linear stage is used to advance the curved compliant anchor (red) through the non-threaded rigid cannulated anchor (yellow) and the bone phantom via the connector (orange). Buckling of the compliant anchor is prevented by the rigid guide (green) and a compression spring (blue).

accurately. Subsequently, the radius of the curved compliant anchor's path was determined by selecting 10 points alongside the circular arch of the anchor path with a mouse click. The radius of the curved compliant anchor was then constructed using the least square error method.

3.3.6. ANCHOR PLACEMENT RESULTS

The results of the experiment are presented in Figure 3.6. Figure 3.6a displays the radius of the curved compliant anchor in bone phantom material with a compressive strength of 5, 10 and 15 PCF, respectively. The radius of the complaint anchor was 15 mm in free space, 22.1 mm (SD ± 0.4 mm) in 5 PCF bone phantom, 29.0 mm (SD ± 0.8 mm) in 10 PCF bone phantom, and 35.8 mm (SD ± 0.2 mm) in 15 PCF bone phantom material. Figure 3.6b illustrates a boxplot of the radii of the curved compliant anchor in bone phantom material with a compressive strength of 5, 10, and 15 PCF. Due to the low number of repetitions, no formal statistical tests were performed. The purpose of these initial experiments was to provide a preliminary evaluation on the precision of the curved compliant anchor path in bone phantoms with different densities.

(a)

5 PCF

r = 22 mm   r = 22 mm   r = 22 mm

10 PCF

r = 28 mm   r = 30 mm   r = 29 mm

15 PCF

r = 36 mm   r = 36 mm   r = 36 mm

(b)
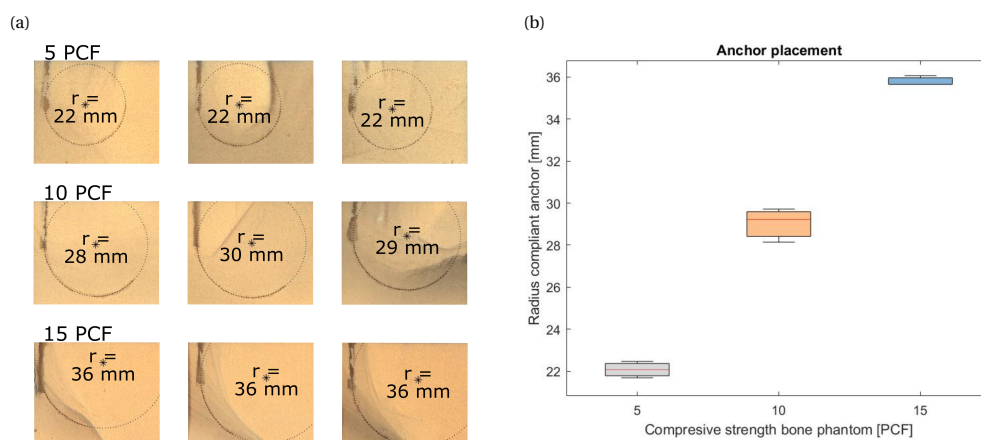
Figure 3.6: Results Placement Validation. (a) Cut through of the bone phantom showing the path of the curved compliant anchor and the corresponding radius. (b) Boxplot showing the radius of the curved compliant anchor for 5, 10 and 15 Pound per Cubic Foot (PCF) bone phantom.

3.4. ANCHOR FIXATION EXPERIMENT

3.4.1. EXPERIMENTAL GOAL

The objective of the Anchor Fixation Experiment was to investigate the fixation strength of the curved compliant anchor in bone phantom material. The preliminary aim was to assess the impact on pull-out resistance of the curved compliant anchor without the use of a screw thread. Subsequently, the impact on pull-out resistance of the curved compliant anchor in conjunction with a rigid cannulated anchor with screw thread was compared to the pull-out resistance of a stand-alone rigid cannulated anchor with screw thread.

3.4.2. EXPERIMENTAL VARIABLES

The independent variable in the Anchor Fixation Experiment was the anchor type. Pull-out tests were conducted using three different anchor configurations: 1) the curved compliant anchor with the non-threaded rigid cannulated anchor, 2) a stand-alone threaded rigid cannulated anchor, and 3) the curved compliant anchor in conjunction with the threaded rigid cannulated anchor.

The dependent variables were the initial pull-out force and the maximal pull-out force. The pull-out force is defined as the axial force exerted on the anchor and was measured using a force sensor (Futek, LCM300, 4448 N). The initial pull-out force refers to the amount of force required to begin the dislodgement or loosening of the screw from the bone, while the maximum pull-out force is the highest force needed to remove the screw entirely once loosening has commenced. Clinically, the initial pull-out force is the more relevant parameter, as it represents the threshold at which screw loosening starts, which is the primary concern in maintaining the stability of the fixation. Understanding

this distinction helps to focus on the factors that affect initial loosening, which is critical for ensuring successful outcomes in bone fixation procedures.

The controlled variable were the bone density (10 PCF, Sawbones), the pull-out velocity (3.5 mm/min), and the radius and length of the complaint anchor (radius: 15 mm, length: 70 mm). These variables remained constant throughout the experiment.

3.4.3. Experimental Facility

The experimental facility is illustrated in Figure 3.7. The facility allows for controlled extraction of the anchor from the bone phantom while continuously measuring the pull-out force using a force sensor (Futek, LCM300, 4448 N). The initial and maximum pull-out forces were measured using this mechanical experimental facility that simulated the *in-vitro* conditions for pedicle screw fixation. For the pull-out experiment, the bone phantom containing the pedicle screws, with and without the curved compliant anchors was positioned within the container, with the proximal end of the anchor connected to the slider. The extraction of the anchor from the bone phantom was facilitated by an electric motor (Modelcraft, RB 35, 1:600) equipped with a gear transmission (9:1), resulting in a translation speed of the slider of 3.5 mm/min. Subsequently, the screws were subjected to a continuous axial pull-out load at this constant displacement rate. Additionally, to determine the force required to initiate the extraction of the anchor, the facility was used to measure the relative displacement of the anchor with respect to bone using a linear potentiometer (Althen, 13FLP12A). The initial pull-out force was defined as the load corresponding to the initial relative displacement of the anchor with respect to the bone phantom. The maximum pull-out force was defined as the highest recorded force just before failure, characterised by a sudden drop in resistance or displacement of the screw.

3.4.4. Experimental Protocol

Bone phantoms (20 mm x 60 mm x 60 mm) were prepared with a bandsaw, after which a cylindrical hole ($\varnothing$ 3 mm, length: 30 mm) was created using a drill press. The bone phantoms were composed of material with a compressive strength of 10 PCF, representing osteoporotic bone. The rigid cannulated anchor was inserted into the bone phantom using the same method as employed in the Anchor Placement Experiment. A linear stage was utilised to advance the curved complaint anchor through the rigid cannulated anchor into the bone phantom at a velocity of 1 mm/s. Following the placement of the curved compliant anchor in the bone phantom, the curved compliant anchor was secured to the rigid cannulated anchor using a bolt (M 0.9). The bone phantom with the anchors was then positioned in the container of the experimental facility. The rigid cannulated anchor was connected to the slider using two bolts (M 2.5). The slider was then moved by the electric motor such that the linear potentiometer was fully retracted and in contact with the container and the shaft. The collected data were analysed using Matlab R2019b. To ensure consistency in data interpretation, the data were normalised such that the anchors started moving at t=0.
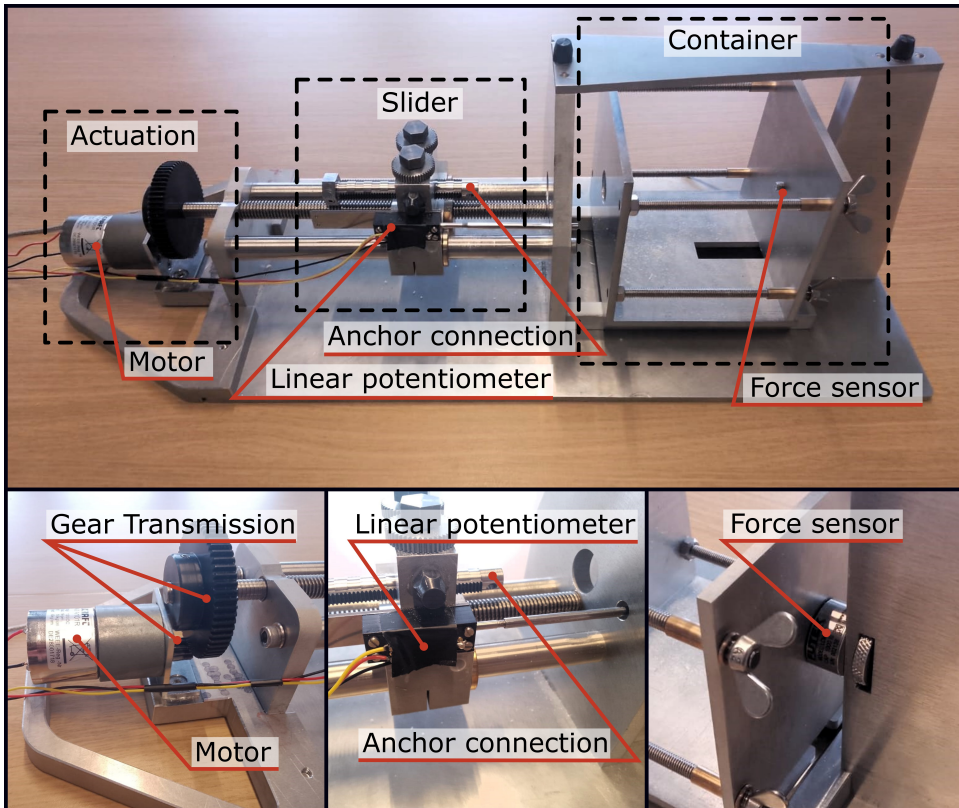
Figure 3.7: Experimental facility Anchor Fixation Validation including the actuation that pulls the anchor via the slider out of the bone that is placed within the container. The pull-force and displacement of the anchor with respect to the bone is measured by the force sensor and the linear potentiometer.

3.4.5. ANCHOR FIXATION RESULTS

The pull-out force of curved compliant anchor with the non-threaded rigid cannulated anchor, the stand-alone threaded rigid cannulated anchor, and the curved compliant anchor with the threaded rigid cannulated anchor is presented in Figure 3.8a. Figure 3.8b presents a boxplot representing the initial and maximum pull-out force of each anchor type. The mean initial pull-out force for the curved compliant anchor with the non-threaded rigid cannulated anchor, the stand-alone threaded rigid cannulated anchor, and the curved compliant anchor with the threaded rigid cannulated anchor is 20 N, 148 N and 157 N respectively. Additionally, the mean maximum pull-out force for the curved compliant anchor with the non-threaded rigid cannulated anchor, the stand-alone threaded rigid cannulated anchor, and the curved compliant anchor with the threaded rigid cannulated anchor is 30 N, 254 N, and 290 N respectively. The addition of a curved compliant anchor to the pedicle screw resulted in an average increase of 6% in initial pull-out resistance and a 14% increase in maximal pull-out force as compared to the stand-alone pedicle screw. Note that due to the low number of repetitions,

no formal statistical tests were performed. The purpose of these initial experiments was to provide a preliminary evaluation of the potential impact, in terms of pull-out force, of the curved compliant anchor.

3.5. Discussion

3.5.1. Main Findings

This study presents a novel design for a curved compliant bone anchor for use in conjunction with conventional cannulated pedicle screws. The anchor consists of a pre-curved compliant nitinol rod ($\varnothing$ 1.25 mm) with a radius of curvature of 15 mm and a length of 70 mm that is advanced through a rigid cannulated and threaded anchor. Placement of the combined compliant and threaded rigid cannulated anchor into the vertebra is similar to the placement of the conventional pedicle screw, with the addition of advancing the curved compliant anchor through the cannulated pedicle screw into the vertebral body after pedicle screw placement. Similarity in placement enables easy integration in the current practice of spinal fusion surgery.

Two experiments were performed to determine whether the curved compliant anchor allows for accurate placement and increases the pull-out force of current pedicle screws. In the Anchor Placement Experiment, the ability of the anchor to follow a predetermined path through cancellous bone was investigated. The radius of the complaint anchor's path was 22 mm in a severe osteoporotic bone phantom and 36 mm in a healthy bone phantom. It was found that although the path of the curved compliant anchor is dependent on the bone density, the anchor path showed a low variability (<1 mm) between samples with the same bone density. The use of pre-operative measurement of bone density, such as a Computed Tomography (CT)-scan or Dual-energy X-ray absorptiometry (DXA) [3] could be used to account for the influence of bone density of the radius of the curved compliant anchor's path. Alternatively, real-time sensing techniques such as Diffuse Reflectance Spectroscopy (DRS), could provide feedback to alert the clinician of potential cortical breaches during placement [5].

In the second experiment, the effect of the curved compliant anchor on the pull-out resistance was investigated. The curved compliant anchor in conjunction with the threaded rigid cannulated anchor fixation strength increased by up to 14% (maximum pull-out force: 290 N) compared to the threaded rigid cannulated anchor without the curved compliant anchor. Furthermore, it was seen that the initial pull-out force was increased with 6%, which can prevent early screw loosening. The wider range of initial pull-out force in the threaded rigid anchor group may be attributed to variations in the material properties of the phantom, such as density or composition, which impact the anchor's grip. These variations can lead to less consistent force measurements and instances where the initial pull-out force is higher without the compliant anchor.

In comparing the additional pull-out strength provided by the compliant anchor to that achieved with cement augmentation, it is important to note that while the increase (6% in initial pull-out resistance and 14% in maximum pull-out force) is modest, it represents a potentially meaningful improvement in scenarios where cement augmentation is not feasible or desired. This initial data suggests that the technology holds promise, but further refinements may be necessary to enhance its efficacy to levels that could

(a)

(b)
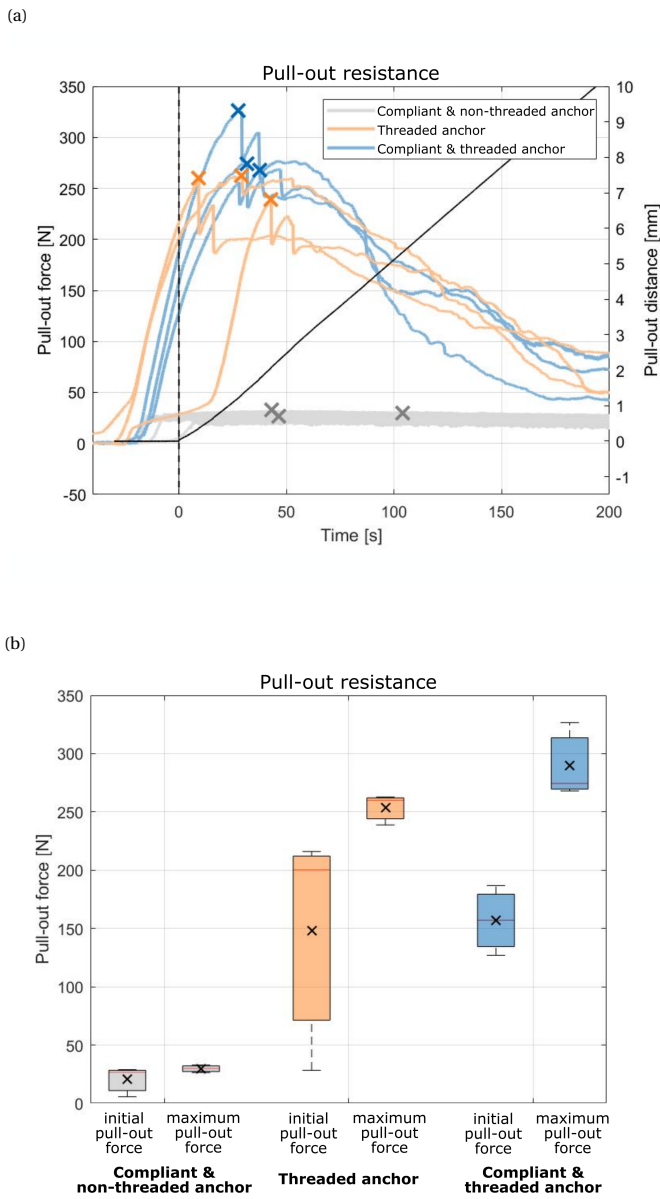
Figure 3.8: Pull-out force of the compliant anchor with the non-threaded rigid cannulated anchor, the stand-alone threaded rigid cannulated anchor, and the compliant anchor with the threaded rigid cannulated anchor. (a) Measured pull-out force of the different anchor types. Maximum pull-out force is indicated with an 'X'. (b) Boxplot showing the maximum pull-out force of the different anchor types. The mean pull-out force for each of the anchor types is indicated with the black 'X'

justify broader clinical adoption. Additionally, the potential benefits of using multiple compliant anchors should be considered, as incorporating several anchors could lead to a cumulative increase in pull-out resistance, potentially making the technology more competitive with existing solutions. Thus, while the current form of the compliant anchor shows potential, further development and evaluation are needed to determine its optimal use and effectiveness in clinical practice.

3.5.2. Limitations and Future Research

The validated curved compliant anchor is constructed from a super elastic nitinol with a diameter of 1.25 mm. A curved compliant anchor with a larger diameter is likely to increase the pull-out resistance further as this would increase the stiffness of the curved compliant anchor. However, plastic deformation of the curved compliant anchor when feeding it through the straight lumen of the rigid cannulated anchor must be avoided. This result in a maximum nitinol rod diameter of 2.2 mm using Equation 2 with an allowable strain of 0.08, and a curve radius of 15 mm. Using a larger rod diameter or a smaller curve radius also implies that a higher force is required to deform the curved compliant anchor such that is can be placed within the straight lumen of the rigid cannulated anchor and possibly that more force is required to advance the curved compliant anchor through the rigid cannulated anchor. Future research into the effects of rod diameter and curve radius on pull-out resistance seems an interesting step.

The curved compliant anchor allows for various placement orientations, potentially increasing fixation strength by expanding contact with the vertebra (Figure 3.9). While our findings indicate low variability in the radius of the anchor's path within samples of the same bone density, we acknowledge that the actual direction of this path remains unpredictable, which presents several clinical challenges. A potential concern with the use of curved compliant anchors is the risk of migration into the ventral prevertebral space, which could result in injury to surrounding tissue including nervous tissue and vascular tissue. To address these challenges, a redesign of the screw head could allow for precise control of the anchor's insertion direction and depth. Pre-operative selection of the anchor path, considering both bone density and vertebral size, will be essential. Furthermore, the use of advanced surgical navigation systems and real-time monitoring during anchor deployment could provide continuous feedback to the surgeon, helping to avoid unintended anchor migration.

Not all vertebrae may accommodate the current anchor paths, and smaller radii should be explored to enable use in a broader range of vertebrae. Relocating the anchor's exit point midway along the pedicle screw body could also allow for bicortical purchase, as well as offer higher versatility in anchor placement, potentially increasing pull-out strength. Nonetheless, the potential for the anchor to traverse the disc space or exit the vertebral body raises significant safety concerns, as these scenarios could cause damage to adjacent segments, interfere with interbody fusion procedures, or even result in injury to surrounding structures. While the outer cortical bone may limit the anchor's path, further investigation is needed to ensure this assumption is valid and that the technology can be safely implemented.

While this study focused on pull-out resistance as a measure of fixation strength, future research should explore the impact of curved anchors on alternative load cases
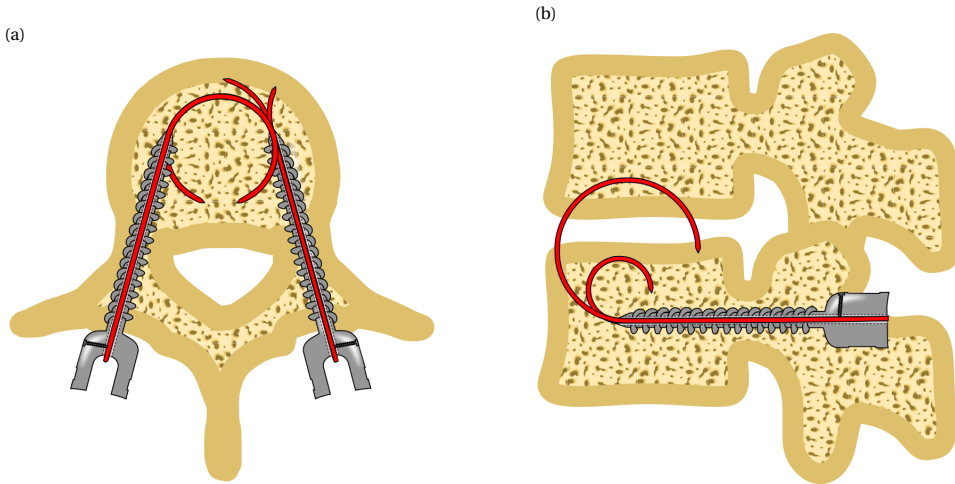
Figure 3.9: Alternative anchor designs using a compliant pre-curved anchor. (a) The use of multiple pre-curved anchors could further increase the fixation strength. (b) Anchor paths through the cortical bone layer allows for a fixation that spans multiple vertebrae The use of multiple pre-curved anchors could further increase the fixation strength.

as well as cyclic load cases that may result in toggling of the anchor. Toggling resistance is crucial in preventing pedicle screw loosening as the pivoting motion of bone anchors is known to compromise the fixations strength [14]. Investigating alternative and cyclic load cases would provide a more comprehensive understanding of the anchor's stability and resistance to loosening under various loading conditions.

The presented curved compliant anchor was designed as a spinal bone anchor in conjunction with a cannulated pedicle screw. We acknowledge that the integration of the nitinol anchor with the standard pedicle screw head does not allow for rod placement in its current form. To address this, the screw head needs to be redesigned to accommodate the nitinol anchor deeper inside the pedicle screw, which will ensure sufficient space for rod placement. This adjustment will facilitate easy integration of the anchor into the current practice of spinal fusion surgery, making it a viable option for clinical use. Additionally, the curved compliant anchor bears resemblance to the K-wires used in orthopaedic procedures for fixating bone fragments. Curved compliant anchors could, therefore, potential be used as an alternative for K-wires for increased fixation strength. Besides increased fixation, curved compliant K-wires could also be used to follow the shape of more organically shaped bones, such as the pelvis, to prevent protrusion out of the bone such that damage to surrounding tissue is limited.

The experiments performed in this study were conducted using SawBones Solid Foam bone phantom material with mechanical properties similar to human bone [23]. However, its homogeneity and closed cell structure may not fully replicate the complexity of real human bone, potentially influencing anchor behaviour. We acknowledge that bone density is likely to influence the performance of the curved anchors, with more

osteoporotic bone potentially reducing the pull-out force, and recommend further experiments using bone phantoms with varying densities to better understand this effect. Furthermore, solely the interaction of the curved anchor within cancellous bone were investigated, neglecting the impact of the cortical bone layer. Future research should consider investigating the influence of the cortical bone layer on anchor performance. Therefore, further *ex-vivo* and *in-vivo* experiments are warranted to validate the performance of the curved anchor in more realistic bone environments. Additionally, we recognise that future studies will require a larger sample size and appropriate statistical analysis to determine the statistical significance of these findings and to validate the observed trends.

3.6. CONCLUSION

The curved compliant spinal bone anchor introduced in this study featured a compliant nitinol curved rod capable of being advanced through a cannulated pedicle screw. The trajectory of the curved compliant anchor proved highly predictable, even though the path is dependent on the bone density. When utilized independently, the curved compliant anchor exhibited a pull-out resistance of 30 N. Using the curved compliant anchor combined with a threaded rigid cannulated anchor, the mean pull-out resistance increased substantially to 290 N, marking a 14% enhancement in pull-out resistance compared to the threaded rigid cannulated anchor without the curved compliant anchor. Employing multiple curved compliant anchors and exploring alternative paths could further augment the pull-out resistance of pedicle screws. The curved compliant bone anchor evaluated in the present study represents a first step towards enhancing the fixation strength of bone screws in a variety of orthopaedic procedures, including spinal fusion surgery.

BIBLIOGRAPHY

[1]   Kamran Aghayev et al. "Transdiscal screw". U.S. pat. 10314631B2. H Lee Moffitt Cancer Ct & Res. June 11, 2019.

[2]   Asaf Ben-Arye, Arnon Epstein, and Yuval Shezifi. "Bone Anchoring System". U.S. pat. 2010305700A1. Ben-Arye Asaf; Epstein Arnon; Scorpion Surgical Technologies Ltd; Shezifi Yuval. Dec. 2, 2010.

[3]   Josephine Berger-Groch et al. "Determination of bone density in patients with sacral fractures via CT scan". In: *Orthopaedics & Traumatology: Surgery & Research* 104.7 (2018), pp. 1037–1041.

[4]   Andrey Bokov et al. "Pedicle screws loosening in patients with degenerative diseases of the lumbar spine: potential risk factors and relative contribution". In: *Global spine journal* 9.1 (2019), pp. 55–61.

[5]   Gustav Burström et al. "Diffuse reflectance spectroscopy accurately identifies the pre-cortical zone to avoid impending pedicle screw breach in spinal fixation surgery". In: *Biomedical Optics Express* 10.11 (Oct. 24, 2019), pp. 5905–5920. (Visited on 09/16/2021).

[6]   Daniel J. Burval et al. "Primary Pedicle Screw Augmentation in Osteoporotic Lumbar Vertebrae: Biomechanical Analysis of Pedicle Fixation Strength". In: *Spine* 32.10 (May 1, 2007), pp. 1077–1083. (Visited on 06/04/2021).

[7]   Paolo A. Cortesi et al. "Epidemiologic and Economic Burden Attributable to First Spinal Fusion Surgery: Analysis From an Italian Administrative Database". In: *Spine* 42.18 (Sept. 15, 2017), pp. 1398–1404. (Visited on 12/01/2021).

[8]   John A. Cowan Jr. et al. "Changes in utilization of spinal fusion in the united states". In: *Neurosurgery* 59.1 (July 1, 2006), pp. 15–20. (Visited on 04/23/2021).

[9]   Fabio Galbusera et al. "Pedicle screw loosening: a clinically relevant complication?" In: *European spine journal* 24 (2015), pp. 1005–1016.

[10] Chad Glerum et al. "Pedicle-Based Intradiscal Fixation Devices and Methods". U.S. pat. 2021307924A1. Globus Medical Inc. Oct. 7, 2021.

[11] Toru Hirano et al. "Structural characteristics of the pedicle and its role in screw stability". In: *Spine* 22.21 (1997), pp. 2504–2510.

[12] Haruo Kanno et al. "Innovation of surgical techniques for screw fixation in patients with osteoporotic spine". In: *Journal of Clinical Medicine* 11.9 (2022), p. 2577.

[13] Esther P. de Kater et al. "Beyond the pedicle screw–a patent review". In: *European Spine Journal* 31.6 (June 1, 2022), pp. 1553–1565. (Visited on 12/06/2022).

[14] Kazuyoshi Kobayashi et al. "Epidemiological trends in spine surgery over 10 years in a multicenter database". In: *European Spine Journal* 27.8 (Aug. 1, 2018), pp. 1698–1703. (Visited on 12/01/2021).

[15] Michael Hannes Krenn et al. "Influence of thread design on pedicle screw fixation". In: *Journal of Neurosurgery: Spine* 9.1 (2008), pp. 90–95.

[16] Yao Liu et al. "Notched K-wire for low thermal damage bone drilling". In: *Medical Engineering & Physics* 45 (2017), pp. 25–33.

[17] Yuanqiang Luo, Lei Chen, and Albert J Shih. "Hollow notched K-wires for bone drilling with through-tool cooling". In: *Journal of Orthopaedic Research®* 37.11 (2019), pp. 2297–2306.

[18] Brook I Martin et al. "Trends in lumbar fusion procedure rates and associated hospital costs for degenerative spinal diseases in the United States, 2004 to 2015". In: *Spine* 44.5 (2019), pp. 369–376.

[19] M Martín-Fernández et al. "Potential risks of using cement-augmented screws for spinal fusion in patients with low bone quality". In: *The Spine Journal* 17.8 (2017), pp. 1192–1199.

[20] Amir M. Matityahu, Robert Trigg Mcclellan, and William H. Dillin. "Posterior Spinal Fastener". European pat. 2299921A1. Total Connect Spine Llc. Mar. 30, 2011.

[21] Robert N. Meek, Carly Anderson Thaler, and Steven Charles Dimmer. "Bone-Fixation Device and System". Pat. WO2020077457A1. Univ British Columbia. Apr. 23, 2020.

[22] Jan U. Mueller et al. "Cement leakage in pedicle screw augmentation: a prospective analysis of 98 patients and 474 augmented pedicle screws". In: *Journal of Neurosurgery: Spine* 25.1 (July 2016), pp. 103–109.

[23] Srinidhi Nagaraja and Vivek Palepu. "Comparisons of Anterior Plate Screw Pullout Strength Between Polyurethane Foams and Thoracolumbar Cadaveric Vertebrae". In: *Journal of Biomechanical Engineering* 138.10 (Oct. 1, 2016), p. 104505. (Visited on 01/04/2022).

[24] Tetsuro Ohba et al. "Risk factors for clinically relevant loosening of percutaneous pedicle screws". In: *Spine Surgery and Related Research* 3.1 (2019), pp. 79–85.

[25] iData Research. *How Many Spinal Fusions are Performed Each Year in the United States?* iData Research. May 25, 2018. (Visited on 09/24/2021).

[26] Elke Rometsch et al. "Screw-related complications after instrumentation of the osteoporotic spine: a systematic literature review with meta-analysis". In: *Global spine journal* 10.1 (2020), pp. 69–88.

[27] M. Stańczyk and B. van Rietbergen. "Thermal analysis of bone cement polymerisation at the cement–bone interface". In: *Journal of Biomechanics* 37.12 (Dec. 1, 2004), pp. 1803–1810. (Visited on 05/07/2021).

[28] Caroline P. Thirukumaran et al. "National Trends in the Surgical Management of Adult Lumbar Isthmic Spondylolisthesis: 1998 to 2011". In: *Spine* 41.6 (Mar. 15, 2016), pp. 490–501. (Visited on 12/01/2021).

[29] Robert J Webster, Allison M Okamura, and Nah J Cowan. "Toward active cannulas: Miniature snake-like surgical robots". In: *2006 IEEE/RSJ international conference on intelligent robots and systems*. IEEE. 2006, pp. 2857–2863.

[30] James N. Weinstein, Bjorn L. Rydevik, and Wolfgang Rauschning. "Anatomic and Technical Considerations of Pedicle Screw Fixation:" in: *Clinical Orthopaedics and Related Research* &NA;284 (Nov. 1992), pp. 34–46. (Visited on 12/17/2021).

[31] Jau-Ching Wu et al. "Pedicle screw loosening in dynamic stabilization: incidence, risk, and outcome in 126 patients". In: *Neurosurgical Focus* 31.4 (Oct. 2011), E9.

[32] Jin Sup Yeom et al. "Leakage of cement in percutaneous transpedicular vertebroplasty for painful osteoporotic compression fractures". In: *The Journal of bone and joint surgery. British volume* 85.1 (Jan. 2003), pp. 83–89.

[33] M R Zindrick et al. "A biomechanical study of intrapeduncular screw fixation in the lumbosacral spine". In: *Clinical orthopaedics and related research* 203 (Feb. 1, 1986), pp. 99–112.

3

DESIGN OF A TOGGLING RESISTANT BONE ANCHOR

4

Loosening of pedicle screws after spinal fusion surgery can prevent the desired fusion between vertebrae and may be a reason for revision surgery. Especially in osteoporotic bone, toggling of pedicle screws is a common problem that compromises the fixation strength of these screws and can lead to loosening or axial pull-out of the screw. In this study, we explore the use of an in-pedicle expandable anchor that shapes to the pedicle to increase the toggling resistance of the anchor by increasing the contact area between the anchor and the dense cortical bone of the pedicle. A scaled-up, two-dimensional prototype was designed. The prototype consists of a bolt and ten stainless steel wedges that expand by tensioning the bolt. During the expansion, the wedges are required to compress the cancellous bone. Based on the first preliminary experiment, it was found that the expansion of the wedges resulted in successful compression of 5 PCF cancellous bone phantom (Sawbones). This preliminary study shows that an expandable in-pedicle anchor could be a feasible option to increase the toggling resistance of spinal bone anchors, especially in osteoporotic bone.

4.1. Introduction

4.1.1. Pedicle Screw Fixation

Spinal fusion surgery is commonly performed to restore stability to the spine in case of deformity, fractures or pain. During spinal fusion surgery, two or more adjacent vertebrae are fused by eliminating all motion between the vertebrae using pedicle screws and rods. The strength of the construct and thus the success rate of spinal fusion surgery relies on the purchase of the screw in the vertebra [14]. Vertebrae have a shell of dense cortical bone that surrounds the porous cancellous bone. Each vertebra has two pedicles that connect the vertebral arch to the vertebral body (Figure 4.1). The pedicle has an hourglass shape with a smaller cross-section in the middle of the pedicle and a larger cross-section more anterior and posterior.

Pedicle screws are placed through the pedicle into the vertebral body. A larger screw diameter increases the fixation strength as it increases the contact surface between the screw and the dense cortical bone. The pedicle is surrounded by delicate anatomical structures such as the spinal cord and spinal nerve roots [10]. To avoid damage to these structures, it is advised to use a screw with a diameter of 80% of the diameter of the pedicle at the most narrow location [7]. The limited diameter of the screw and the hourglass shape of the pedicle result in limited contact between the screw and the dense cortical bone layer. This contact is even more limited due to the oval cross-section of the pedicle.

The fixation strength of pedicle screws is often indicated by the screw's pull-out strength which is the force necessary to axially pull the screw from the vertebra. The pull-out strength relies for 60% on the fixation of the screw in the pedicle as this is the location where the screw has purchase in the dense cortical bone layer [14, 10]. The pull-out strength can be compromised due to small rotations of the screw around the pivoting point, which is known as toggling [1]. Toggling is caused by a cyclic loading that is exerted on the screw, for instance during walking or bending of the back, and is especially a problem in caudocephalad (from tail to head) direction, due to the oval cross-section of the pedicle. A toggling force $F_{toggling}$ of 200 N applied on a single pedicle screw placed in a vertebra that is not connected to a rod, can result in a large toggling displacement of 8 mm [4]. During toggling the cancellous bone that surrounds the screw is compressed which compromises the fixation strength of the screw [14, 4].

Due to the ageing of the population, more patients undergoing spinal fusion surgery suffer from osteoporosis. Osteoporosis is characterized by the resorption of mainly the porous cancellous bone. This decrease in bone density of the cancellous bone decreases the provided resistance to toggling and compromises the fixation strength [14, 11].

4.1.2. State-of-the-Art: Spinal Bone Anchors

The success rate of spinal fusion surgery could be improved by using spinal bone anchors that have an improved fixation strength compared to the conventional pedicle screw, especially in osteoporotic bone. Different methods have been developed to improve the fixation strength of pedicle screws in osteoporotic bone. The use of cement augmented screws can almost double the pull-out strength [14] but has as a drawback the heat generation during curing of the cement which can result in bone necrosis [8]. Furthermore, leaking of cement out of the vertebral body, via veins or cortical defects,
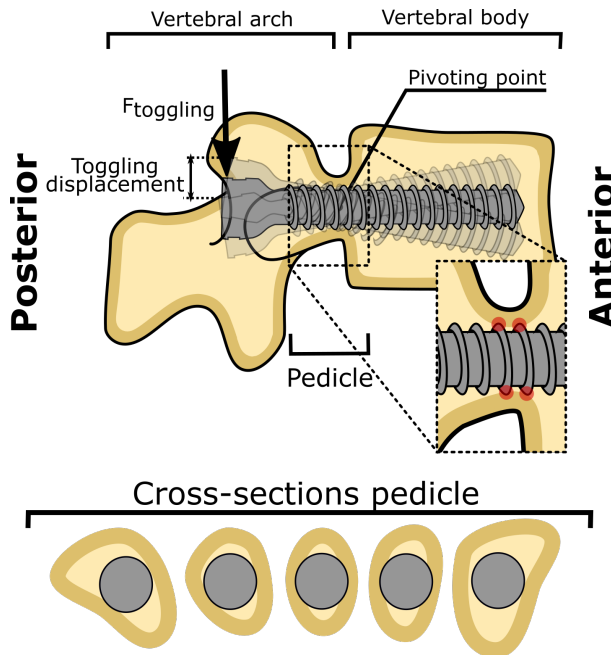
Figure 4.1: Schematic representation of pedicle screw toggling. The toggling force ($F_{toggling}$), results in a pivoting motion of the screw around the pivoting point causing compression of the cancellous bone and compromising the fixation strength. The oval cross sections of the pedicle show the hourglass shape of the pedicle. The red dots indicate the contact points between the pedicle screw and the cortical bone layer of the pedicle.

often occurs and can, in rare cases, result in serious complications such as pulmonary embolisms [13]. Lastly, cement augmented anchors are difficult to remove which can be required during revision surgery. During removal of the cement augmented anchor, the vertebra is often damaged [14].

A second means to increase the fixation of spinal bone anchors is the use of a bone ingrowth inducing coating such as hydroxyapatite. Such a coating can successfully increase the fixation strength but as a drawback, also makes it more challenging to remove the anchor in case of a revision surgery [2, 6].

In patent and scientific literature, expandable anchors are also proposed as a solution to increase the fixation strength of bone anchors. The anchors often have an expandable distal tip that anchors inside the vertebral body by creating a shape-lock which significantly increases the fixation strength [12, 9]. This explored method to increase the fixation strength of spinal bone anchors relies on increasing the fixation within the cancellous bone of the vertebral body. Although the contact area between the screw and the cortical bone layer is slim due to the cylinder shape of the screw and the oval and hourglass shape of the pedicle, the pedicle accounts for 60% of the pull-out resistance and 80% of the toggling resistance [3]. The increase in the contact area between the cortical bone and the bone anchor in the pedicle could, therefore, be more beneficial than an expandable section within the cancellous bone of the vertebral body. In osteoporotic
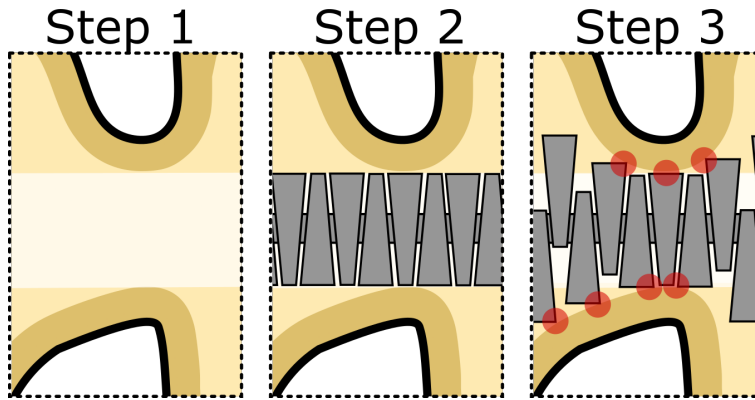
Figure 4.2: Schematic visualisation of the working principle of the in-pedicle expandable anchor. The first step is to make a tunnel through the pedicle (step 1) after which the anchor is placed in the collapsed state (step 2). After correct placement. The anchor can expand (step 3). The expansion results in multiple contact points between the anchor and the cortical bone layer (indicated with red dots).

patients, the advantage of increasing the fixation strength by increasing the contact area with the cortical bone could be even greater, as the cortical bone layer is often less compromised than the cancellous bone [11].

4.1.3. RESEARCH GOAL

To ensure a long-term fixation of the screw within the vertebra, toggling of spinal bone anchors should be avoided. The goal of this study is to design an in-pedicle expandable anchor to increase the toggling resistance by increasing the contact area between the anchor and the cortical bone layer of the pedicle.

4.2. METHOD

4.2.1. DESIGN DIRECTION

The in-pedicle anchor should deform to the pedicle to increase the toggling resistance, which will be achieved by expansion. The current bone anchors use screw thread for fixation in the vertebra. This requires the anchors to have a circular cross-section in order to screw the anchor into the vertebra. Since the proposed in-pedicle anchor uses expansion to fixate within the vertebra, the screw thread is not required and thus is the anchor not limited to having a circular cross-section. Designing the anchor with an oval cross-section, similar to the cross-section of the pedicle, increases the contact between the anchor and the cortical bone layer. This in combination with expansion in the caudo-cephalad direction could make the anchor more resistant to toggling as toggling is most severe in this direction.

We expect that, in clinical use, a tunnel is made through the pedicle before the in-pedicle bone anchor is placed. The anchor is placed in the collapsed state and once in the correct position, the anchor can expand to deform to the cortical bone layer of the pedicle (Figure 4.2).

(a)

(b)
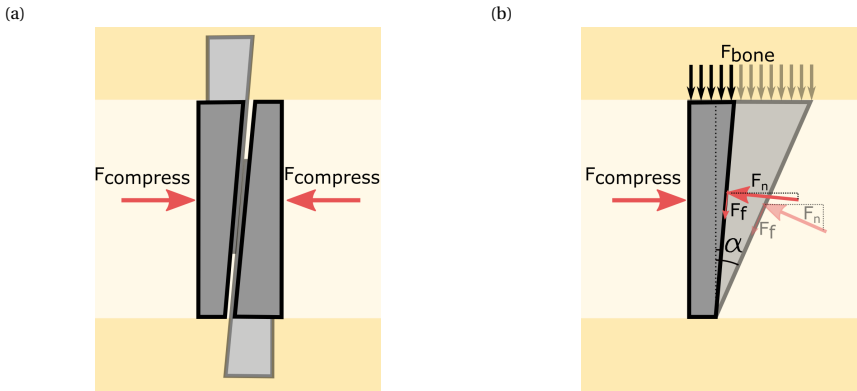
Figure 4.3: Wedge principle. (a) A compressive force $F_{compress}$ results in expansion of the wedges. (b) Free body diagram of the forces acting on a single wedge during expansion. The compressive force results in a normal force F_n which is dependent on the inclination angle α, and friction forces F_f When the wedges expand the wedge will compress the cancellous bone by overcoming F_{bone}.

The proposed in-pedicle bone anchor consists of ten wedges with one bolt through the centre. Tightening the bolt presses the wedges together and, due to the slanted edges, causes the wedges to expand (Figure 4.3a). The idea is that the resistance of the cancellous bone is slim and will thus not prevent the expansion of the wedges. The much denser cortical bone wall is expected to prevent further expansion upon impact. This way the anchor will deform to the cortical bone layer of the pedicle and increase the number of contact points with the cortical bone layer, making the anchor more toggling resistant compared to the conventional pedicle screw.

4.2.2. EXPANSION WORKING PRINCIPLE

Wedges have an inclined side that can be used to convert a force. In this design, a compressive force will result in an angulated normal force which will cause the wedge to expand (Figure 4.3b). Besides the normal force that is generated, friction forces will be induced. These friction forces will oppose the expansion and are highly dependent on the friction coefficient between the two wedges. The wedges of the prototype are intended to expand within the pedicle. This requires the wedges not only to overcome the friction force between the wedges but also to exert enough force to compress the cancellous bone. Wedges with a larger inclination (larger angle α) require a smaller compression force to obtain the desired expansion, which is advantageous. However, the larger the inclination, the wider the wedges will become, and thus the more cancellous bone must be compressed to allow the wedges to expand. This will increase the forces opposing the expansion. Besides this, the pedicle has a limited length, thus an increasing width of the wedges would also decrease the number of wedges that fit within the pedicle and thus result in fewer contact points between the anchor and the cortical bone layer of the pedicle. Therefore, a smaller inclination is beneficial as long as the inclination is large enough to allow the wedges to expand when exerting a limited compressive force.
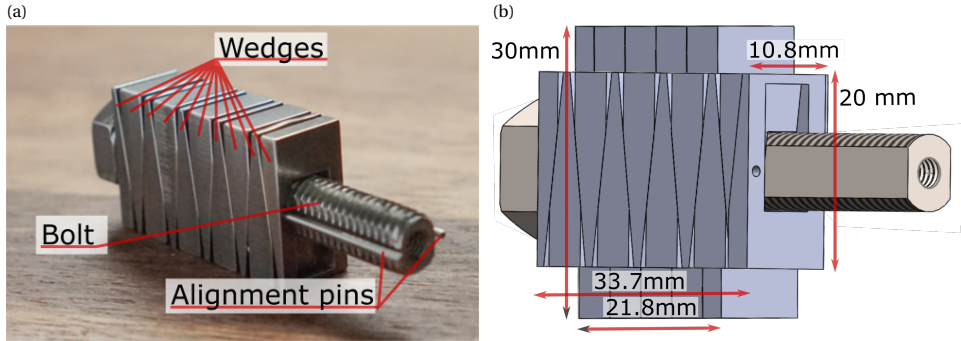
Figure 4.4: Prototype design. (a) Photograph of the prototype consisting of ten wedges, a bolt that runs through the centre and two alignment pins. (b) Dimensions of the prototype in the collapsed and expanded state.

4.2.3. PROTOTYPE

To explore the idea of increasing the toggling resistance using an in-pedicle expandable bone anchor, a two-dimensional (2D) prototype was designed. This 2D prototype should be able to deform to a 2D cross-section of the pedicle.

The prototype comprises a stainless steel M8 bolt and ten stainless steel (316L) wedges made by electrical discharge machining (EDM) (Figure 4.4a). The bolt is flattened at the sides to avoid rotation of the wedges around the bolt during insertion and expansion. To prevent the wedges from expanding before insertion, two alignment pins are used. After placement of the anchor, these alignment pins are removed such that the wedges can expand. The eight wedges in the middle have two slanted sides such that from both sides compression will cause the wedge to move outwards. The first and last wedges have one slanted side where the wedge is in contact with an adjacent wedge to allow for expansion. The other side of the wedge, where it is in contact with the nut or the head of the bolt, is straight to increase the contact area to avoid peak forces that could damage the prototype. The anchor is scaled up (~200%) to ease the fabrication and allow for visual observations during the validation process. The prototype has a width of 10.8 mm, a height of 20 mm and a length of 33.7 mm when in the collapsed state, and a height of 30 mm and a length of 21.8 mm when in the expanded state (Figure 4.4b).

4.2.4. PRELIMINARY EXPERIMENT

The main function of this in-pedicle expandable prototype is that tightening of the bolt must result in the expansion of the wedges which causes compression of the surrounding cancellous bone. In this preliminary experiment, the expansion of the wedges through the cancellous bone will be investigated.

For this experiment, the prototype will be placed between two plates of 5 Pound-force per Cubic Foot (PCF) solid foam cancellous bone phantom (Sawbones) which has similar mechanical properties as osteoporotic cancellous bone [5].

The bolt will be tightened to 7 Nm. The initial state of the wedges and the expanded state after tightening the bolt up to 7 Nm will be captured by a camera (Sony A6000). This
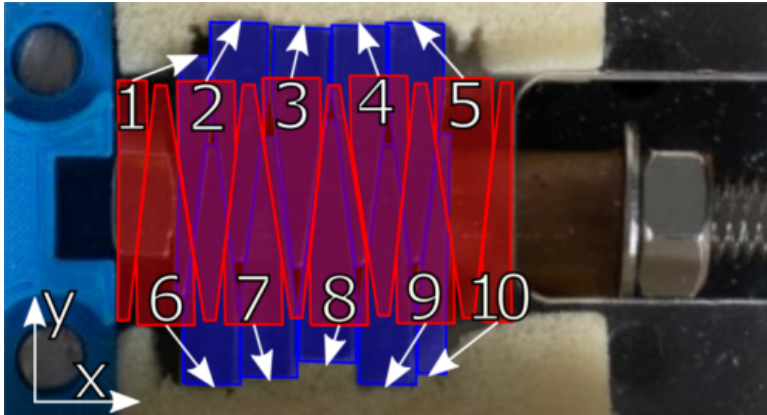
Figure 4.5: Expansion process when exerting a force of 7 Nm. The numbered wedges in the collapsed state (red) and the expanded state (blue) with the expansion path indicated with the white arrow.

test will be repeated three times in a new block of 5 PCF cancellous bone phantom.

Photographs of the wedges were analysed using Matlab 2019b to determine the displacement of each of the wedges in the x and y-direction.

4.3. RESULTS

Figure 4.5 shows the expansion of the wedges when tightening the bolt to 7 Nm. The red indicated wedges show the collapsed position and the blue wedges show the expanded position of the wedges. The white arrows indicate the expansion path of the wedges. Figure 4.6 shows the mean displacement and the standard deviation in the x and y-direction for each of the wedges.

4.4. DISCUSSION

4.4.1. MAIN FINDINGS

This preliminary study presents the idea of using in-pedicle expansion to increase the toggling resistance of spinal bone anchors. A prototype was developed consisting of ten wedges with a bolt that runs through the centre of the wedges. Tightening of the bolt results in expansion of the wedges. The first preliminary experiment showed that the wedges were able to successfully expand within 5 PCF solid foam (Sawbones), which corresponds to osteoporotic cancellous bone [5]. Due to the slanted sides of the wedges, expansion of the anchor also leads to shortening of the anchor. It can be observed that the wedges tend to contract to the centre of the anchor.

4.4.2. LIMITATIONS AND FUTURE RESEARCH

The preliminary experiment shows that the use of wedges to expand through cancellous bone is a possible option to create an in-pedicle expandable anchor to prevent toggling. In future research, the abilities of the anchor to deform to the pedicle must be investigated as well as the toggling resistance of the in-pedicle expandable anchor.

Displacement of the individual wedges during expansion when exerting a torque of 7 Nm
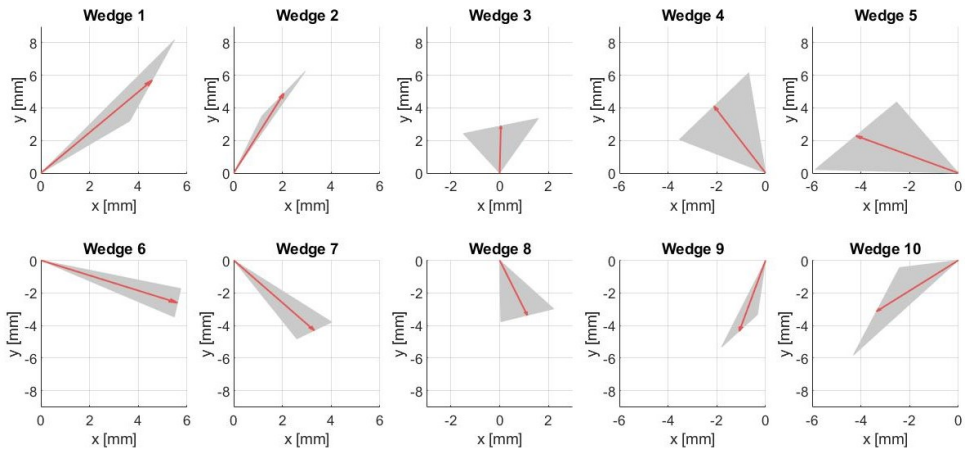
Figure 4.6: Displacement of the wedges during expansion in the x and y-direction. The mean is indicated with the red arrow and the standard deviation is indicated with the grey triangle.

After validation of using in-pedicle expansion to increase the toggling resistance, future research should be conducted such that the anchor can be used in a clinical setting. The current prototype is scaled-up and made in 2D, as this allowed for better visual observations during the preliminary validation. Future experiments will be carried out such that they are closer to the clinical setting in which the anchor is intended to be used. For these experiments, a new prototype must be designed that is scaled to the required size and works in 3D. Furthermore, the current is made of stainless steel prototype, and although stainless steel is listed as a biocompatible material, it is not used for long term implants. For clinical use, the prototype should be redesigned in a material suitable for long term implants such as titanium.

The tests presented in the study are performed using Sawbones 5 PCF solid foam and although this is a good alternative to real bone as it has similar mechanical properties, the phantom is very homogeneous while real bone has a more heterogeneous character which could influence the expansion of the prototype. Furthermore, the pedicle shape is different from person to person and from vertebra to vertebra. Both *ex-vivo* and *in-vivo* tests will give more insight into the adaptability of the anchor for these different pedicle shapes and bone characteristics. In this preliminary study in-pedicle expansion is investigated as a single means of anchoring. It would be interesting to look into combining in-pedicle expansion with currently used spinal bone anchors, such as the conventional pedicle screw. This preliminary study presents a first step in using in-pedicle expansion to increase the toggling resistance and could in the future serve as a means to increase the fixation strength of spinal bone anchors, especially in osteoporotic bone.

4.5. CONCLUSION

The use of in-pedicle expansion to increase the toggling resistance of a spinal bone anchor is explored in this paper. A scaled-up prototype was manufactured consisting of a bolt running through the centre of ten wedges. After placement of the anchor in a premade cavity, the bolt can be tightened which will cause the wedges to expand. The wedges were able to successfully compress a cancellous bone phantom during expansion. The presented prototype is a promising step to explore the use of expandable structures within the pedicle to increase the fixation strength and the toggling resistance of spinal bone anchors.

4

4

BIBLIOGRAPHY

[1]   Mehmet Aycan and Teyfik Demir. "Toggling effect on pullout performance of pedicle screws: Review". In: *International Advanced Researches and Engineering Journal* 4 (Dec. 15, 2020), pp. 161–172.

[2]   Toru Hasegawa et al. "Hydroxyapatite-coating of pedicle screws improves resistance against pull-out force in the osteoporotic canine lumbar spine model: a pilot study". In: *The Spine Journal* 5.3 (May 1, 2005), pp. 239–243. (Visited on 04/26/2021).

[3]   Toru Hirano et al. "Structural characteristics of the pedicle and its role in screw stability". In: *Spine* 22.21 (1997), pp. 2504–2510.

[4]   M Law, A F Tencer, and P A Anderson. "Caudo-cephalad loading of pedicle screws: mechanisms of loosening and methods of augmentation". In: *Spine* 18.16 (Dec. 1, 1993), pp. 2438–2443. (Visited on 12/14/2021).

[5]   Srinidhi Nagaraja and Vivek Palepu. "Comparisons of Anterior Plate Screw Pullout Strength Between Polyurethane Foams and Thoracolumbar Cadaveric Vertebrae". In: *Journal of Biomechanical Engineering* 138.10 (Oct. 1, 2016), p. 104505. (Visited on 01/04/2022).

[6]   Bengt Sandén et al. "Improved extraction torque of hydroxyapatite-coated pedicle screws". In: *European spine journal* 9.6 (Dec. 2000), pp. 534–537.

[7]   Giovanni F. Solitro et al. "Currently Adopted Criteria for Pedicle Screw Diameter Selection". In: *International Journal of Spine Surgery* 13.2 (Apr. 1, 2019), pp. 132–145. (Visited on 09/16/2021).

[8]   M. Stańczyk and B. van Rietbergen. "Thermal analysis of bone cement polymerisation at the cement–bone interface". In: *Journal of Biomechanics* 37.12 (Dec. 1, 2004), pp. 1803–1810. (Visited on 05/07/2021).

[9]   Srilakshmi Vishnubhotla et al. "A titanium expandable pedicle screw improves initial pullout strength as compared with standard pedicle screws". In: *The Spine Journal* 11.8 (Aug. 1, 2011), pp. 777–781. (Visited on 05/18/2021).

[10]   James N. Weinstein, Bjorn L. Rydevik, and Wolfgang Rauschning. "Anatomic and Technical Considerations of Pedicle Screw Fixation:" in: *Clinical Orthopaedics and Related Research* &NA;284 (Nov. 1992), pp. 34–46. (Visited on 12/17/2021).

[11]   Steven Wray et al. "Pedicle screw placement in the lumbar spine: effect of trajectory and screw design on acute biomechanical purchase". In: *Journal of Neurosurgery: Spine* 22.5 (May 1, 2015), pp. 503–510. (Visited on 12/22/2021).

[12]   Zi-xiang Wu et al. "A comparative study on screw loosening in osteoporotic
        lumbar spine fusion between expandable and conventional pedicle screws". In:
        Archives of Orthopaedic and Trauma Surgery 132.4 (Apr. 1, 2012), pp. 471–476.
        (Visited on 05/06/2021).

[13]   Jin Sup Yeom et al. "Leakage of cement in percutaneous transpedicular vertebro-
        plasty for painful osteoporotic compression fractures". In: *The Journal of bone
        and joint surgery. British volume* 85.1 (Jan. 2003), pp. 83–89.

[14]   M R Zindrick et al. "A biomechanical study of intrapeduncular screw fixation in
        the lumbosacral spine". In: *Clinical orthopaedics and related research* 203 (Feb. 1,
        1986), pp. 99–112.

4

5

DESIGN OF AN L-SHAPED BONE ANCHOR

The success rate of spinal fusion surgery is mainly determined by the fixation strength of the spinal bone anchors. This study explores the use of an L-shaped spinal bone anchor that is intended to establish a macro-shape lock with the posterior cortical layer of the vertebral body, thereby increasing the pull-out resistance of the anchor. The performance of this L-shaped anchor was evaluated in lumbar vertebra phantoms (L1-L5) across four distinct perpendicular orientations (lateral, medial, superior, and inferior). During the pull-out experiments, the pull-out force, and the displacement of the anchor with respect to the vertebra was measured which allowed the determination of the maximal pull-out force (mean: 123 N ± 25 N) and the initial pull-out force, the initial force required to start motion of the anchor (mean: 23 N ± 16 N). Notably, the maximum pull-out force was observed when the anchor engaged the cortical bone layer. The results demonstrate the potential benefits of utilising a spinal bone anchor featuring a macro-shape lock with the cortical bone layer to increase the pull-out force. Combining the macro shape-lock fixation method with the conventional pedicle screw shows the potential to significantly enhance the fixation strength of spinal bone anchors.

5.1. Introduction

5.1.1. Spinal Fusion Surgery

Spinal fusion surgery is an orthopaedic procedure that aims to fuse adjacent vertebrae to enhance spinal stability, alleviate pain, and address spinal deformities [20]. The gold standard to achieve spinal fusion entails the use of rods, firmly secured to the vertebrae with pedicle screws inserted through the pedicles into the vertebral body (Figure 5.1a). The overall success of spinal fusion surgery is highly dependent on the fixation strength of these pedicle screws within the vertebra, as even the slightest micro-movement between the adjacent vertebrae can hamper the desired fusion [23].

Although pull-out of pedicle screws is a very unlikely cause of implant failure, the fixation strength of pedicle screws is commonly quantified through the measurement of pull-out force, which represents the axial force required to pull the screw from the vertebra [14]. This pull-out force is the result of the interaction of the pedicle screw with the vertebra. Vertebrae comprise a thin compact layer of cortical bone that encapsulates the porous cancellous bone. The cortical bone layer shows considerable resilience against external forces due to its dense structure. While cortical bone possesses the potential to offer great fixation strength for spinal bone anchors, the majority of the currently used pedicle screws are embedded within the porous cancellous bone. Only the section of the screw located within the pedicle is in contact with the cortical bone layer. Remarkably, this relatively small section is responsible for 60% of the overall pull-out resistance [9, 22].

Correct placement of the pedicle screw is vital for the success of the spinal fusion surgery. The spinal column comprises vertebrae separated by intervertebral disks providing both stability and mobility to the spine. Additionally, the vertebrae play an important role in protecting the spinal cord, which runs through the spinal canal (Figure 5.1a, Figure 5.1b). The spinal column is surrounded by delicate and vital structures such as the spinal cord, vascular and nervous tissue. This presents a challenges in the placement of pedicle screws, as a misalignment may result in damage to these critical anatomical structures or lead to suboptimal screw fixation [21, 18]. When striving to enhance the fixation strength, a larger screw diameter appears advantageous, as it increases contact with the cortical bone layer within the pedicle, consequently increasing the fixation strength [1]. However, a larger screw diameter also elevates the risk of breaching the cortical bone layer and potentially damaging the surrounding anatomy.

5.1.2. Anchor Trajectory Optimisation

The search for enhanced pedicle screw fixation has led to a variety of innovative strategies, including various screw thread types and the use of cement-augmented screws [11, 6]. Another approach to enhance the fixation strength of spinal bone anchors entails optimising the screw trajectory. For instance, in bi-cortical placement the pedicle screw is inserted to ensure fixation of screw tip within the anterior cortex [23, 3] (Figure 5.1a, Figure 5.1c). This screw trajectory offers increased fixation strength, even with an average cortical bone layer thickness of only 0.4 mm [23, 3, 4]. Another alternative screw trajectory is the cortical bone trajectory for lumbar pedicle screw placement. This more lateral and caudo-cranial trajectory engages more cortical bone, thereby enhancing the

pull-out resistance by approximately 30% [15, 10] (Figure 5.1a, Figure 5.1c).

The posterior cortex of the vertebral body, with its perpendicular orientation to the pedicle, presents an ideal opportunity for a spinal bone anchor to establish a macro-shape lock, potentially enhancing pull-out resistance. However, the posterior cortex is currently underutilised in terms of contributing to the fixation strength of pedicle screws due to design and placement limitations that do not accommodate the required L-shape. A number of patents feature spinal bone anchors with outward-curving sections aimed at creating an L-shape macro shape-lock with the posterior cortex of the vertebral body [8, 5]. However, to our knowledge, these designs have not undergone testing in a close to clinical setting. Furthermore, there remains a limited understanding of the potential fixation strength of a macro-shape lock with the posterior cortex of the vertebral body and the optimal orientation for these types of L-shaped anchors. The anchor design presented by Shae *et al.* [17] demonstrates the potential of an expanding lateral pin, employing a rotational motion for anchor deployment. However, the undesirable consequence of this rotational motion of the lateral pin is the compression of the surrounding cancellous bone, potentially compromising the fixation strength of the anchor.

5.1.3. GOAL OF THIS STUDY

The goal of this research is to investigate and optimise the use of L-shaped spinal bone anchor designs that leverage the advantages of a macro-shape lock with the posterior cortex of the vertebral body to enhance pull-out resistance. This study aims to assess the fixation strength and potential benefits of these anchor designs, including their optimal orientation. Additionally, we seek to expand our understanding of the safety implications associated with these anchor designs, particularly in unforeseen circumstances that could lead to complete anchor pull-out from the vertebra. Our research aims to contribute valuable insights into improving the effectiveness and safety of spinal fusion procedures by enhancing the fixation strength of spinal bone anchors.

5.2. METHOD

5.2.1. ANCHOR DESIGN

The currently utilised pedicle screws are inserted through the pedicle of the vertebra into the vertebral body to provide essential stability and fixation strength [9, 22]. Introducing a pedicle screw with a lateral pin resulting in an L-shaped anchor through the same pedicular path allows for the same level of fixation strength as the currently used pedicle screw with the added possibility to establish a robust macro-shape lock with the posterior cortex of the vertebral body, thus enhancing the pull-out resistance. Figure 5.2a presents our conceptual design of a pedicle screw with an integrated L-shaped rod designed to create the desired macro-shape lock with the posterior cortex. The expansion of the rod enables placement of the pedicle screw through a single entry hole, similar to current pedicle screws. Furthermore, the expansion of the lateral pin is achieved by a translational motion which does not result in the undesired compression of the surrounding cancellous bone as a rotational expansion would. Besides placement, removal of spinal bone anchors is of importance, as implant removal can be required due to non-fusion, occurrence of infection or implant loosening [13]. The lateral pin of the L-shaped

5
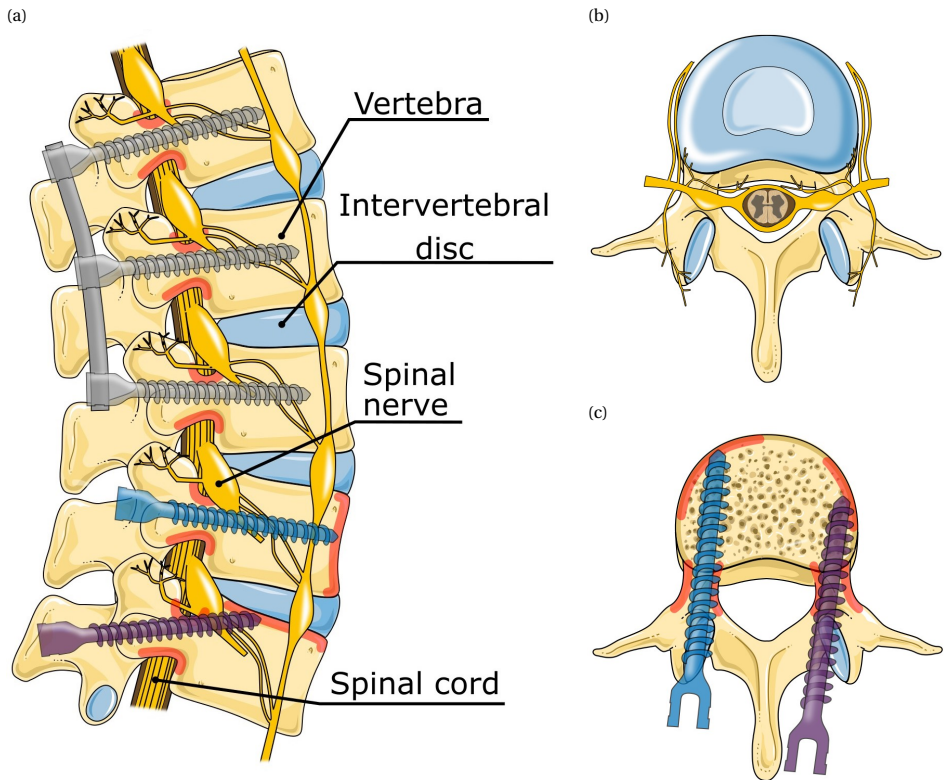
Figure 5.1: Lumbar vertebrae anatomy and placement of pedicle screws (grey), bi-cortical pedicle screws (blue), and cortical pedicle screws (purple). The contact area with the cortical layer using such screws is indicated in red. (a) Lumbar vertebrae (L1-L5), intervertebral discs, spinal cord nerves and pedicle screw placement (sagittal plane). (b) Lumbar vertebra (transverse plane). (c) pedicle screw placement (transverse plane). Illustration adapted from Servier Medical Art by Servier, licensed under a Creative Commons Attribution 3.0 Unported License.

anchor can be retracted by removing the expansion rod, and subsequently introducing it such that it will result in retraction of the pin as illustrated in Figure 5.2a.

The primary research objective of this study is to investigate the potential additional fixation strength of this macro-shape lock compared to the conventional pedicle screw, and determine the optimal orientation of the L-shaped anchor for both strength and safety. To achieve this, an L-shaped anchor without screw thread comprising a central pin and a lateral pin at the tip has been developed (Figure 5.2b). This anchor is not expandable and is merely intended as a means of researching the potential of utilising a macro-shape lock with the cortical bone layer. The length of the lateral pin of the L-shaped anchor was designed to be equal to the diameter of the anchor as this is theoretically the maximum length that would allow for the anchor to be placed through a single entry hole following the design presented in Figure 2a. In this research four orientations of the L-shaped anchor each with a 90-degree rotation were considered (A-D, Figure 5.2c).

5.2.2. EXPERIMENTAL GOAL

The primary aim of this research is to explore the effect of an L-shaped macro lock with the proximal cortical bone layer on the fixation strength of spinal bone anchors. An experiment was carried out to assess the influence of the anchor orientation across various lumbar vertebra. The two most important factors in evaluating spinal bone anchors are the fixation strength and safety. These two factors were investigated based on 1) pull-out resistance of the anchor and 2) damage to the vertebra after complete pull-out of the anchor. Both factors were compared to the conventional pedicle screw.

5.2.3. EXPERIMENTAL VARIABLES

The following independent variables were varied during the experiment:

- Anchor orientation: The pull-out experiment was conducted using the L-shaped anchor in four orientations with the lateral pin pointing in the cranial direction, caudal direction, medial direction, and lateral direction, respectively (Orientation A-D, Figure 5.2c).

- Vertebra type: The pull-out experiment was conducted using lumbar vertebra phantoms provided by Synbone® (Spine Vertebra L1-L5, LSS material). These vertebra phantoms closely mimic real vertebrae, featuring a porous cancellous bone structure [19].

- Anchor type: The pull-out experiment was conducted with the L-shaped anchor as well as with a conventional pedicle screw as presented in Figure 5.2b. The pedicle screw was only tested in a single orientation and only in the L2 vertebra.

The following variable was kept constant during the experiment:

- Pull-out velocity: The L-shaped anchor was pulled out of the vertebra at a constant velocity of 0.5 mm/s.

The following dependent variables were measured during the experiment:

5
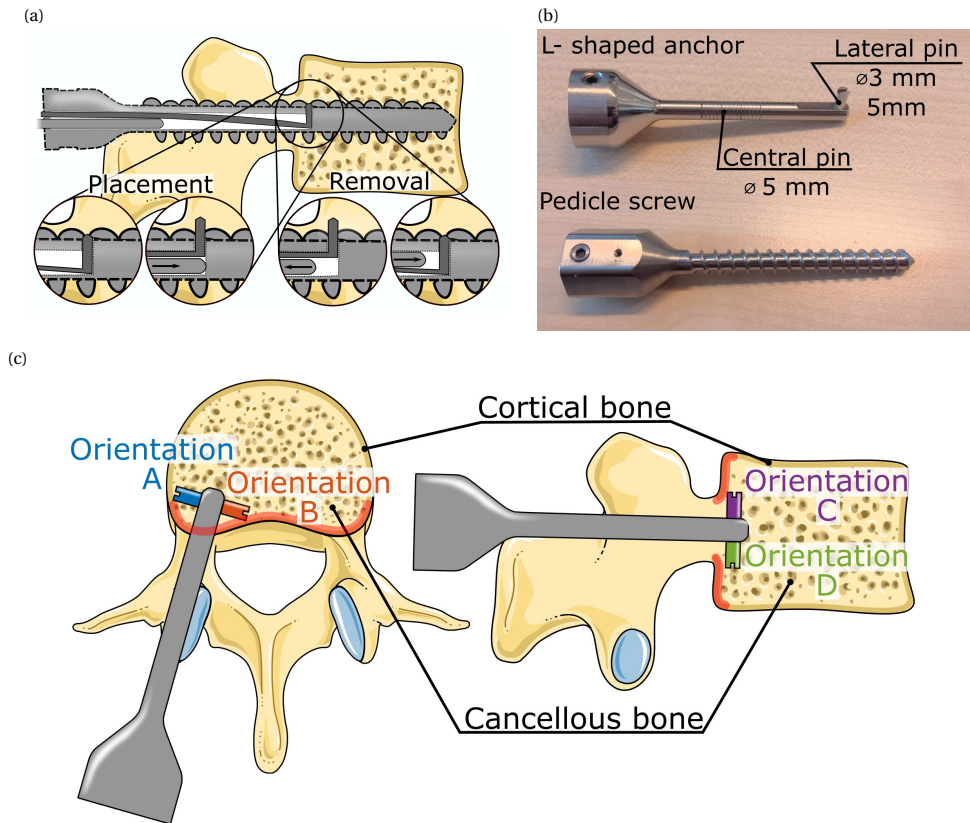
Figure 5.2: L-shaped spinal bone anchor design and placement. (a) Possible expansion mechanism that allows placement of the L-shaped anchor through a single entry point as well as the removal of the anchor. (b) Photograph of the L-shaped spinal bone anchor without screw thread, and a reference pedicle screw. The L-shape anchor comprises a central pin with a series of grooves that serve as indication of the insertion depth. (c) Four orientations (A-D) of the L-shaped anchor that were evaluated in the experiment. The proximal cortex of the vertebral body is indicated in red. Illustration adapted from Servier Medical Art by Servier licensed under a Creative Commons Attribution 3.0 unported license.
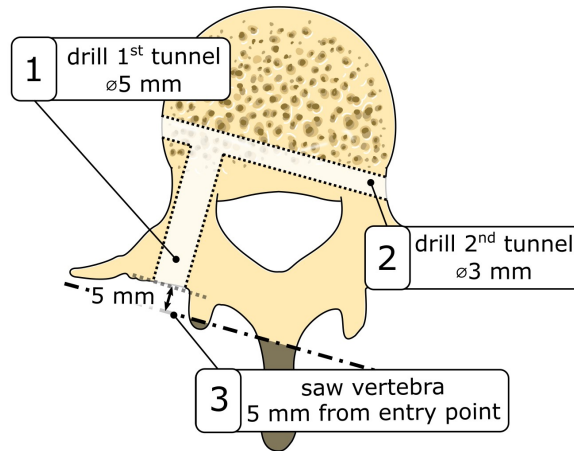
Figure 5.3: Vertebra preparation steps before placement of the L-shaped anchor.

- Pull-out force: The pull-out force of the anchor was measured continuously during the experiment. This allows for the determination of the maximum pull-out force (i.e., the maximum force required to pull the anchor from the vertebra) and the initial pull-out force (i.e., the force required to initiate the pull-out of the anchor from the vertebra).

- Pull-out distance: The relative displacement of the anchor with respect to the vertebra was measured. This measurement, combined with the continuously measured pull-out force allows for the determination of the initial pull-out force.

- Pull-out damage: The damage to the vertebra after complete pull-out of the anchor was categorised as follows: 1) clean pull-out: no breach detected, 2) posterior breach: breach at the entry point of the anchor, 3) pedicle breach: breach of the cortical layer of the pedicle. Damage to the cortical bone layer could indicate damage to the surrounding anatomy and is considered less safe.

5.2.4. VERTEBRA PREPARATION
To accommodate the central pin of the L-shaped bone anchor, a first ⌀ 5 mm tunnel was drilled through the central axis of the pedicle of the vertebra phantom taking the variations in angulation across different spinal levels (L1-L5) into account (Figure 5.3, step 1). Subsequently, a perpendicular ⌀ 3 mm tunnel was drilled to accommodate the lateral pin of the bone anchor (Figure 3, step 2). For this, a 3D printed guide was utilised to guarantee both the perpendicularity of the two tunnels and their correct alignment within the vertebral anatomy. The same procedure for drilling the first tunnel was used to create a tunnel to accommodate the conventional pedicle screw.

To mitigate potential stress concentrations on the vertebrae's processes during the pull-out experiment, a portion of the processes was sawed off. The sawing was performed perpendicular to the first tunnel and the inferior vertebral endplate (Figure 3, step 3). After the completion of these preparatory steps, the anchor was securely po-

sitioned. For the L-shaped anchor, the central pin was carefully inserted and oriented such that the lateral pin could be introduced through the second tunnel and screwed into the central pin.

5.2.5. Experimental Facility

For the experiment a dedicated test facility was designed that is shown in Figure 5.4. This facility enables the controlled extraction of the anchor from the vertebra at a constant velocity while simultaneously measuring the pull-out force and relative displacement of the anchor with respect to the vertebra.

The vertebra, with the anchor securely positioned within it, was positioned within the container (Figure 5.4, Purple). In turn, a force sensor (Futek, LCM300, 4448 N) was connected to the container and the fixture, facilitating continuous force measurement throughout the experiment. The anchor was connected to the slider (Figure 5.4, Orange) through the anchor connection. The slider performs linear translations actuated by the actuation mechanism (Figure 5.4, Blue) consisting of an electro-motor (Modelcraft, RB 35, 1:600) with a gear transmission (9:1). The linear motion of the slider, and consequently the relative displacement between the anchor and the vertebra, was precisely measured using a linear potentiometer (Althen, 13FLP12A).

5.2.6. Experimental Protocol

The following steps were executed during the experiment. The vertebra, containing the securely placed L-shaped anchor or pedicle screw, was positioned within the container so that the sawing plane of the vertebra was in contact with the endplate of the container. Subsequently, the proximal end of the anchor was connected to the slider. The slider was carefully arranged to ensure contact between the vertebra and the endplate of the container. The tip of the linear potentiometer was secured to the container using an integrated magnet such that the displacement between the anchor and the vertebra could be measured.

After completing these preliminary steps, the motor was activated to initiate linear translation of the slider. This motion continued until the anchor was completely extracted from the vertebra at a constant velocity of 0.5 mm/s. Throughout this procedure, the force sensor continuously measured the pull-out force, while the linear potentiometer captured the linear displacement between the anchor and the vertebra such that the initial pull-out force could be determined. As the used linear potentiometer has a 12 mm range, the pull-out force was recorded over 12 mm.

5.2.7. Data Analysis

The force data were normalised by accounting for the force measured after complete pull-out of the anchor, compensating for any forces potentially exerted by the initial positioning of the slider at the start of the experiment. Furthermore, the displacement data were normalised such that the anchor starts moving at t=0. The measured pull-out force at this point represents the initial pull-out force, as this is the force required to start the pull-out of the anchor. All data analysis was performed in Matlab R2019b.

Following the complete pull-out of the anchor, the vertebra was visually inspected for breaches in the cortical layer. Only the most severe breach was recorded. For instance,
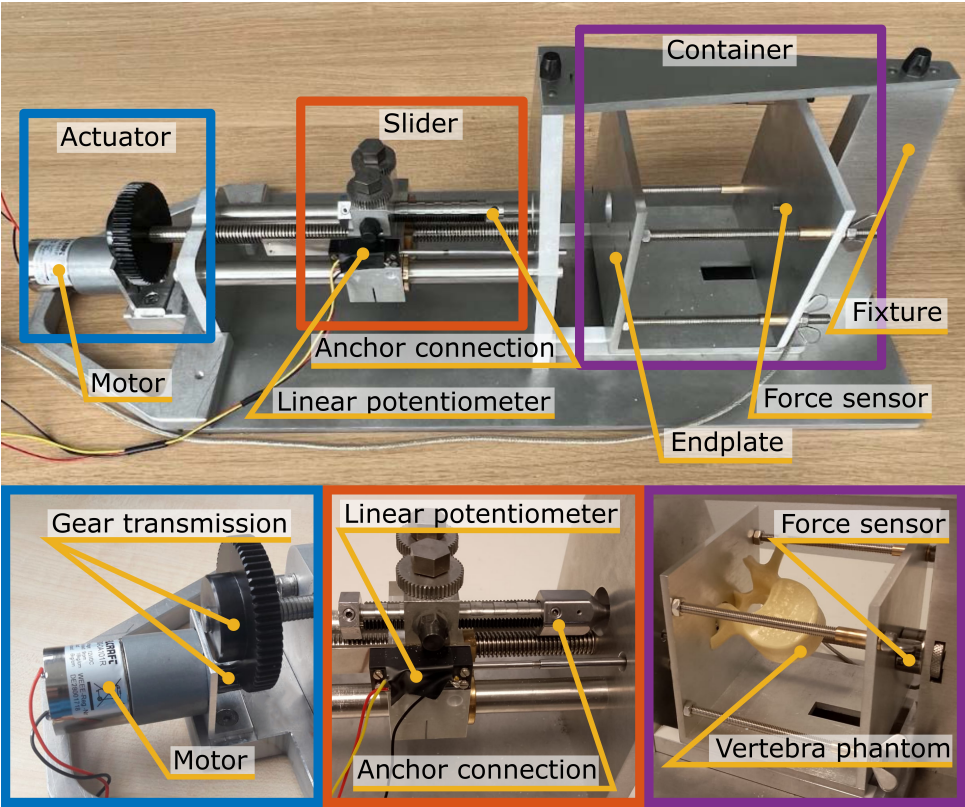
Figure 5.4: Experimental facility consisting of the actuator that pulls the slider and the anchor out of the vertebra that is contained in the container. The force is measured using the force sensor and the displacement of the L-shaped anchor with respect to the vertebra is measured using the linear potentiometer.

Table 5.1: Pull-out test results for L-shaped anchor in four orientations and the pedicle screw.

Anchor	Vertebra type	Initial pull-out force [N]	Maximal pull-out force [N]	Pull-out damage
L-shaped anchor Orientation A	L1	41	90	Pedicle breach
	L2	34	109	Pedicle breach
	L3	53	134	Pedicle breach
	L4	10	129	Clean pull-out
	L5	7	125	Clean pull-out
L-shaped anchor Orientation B	L1	12	122	Pedicle breach
	L2	39	145	Pedicle breach
	L3	53	124	Pedicle breach
	L4	7	86	Clean pull-out
	L5	14	122	Clean pull-out
L-shaped anchor Orientation C	L1	34	138	Posterior breach
	L2	28	156	Pedicle breach
	L3	18	86	Posterior breach
	L4	3	130	Posterior breach
	L5	20	135	Pedicle breach
L-shaped anchor Orientation D	L1	16	56	Posterior breach
	L2	23	138	Posterior breach
	L3	37	107	Posterior breach
	L4	30	126	Pedicle breach
	L5	48	180	Pedicle breach
Pedicle screw	L2	203	339	Pedicle breach
	L2	40	348	Pedicle breach
	L2	3	369	Pedicle breach
	L2	142	426	Pedicle breach

if both a breach at the pedicle and posterior breach was present, only the pedicle breach was recorded, as this type of breach holds more severe clinical implications.

5.3. RESULTS

The initial pull-out force, maximal pull-out force and damage to the vertebra after complete pull-out of the pedicle screw and the L-shaped anchor in the four evaluated orientations (A-D) is listed in Table 5.1. The measured pull-out force of the pedicle screw and the L-shaped anchor in the different anchor orientations (A-D) is illustrated in Figure 5. The close-up view also demonstrates how the initial pull-out force was determined.

Based on the measured pull-out force of the L-shaped anchor, three distinct force profiles were identified: 1) a double force peak profile, 2) a single force peak profile and 3) no force peak profile. After inspecting the vertebrae cross-section, it was found that the force peaks correlate to the presence of a cortical layer, as shown in Figure 5.6. A double force peak profile indicates that the L-shaped anchor was pulled through two
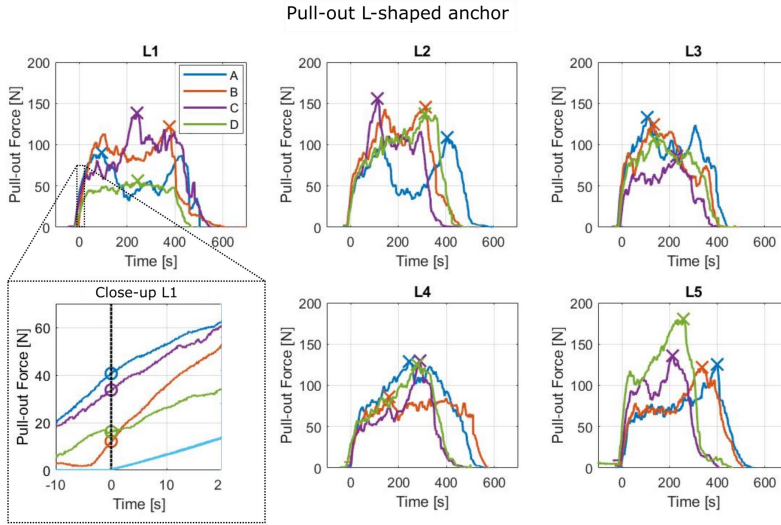
Figure 5.5: Pull-out force of the L-shaped anchor in different anchor orientations (A-D) for different vertebra (L1-L5). The maximum pull-out force is indicated with an 'X'. The close-up shows the determination of the initial pull-out force indicated with an 'o'

cortical bone layers, a single force peak profile indicates that the L-shaped anchor was pulled through a single cortical layer and the lack of a clear force peak indicates that the L-shaped anchor was pulled only through cancellous bone without encountering a cortical bone layer.

The L-shaped anchor has a mean initial pull-out force of 23 N ± 16 N and a mean maximum pull-out force of 123 N ± 25 N. The measured pull-out force of the pedicle screw in an L2 vertebra phantom is presented in Figure 5.7.

In four of the twenty pull-out experiments (20%) with the L-shaped anchor, clean pull-out (no breaches) was observed (L4A, L4B, L5A, L5B). In six cases (30%) breach of the posterior cortex was observed and in the remaining ten cases (50%) cortical breach of the pedicle was observed. Complete pull-out of the pedicle screw resulted to pedicle breach in 100% of the performed experiments Figure 5.8 presents a boxplot with the initial and maximal pull-out force of the L-shaped anchor for the identified damage to the vertebra.

5.4. DISCUSSION

5.4.1. MAIN FINDINGS

This study aimed to explore the effectiveness of a macro-shape lock with posterior cortex of the vertebral body to enhance the fixation strength of spinal bone anchors. An L-shaped anchor was developed and evaluated in four perpendicular orientations to assess the pull-out resistance and the safety in use. The pull-out force measurements showed three distinct force profiles: 1) double force peak profile, 2) single force peak profile and 3) no force peak profile. The pull-out force peaks could be linked to the existence of a
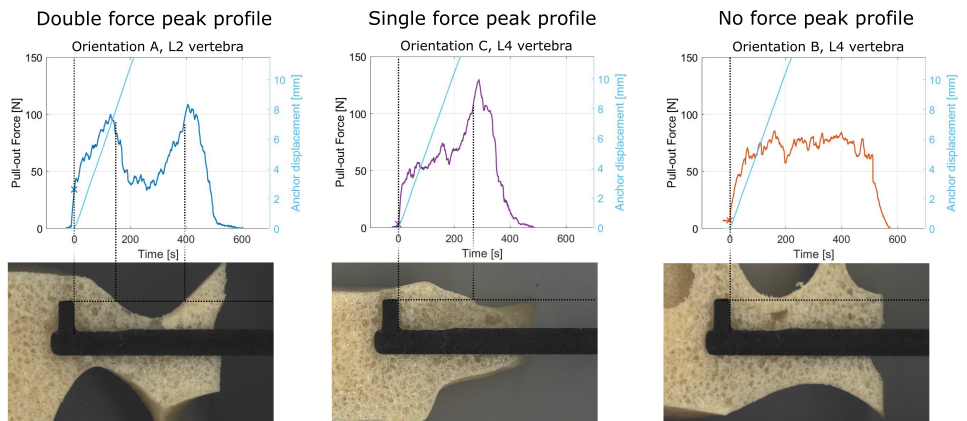
Figure 5.6: Pull-out force linked to the cross-section of the vertebra. Left: Double force peak profile linked to Orientation A in the L2 vertebra, Middle: Single force peak profile linked to Orientation C for the L4 vertebra, Right: No force peak profile linked to Orientation B in the L4 vertebra.

5
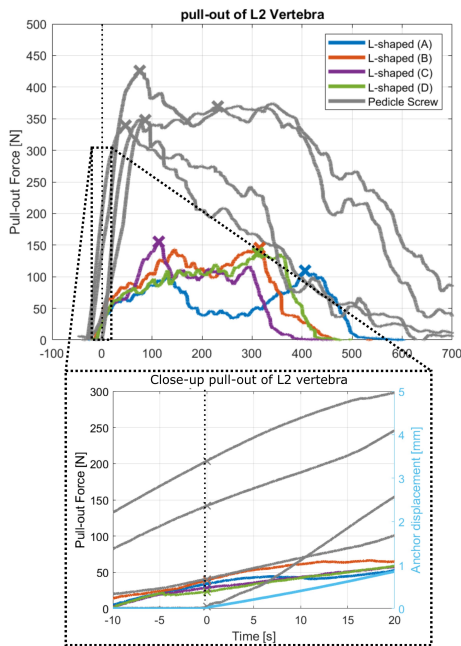
Figure 5.7: Pull-out force of the pedicle screw and L-shaped anchor in Orientation (A-D) each for four repetitions in a L2 vertebra phantom. The maximum force is indicated with an 'X' and the initial pull-out force is indicated with an 'o' in the close up.
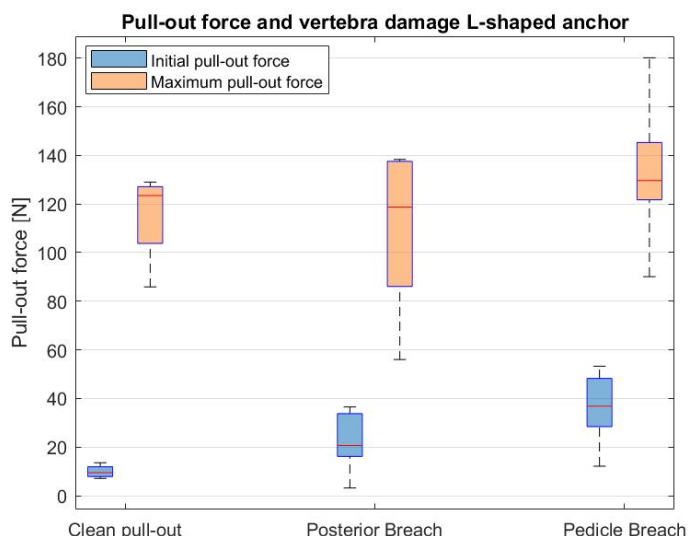
Figure 5.8: Boxplot presenting the initial (blue) and maximum pull-out force (orange) for the three identified degrees of cortical bone damage: 1) clean pull-out, 2) posterior breach and 3) pedicle breach for the experiments performed with the L-shaped anchor.

macro-shape grip with the L-shaped anchor and the cortical bone layer indicating that a shape lock with the cortical bone layer increases the pull-out resistance of a spinal bone anchor. The mean maximum pull-out force of the L-shaped anchor was 123 N ± 25 N which is significantly lower than the maximum pull-out force of a pedicle screw (370 N ± 39 N) tested in the same bone phantoms and the pull-out force of pedicle screws reported in literature (287 N) [15]. Although the fixation strength of the L-shaped anchor is less than the conventional pedicle screw, utilising a macro-shape lock with the proximal cortex as an add-on for the current pedicle screws could potentially increase the pull-out strength with up to 33%, although further research is required.

Alternative means to increase the fixation strength of pedicle screw reported in literature include double threaded screws or bi-cortical fixation, both have resulted in an increase fixation strength of 20% [23, 16]. These means for improved fixation can be included for the pedicle screw that is equipped with the L-shaped anchor. The use of a hydroxyapatite-coating to induce bone ingrowth can also increase the fixation strength of spinal bone anchors by 50% [7] which is more than can be expected of the L-shaped anchor. However, since the increased fixation of the hydroxyapatite-coating is established due to the surrounding bone growth into the spinal bone anchor, it takes days to weeks to establish this increased fixation, while the use of a macro-shape lock can be loaded directly. Cement augmented pedicel screws can double the pull-out resistance after placement [23]. However, removal of these screws remains a challenge without damaging the vertebra. The removal of the L-shaped anchor can be achieved as illustrated in Figure 5.2a. Further research is required to investigate if the use a macro-shape
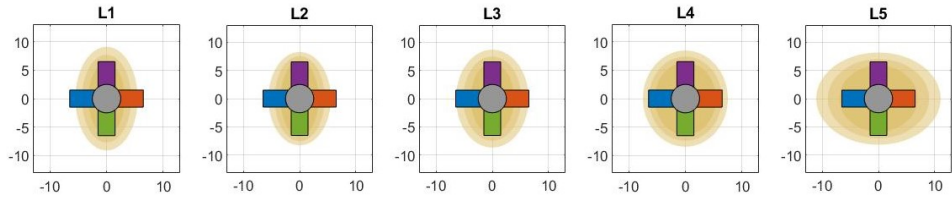
Figure 5.9: Schematic representation of the varying shape of the L1-L5 pedicle cross-section, with the L-shaped anchor in four orientations (Orientation A: blue, Orientation B: red, Orientation C: yellow, Orientation D: purple). Based om pedicle measures reported by Zindrick *et al.* [24].

fixation in combination with the pedicle screw can result in the required increase in fixation strength and its ability for implant removal without damaging the vertebra.

The maximum pull-out force was found to be higher than the initial pull-out resistance for all tests with the L-shaped anchor, which suggest that the L-shaped anchor did not create a macro-shape lock in the initial position. To validate this hypothesis, a number of vertebrae were cut through such that the pull-out path of the L-shaped anchor could be investigated (Figure 5.6). Pull-out of the L-shaped anchor initially resulted in compression of cancellous bone. Upon contact with the cortical bone layer the maximum pull-out force was achieved resulting in the maximum pull-out force. This underscores the importance of correct initial anchor placement to establish an effective macro shape-lock with the highest pull-out resistance from the start.

After complete pull-out of the L-shaped bone anchor, damage to the vertebra could be observed in 80% of cases. In 50% of cases breach of the cortical layer at the pedicle could be observed, which could be an indication of damage to surrounding anatomy due to nerves and spinal cord located near the pedicle. Complete pull-out of the pedicle screw resulted in significant damage to the pedicle in 100% of the pull-out experiments with the pedicle screw. It is important to note that complete pull-out of a pedicle screw is very unlikely. Nevertheless, literature reports that in 16.2% of the anchored pedicle screws, partial pull-out of the screw is observed during rod connection in which the pedicle screw is connected to the Harrington rod [12]. A higher initial pull-out resistance of the L-shaped anchor was associated with more severe damage to the vertebra phantom after complete anchor extraction, with the degree of damage varying depending on the anchor's orientation. A possible explanation is the variety in pedicle shape over the different vertebra as illustrated in Figure 5.9. Due to the ascending oval shape of the L1-L3 pedicle cross-section, orientation A and B of the L-shaped anchor are expected to create a more effective macro-shape lock with the cortical bone layer. However, the flat oval cross-section of the L5 pedicle makes orientation C and D of the L-shaped anchor more likely to generate an effective macro-shape lock. The preferred orientation of the L-shaped anchor is, therefore, dependent on the vertebra shape. Pre-operative image analysis can help in determining the most optimal anchor orientation based on the geometrical properties in the target vertebra.

Possibly, the initial pull-out resistance can be increased without increasing the risk on damage to the vertebra by initially placing the L-shaped anchor in the position in which the maximal pull-out resistance was achieved. This optimal placement of the L-
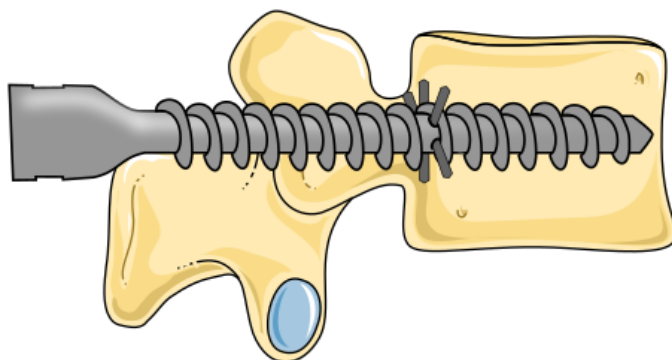
Figure 5.10: Future vision of an L-shaped anchor to increase the pull-out resistance of spinal bone anchors with the utilisation of multiple L-shaped anchors to create a larger contact area with the proximal cortex of the vertebral body which could increase the pull-out resistance further. Illustration adapted from Servier Medical Art by Servier, licensed under a Creative Commons Attribution 3.0 Unported License.

shaped anchor right behind the cortical bone layer could be achieved in a safe manner by implementing real-time feedback for instance by using Diffuse Reflectance Spectroscopy (DRS) to reliably detect the cortical bone layer [2].

5.4.2. LIMITATIONS AND FUTURE RESEARCH

The evaluation of the L-shaped anchor in this study was performed using vertebra models designed to mimic the mechanical properties of human vertebrae. Nevertheless, these models exhibited variations, such as air pockets and regions with differing structural densities, potentially influencing the measurements. Future research should incorporate *ex-vivo* and *in-vivo* experiments to provide a more accurate representation of real bone structures, helping to thoroughly assess potential fixation strength and damage to the surrounding anatomy following complete anchor pull-out.

Means to enhance the fixation strength of and L-shaped add-on to the pedicle screw deserves exploration. For instance, integrating the use of multiple laterally expanding elements (Figure 5.10) could create an umbrella-like structure that expands behind the pedicle, establishing a macro-shape lock with the proximal cortex of the vertebral body and spreading the stress more evenly over a larger surface area. This has the potential to further enhance the anchor's fixation strength due to increased contact with the cortical bone layer.

In this study, axial pull-out resistance of the anchor was considered. In future experiments alternative load cases such as perpendicular loads and cyclic loading can be investigated. Beyond increasing the pull-out resistance, the placement of the L-shaped anchor is thought to enhance the toggling resistance of the spinal bone anchor. Toggling, a pivoting motion of the pedicle screw around the contact point with the cortical bone layer in the pedicle, compresses the cancellous bone surrounding the screw and diminishes the screw's fixation strength. A correctly placed L-shaped anchor creates additional contact with the cortical bone layer, preventing this toggling motion and thus increasing the anchor's fixation strength.

5.5. CONCLUSION

The L-shaped anchor presented in this study can be used to create a shape-lock with the proximal cortex of the vertebral body. The use of a macro-shape lock with the cortical bone layer represents a promising innovation in spinal instrumentation with its potential to enhance pull-out resistance with a maximum pull-out force of 123 N ± 25 N in bone phantoms. However, it is essential to acknowledge the challenges associated with this technology, including the risk of cortical breach and the technical difficulty involved in its precise placement. The presented L-shaped anchor presents the ability to increase the pull-out resistance and hold the potential to be used in combination with the current golden standard of the pedicle screw to increase the pull-out resistance. With further research and development, the use of an L-shaped anchor that utilises a macro-shape lock with the cortical bone layer could provide a significant increase in the fixation strength of spinal bone anchors.

BIBLIOGRAPHY

[1] A. G. Brantley et al. "The effects of pedicle screw fit. An in vitro study." In: *Spine* 19.15 (1994), pp. 1752–1758.

[2] Gustav Burström et al. "Diffuse reflectance spectroscopy accurately identifies the pre-cortical zone to avoid impending pedicle screw breach in spinal fixation surgery". In: *Biomedical Optics Express* 10.11 (Oct. 24, 2019), pp. 5905–5920. (Visited on 09/16/2021).

[3] Luc P. Cloutier, Carl-Eric Aubin, and Guy Grimard. "Biomechanical study of anterior spinal instrumentation configurations". en. In: *European Spine Journal* 16.7 (July 2007), pp. 1039–1045. (Visited on 06/12/2023).

[4] Senthil K Eswaran et al. "Cortical and trabecular load sharing in the human vertebral body". In: *Journal of Bone and Mineral Research* 21.2 (2006), pp. 307–314.

[5] Yafei Feng et al. "Medical anchor type vertebral pedicle screw". Pat. CN103860251A. Fourth Military Medical Univ. June 18, 2014.

[6] Bruce M. Frankel, Sabino D'Agostino, and Chiang Wang. "A biomechanical cadaveric analysis of polymethylmethacrylate-augmented pedicle screw fixation". In: *Journal of Neurosurgery: Spine* 7.1 (2007). Publisher: American Association of Neurological Surgeons, pp. 47–53.

[7] Toru Hasegawa et al. "Hydroxyapatite-coating of pedicle screws improves resistance against pull-out force in the osteoporotic canine lumbar spine model: a pilot study". In: *The Spine Journal* 5.3 (May 1, 2005), pp. 239–243. (Visited on 04/26/2021).

[8] John Riley Hawkins, Alexander Grinberg, and Michael Michielli. "Revisable Orthopedic Anchor and Methods of Use". U.S. pat. 2016008033A1. Depuy Synthes Products Inc. Jan. 14, 2016.

[9] Toru Hirano et al. "Structural characteristics of the pedicle and its role in screw stability". In: *Spine* 22.21 (1997), pp. 2504–2510.

[10] Kota Kojima et al. "Cortical bone trajectory and traditional trajectory—a radiological evaluation of screw-bone contact". In: *Acta neurochirurgica* 157 (2015), pp. 1173–1178.

[11] Luigi La Barbera. "Chapter 17 - Fixation and Fusion". In: *Biomechanics of the Spine*. Ed. by Fabio Galbusera and Hans-Joachim Wilke. Academic Press, Jan. 1, 2018, pp. 301–327. ISBN: 978-0-12-812851-0. (Visited on 02/25/2021).

[12] Tetsuro Ohba et al. "Risk factors for clinically relevant loosening of percutaneous pedicle screws". In: *Spine Surgery and Related Research* 3.1 (2019), pp. 79–85.

5

[13] Mark A Pichelmann et al. "Revision rates following primary adult spinal deformity surgery: six hundred forty-three consecutive patients followed-up to twenty-two years postoperative". In: *Spine* 35.2 (2010), pp. 219–226.

[14] Bengt Sandén et al. "Improved Bone–Screw Interface With Hydroxyapatite Coating: An: In Vivo: Study of Loaded Pedicle Screws in Sheep". In: *Spine* 26.24 (2001), pp. 2673–2678.

[15] BG Santoni et al. "Cortical bone trajectory for lumbar pedicle screws". In: *The Spine Journal* 9.5 (2009), pp. 366–373.

[16] Wei Ren Daniel Seng et al. "Pedicle Screw Designs in Spinal Surgery: Is There a Difference? A Biomechanical Study on Primary and Revision Pull-Out Strength". In: *Spine* 44.3 (Feb. 1, 2019), E144. (Visited on 01/21/2022).

[17] Thomas M Shea et al. "Balancing rigidity and safety of pedicle screw fixation via a novel expansion mechanism in a severely osteoporotic model". In: *BioMed Research International* 2015 (2015).

[18] Se-II Suk et al. "Thoracic Pedicle Screw Fixation in Spinal Deformities: Are They Really Safe?" In: *Spine* 26.18 (Sept. 15, 2001), pp. 2049–2057. (Visited on 12/09/2021).

[19] Synbones. *LSS Spine models*. Accessed: 09-08-2023.

[20] Venkata Ramakrishna Tukkapuram, Abumi Kuniyoshi, and Manabu Ito. "A Review of the Historical Evolution, Biomechanical Advantage, Clinical Applications, and Safe Insertion Techniques of Cervical Pedicle Screw Fixation". In: *Spine Surgery and Related Research* 3.2 (Apr. 27, 2019), pp. 126–135. (Visited on 02/09/2021).

[21] Bernd Wegener et al. "Delayed perforation of the aorta by a thoracic pedicle screw". In: *European Spine Journal* 17.2 (Sept. 1, 2008), pp. 351–354. (Visited on 12/09/2021).

[22] James N. Weinstein, Bjorn L. Rydevik, and Wolfgang Rauschning. "Anatomic and Technical Considerations of Pedicle Screw Fixation:" in: *Clinical Orthopaedics and Related Research* &NA;284 (Nov. 1992), pp. 34–46. (Visited on 12/17/2021).

[23] M R Zindrick et al. "A biomechanical study of intrapeduncular screw fixation in the lumbosacral spine". In: *Clinical orthopaedics and related research* 203 (Feb. 1, 1986), pp. 99–112.

[24] Michael R. Zindrick et al. "Analysis of the Morphometric Characteristics of the Thoracic and Lumbar Pedicles". en-US. In: *Spine* 12.2 (Mar. 1987), pp. 160–166. (Visited on 09/27/2022).

5

II

ANCHOR PLACEMENT
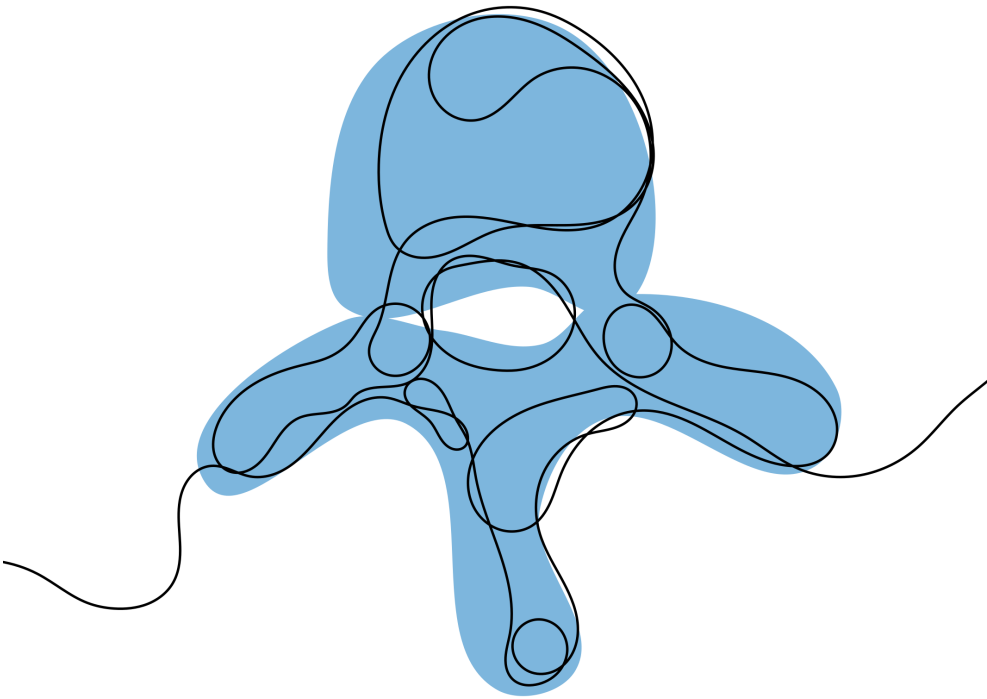
6

STATE-OF-THE-ART IN STEERABLE BONE DRILLS

Orthopaedic procedures often require drilling of tunnels through bone, for instance for the introduction of implants. The currently used rigid bone drills make it challenging to reach all target areas without damaging surrounding anatomy. Steerable bone drills are a promising solution as they enable access to larger volumes and the creation of curved tunnels thereby reducing the risk of harm to surrounding anatomical structures. This review provides a comprehensive overview of steerable bone drill designs identified in patent literature via the Espacenet database and in scientific literature accessed via the Scopus data base. A Boolean search combined with pre-set inclusion criteria returned 78 literature references describing a variety of drill designs. These drill designs could be categorised based on how the drilling trajectory was defined. Three methods to influence the drilling trajectory were identified: 1) the device (57% of the sources), 2) the environment (15% of the sources): the path is defined based on the tissue interaction forces with the surrounding bone or 3) the user defines the drilling trajectory (28% of the sources). The comprehensive overview of steerable drilling methods provides insights in the possibilities in drill design and may be used as a source of inspiration for the design of novel steerable drill designs.

6.1. Introduction

6.1.1. Steerable Bone Drilling

Bone drilling is widely employed surgical technique in various medical procedures, playing an important role in fracture fixation, implant placement, and facilitating access to specific treatment sites (Figure 6.1) [48]. Bone drills are usually rigid devices containing an axially rotating cutting head. They are often used in conjunction with surgical screws and plates to treat a wide variety of injuries and diseases. Although bone drills are effective in open surgery, the strive for minimal invasive surgeries and optimal patient outcomes poses a challenge when using conventional rigid and straight bone drills especially, when navigating through tight spaces, such as joints [68].

For instance, Anterior Cruciate Ligament (ACL) reconstruction aims to restore knee function and eliminate pain and discomfort caused by a damaged or torn ACL [89]. Precision drilling is crucial to create the tunnels in the femur and tibia such that the damaged or torn ligament can be reattached with a pin [18]. A reconstruction of the ACL that more closely resembles the anatomical structure before injury is associated with an improved biomechanical outcome [100]. However, drilling of the tunnels required for this anatomical reconstruction with rigid drills is challenging [31].

Similarly, osteonecrosis treatment, particularly in the femoral head, involves drilling to remove lesions areas to prevent collapse of the femoral head due to disrupted blood supply [50]. Conventional rigid drills complicate the removal of the entire lesion area without causing substantial damage to surrounding healthy tissue.

The integration of steerable bone drills in orthopaedic procedures offers the potential to remove entire lesions through a single entry point, as the steerability allows for reaching specific locations within the bone, and drilling along preferred trajectories, thus minimising damage to surrounding anatomy [59]. Furthermore, steerable drills may enable alternative drilling trajectories to reach lesions, further minimising damage to healthy surrounding tissue. The versatility of steerable bone drills presents a promising solution across various medical procedures, as the steerability potentially increases the precision, reduces the complication rates improves patient outcomes.

Steerable bone drills, with enhanced manoeuvrability, offer potential benefits across a spectrum of (orthopaedic) procedures. In procedures such as bone harvesting, where complications such as pain, nerve injury, and fracture may occur [14], steerable bone drills might provide a solution to minimise these risks. Especially in patients with compromised bone quality due to osteoporosis, fractures may occur if multiple grafts are taken too close together in order to obtain sufficient graft material [47].

Despite their clear utility, only a limited number of these steerable bone drills are currently available for clinical use. Achieving a balance between the required flexibility for bending and steering while simultaneously accomplishing the required axial rigidity to facilitate bone drilling is challenging.

Examples of commercially available bone drills are the *Stryker MicroFX OCD* [58] and the *Carevature Dreal* [27]. These flexible drills are used in combination with a curved external guide, facilitating easier access to entry points without compromising surrounding anatomy. However, the drilling trajectory through the bone remains fixed, lacking the flexibility for clinicians to adapt the trajectory during the procedure.
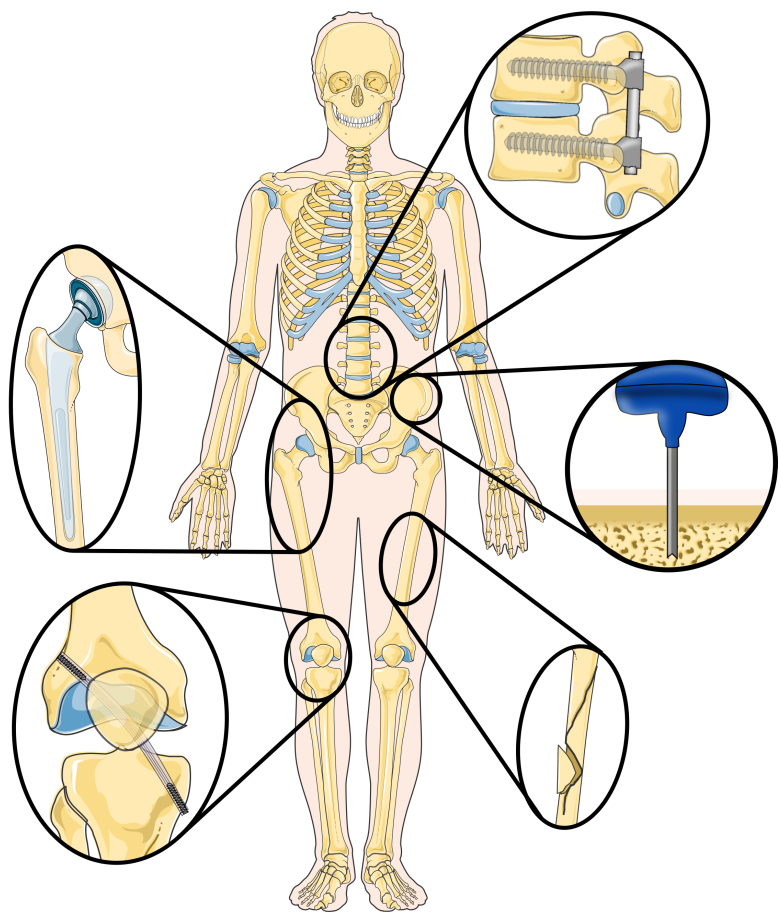
Figure 6.1: Overview of (orthopaedic) procedures where the use of steerable bone drills can provide advantages, including implant placement, ligament reconstruction, fracture fixation and bone harvesting. Illustration adapted from Servier Medical Art by Servier, licensed under a Creative Commons Attribution 3.0 Unported License.

6.1.2. Goal of this Study

While commercially available steerable bone drills are still in their initial stages, a multitude of innovative designs are documented in scientific and patent literature. Currently available reviews on bone drilling focus on scientific literature [48, 41] describing the parameters affecting the drilling performance and thermal reactions of rigid drills, with limited attention given to the validation and practical application of steerable designs. The review of Sendrowicz *et al.* [76] focuses on steerable bone drill designs presented in patent literature, however the validation of these designs and the drilling performance of these designs is limited. The current study expands its focus by incorporating both scientific literature and patent literature as scientific literature provides information on the current capabilities of steerable bone drills, while patent literature sheds a light on potential future development areas.

This review aims to present a comprehensive overview of steerable bone drills, highlighting their ability to create curved tunnels for the treatment of challenging lesion areas, or to drill specific paths to reach specific target locations and improve the placement of implants, amongst others. A comprehensive review of steerable bone drills is essential due to the significant potential these devices hold for advancing minimally invasive surgical techniques and improving patient outcomes. Both scientific literature, presenting the current possibilities and patent literature highlighting future developments, are included in this review. The goal is to provide a comprehensive insight into the current state of the art and potential developments in steerable bone drill technologies. By doing so, we highlight innovative design strategies, evaluate their clinical potential, and identify areas for future development. This information is crucial for guiding further research, informing clinical practices, and ultimately enhancing the safety and effectiveness of orthopaedic surgeries.

6.2. Method

6.2.1. Search Method

The identification of relevant literature commenced with a search in the Scopus database to identify scientific literature providing insights into the current possibilities in steerable bone drilling. Additionally, a literature search was conducted in the Espacenet database to identify patent literature illustrating future developments in the field of steerable bone drills.

The scientific literature search performed in the Scopus database facilitated Boolean search queries. The search query in Scopus was categorised into three sections: (1) Application area (bone, osteo*, orthop*), (2) Instrument type (drill*, burr*, ream*, trep*, bore), and (3) Steering functionality (flex*, steer*, maneuv*, manouv*, deflect*, curv*, articulat*, directional*, orient*, deviat*, bend). We did not apply a date range or document type filter to our search query to ensure we encompassed all relevant studies concerning steerable bone drills. The search was, however, limited to English literature using the 'LIMIT-TO' function. The search query used was as follows:

TITLE (drill* OR burr* OR ream* OR trep* OR bore) AND TITLE-ABS ((bone OR osteo* OR ortop*) AND (flex* OR steer* OR maneuv* OR manoeuv* OR deflect* OR curv* OR ar-

ticulat* OR directional* OR orient* OR deviat* OR bend*)) AND (LIMIT-TO (LANGUAGE, "English"))

The patent literature search was conducted in the Espacenet database, which allows for Boolean searches combined with classification searches. A Boolean search was performed within the class "A61B17/16", that includes surgical instruments, devices or methods for bone cutting, breaking or removal means other than saws. The Boolean search was performed to find patent literature with the correct instrument type (drill*, burr*, ream*, trep*, bore) and steering functionality (flex*, steer*, maneuv*, manouv*, deflect*, curv*, articulat*, directional*, orient*, deviat*, bend). The application area was not included in the Boolean search as it was already covered by the classification search. This resulted in the following search query:

cpc = "A61B17/16/low" AND ((ta = "drill*" OR ta = "burr*" OR ta = "ream*" OR ta = "trep*" OR ta = "bore") AND (ta = "flex*" OR ta = "steer*" OR ta = "maneuv*" OR ta = "manoeuv*" OR ta = "deflect*" OR ta = "curv*" OR ta = "articulat*" OR ta = "directional*" OR ta = "orient*" OR ta = "deviat*" OR ta = "bend*"))

Only WO (World) patent applications in English were considered, using the filter options in the Espacenet interface.

6.2.2. INCLUDED LITERATURE
The scientific and patent literature identified underwent screening to determine eligibility based on pre-set criteria. As this study aims to present an overview of steerable bone drills it was decided to only include scientific and patent literature specifically outlining the design of an instrument capable of creating a curved tunnel through bone. Literature records solely concentrating on aspects such as instrument handle design, path planning, or tissue interaction forces were excluded from consideration. Initially, the title and abstract of each record were screened to assess eligibility. For papers that could not be excluded based on title and abstract alone, the full text was screened for eligibility

6.3. RESULTS

6.3.1. IDENTIFIED STEERABLE BONE DRILLS
The search in the Scopus and Espacenet database resulted in 337 identified articles and 339 identified patents (September 2023), respectively. After exclusion of inaccessible records and duplicates, and evaluation based on the eligibility criteria, 19 references from the scientific literature and 59 references from the patent literature were deemed eligible, resulting in a total of 78 included records in this study.

6.3.2. CLASSIFICATION STEERABLE BONE DRILLS
Based on the identified scientific literature and patents on steerable bone drills, a comprehensive classification was defined based on the method of steering employed, namely: 1) Device-defined, 2) Environment-defined, and 3) User-defined steering (Figure 6.2). Device-defined steering utilises inherent mechanisms within the drill itself to

(a) Device-defined steering

(b) Environment-defined steering

(c) User-defined steering

[13, 15, 85, 64, 16, 72, 71, 70, 26, 67, 36, 75, 44, 33, 19, 52, 87, 39, 2, 42, 74, 32, 46, 73, 21, 38, 83, 93, 96, 34, 49, 94, 84, 99, 55, 12, 29, 88, 54, 90, 11, 24, 91, 79, 80, 23, 95]

[23, 60, 92, 56, 62, 61, 63, 66, 69, 78, 45, 17]

[74, 95, 17, 97, 4, 3, 37, 86, 10, 6, 9, 8, 77, 25, 5, 81, 98, 51, 53, 7, 82, 43, 35]
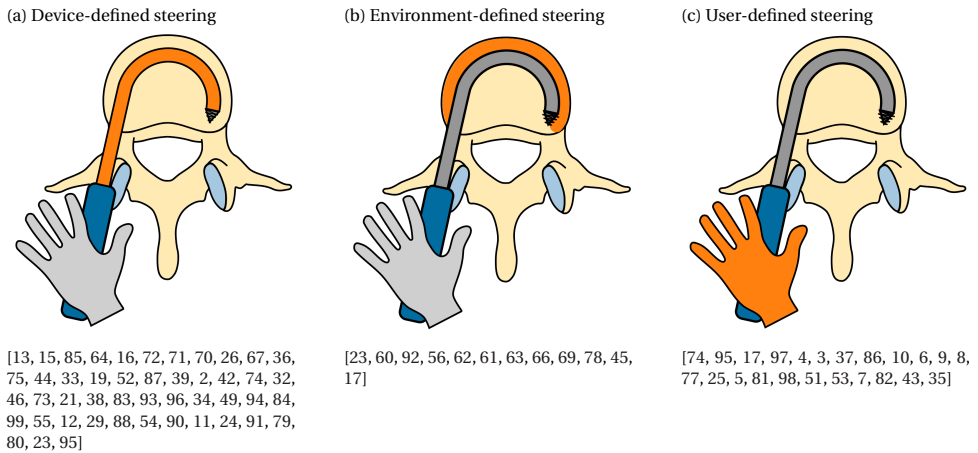
Figure 6.2: Overview of the three identified steering methods utilised by steerable bone drills: 1) Device-defined, 2) Environment-defined, and 3) User-defined steering.

control the drill path, often involving curved drills or integrated guides that determine the drill's path according to pre-programmed trajectories. Environment-defined steering relies on external factors, such as the interaction between the drill and the bone tissue or other environmental cues, which guide the drill's trajectory. Finally, user-defined steering places the control of the drill path in the hands of the operator, allowing for manual adjustment of the drill's direction based on real-time observations and decisions made during the procedure. In the upcoming sections, the identified drills per category will be discussed in detail.

6.3.3. Device-Defined Steering

Forty-seven (47) references describe bone drills in which the device primarily determines the path drilled [13, 15, 85, 64, 16, 72, 71, 70, 26, 67, 36, 75, 44, 33, 19, 52, 87, 39, 2, 42, 74, 32, 46, 73, 21, 38, 83, 93, 96, 34, 49, 94, 84, 99, 55, 12, 29, 88, 54, 90, 11, 24, 91, 79, 80, 23, 95]. The instrument itself defines the pathway, either without (six references) or with a guide (41 references), shaping the curve of the drilled tunnel.

In six references [13, 15, 85, 64, 16, 23], the insertion of a curved drill to create a curved tunnel in bone is presented. These drills deviate from conventional axially rotating bone drills, and instead rely solely on a pushing force to advance the curved drill into the bone, thus creating the desired curved tunnel. For instance, Blain and Kovach [13] propose a tool that allows the surgeon to advance two curved arms with a flat, bevelled, or stepped tip into the bone to create a circular tunnel (Figure 6.3a). Similar rigid curved members are proposed to increase the fixation strength of bone anchors [15]. Sohn [85] introduces a curved needle designed for insertion into the bone to create a curved tunnel for suture placement. The needle, constructed from an elastic material like nitinol, possesses the capability to be straightened using a guide prior to ejection, facilitating access to the suture site. Upon ejection, the needle disengages from the guide and re-

verts to its original curved shape, effectively creating the desired curve. Orbay *et al.* [64] outline a similar principle for fixing bone fractures using curved nails and Brockman and Vangemert [16] utilise the concept to create a curved void for spinal decompression. In contrast, Coope [23] introduces a elastic but straight nail with only an angulated tip, which results in the creation of a curved path due to the resultant forces of the tip and the angulation of the tip when hammering the nail in the bone.

An axially rotating drill, utilising a rigid guide, can create a tunnel along a pre-defined curve [72, 71, 70, 26]. These types of drills consist of a drill tip actuated with a flexible drive shaft, loosely connected to the rigid guide. Advancing the drill with the curved guide into the bone results in the drilling of a curved tunnel. An example of a drill utilising this principle uses disposable cartridges, each including two individual drill bits ($\varnothing$ 2 mm) working together to form one curved tunnel with a diameter of approximately 8 mm (Figure 6.3b) [26]. The drill tip operates at a speed up to 700 rpm, and each cartridge is capable of drilling three to five tunnels [70, 26].

The use of an external guide in combination with a flexible drill allows the surgeon to access certain entry points without risking damage to surrounding tissue, as the guide steers the drill in the desired direction while shielding the surrounding tissue from the rotating drill bit [67, 36, 75, 44, 33, 19, 52, 87, 39, 2, 42, 74, 32, 46, 73, 21, 38, 83, 93]. Saw *et al.* [74] describe a drill design comprising a drill bit actuated by a drive shaft with increased flexibility due to laser-cut slots (Figure 6.3c). The driveshaft is fed through a curved external guide, ensuring the drill tip is oriented in the desired direction to reach the entry point. A serrated edge on the distal end of the guide can be added to engage with the bone, preventing slipping of the drill tip [52, 87].

Besides curving the drill to reach the desired entry points and shielding the surrounding tissue from damage, an external guide can also be used to create a curved tunnel in bone (Figure 6.3d) [32, 46, 73, 21, 38]. Siegal *et al.* [83] propose the use of a segmented guide that, once extended from the rigid and straight outer sleeve, curves in a pre-determined manner based on the tensioning element and the shape of the segments that may interlock. This way, the flexible driveshaft and drill tip is oriented to drill a curved tunnel. A flexible drive shaft used in combination with an external guide can be achieved by employing a flexible material such as nitinol [19, 52, 39], incorporating (laser) cut notches or a spiral pattern [75, 52, 74], using interlocking rigid segments [52], implementing a reduction in diameter [44, 19, 87] or employing a drive cable [33, 2, 42, 46, 21, 38].

Alternatively, instead of using an external guide, an internal guide can be employed to direct the drilling trajectory of a bone drill [96, 34, 49, 94, 84, 99, 55, 12, 29, 95]. These drills comprise a cannulated drill bit actuated with a flexible driveshaft featuring a central lumen. The drill can be advanced over a pre-placed guide that defines the drilling trajectory. The drill design proposed by Walker [96] introduces a drill tip ($\geq \varnothing$ 4.5 mm) and a flexible drive shaft with a central lumen, enabling advancement of the drill over a pre-placed guide wire (Figure 6.3e). The flexibility of the drive shaft is achieved through the use of a flexible material [99], hinged rigid parts, a hollow torsion cable [49, 94], or the use of interlocking segments [96, 34, 84, 55, 12]. Billon *et al.* [12] also propose a cannulated drill that can be advanced over an internal guide. However, in this design a set of guide pins with varying radii is introduced, allowing the surgeon to choose the

6

6

Figure 6.3: Steerable bone drills in which the drilling trajectory is defined by the device comprising a drill bit (yellow), a drive shaft (blue), an outer shaft (green) and a means to steer the drill bit (red). (a) Drill proposed by Blain and Kovach [13] comprising two curved arms (red) with a drill tip (yellow) to create a curved tunnel. (b) Drill proposed by Romano [72] comprising two individual drill bits to create a curved tunnel. (c) Drill proposed by Saw *et al.* [74] with an external guide (red) that bends the drill bit, actuated with a flexible drive shaft (blue), to reach a desired entry point. (d) Drill proposed by Hoigne and Nolte [38] using an external guide (red) to create curved tunnels. (e) Drill proposed by Walker [96] using an internal guide wire (red) over which the tubular flexible drill (blue and yellow) is advanced. (f) Drill proposed by Cragg and Kegan [24] comprising two concentric tubes that can be rotated and translated with respect to each other such that the curved inner tube (red) can be used to steer the drill.

appropriate guide to arrive at the desired location. For drills that curve due to the use of a guide, the friction between the flexible drive shaft and a rigid outer tube can be minimised by incorporating a low-friction coating such as PolyTetraFluoroEthylene (PTFE) [12] or electroplating nickel to create a precise finish [88].

Lv *et al.* [54] propose using a nitinol guide over which the flexible cannulated drill can be advanced. The super-elastic nitinol internal guide allows drilling straight tunnels by retracting the drill with the internal guide within the straight rigid sleeve. After drilling the straight tunnel, the internal guide can be advanced to drill a curved tunnel. Teitel-baum *et al.* [90] describe using two concentric guides through which a flexible drive shaft runs, actuating the drill bit at the distal end. The outer guide is rigid and straight while the second tubular guide is made of a more flexible material and has a curvature. This drill can create straight holes when the second guide is completely withdrawn within the straight outer guide. After reaching the desired length of the straight tunnel, the flexible drill with the flexible guide can be advanced to drill a circular arch (Figure 6.3f). A similar working principle is described in the patents by Amadio *et al.* [11] and Cragg and Kegan [24] and scientific papers [91, 79, 80]. For example, Sharma *et al.* [79] propose using a flexible torque coil to actuate the drill tip, a curved nitinol guide, and a surrounding rigid stainless steel guide. The achieved radius of the drill was 35.7 mm with a $\varnothing$ 6.7 mm drill bit. Deviations in the drill path caused by deformations of the nitinol guide due to the interaction forces with the bone could be decreased by increasing the rotational speed of the drill tip and decreasing the insertion speed of the drill [79].

6.3.4. ENVIRONMENT-DEFINED STEERING

Twelve (12) bone drills create a curved pathway, where the interaction with the environment is the major determinant of the drilled path [23, 60, 92, 56, 62, 61, 63, 66, 69, 78, 45, 17]. The interaction forces with the bone can be used to deflect the drill and influence the drilling trajectory as proposed by Tornier *et al.* [92]. The proposed drill consists of a single tube with a flexible section created by a cut spiral pattern with interlocking teeth. These teeth allow for the transmission of the oscillatory actuation of the drill tip, and the shape of the teeth also defines the radius of curvature of the drill.

Other references describe the utilisation of the difference in resistance between the compact cortical outer layer and the softer porous cancellous bone on the inside of bone to steer the bone drill [56, 62, 61, 63, 66, 69, 78, 45, 17]. These variations in tissue interaction forces cause the drill to deflect, taking the path of the least resistance and creating a curved tunnel. These bone drills include flexible drive shafts that actuate the drill tip and steers passively based on the tissue interaction forces. The design by McManus [56] employs an eccentric drill tip connection to aid the deflection of the drill to create a tunnel along the cortical wall for improved intermedullary nail fixation (Figure 6.4a). The flexible drill by Ohashi *et al.* [62] is designed for bone graft harvesting and comprises a flexible stainless-steel rod to transmit a rotating motion to the drill tip. The drill includes a flexible outer cannula with an outer diameter of 3.5 mm and a length of 250 mm through which the graft material is harvested [62, 61, 63]. The drill design described by Papenfuss [66] is also intended for bone marrow collection and features a drive shaft used to actuate the drill tip at the distal end while allowing for bone marrow collection through the lumen (Figure 6.4b). The flexible hollow drive shaft consists of rigid inter-
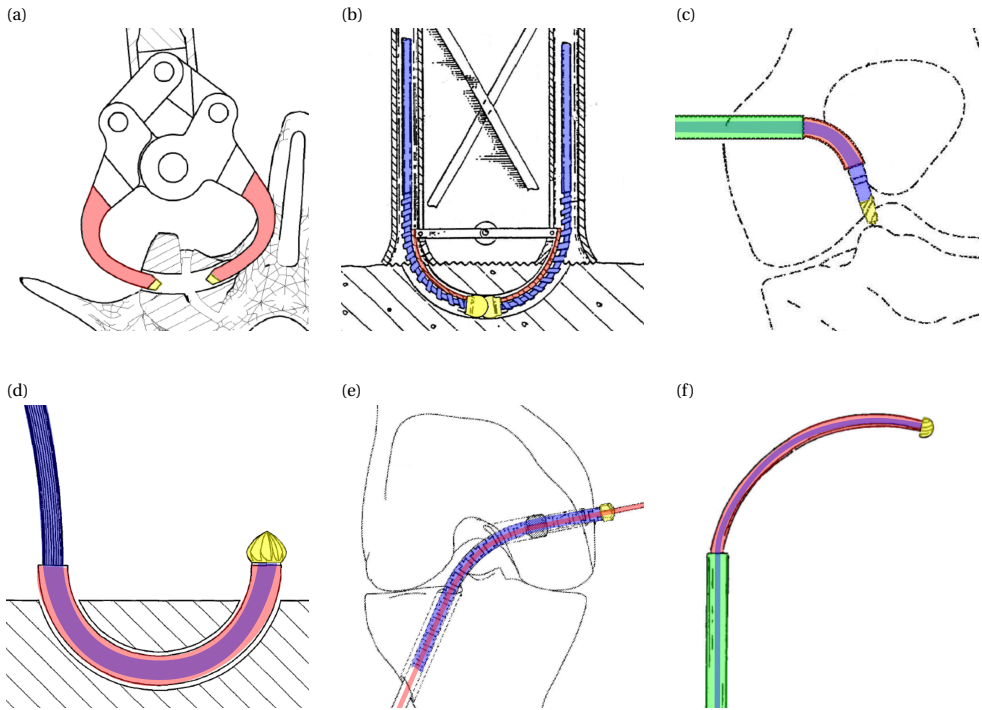
(a)

(b)

(c)

6

Figure 6.4: Steerable bone drills in which the drilling trajectory is defined by the environment comprising a drill bit (yellow) and a flexible drive shaft (blue). (a) Bone drill proposed by McManus [56] with an eccentric drill bit aiding bending of the drill. (b) Bone drill proposed by Papenfuss [66] with a flexible drill shaft (blue) comprising interlocking teeth. (c) Drill developed by de Kater *et al.* [45] comprising two stacked leaf springs (blue) that allow for planar bending of the drill bit (yellow).

locking segments [66, 69, 17].

Where all environment-defined steering drills described thus far utilise an axially rotating motion of the drill bit, the drill by de Kater *et al.* [45] employs an oscillating rotation perpendicular to the drilling direction using and abrasive wheel (Figure 6.4c). This unique drill tip is actuated by two stacked leaf springs, allowing the drill to deflect in a single plane and follow the cortical bone layer.

6.3.5. USER-DEFINED STEERING

Twenty-three (23) bone drills create a curved tunnel in which the user is the major determinant of the drilling trajectory [74, 95, 17, 97, 4, 3, 37, 86, 10, 6, 9, 8, 77, 25, 5, 81, 98, 51, 53, 7, 82, 43, 35]. The user can actively articulate the drill tip, enabling the user to steer the drill along the desired trajectory during the procedure. This steering motion is often facilitated by cables running through the drill, attached at the distal end of the drill. Pulling on one of these cables introduces a specific direction of bending in the drill, giving the user control over the drilling trajectory.

Five found drill designs [17, 97, 4, 3, 37] consist of a discrete number of rigid segments connected by joints that can be bent by the user. The drill presented by Wang

et al. [97] has a tip segment that is able to make sharp curves due to the geared rolling joint connecting the segment to the rigid shaft ($\varnothing$ 4.5 mm). The articulation of the drill tip is achieved by steering wires, and the drill tip is actuated with a U-joint transmission through the central lumen of the drill. Similar designs are proposed in the scientific literature, comprising three jointed segments that can be articulated with steering wires, allowing the drill to drill curved tunnels [4, 3]. The drill tip is actuated by a flexible drive shaft located in the centre of the segments, allowing a rotational speed of up to 3000 rpm. The drill bit can also be actuated by a sleeve of interlocking segments as presented by Bromer (Figure 6.5a) [17]. This drill design can drill curved tunnels based on the interaction forces with the surrounding bone tissue, but the drill tip can also be articulated by the user by either tensioning or loosening one of the two spines that runs through the centre of the drill, causing the drill tip to deflect.

Eleven drill designs [74, 86, 10, 6, 9, 8, 77, 25, 5, 81, 35] describe the use of a central flexible drive shaft for actuation of the drill tip. This drive shaft is surrounded by a notched cannula which establishes a flexible outer sleeve due to compliant hinges. The advantage is that these compliant hinges are easier to manufacture at a small scale compared to regular joints, making miniaturisation of these drills more feasible (Figure 6.5b). The drill of Solzbacher *et al.* [86] comprises a notched outer sleeve ($\varnothing$ 8 mm) of nitinol, allowing the drill to make a 90° curve in one plane while generating high stiffness in the perpendicular plane. Steering cables run through the outer sleeve and are connected to the distal end to bend the drill bit in the desired direction. An alternative to the notched outer sleeve is a helical spring-like structure that can be used to create a flexible outer sleeve [98, 51, 53] (Figure 6.5c). Watanabe *et al.* [98] propose the use of an outer sleeve in a drill design that comprises a number of springs. Deflection of the drill tip is aided by incorporating springs with a lower stiffness closer to the drill tip, while the springs at the base of the drill are stiffer to ensure that input via the steering cables have a minimal effect on the drill shaft.

Steering the drill by changing the drill tip configuration or orientation is also proposed to allow the user to influence the drilling trajectory [95, 7, 82]. The drill design presented by Voor *et al.* [95] comprises a flexible outer shaft with a bevelled end through which the drive shaft for the drill bit with a conical end runs (Figure 6.5d). Pulling the drill tip in the flexible shaft results in a change in the orientation of the drill tip and thus a change in the drilling trajectory. The drill design presented by Alambeigi and Liu [7] proposes an alternative drill design that comprises two flexible concentric tubes, of which the inner tube has an eccentric hole through which the flexible drive shaft runs (Figure 6.5e). Translating and rotating the inner tube relative to the outer tube changes the exit angle of the drill bit, allowing the user to change the drilling trajectory. A similar principle is proposed by Siccardi *et al.* [82].

Ju [43] presents a drill that does not use axial rotation but employs an electrode to remove material surrounding the drill bit by bringing the tissue in a gaseous state through the creation of a high energy electric field. This design minimises the forces acting on the drill, allowing the use of a catheter tube containing the electrodes and steering cables to influence the drilling trajectory.

6

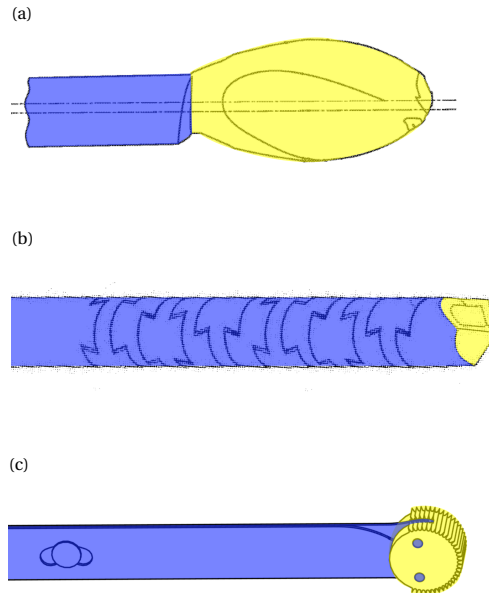(a)   (b)

(c)   (d)

(e)
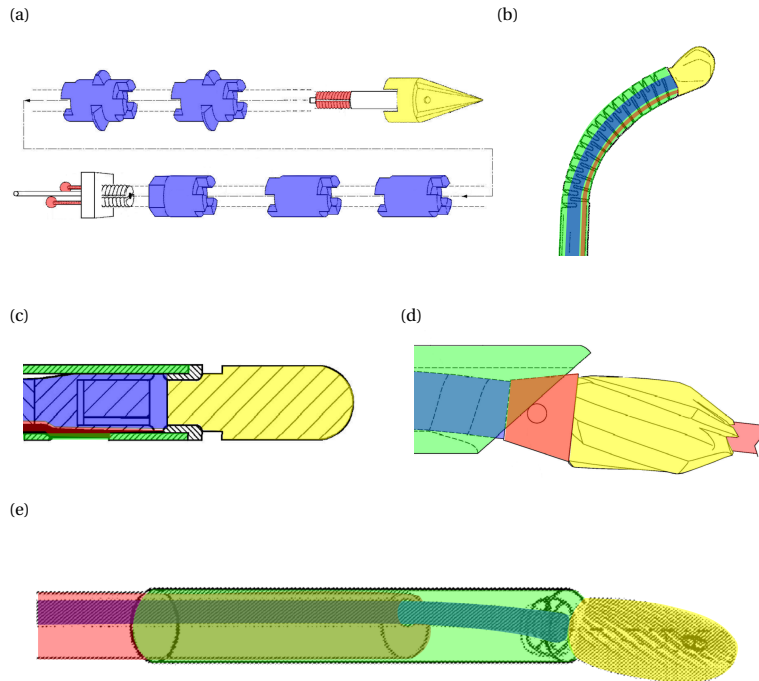
Figure 6.5: Steerable bone drills in which the drilling trajectory is defined by the user comprising a drill bit (yellow), a drive shaft (blue), an outer shaft (green) and a means of steering (red).(a) Steerable bone drill proposed by Bromer [17] comprising two spines that allow articulation of the drill bit to steer the drill in the desired drilling trajectory. (b) Steerable drill proposed by Alambeigi *et al.* [6] using a steering cable (red) that can be pulled to steer the drill in the desired direction. (c) Drill proposed by Liu *et al.* [51] with a drill tip comprising a helical spring-like outer shaft (green) that can be bend by tensioning the steering cable (red). (d) Bone drill proposed by Voor *et al.* [95] using an internal guide (red) as well as a drive shaft (blue) with a conical end (red) that can be tensioned to change the drill tip orientation. (e) Steerable bone drill design proposed by Alambeigi and Liu [7] comprising two concentric flexible tubes that can be translated and rotated with respect to each other to articulate the drill tip through the eccentric drive shaft (blue).

6.4. DISCUSSION

6.4.1. COMPARATIVE ANALYSIS

The objective of this study was to provide a comprehensive overview of steerable bone drills as documented in both scientific and patent literature. The steering methods utilised by these bone drills were categorised in three groups: 1) device-defined, 2) environment-defined and 3) user-defined steering. Notably, more than half (57%) of the steerable drill designs utilises a steering method in which the device plays a major role in determining the drill path, resulting in predefined drill paths.

The majority of drill designs discussed in this review originate from patent literature (76%). While these designs exhibit potential, a validation via proof-of-principle experiments is not required before patent publication. Consequently, the feasibility of these drill designs in a clinical setting remains uncertain. Even with the proof-of-principle experiments found in the scientific literature, not all critical aspects are thoroughly explored. For instance, prolonged heat generation during drilling can lead to bone necrosis [65], but is not specifically explored in the drill designs presented in the included literature, leaving these effects unknown.

The three primary steering methods for steerable bone drills — device-defined, environment-defined, and user-defined steering — each come with distinct advantages and disadvantages that influence their clinical application. Device-defined steering offers predefined drill paths through integrated mechanisms, inhibiting active adjustment of the drill path, but operating at increased precision over environment- and user-defined steering methods. As of now, device-defined steering drills are the only commercially available option and include examples like the *Carevature Dreal* [27], the *Stryker MicroFX OCD* [58], the *Lenkbar FlexMetric* ® [1], the *Zimmer Biomet Precision Flexible Reaming system* [57] and the *DePuy Synthes Cavity Creation Instrument* [22]. In contrast, environment-defined steering adapts to changes in the material properties of the surrounding bone, offering a more responsive and adaptive approach. This method, however, relies on passive steering mechanisms sensitive to individual variations in bone density, posing safety concerns due to unpredictable drill paths. Despite their straightforward design and potential advantages, these drills have not yet reached commercial markets, possibly due to concerns about the risk of cortical bone breach, especially in patients with conditions like osteoporosis. User-defined steering provides surgeons with direct control over the drill's trajectory, allowing for immediate adjustments and flexibility during procedures. While this method can enhance surgical precision, it is more prone to user error and requires complex, user-friendly interfaces to provide precise information about the drill tip's location and orientation. The need for advanced navigation systems may explain why user-defined drills remain in the pre-clinical phase. Each steering method presents a unique balance of control, adaptability, and reliance on either technology or user skill. To address these challenges, the development of hybrid drilling systems that incorporate elements from all three steering methods —combining device-defined precision, environment-defined adaptability, and user-defined flexibility— could provide greater efficacy and safety in complex surgical scenarios, paving the way for future advancements in orthopaedic surgery.

The primary application areas of the drills presented in the included literature is for spine surgery procedures (33%), see Figure 6.6a. These procedures range from fracture

fixation and vertebra decompression to reaching specific target sites such as the intervertebral disk, lesion areas or tumours. Another substantial application area involves steerable drilling through joints. In this application field, the scientific and patent literature records propose steerable bone drills for ligament reconstructions, arthroplasty to restore the function of a joint by resurfacing the bone, or placement of an artificial joint. Ten records (13%), all of which are patents, do not clearly specify an application area for the proposed steerable drill design.

From the temporal distribution of the included literature, it becomes evident that the development of steerable bone drills is relatively recent, arising from 1990 onwards (Figure 6.6b). Since then, the number of steerable bone drills described in literature has been steadily increasing over the years. The development of drills that use a user-defined steering method is more recent, with literature published from 2000 onwards. This trend may be attributed to the need for a user-friendly interface to steer the drill in the desired direction, which may increase the design complexity. Furthermore, effective use of a user-defined steerable bone drill demands real-time and accurate information of the drill's location allowing the user to steer the drill in the desired path to avoid damage to the surrounding tissue. While fluoroscopy is currently employed in spine surgery for real-time 2D navigation, this method exposes both the patient and clinicians to radiation [40]. Alternative navigation possibilities, such as Diffuse Reflectance Spectroscopy (DRS), could be explored in order to real-time detect cortical breaches to prevent damage to surrounding anatomy [20].

6.4.2. Limitations and Future Research

This review offers a comprehensive overview of steerable bone drills described in both patent and scientific literature. The majority of the drills included in this review employ a conventional axial rotating drill bit. For future research, exploring alternative drilling methods and their implications on steerable bone drill development would be insightful. Alternative drilling methods, such as water jet drilling or piezoelectric drilling, are associated with higher quality of the cuts and less thermal damage to the surrounding bone [28, 30]. Furthermore, waterjet drilling is presented as an alternative drilling method that could potentially ease the development of a steerable bone drill by using flexible tubing [28]. However, these alternative drilling methods have not been utilised in the included steerable bone drills, making them an interesting topic for future research.

The broader clinical adoption of steerable bone drills faces several technological challenges that must be addressed to enhance their effectiveness and integration into surgical practices, see Table 6.1. One primary limitation is the precision and reliability of current steering mechanisms. Although, the included literature presents various validation experiments were generally limited to phantom studies, which usually entail homogenous materials, indicating that there are still steps to be taken before steerable bone drills can be applied in a clinical setting.

Comparing the various steering methods of steerable bone drills with traditional straight-path drilling in quantitative terms reveals significant advantages in terms of surgical precision. Additionally, these advanced steering technologies have the potential to decrease the operative time by allowing more precise targeting of the lesion and improving patient outcomes. However, another factor that needs to be considered is the poten-

(a)

(b)
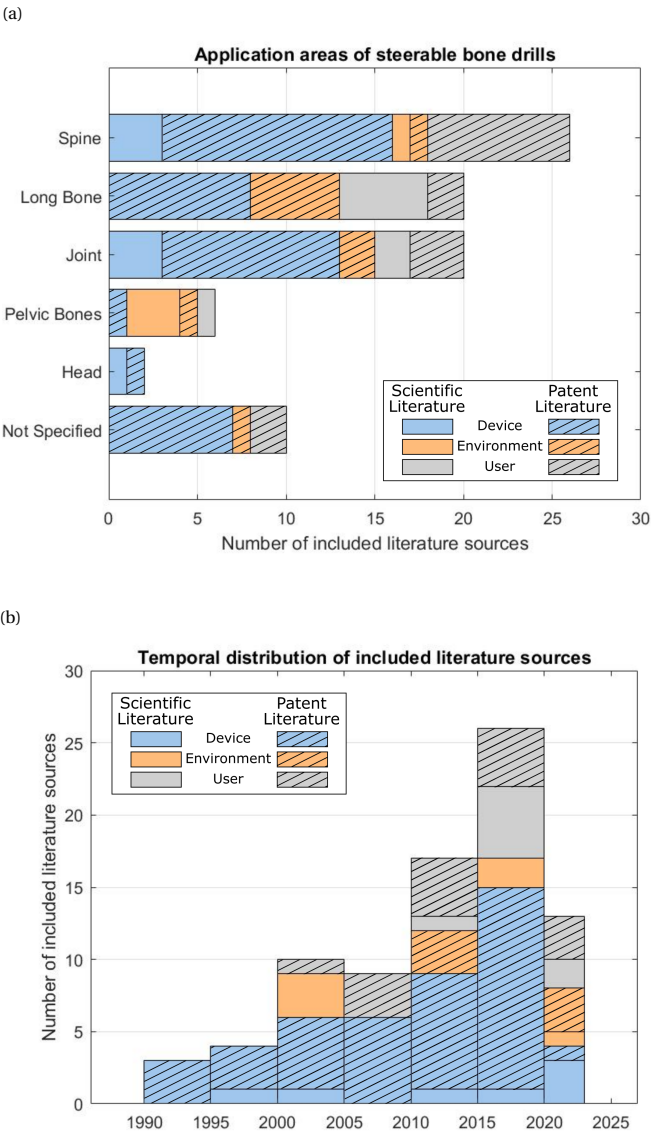
Figure 6.6: Overview of the included literature. (a) Application area of the steerable bone drills described in the included scientific and patent literature. (b) Temporal distribution of the publication date of the included literature.

Table 6.1: Comparison of Steering Methods of Steerable Bone Drills.

Steering Method	Device-defined Steering	Environment-defined Steering	User-defined Steering
Versatility	Low versatility, due to predetermined drill path defined by the device. Path adjustments impossible during the procedure.	Medium versatility, potential path adjustments based on the interaction forces with the environment and potential to drill a path along the cortical bone layer.	High versatility, adjustment to the path during the procedure possible by inputs of the user.
Precision	High precision due to predetermined drill paths using rigid guides.	Precision dependent on the bone quality and thus interaction forces.	Precision dependent on the user. Potential high precision with proper feedback systems.
Reliability	Very reliable due to the use of rigid guides.	Reliable, but failure possible when encountering excessive interaction forces.	Reliable, but failure possible due to flexible moving drill elements.
Safety	High, dependent on proper pre-operative planning.	Medium, dependent on bone quality. Potential of cortical breach with low bone quality.	Medium, dependent on the skill of the operator. Prone to user error.

tial increased risk of complications due to user-error. Further research should, therefore, be executed to determine the advantages of using non-straight drill paths on the long-term success rates of orthopaedic procedures.

Another aspect that is partly overlooked, but necessary to enable steerable bone drilling in a clinical setting, is the navigation of the drill. Using a steerable bone drill in clinical practice requires extensive real-time knowledge of the drill's location and the patient's anatomy. Particularly, drills intended for actively steering by the user necessitate real-time awareness of the drill's location within the patient's anatomy, allowing the surgeon to guide the drill in the preferred direction during the procedure and can be used as a means of safeguarding patient safety. Unfortunately, the integration of advanced sensors and feedback systems to improve steering precision remains a technical challenge due to the dimensional constraints. Especially in environment-defined steering inte-

grating feedback systems is challenging, as these systems need to be highly responsive and adaptive to dynamic changes in bone morphology and density during procedures. Incorporating real-time navigation techniques for steerable bone drills would be crucial for advancing their development.

The integration of steerable bone drills with robotic systems presents a promising avenue for overcoming these challenges. Robotics can enhance the precision and repeatability of steerable drills by incorporating advanced algorithms for path planning and real-time adjustments of the drill path. Robotic systems can also integrate sophisticated imaging or shape sensing technologies, such as Computed Tomography (CT) or optical fibers containing Fiber Bragg Gratings (FBGs), to provide continuous feedback and improve the accuracy of the different steering methods. Future research should focus on developing robotic platforms that can be integrated with steerable drills and allow for easy integration into the orthopaedic procedures.

6.5. CONCLUSION

Steerable bone drills have potential to significantly benefit a range of (orthopaedic) procedures by enhancing manoeuvrability, facilitating access to target areas, and minimising damage to surrounding anatomy. This study offers a comprehensive overview of steerable bone drill designs as documented in both patent and scientific literature. The search query, coupled with pre-defined inclusion and exclusion criteria, resulted in the inclusion of 59 patent and 19 scientific literature references. Based on the included references, it was found that the drilling trajectory could be defined by: (1) the device, (2) the environment, or (3) the user. In the first category, the drilling trajectory is integrated into the bone drill and is thus predetermined before the procedure. In the second category, the drilling trajectory is defined during the procedure based on the tissue interaction forces between the drill and the surrounding tissue. The drills in the third category enable the user to adapt the drilling trajectory during the procedure. This comprehensive overview aims to provide insights into the current and future development of steerable bone drills, serving as a valuable source of inspiration for the development of innovative steerable bone drill designs.

6

BIBLIOGRAPHY

[1] *ACL Reamers – Lenkbar*. en-US. (Visited on 08/10/2022).

[2] Chandra M. Agrawal, Kyriacos a Athanasiou, and Dan R. Lanctot. "Creating Holes in Bone Via the Medullary Cavity". WO9912485A1. Mar. 1999.

[3] Ahmad Nazmi Bin Ahmad Fuad et al. "A Robotic Flexible Drill and Its Navigation System for Total Hip Arthroplasty". en. In: *Annals of Biomedical Engineering* 46.3 (Mar. 2018), pp. 464–474. (Visited on 07/21/2023).

[4] Ahmad Nazmi Bin Ahmad Fuad et al. "On the development of a new flexible drill for orthopedic surgery and the forces experienced on drilling bovine bone". en. In: *Proceedings of the Institution of Mechanical Engineers, Part H: Journal of Engineering in Medicine* 232.5 (May 2018), pp. 502–507. (Visited on 06/12/2023).

[5] John Martin Aho and Andrew R. Sennett. "Devices and Methods for Vertebrostenting". WO2010111246A1. Sept. 2010.

[6] Farshid Alambeigi and Mehran Armand. "Steerable Device for Treatment of Hard-Tissue-Related Diseases and Minimally Invasive Surgery". WO2018160269A1. Sept. 2018.

[7] Farshid Alambeigi and Yang Liu. "Fully Steerable Flexible Curved-Drilling Robot Device, System and Method". WO2023023634A1. Feb. 2023.

[8] Farshid Alambeigi et al. "A Curved-Drilling Approach in Core Decompression of the Femoral Head Osteonecrosis Using a Continuum Manipulator". In: *IEEE Robotics and Automation Letters* 2.3 (July 2017). Conference Name: IEEE Robotics and Automation Letters, pp. 1480–1487.

[9] Farshid Alambeigi et al. "Design and characterization of a debriding tool in robot-assisted treatment of osteolysis". In: *2016 IEEE International Conference on Robotics and Automation (ICRA)*. May 2016, pp. 5664–5669.

[10] Farshid Alambeigi et al. "Inroads Toward Robot-Assisted Internal Fixation of Bone Fractures Using a Bendable Medical Screw and the Curved Drilling Technique". In: *2018 7th IEEE International Conference on Biomedical Robotics and Biomechatronics (Biorob)*. ISSN: 2155-1782. Aug. 2018, pp. 595–600.

[11] Jordan Amadio, Farshid Alambeigi, and Susheela Sharma. "Concentric Tube Drilling Robot Device, System and Method". WO2023077071A1. May 2023.

[12] Adrien Billon et al. "Drilling Device for Making a Bone Canal with a Curved Profile Inside the Body of a Vertebra". WO2012101354A1. Aug. 2012.

[13] Jason Blain and Eric Kovach. "Vertebral Facet Joint Drill and Method of Use". WO2012024162A1. Feb. 2012.

6

[14]   David W Boone. "Complications of iliac crest graft and bone grafting alternatives in foot and ankle surgery". en. In: *Foot and Ankle Clinics* 8.1 (2003), pp. 1–14.

[15]   Dale G. Bramlet, Peter Sterghos, and John Sodeika. "Surgical Fastener Assembly". WO0044293A1. Aug. 2000.

[16]   Christopher Scott Brockman and Geoffrey James Vangemert. "Device for Creating a Void Space in a Living Tissue, the Device Including a Handle with a Control Knob That Can Be Set Regardless of the Orientation of the Handle". WO2015057195A1. Apr. 2015.

[17]   Nicholas Bromer. "Articulated Bone Drill and Tap". WO2014185887A1. Nov. 2014.

[18]   Andreas Burkart et al. "Precision of ACL Tunnel Placement Using Traditional and Robotic Techniques". In: *Computer Aided Surgery* 6.5 (Jan. 2001). Publisher: Taylor & Francis _eprint: https://doi.org/10.3109/10929080109146092, pp. 270–278. (Visited on 12/18/2023).

[19]   J. Brook Burley et al. "Flexible Drill Bit and Angled Drill Guide for Use with the Same". WO2014107729A3. Feb. 2015.

[20]   Gustav Burström et al. "Diffuse reflectance spectroscopy accurately identifies the pre-cortical zone to avoid impending pedicle screw breach in spinal fixation surgery". In: *Biomedical Optics Express* 10.11 (Oct. 24, 2019), pp. 5905–5920. (Visited on 09/16/2021).

[21]   Allen Carl et al. "Systems, Devices and Apparatuses for Bony Fixation and Disk Repair and Replacement Methods Related Thereto". WO2007079242A2. July 2007.

[22]   *Cavity Creation Instrument | DePuy Synthes*. en-US. (Visited on 01/26/2024).

[23]   Robin John Noel Coope. "Cannulated Hammer Drill Attachment". WO2014075165A1. May 2014.

[24]   Andrew H. Cragg and Jonathan Kagan. "Apparatus for Forming Shaped Axial Bores Through Spinal Vertebrae". WO0160262A1. Aug. 2001.

[25]   Lawrence Crainich, Andrew R. Sennett, and Joseph E. Trabka. "Drills and Methods for Vertebrostenting". WO2008076330A1. June 2008.

[26]   Gary L. Dockery. "The romano drill: A new surgical curved drill system". In: *The Journal of Foot and Ankle Surgery* 34.3 (May 1995), pp. 273–275. (Visited on 09/27/2023).

[27]   *Dreal*. en-US. (Visited on 01/11/2024).

[28]   Steven den Dunnen et al. "How do jet time, pressure and bone volume fraction influence the drilling depth when waterjet drilling in porcine bone?" en. In: *Journal of the Mechanical Behavior of Biomedical Materials* 62 (Sept. 2016), pp. 495–503. (Visited on 07/19/2023).

[29]   Alfred A. Durham. "Method and Devices for Use in Bone Fixation Procedures". WO0012036A1. Mar. 2000.

[30] Jônatas Caldeira Esteves et al. "Dynamics of bone healing after osteotomy with piezosurgery or conventional drilling– histomorphometrical, immunohistochemical, and molecular analysis". In: *Journal of Translational Medicine* 11.1 (Sept. 2013), p. 221. (Visited on 07/19/2023).

[31] Brian Forsythe et al. "Optimization of Anteromedial Portal Femoral Tunnel Drilling With Flexible and Straight Reamers in Anterior Cruciate Ligament Reconstruction: A Cadaveric 3-Dimensional Computed Tomography Analysis". en. In: *Arthroscopy: The Journal of Arthroscopic & Related Surgery* 33.5 (May 2017), pp. 1036–1043. (Visited on 06/12/2023).

[32] Eduardo Gonzalez-Hernandez. "Curved Assembly for Reattachment of Fragmented Bone Segments". WO2008128067A2. Oct. 2008.

[33] Gary L. Graham et al. "Torqueable Control Handle with Locking Mechanism". WO2015050940A1. Apr. 2015.

[34] Jeremy Granville-Chapman, R. Steve Bale, and Ian A. Trail. "Use of flexible elbow reamers for cement removal in the humerus during revision shoulder arthroplasty". en. In: *Shoulder & Elbow* 9.2 (Apr. 2017). Publisher: SAGE Publications Ltd, pp. 133–135. (Visited on 09/27/2023).

[35] Jerry R. Griffiths and Jose Fernandez. "System and Method for Forming a Curved Tunnel in Bone". WO2014081759A1. May 2014.

[36] Bryan D. Haughom et al. "Arthroscopic Acetabular Microfracture With the Use of Flexible Drills: A Technique Guide". In: *Arthroscopy Techniques* 3.4 (Aug. 2014), e459–e463. (Visited on 12/07/2023).

[37] Gregory a Helm et al. "Method and System for Fusing a Spinal Region". WO0067650A1. Nov. 2000.

[38] Dominik J. Hoigne and Lutz Nolte. "Surgical Drilling Device". WO2008031245A2. Mar. 2008.

[39] Bryan Patrick Howard et al. "Suture Anchor Implantation Instrumentation System". WO2011009043A1. Jan. 2011.

[40] Ibrahim Hussain et al. "Evolving Navigation, Robotics, and Augmented Reality in Minimally Invasive Spine Surgery". In: *Global Spine Journal* 10.2 (Apr. 1, 2020), 22S–33S. (Visited on 12/01/2021).

[41] Muhammad Jamil et al. "Comprehensive analysis on orthopedic drilling: A state-of-the-art review". en. In: *Proceedings of the Institution of Mechanical Engineers, Part H: Journal of Engineering in Medicine* 234.6 (June 2020), pp. 537–561. (Visited on 06/12/2023).

[42] Wesley D. Johnson et al. "Flexible Cutting Tool and Methods for Its Use". WO9731577A1. Sept. 1997.

[43] Don Soo Ju. "Electrode Suction Drill System". WO2020096220A1. May 2020.

[44] Geoffrey Ian Karasic et al. "Anchor Delivery System". WO2018237280A1. Dec. 2018.

6

[45] Esther P. de Kater et al. "Tsetse fly inspired steerable bone drill—a proof of concept". In: *Frontiers in Bioengineering and Biotechnology* 11 (2023). (Visited on 06/12/2023).

[46] Kaj Klaue. "Device for Introducing a Bent Nail into a Bone". WO2010133933A1. Nov. 2010.

[47] Douglas A. Kuhn and Morey S. Moreland. "Complications Following Iliac Crest Bone Grafting:" en. In: *Clinical Orthopaedics and Related Research* 209.&NA; (Aug. 1986), pp. 224–226. (Visited on 12/01/2023).

[48] JuEun Lee, Craig L. Chavez, and Joorok Park. "Parameters affecting mechanical and thermal responses in bone drilling: A review". In: *Journal of Biomechanics* 71 (Apr. 2018), pp. 4–21. (Visited on 12/18/2023).

[49] Jean Yves Leroy et al. "Flexible and Cannulated Cutting Device". WO2017125667A1. July 2017.

[50] Jay R. Lieberman et al. "Osteonecrosis of the Hip: Management in the Twenty-first Century". en-US. In: *JBJS* 84.5 (May 2002), p. 834. (Visited on 09/21/2023).

[51] Y. King Liu et al. "Steerable Curvable Vertebroplasty Drill". WO2010135606A1. Nov. 2010.

[52] Marc Long, Kyle Craig Pilgeram, and Marc Charles Wennogle. "Flexible Micro-drilling Instrumentation, Kits and Methods". WO2012109334A2. Aug. 2012.

[53] Antony Lozier, Nicolas Pacelli, and John Dawson. "Instruments, Implants, and Methods for Fixation of Vertebral Compression Fractures". WO2009089252A1. July 2009.

[54] Shiwen Lv et al. "Vertebral Balloon Dilation System". WO2015085837A1. June 2015.

[55] Thomas Martin. "Flexible Spinal Driver or Drill with a Malleable Core, and/or Fixed Core Radius". WO2015200018A1. Dec. 2015.

[56] Joshua McManus. "Clavicle Reamer". WO2015069675A1. May 2015.

[57] *Medial Portal ACL Reconstruction*. en-US. (Visited on 08/10/2022).

[58] *MicroFX OCD - Osteochondral Drilling System*. en-US. (Visited on 08/10/2022).

[59] Genya Mitani et al. "Tibia Rotational Technique to Drill Femoral Bone Tunnel in Anatomic Double-Bundle Anterior Cruciate Ligament Reconstruction". en. In: *Arthroscopy Techniques* 3.4 (Aug. 2014), e495–e499. (Visited on 07/19/2023).

[60] Masanori Mizukami et al. "Bone Drill Reamer". WO2017042914A1. Mar. 2017.

[61] K. Ohashi et al. "A manipulator with flexible drilling unit for hematopoietic stem cell harvesting". In: *Proceedings of the Second Joint 24th Annual Conference and the Annual Fall Meeting of the Biomedical Engineering Society] [Engineering in Medicine and Biology*. Vol. 1. ISSN: 1094-687X. Oct. 2002, 689–690 vol.1. (Visited on 09/27/2023).

[62] K. Ohashi et al. "Stem cell harvesting device with passive flexible drilling unit for bone marrow transplantation". In: *IEEE Transactions on Robotics and Automation* 19.5 (Oct. 2003). Conference Name: IEEE Transactions on Robotics and Automation, pp. 810–817.

[63] Kota Ohashi et al. "A Stem Cell Harvesting Manipulator with Flexible Drilling Unit for Bone Marrow Transplantation". en. In: *Medical Image Computing and Computer-Assisted Intervention — MICCAI 2002.* Ed. by Takeyoshi Dohi and Ron Kikinis. Lecture Notes in Computer Science. Berlin, Heidelberg: Springer, 2002, pp. 192–199. ISBN: 978-3-540-45786-2.

[64] Jorge L. Orbay, Javier Castaneda, and Ernesto Hernandez. "Fracture fixation system". EP2292166A1. Mar. 2011.

[65] Rupesh Kumar Pandey and SS Panda. "Drilling of bone: A comprehensive review". In: *Journal of clinical orthopaedics and trauma* 4.1 (2013), pp. 15–30.

[66] Erik Papenfuss. "Cutting Head for Tissue Collection Device". WO2021050046A1. Mar. 2021.

[67] John Peloza et al. "The use of a new high-speed shielded curved drill is associated with improved intraoperative and clinical outcomes after cervical corpectomy and fusion procedures: a retrospective case series". en. In: *Journal of Orthopaedic Surgery and Research* 18.1 (May 2023), p. 364. (Visited on 09/27/2023).

[68] Peter Plinkert and Hubert Löwenheim. "Trends and Perspectives in Minimally Invasive Surgery in Otorhinolaryngology-Head and Neck Surgery". en. In: *The Laryngoscope* 107.11 (1997). _eprint: https://onlinelibrary.wiley.com/doi/pdf/10.1097/00005537-199711000-00011, pp. 1483–1489. (Visited on 09/20/2023).

[69] Jose Rivera. "Flexible Trephine Reamer". WO2020247063A1. Dec. 2020.

[70] Jack W. Romano. "Apparatus for Drilling a Curved Bore". WO9426177A1. Nov. 1994.

[71] Jack W. Romano. "Curved Bore Drilling Apparatus". WO9111962A1. Aug. 1991.

[72] Jack W. Romano. "Curved Bore Drilling Method and Apparatus". WO9111961A1. Aug. 1991.

[73] Jude L. Sasing et al. "Surgical Cutting Devices and Methods". WO2008054752A2. May 2008.

[74] Khay Yong Saw, Nathan C. Maier, and Sureshan Sivananthan. "Arthroscopic Drill Blade and Arthroscopic Drill Access System Made Therefrom". WO2018058126A1. Mar. 2018.

[75] Jeffrey M. Schwamb, Phillip J. Berman, and John R. Prisco. "Surgical Bur and Related Surgical Instruments". WO2019168583A1. Sept. 2019.

[76] Alexander Sendrowicz et al. "Surgical drilling of curved holes in bone–a patent review". In: *Expert review of medical devices* 16.4 (2019). Publisher: Taylor & Francis, pp. 287–298.

6

[77] Andrew R. Sennett, Randy J. Beyreis, and Brett A. Williams. "Devices and Methods for Fracture Reduction". WO2009155319A1. Dec. 2009.

[78] Andrew William Seykora, Larry W. Ehmke, and Brent Lane Norris. "Bone Harvesting System". WO2020068592A1. Apr. 2020.

[79] Susheela Sharma et al. "A Concentric Tube Steerable Drilling Robot for Minimally Invasive Spinal Fixation of Osteoporotic Vertebrae". In: *IEEE Transactions on Biomedical Engineering* (2023). Conference Name: IEEE Transactions on Biomedical Engineering, pp. 1–11.

[80] Susheela Sharma et al. "A novel concentric tube steerable drilling robot for minimally invasive treatment of spinal tumors using cavity and u-shape drilling techniques". English. In: *2023 IEEE International Conference on Robotics and Automation (ICRA)*. IEEE, July 2023, pp. 4710–4716. (Visited on 09/27/2023).

[81] Bifeng Shen, Dawei Zhu, and Lianghui Fu. "Controllably Bendable Vertebroplasty Device and Component and Method Thereof". WO2020119736A1. June 2020.

[82] Francesco Siccardi et al. "Guide for Flexible Bone Drill and Bone Resection Instrument". WO2018122687A1. July 2018.

[83] Tzony Siegal, Oded Loebl, and Didier Toubia. "Surgical Device with Combined Differential Gearing and Deflection Mechanism". WO2015004667A1. Jan. 2015.

[84] Leon Slobitker and Ran Weisman. "Flexible Bone Tool". WO2015121869A1. Aug. 2015.

[85] Ze Ev Sohn. "Suture Insertion Device for the Treatment of Urinary Stress Incontinence". WO9747246A1. Dec. 1997.

[86] Rene M Solzbacher et al. "Bone cyst surgery robot with bendable drilling and remote control". en. In: *Journal of Computational Design and Engineering* 9.6 (Nov. 2022), pp. 2495–2505. (Visited on 07/21/2023).

[87] Peter Klindt Sorensen et al. "A System for Use in Tissue Repair". WO2012048050A1. Apr. 2012.

[88] Stanley D. Stearns and H. Max Loy. "Bone Drill and Methods of Treatment Delivery". WO2008103606A2. Aug. 2008.

[89] S. Tashman et al. "Abnormal rotational knee motion during running after anterior cruciate ligament reconstruction". English. In: *American Journal of Sports Medicine* 32.4 (2004), pp. 975–983.

[90] George P. Teitelbaum et al. "Methods and Devices for Transpedicular Discectomy". WO2004107955A2. Dec. 2004.

[91] George P. Teitelbaum et al. "Transpedicular Intervertebral Disk Access Methods and Devices". WO2004043271A1. May 2004.

[92] Alain Tornier et al. "Articulated Drill and the Reciprocating Motion Drive Device Thereof". WO2013079845A1. June 2013.

[93] Matteo Tutino et al. "Endoscopic Intracranial Craniofacial and Monobloc Osteotomies with the Aid of a Malleable High-Speed Pneumatic Drill: A Cadaveric and Clinical Study:" en. In: *Annals of Plastic Surgery* 44.1 (Jan. 2000), pp. 1–7. (Visited on 07/19/2023).

[94] Guy Viart et al. "Device for Percutaneous Transpedicular Fusion". WO2016207501A1. Dec. 2016.

[95] Michael J. Voor, David Seligson, and Richard Joseph Ackermann. "Systems and Methods for Intramedullary Preparations". WO2018075925A1. Apr. 2018.

[96] Peter Walker. "Improvements in Anterior Cruciate Ligament Reconstruction". WO2019161436A1. Aug. 2019.

[97] Yan Wang et al. "A Handheld Steerable Surgical Drill With a Novel Miniaturized Articulated Joint Module for Dexterous Confined-Space Bone Work". In: *IEEE Transactions on Biomedical Engineering* (2022). Conference Name: IEEE Transactions on Biomedical Engineering, pp. 1–1.

[98] Hiroki Watanabe et al. "Development of a "steerable drill" for acl reconstruction to create the arbitrary trajectory of a bone tunnel". In: *2011 IEEE/RSJ International Conference on Intelligent Robots and Systems*. ISSN: 2153-0866. Sept. 2011, pp. 955–960.

[99] Christian Woll, Duane Dickens, and Richard Woods. "Orthopedic Intramedullary Fixation System". CA2561552A1. Nov. 2005.

[100] Masayoshi Yagi et al. "Biomechanical Analysis of an Anatomic Anterior Cruciate Ligament Reconstruction". en. In: *The American Journal of Sports Medicine* 30.5 (Sept. 2002). Publisher: SAGE Publications Inc STM, pp. 660–666. (Visited on 12/18/2023).

6

7

DESIGN OF A FLEXIBLE BONE DRILL

Orthopaedic surgery relies on bone drills to create tunnels for fracture fixation, bone fusion, or tendon repair. Traditional rigid and straight bone drills often pose challenges in accessing the desired entry points without risking damage to the surrounding anatomical structures, especially in minimal invasive procedures. In this study, we explore the use of hydraulic pressure waves in a flexible bone drill design. The HydroFlex Drill includes a handle for generating a hydraulic pressure wave in the flexible, fluid-filled shaft to transmit an impulse to the hammer tip, enabling bone drilling. We evaluated seven different hammer tip shapes to determine their impact on drilling efficiency. Subsequently, the most promising tip was implemented in the HydroFlex Drill. The HydroFlex Drill Validation demonstrated the drill's ability to successfully transfer the impulse generated in the handle to the hammer tip, with the shaft in different curves. This combined with the drill's ability to create indentations in bone phantom material is a promising first step towards the development of a flexible or even steerable bone drill. With ongoing research to enhance the drilling efficiency, the HydroFlex Drill opens possibilities for a range of orthopaedic surgical procedures where minimally invasive drilling is essential.

7

7.1. Introduction

7.1.1. Challenges in Orthopaedic Surgery

Orthopaedic surgery with its focus on the musculoskeletal system, confronts persistent challenges in procedures such as drilling through bone for fracture fixation, bone fusion, or tendon repair [4]. While conventional rigid and straight bone drills have proven user-friendly, reaching all desired locations with these drills poses challenges due to their limited manoeuvrability, especially in minimally invasive procedures. The introduction of flexible and steerable bone drills holds promise in overcoming these limitations, offering enhanced reachability in challenging areas, minimising damage to surrounding tissue, and creating superior tunnels for fixation of tendons and bone anchors. As an example, steerable bone drills allow for the integration of curved tunnels and innovative bone anchors which has the potential to enhance the fixation strength of the currently used spinal bone anchors [1].

7.1.2. Steerable Bone Drills: State-of-the-Art

Despite a variety of steerable bone drills presented in patent literature, there are currently no commercial bone drills available that allow real-time trajectory adjustment during surgery [9]. Although steerable bone drills are not commercially available, there are bone drills that allow for drilling of slightly more complex tunnels. These drills comprise a flexible drive shaft connected to a rotating drill tip creating a flexible drill that can be advanced through a curved guide [2], or, in case of a tubular drill, can be advanced over a pre-placed guide wire [5]. With the aid of a guide slightly curved or slightly angulated tunnels can be created. Several steerable bone drill designs are presented in scientific literature. These drills also comprise a flexible drive shaft that actuates a rotating drill tip that can be angulated by the use of steering cables [12, 10]. Although the presented designs are promising the design of a steerable bone drill that uses an axially rotating drill tip to advance through the bone tissue presents a challenge as the required flexibility for creating a curved tunnel compromises the drill's buckling resistance needed to advance through hard materials like bone. Furthermore, heat generation during drilling can result in bone necrosis. Although there is a lot of research describing the factors influencing heat generation, such as drill speed, drill diameter and the use of coolant, heat generation remains a problem when using an axially rotating bone drill [4]. In the case of a steerable drill, the heat generation might even be a larger problem as heat generation is more severe when using a guide as the added friction between the rotating drill and the guide further increases the drills temperature [3]. Alternative drilling methods such as ultrasonic drilling or hammering offer potential advantages over rotating drilling as hammering generates less heat compared to traditional drilling, reducing the risk of bone necrosis [13]. However, the challenge lies in applying an impulse to bone tissue through a flexible shaft.

Addressing this challenge, Sakes *et al.* [6] introduced a flexible catheter filled with a fluid capable of transferring an impulse with the aim to hammer through calcifications in blood vessels. The transfer of the impulse through the flexible catheter is achieved by utilisation of a hydraulic pressure wave. A hydraulic pressure wave is a standing wave that comprises of high-pressure regions and low-pressure regions that can propagate

through a fluid filled tube. While the catheter by Sakes *et al.* has a smaller diameter (1.4 mm) than a bone drill (~4 mm) and calcifications in blood vessels differ in material properties from bone, the use of a hydraulic pressure wave holds promise in the design of a flexible bone drill. The use of a hydraulic pressure wave allows for the transfer of an impulse while facilitating the necessary bending for drilling curved tunnels without the risk of buckling.

   This study proposes the application of a hydraulic pressure wave to transfer an impulse through a flexible fluid-filled bone drill, thereby facilitating the development of the HydroFlex Drill. The HydroFlex Drill comprises a handle in which the pressure wave is generated that propagates through the flexible shaft. At the distal end, the pressure wave is transferred to the hammer tip where a hammer stroke, and thus impact, is generated onto the bone (Figure 7.1).

7.1.3. GOAL OF THIS STUDY
The goal of this study was to design and evaluate a flexible bone drill incorporating the use of a hydraulic pressure wave for the drilling of curved tunnels through bone. A concept design and prototype of the HydroFlex Drill was created and validated. The initial validation involved the evaluation of seven hammer tip shapes based on their penetration rate through bone phantom material. Subsequently, the optimal tip shape, determined through this evaluation, was integrated into the HydroFlex Drill prototype. The drill's performance was then assessed in both straight and curved configurations, providing valuable insights into its potential clinical application and broader implications for orthopaedic surgery.

7.2. HYDROFLEX DRILL DESIGN
7.2.1. CONCEPT DESIGN
The primary function of the handle is to allow the user to generate a hydraulic pressure wave. The handle incorporates a spring, which is tensioned by pulling the knob backwards (Figure 7.2a). Upon loosening the knob, the spring releases and forces a mass forward striking an impulse delivery plunger at the proximal side of the flexible shaft. The generated impulse is transferred from the impulse delivery plunger located within the flexible, fluid-filled shaft to the fluid, minimising losses due to wave reflection.

   In the shaft, efficient transfer of the impulse from the handle to the hammer tip by a hydraulic pressure wave is crucial. Consequently, the shaft is designed as a radially incompressible hollow tube with a smooth inner surface to limit losses during impulse transfer. Additionally, the shaft's flexibility allows for potential future adaptation into a steerable drill. Besides the shaft design, the fluid medium used to transfer the impulse influences the efficiency of the impulse transfer [7]. As the drill is intended for clinical use and the risks related to leaking of the fluid must be minimised, saline solution would be preferred as fluid to transfer the impulse.

   The momentum of the hydraulic pressure wave is effectively transferred to the bone material through the hammer tip. This tip comprises a pin fitting within the drill shaft, facilitating the transfer of the pressure wave's momentum to the surrounding bone. An internal spring within the hammer tip ensures its return to the initial position after each
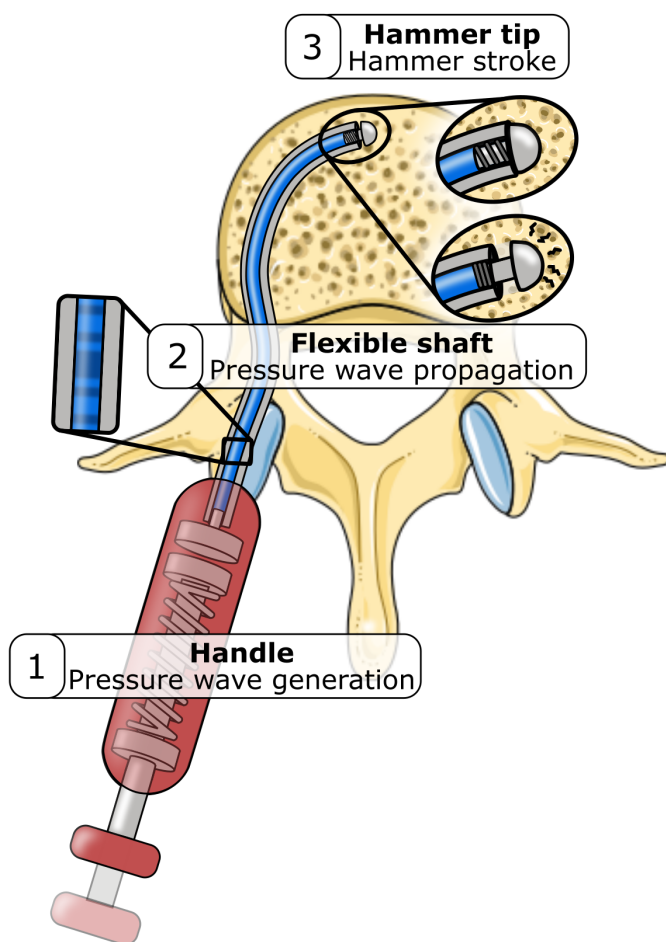
Figure 7.1: Proposed flexible bone drill with hydraulic pressure wave technology including 1) a handle where the pressure wave is generated, 2) a flexible shaft through which the pressure wave propagates and 3) a hammer tip that the hammer stroke on the surrounding bone. Illustration adapted from Servier Medical Art by Servier, licensed under a Creative Commons Attribution 3.0 Unported License.

(a)

(b)
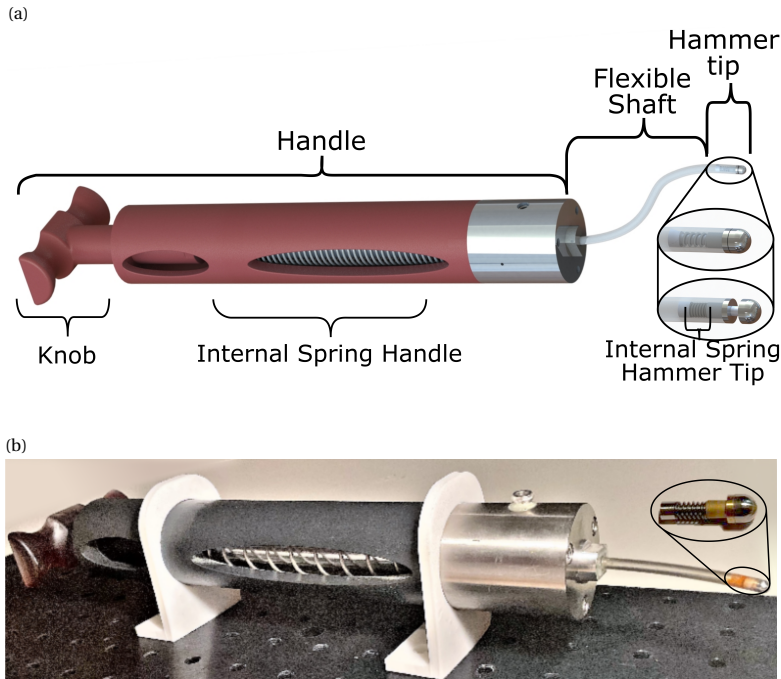
Figure 7.2: HydroFlex Drill prototype. (a) Model of the HydroFlex Drill including a handle to generate a hydraulic pressure wave that propagates through the flexible shaft where up on contact with the hammer tip, the hydraulic pressure wave is transferred via the hammer tip to the bone material. (b) Photo of the HydroFlex Drill prototype.

stroke, enabling repetitive hammering (Figure 7.2a). The optimal tip shape to transfer the impulse to the bone material will be investigate. Only rotational symmetric tip shapes will be considered as rotational symmetric tip shapes have proven to be effective in the transfer of an impulse to brittle material [8].

7.2.2. PROTOTYPE

The assembled prototype, illustrated in Figure 7.2b, was manufactured using a combination of 3D printed parts (Envision TEC R5) and off-the-shelf components such as the spring in the handle ($\varnothing$: 24.4 mm, k: 0.78 N/mm) and the spring in the hammer tip (Amatec, $\varnothing$: 2.5 mm, k: 1.4 N/mm). The selected tube for the flexible drill shaft is a Nylon PA12 Tube (Advanced Fluid Solutions, UK, $\varnothing_{outer}$: 4 mm, $\varnothing_{inner}$: 2.5 mm, length: 40 mm). Although in clinical use saline would be preferred, in this prototype the shaft will be filled with water as the properties of saline and water are negligible [7]. To minimise leakage during the impulse transfer from the handle to the flexible shaft, the distal end of the handle and the hammer tip were precision-milled from stainless steel.

(a)   (b)
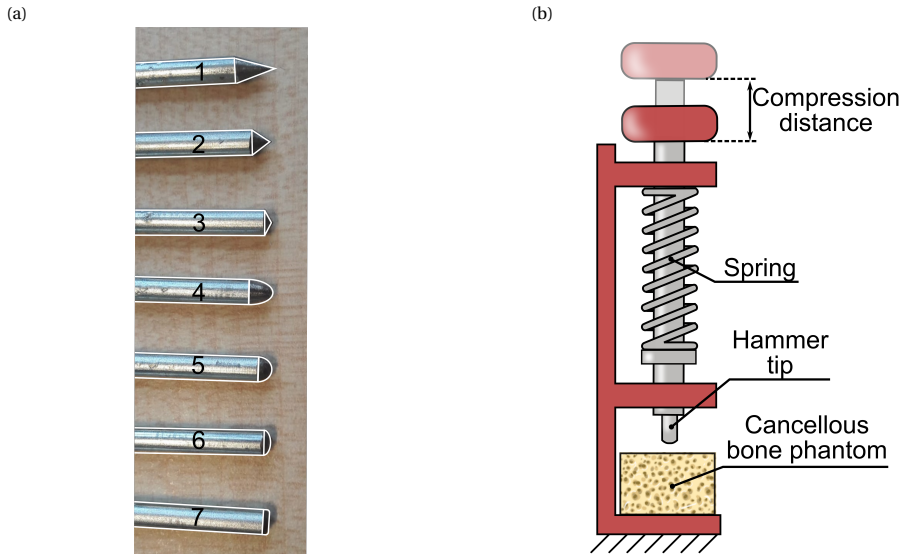
Figure 7.3: The effect of tip shape on performance. (a) Differently shaped hammer tips. (b) Experimental facility used in the Hammer Tip Shape Validation

7.3. Materials and Methods

7.3.1. Experimental Goal

Given the unconventional use of impulse hammering to drill through bone, a thorough investigation of this method is vital. The initial focus was on determining the optimal hammer tip shape for bone drilling, which will then be integrated into the HydroFlex Drill prototype. Subsequently, the drilling performance of this novel design was validated with the flexible shaft in various configuration. Two distinct experimented were preformed: 1) Hammer Tip Shape Validation, exploring the impact of different tip shapes on drilling performance, and 2) HydroFlex Drill Validation, assessing drilling performance of the HydroFlex Drill with its flexible shaft in straight and curved configurations using the identified optimal hammer tip.

7.3.2. Hammer Tip Shape Validation

EXPERIMENTAL VARIABLES

The first independent variable in this study was the hammer tip shape. Seven rational symmetric tip shapes (conical, hemispherical, and cylindrical), all with a 4 mm diameter, were developed and validated (Figure 7.3a). The second independent variable was the compression distance of the spring, influencing the generated force used to hammer the tip into the bone phantom material. Two compression distances, 10 mm and 20 mm were evaluated resulting in a spring force of 7.8 N and 11.7 N being executed on the system, respectively. The dependent variable was the penetration rate [mm/stroke] through the cancellous bone phantom.

Experimental Facility and Protocol

The experimental setup, depicted schematically in Figure 7.3b, comprised a hammer unit capable of generating impulses through a spring-loaded mechanism, similar to the one used in the handle of the HydroFlex drill. The impulse was generated by a spring (∅: 24.4 mm, k: 0.78 N/mm) and transmitted through various hammer tips to the cancellous bone phantom (polyurethane foam). By adjusting the compression distance of the spring, the force used to hammer the drill tip could be varied. The hammer tip was driven into the bone phantom material five times. If no visible penetration occurred, an additional five hammer strokes were performed. The penetration rate [mm/stroke] was determined by dividing the measured penetration depth by the number of a hammer strokes performed, allowing for a comprehensive evaluation of drilling efficiency. Each hammer tip was tested three times. The data analysis used to determine the mean penetration rate and the standard deviation was performed in MATLAB.

Experimental Results

The penetration rates for the seven distinct hammer tip shapes and two different spring compression distances are illustrated in Figure 7.4. Notably, an increase in spring compression corresponds to an increased penetration rate, aligning with expectations. The tip shape showed a limited effect on the penetration rate. However, it was found that the hammer tips with a flatter tip shape (6, 7) showed accumulation of densely packed bone at the tip, potentially impeding drilling efficiency over prolonged use. Furthermore, given the application of the drill in orthopaedic surgery, where safeguarding surrounding anatomy is crucial, the desirability of a sharp tip (1, 2, 3) is diminished due to the increased risk of damage to surrounding soft tissues such as nerves and blood vessels. Consequently, Hammer Tip 4 was selected for incorporation into the final design. This tip demonstrated a relatively high penetration rate with a small variability while featuring a blunt tip, thereby minimising the likelihood of causing harm to surrounding tissues.

7.3.3. HydroFlex Drill Performance Validation

Experimental Variables

The independent variable of this experiment was the HydroFlex Drill shaft configuration (straight, 45° curve, 90° curve). The dependent variable was the generated maximum hammer force by the hammer tip to evaluate the drilling performance of the HydroFlex Drill.

Experimental Facility and Protocol

The experimental setup is illustrated in Figure 7.5. The HydroFlex Drill handle was securely fixed, and the flexible shaft was positioned to reflect three configurations: 1) straight, 2) curved with a 45° angle, and 3) curved with a 90° angle. A compression distance of 40 mm of the spring within the handle was imposed, resulting in an input spring force of 31.2 N. The maximum generated output force by the hammer tip was measured using a load cell (PST, S-type, 150 kg). In each shaft configuration, 10 hammer tip strokes were measured using the force sensor. The measured output force ensures a comprehensive understanding of the HydroFlex Drill performance under varying shaft
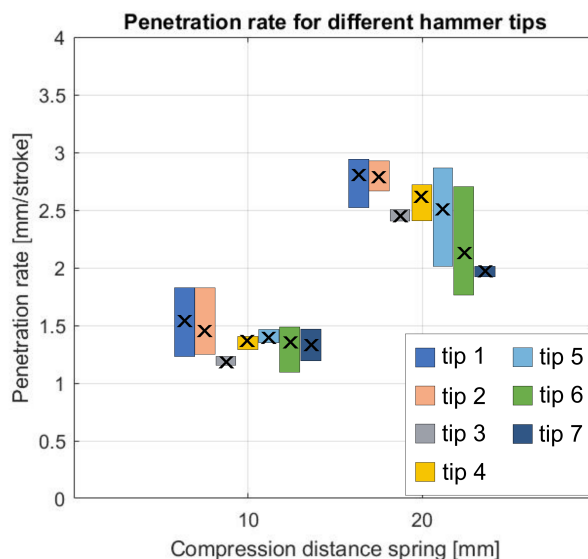
Figure 7.4: Penetration rate for different tip shapes and different compression distances of the impulse generating spring. The crosses indicate the mean value while the boxes indicate the standard deviation.

configurations. The data analysis used to generate a box plot of the maximum hammer force was performed in MATLAB.

EXPERIMENTAL RESULTS

The outcomes of the HydroFlex Drill Validation are depicted in Figure 7.6. The measured output force was 11.1 ±1.3 N with the shaft in straight configuration, 5.7 ±1.6 Ns with the shaft in a 45° curved configuration and 4.1 ±1.2 Ns with the shaft in a 90° curved configuration. It can be observed that the force transferred from the drill tip decreases when a stronger curve is introduced in the flexible shaft. These findings suggest that the presence of a curve in the flexible shaft has significant impact on the transferred impulse, with approximately a 60% decrease from straight to the 90° curved configuration. Testing the HydroFlex Drill on bone phantom material (SawBones) showed that the drill was able to create an indentation after repetitive hammering, thought the penetration rate was low compared to the penetration rate that was achieved in the Hammer Tip Shape Validation.

7.4. DISCUSSION

This study marks a first exploration into the development of a steerable bone drill utilising a hydraulic pressure wave to hammer through bone. The influence of tip shape on penetration rate was found to be limited, but concerns arise regarding the accumulation of densely packed bone when using blunt tips and the imposed risks to damage surrounding tissue when using sharp tips. It is therefore recommended to employ hemispherical tip shapes, which help prevent the issue of packing without causing harm to
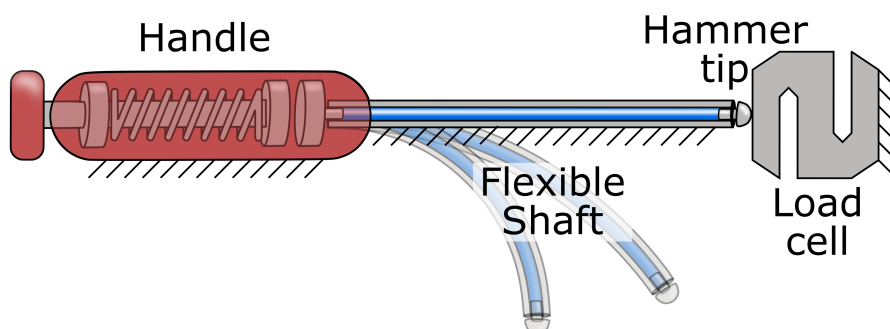
Figure 7.5: Experimental setup with the HydroFlex Drill with the flexible shaft in straight, 45° and 90° curve and a loadcell measuring the force.

surrounding tissue. In this study only rotational symmetric hammer tips were considered, however other tip shapes such as a diamond or trocar shape that is currently used in Kirschner-wires as these tip shapes are designed to propagate through bone.

Implementing this drill tip in the HydroFlex Drill prototype showed that it is possible to transfer high-force impulses with the flexible shaft both in straight and curved configurations. It was found that efficiency of impulse transfer decreases with shaft curvature, possibly due to changes in the cross section of the flexible shaft that result in more losses during the propagation of the hydraulic pressure wave. For efficient wave propagation the shaft must be both axial and radial stiff while maintaining a low bending stiffness. Alternative shaft designs with incorporated braiding or a multi-layer construction could be investigated to minimise the energy loss when bending the shaft. Another source of energy loss could be the dissolved gas within the fluid which could be further minimised.

Validation of the HydroFlex Drill on bone phantom material showed clear decrease in efficiency compared to using a direct impact as was the case in the Hammer Tip Shape Validation. These losses in efficiency are attributed partly to leakage of the fluid resulting in small air bubbles in the shaft which can lower the efficiency considerably due their compressibility. Leakage could be limited through minimising play between the moving hammer tip and the tube or by integrating O-rings, however this is likely to increase the friction between the moving parts and as a result the efficiency will decrease. An alternative solution is to use the drill while ensuring the hammer tip is submerged in fluid such that the fluid that leaks during a hammer stroke will be replaced once the drill tip moves back to the initial position.

Another source of efficiency loss is caused by the energy dissipation by the compression spring in the hammer tip. To address this, future research could focus on redesigning the hammer tip to eliminate the need for a spring in the hammer tip, minimise leakage and integrating steering cables in the flexible shaft to allow for steering to control the drilling direction.

In a clinical setting, the HydroFlex Drill is intended to hammer repetitively in order to drill a tunnel through bone. The drilling speed of the HydroFlex Drill can be adapted by changing the generated input impulse as well as the hammer frequency in order to
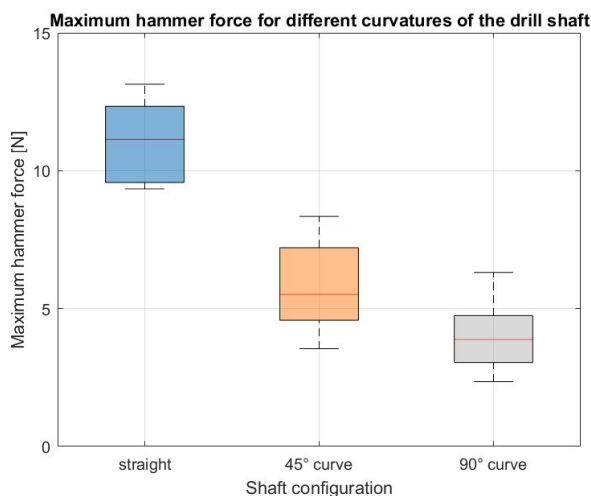
Figure 7.6: Box plot indicating the measured impulse with the flexible drill shaft in a straight configuration and a 45° and 90° curve.

achieve conventional drilling speeds of 6.53 m/min [11]. A larger input impulse will result in a larger output impulse and thus a higher penetration rate, but this will also limit the control of the surgeon on the path and the drilling depth. Possibly an adaptable input impulse would allow a surgeon to change between faster and slower drilling. The drill speed can also be increased by increasing the hammer frequency, however it is important to ensure that the hydraulic pressure waves do not interact such that the efficiency does not decrease due to interaction of the waves.

The current HydroFlex Drill, utilising a hydraulic pressure wave for bone drilling, exhibits promising initial results and represents a foundational step towards the realisation of a steerable bone drill.

7.5. CONCLUSION

This study introduces the HydroFlex Drill with a flexible shaft ($\varnothing$: 4 mm, length: 40 mm) employing a hydraulic pressure wave for bone drilling. The HydroFlex Drill successfully transmitted impulses through the drill shaft in both straight and curved (45°, 90°) configuration. These findings underscore the potential of a hydraulic pressure wave in facilitating efficient bone drilling with a flexible shaft, marking a first step in the development of a steerable bone drill.

BIBLIOGRAPHY

[1]   Esther P. de Kater et al. "Beyond the pedicle screw–a patent review". In: *European Spine Journal* 31.6 (June 1, 2022), pp. 1553–1565. (Visited on 12/06/2022).

[2]   *MicroFX OCD - Osteochondral Drilling System.* en-US. (Visited on 08/10/2022).

[3]   A Ferhat Misir et al. "Effect of surgical drill guide on heat generated from implant drilling". In: *Journal of Oral and Maxillofacial Surgery* 67.12 (2009), pp. 2663–2668.

[4]   Rupesh Kumar Pandey and SS Panda. "Drilling of bone: A comprehensive review". In: *Journal of clinical orthopaedics and trauma* 4.1 (2013), pp. 15–30.

[5]   *Precision Flexible Reaming System for Medial Portal Approach.* (Visited on 01/26/2024).

[6]   Aimée Sakes et al. "Crossing Total Occlusions using a hydraulic pressure wave: a feasibility study". In: *Biomedical Physics & Engineering Express* 4.5 (2018), p. 055019.

[7]   Aimée Sakes et al. "Crossing Total Occlusions Using a Hydraulic Pressure Wave: Development of the Wave Catheter". In: *Frontiers in Medical Technology* 4 (2022), p. 851927.

[8]   Aimée Sakes et al. "Endovascular crossing of chronic total occlusions using an impulse: an explorative design study". In: *Cardiovascular Engineering and Technology* 8 (2017), pp. 145–163.

[9]   Alexander Sendrowicz et al. "Surgical drilling of curved holes in bone–a patent review". In: *Expert review of medical devices* 16.4 (2019). Publisher: Taylor & Francis, pp. 287–298.

[10] Rene M Solzbacher et al. "Bone cyst surgery robot with bendable drilling and remote control". en. In: *Journal of Computational Design and Engineering* 9.6 (Nov. 2022), pp. 2495–2505. (Visited on 07/21/2023).

[11] Toma Udiljak, Damir Ciglar, SJAiPE Skoric, et al. "Investigation into bone drilling and thermal bone necrosis". In: *Advances in Production Engineering & Management* 2.3 (2007), pp. 103–112.

[12] Hiroki Watanabe et al. "Development of a "steerable drill" for acl reconstruction to create the arbitrary trajectory of a bone tunnel". In: *2011 IEEE/RSJ International Conference on Intelligent Robots and Systems.* ISSN: 2153-0866. Sept. 2011, pp. 955–960.

[13] Vidmantas Zegunis, SøRen Toksvig-Larsen, and Robertas Tikuisis. "Insertion of K-wires by hammer generates less heat: a study of drilling and hammering K-wires into bone". In: *Acta Orthopaedica Scandinavica* 64.5 (1993), pp. 592–594.

7

8

DESIGN OF A STEERABLE BONE DRILL

The fixation strength of pedicle screws could be increased by fixating along the much stronger cortical bone layer, which is not possible with the current rigid and straight bone drills. Inspired by the tsetse fly, a single-plane steerable bone drill was developed. The drill has a flexible transmission using two stacked leaf springs such that the drill is flexible in one plane and can drill along the cortical bone layer utilising wall guidance. A proof-of-principle experiment was performed which showed that the Tsetse Drill was able to successfully drill through 5, 10 and 15 PCF cancellous bone phantom which has similar mechanical properties to severe osteoporotic, osteoporotic and healthy cancellous bone. Furthermore, the Tsetse Drill was able to successfully steer and drill along the cortical wall utilising wall guidance for an insertion angle of 5°, 10° and 15°. The experiments conclude that the tsetse fly-inspired drilling method is successful and even allows the drilling along the cortical bone layer. The Tsetse Drill can create curved tunnels utilising wall guidance which could increase the fixation strength of bone anchors and limit the risk of cortical breach and damage to surrounding anatomy.

8

8.1. INTRODUCTION

8.1.1. BONE DRILLING

Orthopaedic surgery concentrates on the fusion, fixation and reshaping of bones using bone drills, saws and screws. An example of orthopaedic surgery is spinal fusion (Figure 8.1a). This surgical procedure accounted for 14,1 billion dollars in aggregate costs in 2018 in the US alone, which is more than any other procedure that year in the US [20]. In spinal fusion surgery, adjacent vertebrae are fused in the correct position using pedicle screws and rods. Fusion is achieved by creating a tunnel that runs through the pedicles into the vertebra body using an awl. A pedicle screw is placed in this pre-made tunnel to provide the required fixation (Figure 8.1b). The success rate of the spinal fusion greatly depends on the fixation strength of the pedicle screws within the bone. Insufficient fixation of the pedicle screw can result in screw loosening, which prevents the desired fusion [32].

The study conducted by Wu *et al.* [30] reported screw loosening in 4.7% of the placed pedicle screws in spinal fusion surgery. A major cause of screw loosening is related to vertebral anatomy. Vertebrae consist of a thin but compact and strong outer layer of cortical bone, which encloses the much softer and porous cancellous bone. The fixation strength of pedicle screws mainly results from contact with the compact cortical bone inside the pedicle. However, the majority of the pedicle screw is surrounded by the softer cancellous bone. Especially for patients suffering from osteoporosis, the fixation strength of pedicle screws is limited due to the decrease of bone density of the cancellous bone [6].

The fixation strength of pedicle screws can be increased using bi-cortical screw fixation in which the insertion path is chosen such that the distal end of the pedicle screw is placed in the cortical bone at the anterior side of the vertebral body (Figure 8.1b). As a result, the pedicle screw has contact with the cortical bone layer in the pedicle and at the distal end of the pedicle screw, which increases the pull-out strength [32, 8]. Following this principle, a curved tunnel along the cortical wall through which the bone anchor can be placed could further increase the fixation strength of the bone anchor due to the increased contact with the cortical bone layer (Figure 8.1b). In addition to the enhanced fixation strength achieved by drilling along the cortical bone layer, the curved path itself can further increase the fixation strength of spinal bone anchors by utilising this macro-shape grip with the bone. However, in order to create a curved tunnel along the cortical bone layer, a steerable bone drill is required. Unfortunately, as of today, there is no steerable bone drill clinically available [25].

8.1.2. STATE-OF-THE-ART: STEERABLE BONE DRILLING

The development of a steerable bone drill is challenging due to the interplay between the need for low bending stiffness to follow a curved trajectory with the need for high axial stiffness that is necessary to drill through bone. Furthermore, the drilled tunnel should remain fully within the cortical bone layer to avoid damage to the surrounding anatomy, which is challenging due to the lack of imaging modalities that can visualise the drill path in real-time. Additionally, the relatively small diameter of the pedicles restricts the outer diameter of the drill to 4 mm, as this is the smallest pedicle diameter measured,
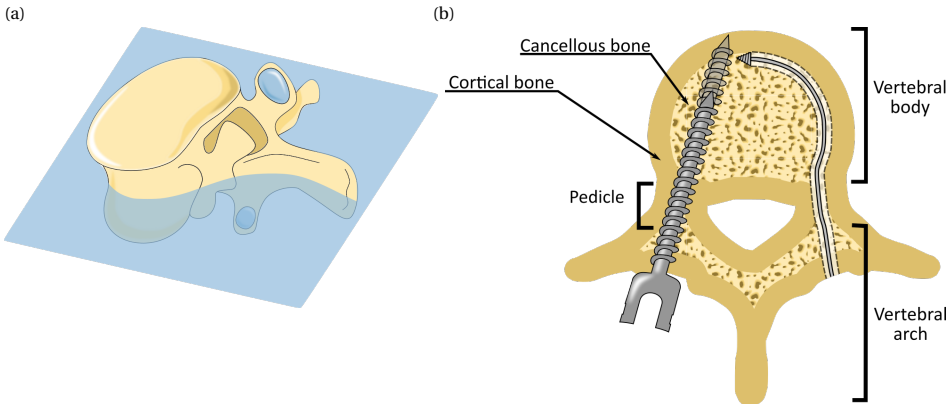
Figure 8.1: Spinal Fusion Surgery. (a) Cross-section of a lumbar vertebra. (b) During spinal fusion surgery pedicle screws are placed through the pedicles (left). The fixation strength of the pedicle screw can be increased using bi-cortical fixation in which the distal tip of the pedicle screw is embedded in the anterior cortical bone layer (left). Drilling of a curved tunnel along the cortical bone layer could further increase the fixation strength of spinal bone anchors (right).

which complicates manufacturing [25].

Currently, there are no commercially available bone drills that can drill curved tunnels through bone and allow for real-time path adaptation. However, flexible reamers in Anterior Cruciate Ligament (ACL) reconstruction in the knee, are commercially available. These devices are utilised to create a pre-determined curved tunnel in the femur, through which a ligament graft can be passed to reconstruct the ACL [10]. Flexible reamers use a bendable but torsion-stiff structure to axially rotate the tip while still allowing for bending motions. Although the reamers can be bent, they do not allow for real-time path adaptation as they are used in combination with an internal or external pre-curved guide (Figures 8.2a, 8.2b) [27, 22, 1, 21]. Drilling along the cortical bone layer in vertebrae with these types of instruments would thus require patient-specific guides that can be used inside the vertebra and need to be manufactured pre-operatively.

The scientific literature describes a variety of steerable bone drill designs that are actively steerable. The proposed drills share many similarities with commercially available reamers, as most drills also use a flexible drive shaft to rotate the drill tip while allowing for the bending of the drill [29, 4, 3, 19, 28]. Wang *et al.* [28] describe a rigid bone drill containing a tip that can deflect using a tendon-driven joint (Figure 8.2c) to target a larger lesion area through a single entry point. However, the drill is not able to drill a curved tunnel due to the rigid design of the shaft. Ahmad Faud *et al.* [3] describe a flexible bone drill that consists of multiple interconnected rigid segments. The drill is intended for use in total hip arthroplasty to create a curved cavity in the femur. Alambeigi *et al.* [4] and Ma *et al.* [19] both describe a steerable bone drill that comprises a bendable but axially stiff structure, utilising compliant joints. The drill tip can deflect by tensioning internal steering cables. Although these drills can in principle drill curved tunnels by selectively pulling the steering cables, the required steering forces are relatively high due to the interaction forces with the surrounding bone when deflecting the
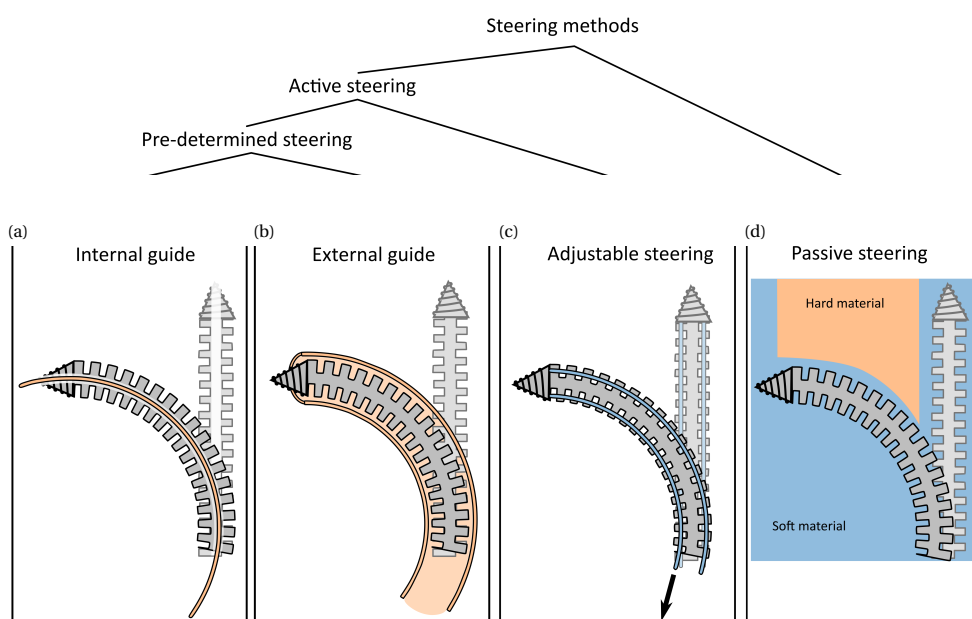
Figure 8.2: Overview of steering techniques for bone drills. Within the category "Active steering" a distinction between "Pre-determined steering" and "Adjustable steering" is made. (a) Use of an internal guide to actively bend the drill. (b) Use of an external guide to actively bend the drill. (c) Adjustable steering methods including the use of tendons. (d) Use of passive steering to passively bend the drill using the environment.

tip of the drill. Watanabe *et al.* [29] try to reduce the required tension forces by making the bendable section more compliant at the tip of the drill. Using this steering principle leads to cable tensioning forces of over 30 N required to generate a drill tip deflection of 20°.

Besides the drill designs presented in scientific literature, the review of Sendrowicz *et al.* [25] shows that in the patent literature, many designs for steerable bone drills are proposed. One thing that must be noted is that the majority of these patents (78%) describe drills that are only able to make pre-defined curved tunnels (Figures 8.2a, 8.2b). The path can thus not be changed during the intervention. As a result, exact information on the patient's anatomy is required to define the path pre-operatively and the drill path cannot be adapted to deformation or displacements that may occur during the procedure. In the overview of Sendrowicz *et al.* [25], only the patent of Bonutti [5] describes a drill design that can drill a multi-curved path that is adjustable during insertion (Figure 8.2c). The patent describes a drill containing inflatable elements in its shaft that allow for deflection of the tip. However, to our knowledge, the design has not been manufactured or tested in a close to clinical setting.

8.1.3. CHALLENGES IN STEERABLE BONE DRILLING

Conventional drills use an axially rotational motion to advance through the target material. To make such a drill flexible, the drill must be flexible in two orthogonal bending planes due to the rotational motion of the shaft. However, for drilling a continuous tunnel along the cortical bone layer of the vertebral body, planar bending in a single plane would in theory be sufficient, as indicated in Figure 8.1. The drill would only need to be flexible in one bending plane while it could be completely rigid in the orthogonal plane, which would eliminate buckling in this plane and could increase the buckling resistance of the drill overall. Furthermore, such a planar bending drill would open pathways for the application of non-rotational drilling methods such as hammering or milling, to achieve the curved pathway in the vertebra.

Steering of a drill can be achieved using internal forces applied on the drill that are initiated by the user, as explained in Section 8.1.2. This includes using steering cables or the use of a pre-curved internal or external guide (Figures 8.2a, 8.2b, 8.2c). The internal forces that are required to bend a drill tip enclosed in bone tissue are often rather high due to the material properties of cancellous bone. This puts high strains on the drill and could in extreme cases cause mechanical failure. An alternative to active steering of the drill would be to passively steer the drill using external forces that are exerted on the drill by the environment (Figure 8.2d). Cortical bone is compact and much stronger than porous cancellous bone. Therefore, drilling through the cortical bone will result in higher cutting forces. These cutting forces could in theory be used to deflect the drill tip such that the drill will take the path of the least resistance and steer along the cortical bone layer. We will refer to this type of steering as "wall guidance".

Wall guidance is based on the drill taking the path of least resistance. When drilling through the softer and porous cancellous bone, the cutting force induced by the cancellous bone ($F_{C\,cancellous}$) is axial and will not cause a deflection, except when the cutting force exceeds the buckling strength of the drill (Figure 8.3). The cutting force will drastically increase when the drill tip comes into contact with the much stronger cortical bone
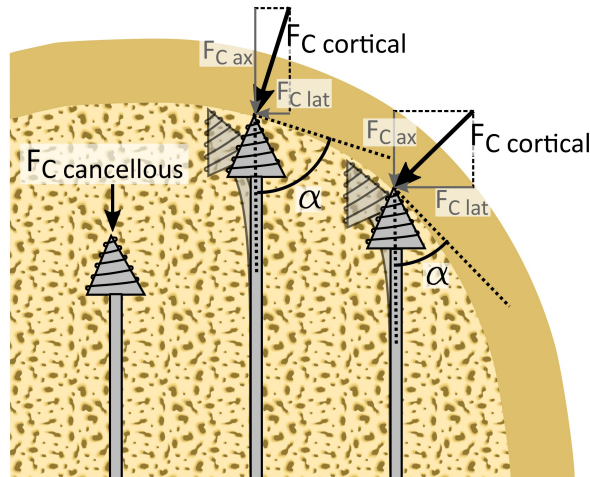
Figure 8.3: Schematic representation of wall guidance steering. Wall guidance allows the drill to passively steer along the cortical bone layer. When the drill is surrounded by cancellous bone, an axial cutting force ($F_{C:cancellous}$) acts on the drill tip. When the drill tip is in contact with the significantly harder cortical bone the cutting force ($F_{C:cortical}$) increases. The orientation of the cutting force depends on the impact angle α between the drill and the cortical bone layer.

($F_{C\,cortical}$). Depending on the impact angle (α) between the drill and the cortical bone, a lateral force ($F_{C\,lat}$) will be introduced, which can be used to deflect the drill (Figure 8.3). This way wall guidance can be used to drill along the cortical bone wall without the need for active steering by the user. However, it should be noted that in vertebrae there is no clear transition point from cancellous to cortical bone. Rather there is an approximately 2 mm thick transition zone where the porous cancellous bone converges in the compact cortical bone [31]. This gradual change in bone density and thus in drilling resistance might complicate steering by wall guidance. Even so, we expect only a small effect due to the low thickness of the transition zone in most vertebrae.

8.1.4. GOAL OF THIS STUDY
The goal of this study is to develop a planar steerable bone drill for use in spinal fusion surgery that can drill along the cortical bone layer to increase the fixation strength of a spinal bone anchor. We explore wall guidance as a method to drill along the cortical bone layer without the need for active steering by the user.

8.2. DEVELOPMENT OF THE TSETSE DRILL
8.2.1. BIO-INSPIRATION: TSETSE FLY PROBOSCIS
Insects can drill through relatively hard materials with their slender ovipositors or mouthpieces. These ovipositors or mouthpieces are often flexible or even steerable during insertion [7]. This makes insects an interesting inspiration source for the design of a novel, steerable bone drill. Especially the drilling method utilised by the tsetse fly to cut through the host's skin is of interest as the rotational motion that is used to cut the skin,
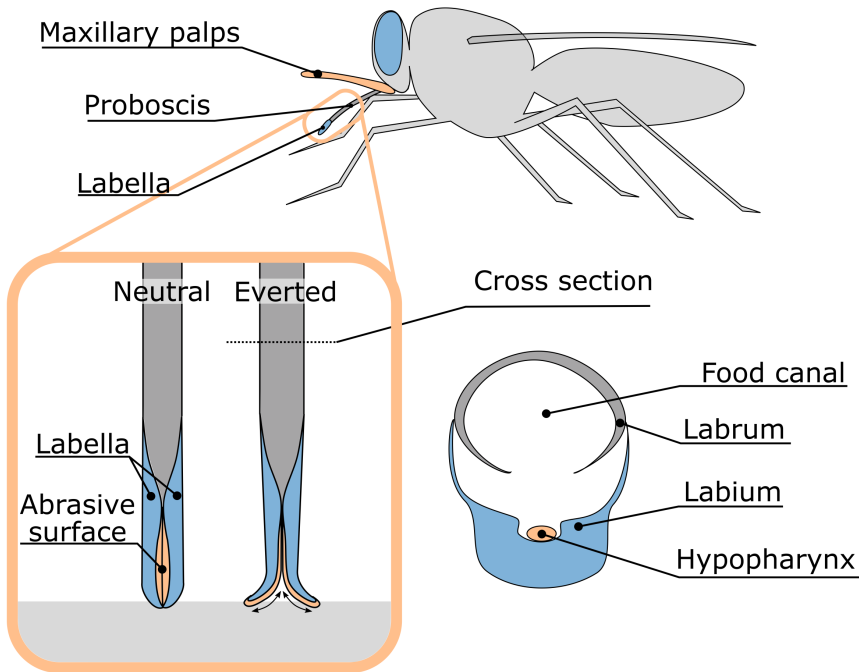
Figure 8.4: Anatomy of the tsetse fly proboscis and the rasping motion of the proboscis during feeding.

occurs around an axis perpendicular to the linear advancement of the proboscis. This makes the drilling mechanism bendable in one plane and thus an interesting inspiration for the development of a planar steerable drill.

The tsetse fly proboscis, a tubular organ used to suck blood, consists of two mouth parts; the labrum and the labium which form the food canal through which the blood is transported (Figure 8.4). The labium is located ventrally from the hypopharynx, a tubular organ through which saliva is transported. The thicker tip of the labium, which is known as the labella, surrounds both the hypopharynx and the labrum and is used to cut through the skin of the host to subsequently feed on the blood of the host. For this purpose, the labella are covered with sharp teeth. Normally the teeth are located within the proboscis, but during feeding, the teeth are repeatedly everted and inverted using a combination of muscle forces and haemostatic pressure to create a rasping motion to cut through the skin [18, 14]. As a result, the proboscis is repetitively pulled into and pushed out of the tissue. A pulling force on the distal tip, to pull the proboscis deeper into the substrate, has a major advantage over pushing the proboscis forward at the proximal end, as it limits the risk of buckling of the proboscis.

8.2.2. Drill Tip Design

The drilling method of the tsetse fly proboscis shows potential for use in an planar flexible bone drill. However, the large number of independently moving and flexible parts
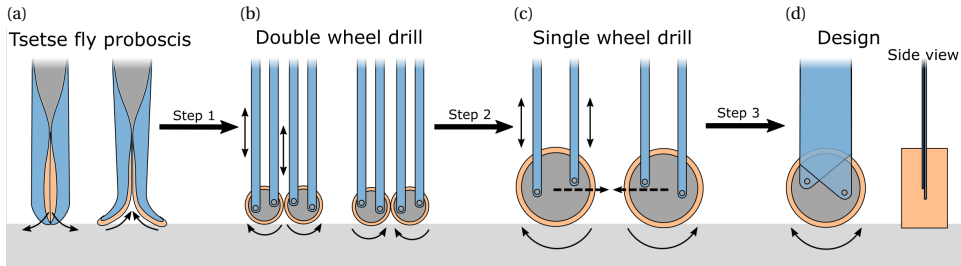
Figure 8.5: Schematic representation of the proboscis of the tsetse fly and the transformation to the drill tip design. (a) Schematic illustration of the tsetse fly proboscis. (b) Double wheel design of the bone drill. (c) Single wheel design of the bone drill. (d) Final conceptual design of the bone drill. The motions of the parts are indicated with arrows. The "walking" behaviour of the drill tip is indicated with the dotted arrow.

are difficult to manufacture with conventional machining techniques and to actuate reliably. The drilling method used by the tsetse fly is, therefore, simplified such that it can be implemented in the design of the steerable bone drill (Figure 8.5a). The motion of the labella during drilling could be simplified as an oscillating rotation of two wheels in opposing directions (Figure 8.5b). The advantage of two oppositely oscillatory rotating wheels is that the lateral forces acting during drilling are counteracted. As a result, the proboscis is repetitively pulled into and pushed out of the substrate.

The drill should be able to fit through the narrow pedicle to prevent damage to the surrounding tissues, resulting in design requirement for the size of the drill. The second lumbar vertebra (L2) has on average the smallest pedicle of the lumbar vertebrae, with an oval cross section of 8.9 mm (SD ± 2.2 mm) by 15 mm (SD ± 1.5 mm) [33]. Manufacturing the two oscillating wheels at this scale is a challenge as the drill diameter is at least twice as large as the wheel diameter. By simplifying the labella motion even further to a single oscillating wheel, the drill can be manufactured with a smaller cross-section and could drill a narrower tunnel (Figure 8.5c). However, by eliminating a second, opposite rotating wheel, there is a chance that during drilling the lateral forces on the front of the oscillating wheel will result in sideways "walking" of the drill tip. The effect can be limited by making the transmission of the drill rigid in the plane of the wheel rotation to avoid bending of the drill due to the lateral forces, but flexible in the orthogonal plane such that the drill can be used for drilling curved tunnels (Figure 8.5d).

The oscillatory motion of the drill tip requires an abrasive surface that can cut in both directions. This can be achieved by a cutting surface with symmetrical teeth. The rake angle of the cutting teeth depends, amongst other characteristics, on the material being cut. For bone saws, a negative rake angle of 10° was found most optimal to limit the resultant forces, while still maintaining sawing efficiency [17]. Based on this, the drill tip was designed with cutting teeth with a negative rake angle of 10°, a height of 0.5 mm and a distance between the teeth tips of 0.4 mm (Figure 8.6). As only the frontal surface of the drill tip will be used to cut through the bone, it was decided to cover only this frontal surface with cutting teeth. To ensure effective drilling, an oscillation amplitude of 15° for the drill tip was chosen, as with this amplitude, the travelled distance of one tooth is
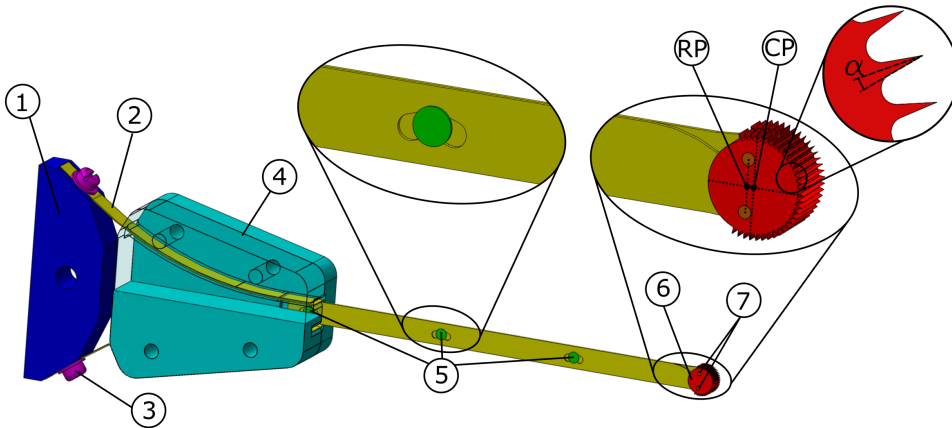
Figure 8.6: Tsetse Drill design. The actuator (not shown) is connected to an oscillation amplifier 1) to which the two leaf springs 2) are connected via two screws 3). The guide 4) directs both leaf springs, which are interconnected using three transmission pins 5). The transmission pins enable the translation of the leaf springs to activate the drill tip 6). The drill tip is attached to the leaf springs using two drill tip pins 7). The Rotation Point (RP) and the Centre Point (CP) of the drill tip are indicated. The negative rake angle of the teeth is indicated with α.

approximately four times the distance between the teeth. It was decided to cover 220° of the drill tip with teeth so that, even in the most rotated orientation of the drill tip, the frontal area of the drill tip would remain fully covered with teeth.

8.2.3. TRANSMISSION DESIGN

The transmission must transfer the oscillatory input from the actuator to the drill tip and be flexible in one plane to allow for wall guidance while being rigid in the orthogonal plane to avoid the effect of 'walking'. This can be achieved by using leaf springs (Figure 8.6, #2, yellow), as leaf springs can easily bend in one plane, but are rigid in the orthogonal plane. Furthermore, the thickness of the leaf springs can be chosen such that the drill can withstand the axial drilling forces with a reduced risk of buckling. The risk of buckling is limited even further by connecting the two leaf springs at distinct points using transmission pins (Figure 8.6, #5, green). The transmission pins are rigidly connected to one of the leaf springs, while the other leaf spring is connected via a slot that acts as a sliding joint. This way, the leaf springs are connected while permitting the required translating motion.

The length of the transmission determines the length of the tunnel that can be drilled. In order to drill a straight path along the longitudinal axis of the pedicle from the posterior cortical bone layer to the anterior cortical bone layer is found to be maximum 62 mm [33]. However if the drilled path would follow the cortical bone layer the required tunnel length will be longer. Therefore, the required transmission length should be at least 100 mm.

When retracting the drill, the tip could get stuck when the drill tip (Figure 8.6, #6, red) is exactly the same size as the tunnel that is cut. To avoid this, the drilled tunnel should
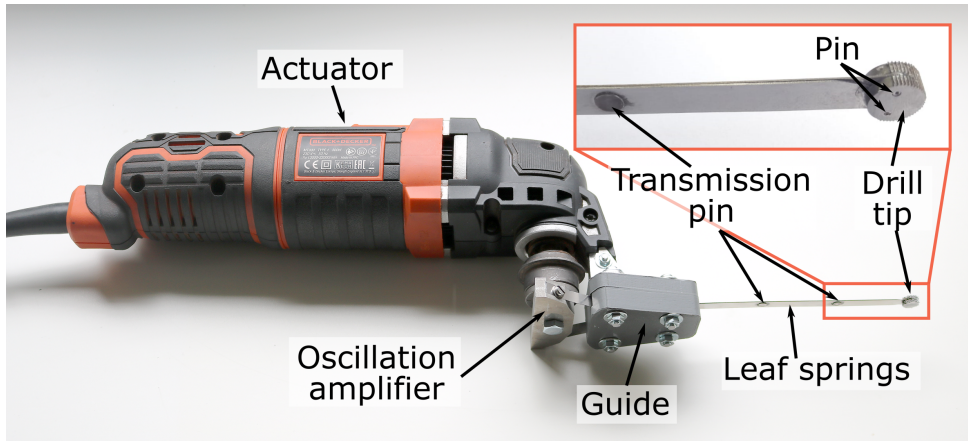
Figure 8.7: Photograph of the actuator and the Tsetse Drill.

be slightly larger than the drill tip. By placing the drill tip pins (Figure 8.6, #7, orange) that connect the drill tip to the leaf springs slightly closer to the actuator, the drill tip will not rotate around its centre, but will rotate around the centre point between the two pins. As a result, the drill tip will make a slight sweeping motion that ensures that the drilled tunnel is slightly larger than the cross-section of the drill tip. This will ensure that the drill can easily be removed from the drilled tunnel.

8.2.4. Actuator and Prototype
The actuation of the drill tip is achieved using an oscillating input provided by a multi-function tool (Black and Decker MT300KA), see Figure 8.7. The multi-function tool has an oscillatory output with an oscillation amplitude of 1.4^o. The oscillation amplitude of the actuator is increased to 15° amplitude of the drill tip using an oscillation amplifier (Figure 8.6, #1, blue), that is placed between the actuator and the leaf spring. The leaf springs (spring steel, thickness 0.3 mm, height 6 mm, length till guide 100 mm, laser cut) are connected to the oscillation amplifier (aluminium, wire EDM and milling), via a guide (Figure 8.6, #4, turquoise, PolyEthylene Terephthalate Glycol, 3D-printed, Ulti-maker 2). The guide has two arc-shaped ridges through which the leaf springs run to prevent buckling of the leaf springs during the actuation of the drill. The leaf springs are connected to each other using three transmission pins ($\varnothing$ 2 mm, tool-steel, turning lathe). The distal end of each of the leaf springs is connected to the drill tip (hardened steel, wire EDM) using a pin ($\varnothing$ 1 mm, tool-steel, turning lathe).

8.3. Materials and Methods

8.3.1. Experimental Goal
The goal of the experiment was two-fold: 1) to evaluate the drilling performance of the prototype through cancellous bone with different bone properties and 2) to investigate the utilisation of wall guidance. Therefore, two different experiments were performed:

1) Drilling Performance Experiment and 2) Wall Guidance Experiment.

8.3.2. DRILLING PERFORMANCE EXPERIMENT

EXPERIMENTAL VARIABLES

Independent Variables

The following variables were manipulated during the Drilling Performance Experiment.

- Tissue density: In order to determine the Tsetse Drill's ability to drill through bone with different mechanical properties, bone phantoms with different compressive strengths were used. The experiment was performed in cancellous bone phantom (Sawbones) with a compressive strength of 5, 10 and 15 Pounds per Cubic Foot (PCF), which is comparable to severe osteoporotic, osteoporotic and healthy cancellous bone respectively [23].
- Feed-rate: The experiment was conducted with a linear advancement of the drill (feed-rate) of 1 mm/s. This feed rate falls in the range of 0.5–1 mm/s that is commonly used in different bone drilling experiments [15, 24]. The experiment on the 15 PCF bone phantom was also conducted with a feed-rate of 0.5 mm/s to investigate whether a lower feed-rate would decrease the axial cutting force.

Dependent Variables

The following variables were measured during the Drilling Performance Experiment.

- Axial drilling force: The axial drilling force was measured using a load cell (FUTEK, 25 lbs) that was placed below the bone phantom. Unsuccessful drilling of the drill tip will prevent the drill tip from advancing further into the bone. As a result, the axial drilling force is expected to increase.
- Success rate: The success rate is defined as the percentage of the experiments that could be performed successfully, see Equation 8.1. The experiment was considered successful if the full drill path was completed without the need for external intervention.

$$succes rate = \frac{\#experiments_{successful}}{\#experiments_{total}} \cdot 100\%$$ (8.1)

EXPERIMENTAL FACILITY

The experimental facility consisted of the prototype with the actuator mounted to a linear stage, which allowed both the feed-rate and the drill depth to be controlled independently (Figure 8.8). The load cell was placed at the base plate of the linear stage. The bone phantom was placed on top of the load cell such that the axial cutting forces could be measured throughout the experiment. A 3D-printed guide was used to guide the drill tip of the prototype during insertion into the bone phantom.

EXPERIMENTAL PROTOCOL

The linear stage was lowered until the drill tip was in close proximity to the bone phantom surface, which was determined by eye. At this time, the guide was placed around the drill. Subsequently, the drill was turned on with a cutting speed of 17,200 RPM, after

Figure 8.8: Experimental facility Drilling Performance Experiment. The experimental facility consisted of the prototype of the Tsetse Drill including the actuator connected to the linear stage. The drill tip was guided using a 3D-printed guide. The bone phantom was placed on top of the load cell (Futek, 25 lbs) such that the axial drilling forces could be measured throughout the experiment.

which the linear stage was turned on and started to move down with the predetermined feed-rate and a drilling depth of 3 cm. The experiment was performed 5 times in the 5, 10 and 15 PCF bone phantoms with a feed-rate of 1 mm/s and 5 times in a 15 PCF bone phantom with a feed-rate of 0.5 mm/s.

DATA ANALYSIS

The data analysis was performed in MATLAB R2019b. The acquired axial drilling force data were corrected for any offset in the measured force based on the mean measured force before the drilling started. Furthermore, the data were normalised such that the insertion of the drill started at time point t = 0 [s] for each experiment. Statistical analysis was conducted by performing ANOVA analysis to investigate the effect of the compressive strength of the bone phantom on the measured axial drilling force.

8.3.3. WALL GUIDANCE EXPERIMENT

EXPERIMENTAL VARIABLES
Independent variables
The following variables were manipulated during the Wall Guidance Experiment.

- Insertion angle: The insertion angle was defined as the angle between the drill path and the cortical bone phantom plate. The experiment was conducted with an insertion angle of 5°, 10° and 15°. Successful deflection of the drill for different insertion angles indicates the adaptability and passive steering capabilities of the drill.

- Tissue density: As the use of a steerable bone drill will mainly be of interest in patients with compromised bone due to osteoporosis, the experiment was conducted using 5 PCF rigid foam bone phantoms (Sawbones), which is comparable to osteoporotic bone [23]. For the 10° insertion angle, the experiment was also conducted using a 10 PCF rigid foam bone phantom (Sawbones), in order to investigate the effect of tissue density on the wall guidance ability.

Dependent Variables
The following variables were measured during the Wall Guidance Experiment.

- Success rate: Successful utilisation of wall guidance results drill deflection upon contact with the cortical bone layer. If the deflection is successful, the drill tip continues drilling through the cancellous bone, following the path of least resistance. However, if the deflection is unsuccessful, the drill tip continues its path through the much harder cortical bone layer, resulting in a significantly higher cutting force on the drill and, as a consequence, buckling of the drill. The experiment was considered successful if the full drill path (4 cm) was completed without the need for external intervention to address drill buckling. The success rate is defined as the percentage of the experiments that could be performed successfully, see Equation 8.1.
- Drill depth in cortical bone: The effectiveness of using wall guidance will be measured based on the drill depth in the cortical bone 1 cm after initial contact with the cortical bone. The ability to deflect after initial contact with the cortical bone phantom is indicated by the depth of the drill path through the cortical bone. The drill depth in the cortical bone is measured using the depth-measuring blade of a calliper.

EXPERIMENTAL FACILITY
The experimental facility is largely comparable to the experimental facility of the Drilling Performance Experiment and consisted of the Tsetse Drill with the actuator mounted to the same linear stage (Figure 8.9). The bone phantom consisted of a short fibre epoxy plate (Sawbones) that mimics the cortical bone layer clamped to a rigid foam cancellous bone phantom (Sawbones) of 5 PCF or 10 PCF. The bone phantom was angled using 3D-printed Stances with an angle of 5°, 10° or 15° that were screwed to the baseplate of the linear stage. The drill tip was placed in a guide that was corrected for the angulation of the bone phantom as can be seen in Figure 8.9.

EXPERIMENTAL PROTOCOL
The bone phantom was placed on a stance with a 5°, 10° or 15° angle to affirm the insertion angle of the drill with respect to the cortical bone layer. Subsequently, the Tsetse Drill with the actuator was connected to the linear stage and levelled such that the drill tip with the guide could be fixed to the bone phantom. After this, the linear stage was engaged with a feed-rate of 0.5 mm/s and the drill would start a cycle in which a 4 cm deep tunnel through the bone phantom was followed at a cutting speed of 17,200 RPM. The experiment was repeated until three successful experiments were conducted for each experimental condition.
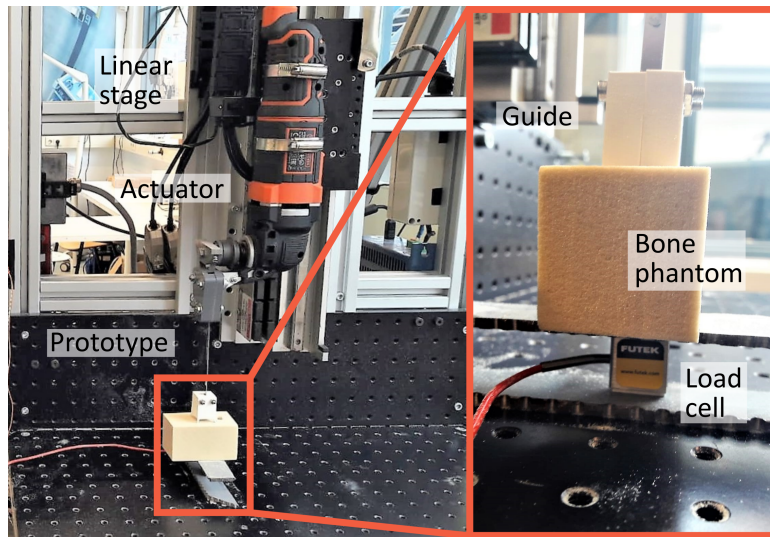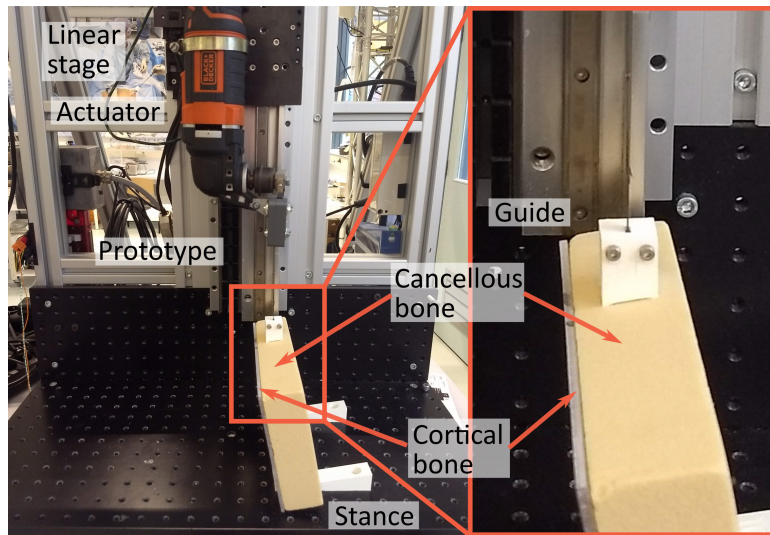
Figure 8.9: Experimental facility Wall Guidance Experiment. The experimental facility consisted of the prototype of the Tsetse Drill including the actuator connected to the linear stage. The drill tip was guided during insertion into the bone phantom by a 3D-printed guide. The bone phantom consisted of cancellous bone and a layer of cortical bone. The bone phantom was angled (0°, 5°, 10° or 15°) using different stances.

8.3.4. DATA ANALYSIS

The data analysis was performed in MATLAB R2019b. An ANOVA analysis was conducted for the statistical analysis of the effect of the insertion angle of the drill and the compressive strength of the bone phantom on the drill depth in the cortical bone.

8.4. RESULTS

8.4.1. DRILLING PERFORMANCE EXPERIMENT

Figure 8.10 shows the axial drilling force versus time through the 5, 10 and 15 PCF bone phantom material for the five repetitions of each experimental condition. The success rate was 100% for the 5, and 10 PCF bone phantom with a feed-rate of 1 mm/s. The success rate was also 100% for the 15 PCF bone phantom with a feed-rate of 0.5 mm/s. For the 15 PCF bone phantom with a feed-rate of 1 mm/s the success rate was 80%. The drill buckled during the first run, resulting in the abortion of the experiment. The high axial forces that were measured during Run 2 and Run 4 suggest that the drill was almost buckling during these two runs. However, the experiment was not aborted and thus these two repetitions were considered successful.

Figure 8.11 shows a boxplot of the maximum axial drilling force for the five repetitions of each experimental condition. The maximum drilling force was 0.61 N (SD ± 0.03 N), 0.92 N (SD ± 0.10 N), 7.59 N (SD ± 6.11 N), for 5 PCF, 10 PCF and 15 PCF bone phantom respectively all with a feed-rate of 1 mm/s. The maximum drilling force was 1.31 N (SD ± 0.62 N) for 15 PCF with a feed-rate of 0.5 mm/s. The buckling of the Tsetse Drill during the first run in the 15 PCF bone phantom with a feed rate of 1 mm/s resulted in a
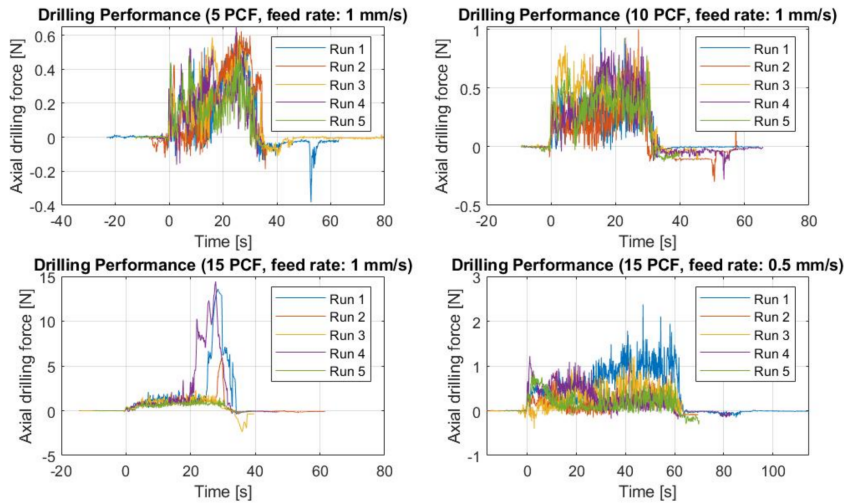
Figure 8.10: Axial drilling force for each of the experimental conditions of the Drilling Performance Experiment. The data of each run are presented.

great variance in the maximum axial drilling force measured. The one-way ANOVA test indicated a statistically significant effect of the compressive strength of the bone phantom material on the measured maximum drilling force (p=$1.4 \cdot 10^{-2}$). It should be noted that a limited number of data points were used for this statistical analysis.

8.4.2. WALL GUIDANCE EXPERIMENT
Figure 8.12a shows the results of the wall guidance test. The success rate was 100% for the experimental conditions with a 5° and a 10° insertion angle. Figure 8.12b presents photographs of the drilled tunnels during the wall guidance experiment. The drill buckled once in the experiments with the 15° insertion angle, resulting in a success rate of 75%. This unsuccessful experiment was not included in the data in Figure 8.12a. The drilling depth in the cortical bone phantom was 0.07 mm (SD ± 0.04 mm), 0.59 mm (SD ± 0.19 mm), 0.44 mm (SD ± 0.39 mm) for an insertion angle of 5°, 10° and 15° all in 5 PCF cancellous bone phantom. The drilling depth in the cortical bone layer with an impact angle of 10° in a 10 PCF cancellous bone phantom was 0.82 mm (SD ± 0.09 mm). The one-way ANOVA test indicated no statistically significant effect of the insertion angle on the drill depth in the cortical bone layer (p=$1.0 \cdot 10^{-1}$). Furthermore, the one-way ANOVA test indicated no statistically significant effect of the compressive strength of the cancellous bone on the drill depth in the cortical bone layer (p=$1.4 \cdot 10^{-1}$).

8.5. DISCUSSION
8.5.1. MAIN RESULTS
The presented Tsetse Drill (outer dimensions: 4 mm × 7 mm, length: 100 mm) has demonstrated successful drilling through bone phantom material and effective steer-
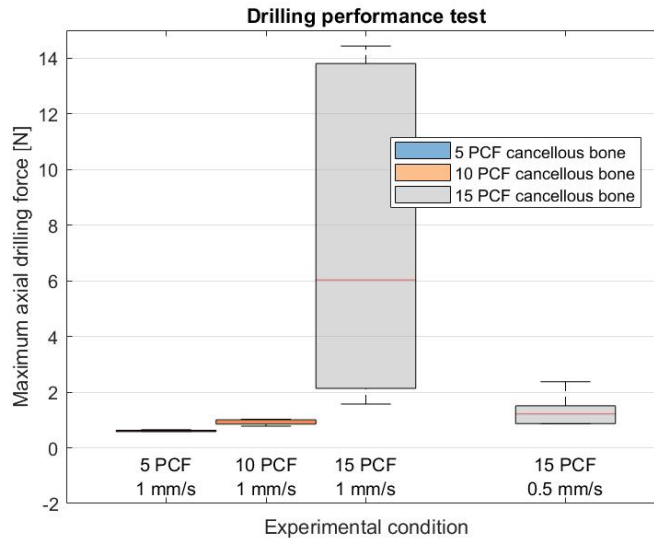
Figure 8.11: Results of the Drilling Performance Experiment. Boxplots of the maximum axial drilling force measured when drilling through 5, 10 and 15 PCF cancellous bone phantoms at a feed rate of 1 mm/s and for drilling though a 15 PCF cancellous bone phantom at a feed rate of 0.5 mm/s.

ing along the cortical bone layer using wall-guidance. Figure 8.13 illustrates a future vision of the Tsetse Drill's application in spinal fusion surgery. In this scenario, the Tsetse Drill is utilised to create a straight pilot hole through the pedicle. Upon impact with the anterior cortical bone layer, the drill deflects and continues to drill along the cortical bone layer using wall-guidance. After creating this curved tunnel, a spinal bone anchor can be placed, such as a segmented screw capable of bending to follow the curved predrilled tunnel. Aghayev *et al.* [2] and Glerum *et al.* [11] have described these spinal bone anchor designs. The fixation path along the cortical bone layer offers the potential for increased fixation of spinal bone anchors due to the large contact area with the strong cortical bone layer and the macro-shape grip that is achieved through the curved drilling path. The Tsetse Drill offers a multitude of potential applications beyond spinal fusion surgery, for a range of orthopaedic interventions. For instance, the Tsetse Drill can be utilised in revision surgeries or tendon repairs to access difficult anatomical sites and minimise damage to surrounding anatomy.

The manufactured proof-of-principle prototype of the Tsetse Drill was able to successfully drill through bone tissue phantoms with a compressive strength of 5 PCF, 10 PCF and 15 PCF representing osteoporotic and health cancellous bone. The axial drilling force increased with increasing compressive strength of the bone phantom. One of the five tests performed on the bone phantom with a 15 PCF compressive strength and a feed-rate of 1 mm/s was unsuccessful due to buckling of the drill. Lowering the feed rate can lower the axial drilling force and prevent buckling in bone with higher compressive strength. A feed rate of 0.5 mm/s resulted in a 100% success rate when drilling through

(a)

(b)
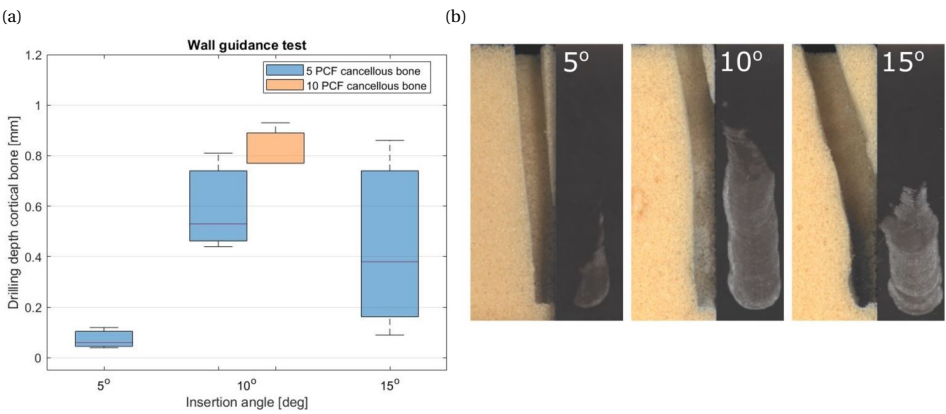
Figure 8.12: Results of the Wall Guidance Experiment. (a) Boxplot of the drilling depth in cortical bone 1 cm after initial contact for three insertion angles (5°, 10° and 15°) in the 5 PCF and 10 PCF cancellous bone phantoms. (b) The drill path for three insertion angles (5°, 10° and 15°) in the 5 PCF bone phantom and the damage to the cortical bone phantom.
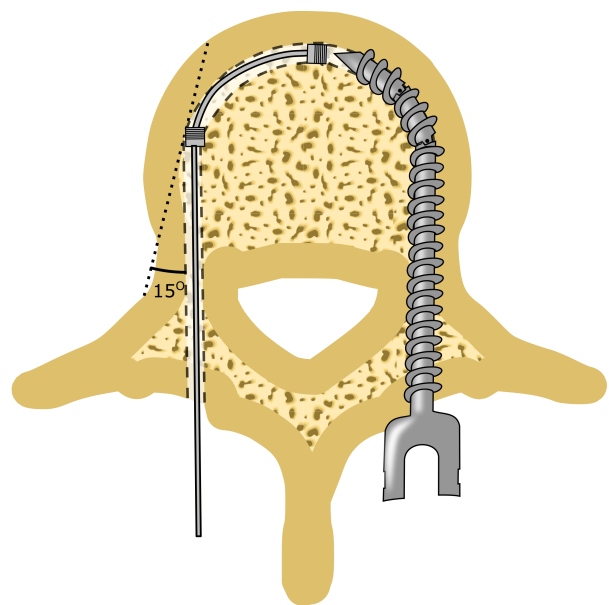
Figure 8.13: Future vision of using the Tsetse Drill in spinal fusion to increase the fixation strength of spinal bone anchors by increase the contact are between the cortical bone layer and the anchor.

15 PCF cancellous bone phantom. This feed rate is comparable to the feed rate used in other studies [15, 26].

The proof-of-principle prototype was able to successfully drill along the cortical bone phantom when inserted under an angle of 5°, 10° or 15°. For an insertion angle of 5°, the average drill depth in the cortical bone was measured to be 0.07 mm (SD ± 0.04 mm) which is below the average vertebral cortical bone layer thickness of 0.4 mm [9]. However, the drill depth in the cortical bone increased to 0.44 mm (SD ± 0.39 mm) for an insertion angle of 15°. Drilling through the cortical bone is undesired as it could result in a cortical breach and increases the forces acting on the drill. Redesign of the abrasive surface of the drill tip, such as the teeth length, could decrease the cutting depth in the cortical bone layer. Furthermore, it would be interesting to investigate the effect of the drill tip shape on the drilling depth in the cortical bone layer.

An interesting characteristic of the Tsetse Drill is that the drilled tunnel has a rectangular cross-section. Furthermore, the cross-sectional shape of the Tsetse Drill and thus the cross-sectional shape of the drilled tunnel can be changed by redesigning the drill tip. In spinal fusion surgery, a tunnel is created through the pedicle into the vertebral body. Subsequently, a pedicle screw is placed through this tunnel. As of now, the fixation of the pedicle screw mainly relies on the contact between the pedicle screw and the strong cortical bone layer. This contact is, however, limited due to the oval cross-section of the pedicle and the round cross-section of the pedicle screw and tunnel. An oval drill path would allow for novel anchors with an oval cross-section that can shape to the pedicle, such as the one designed by de Kater *et al.* [16]. This way the contact area between the anchor and the cortical bone layer in the pedicle could be increased considerably. This would not only result in increased pull-out strength of the anchor, but it can also increase the toggling resistance of the anchor due to the increased contact area with the cortical bone in the caudal and cranial direction.

8.5.2. LIMITATIONS AND FUTURE RESEARCH

The presented Tsetse Drill was able to successfully deflect when encountering the harder cortical bone with angles up to 15°. The achieved deflection is comparable to the deflection of the drill described by Watanabe *et al.* [29] without requiring active steering by the user. Furthermore, the drill does not rely on steering cables that require high tension forces to facilitate the required tip deflection. Although this is a large advantage over fully rigid drills, further research is necessary to investigate the ability to utilise wall guidance for larger insertion angles. Additionally, future research could be conducted into combining wall guidance with additional steering methods to increase the adaptability of the drill. Furthermore, the large contact area between the quickly oscillating drill tip and the surrounding bone may result in heat generation. In future research heat generation should be investigated, as heating of bone tissue can result in bone necrosis [13].

For the proof-of-principle experiments, the drill was tested in artificial bone phantom material. Although the mechanical characteristics of this artificial bone are similar to real bone, they are no replacement for actual bone. The pores in the bone phantom are closed cells and smaller than cancellous bone. Furthermore, the pores in cancellous bone are filled with bone marrow, a fatty liquid. The presence of fluids, such as blood

and bone marrow, could slow down the disposal of the bone chips that are formed during drilling. Furthermore, the transition zone between the cortical and cancellous bone was not considered in the performed experiments and could influence the wall guidance performance, as the transition from cancellous to cortical bone is less abrupt than in the performed experiments.

The Tsetse Drill is currently designed for spinal fusion surgery. However, the Tsetse Drill could also be of great advantage in ligament reconstructions. During this type of surgery, a ligament is reconstructed by placing a ligament graft through the bone via a pre-drilled tunnel. In these reconstructions, a longer tunnel is thought to increase the fixation of the ligaments [12]. With the Tsetse Drill, a curved path could be created to increase the tunnel length. Also in other orthopaedic surgeries, such as implant revision surgeries and bone decompression, a steerable drill that can drill along the cortical bone layer could be preferable over conventional bone drills [4, 3]. Therefore, in future research, we will investigate the Tsetse Drill mechanism for use in a variety of orthopaedic interventions.

8.6. Conclusion

This paper presents a novel passively steerable bone drill design inspired by the tsetse fly proboscis. The Tsetse Drill comprises two stacked leaf springs that transmit the oscillation to the drill tip while allowing for bending of the drill. The drill tip of the Tsetse Drill has an abrasive surface and rotates in an oscillatory fashion perpendicular to the drilling direction. This drilling method allows for the utilisation of wall guidance to drill a curved path along the cortical bone layer of the vertebra. The proof-of-principle prototype was able to successfully drill through bone phantom material with a compressive strength of 5 PCF, 10 PCF and 15 PCF. Furthermore, the Tsetse Drill was able to passively steer utilising wall guidance with insertion angles of 5°, 10° and 15°. The presented Tsetse Drill could be a first step in the direction of steerable bone drilling in a variety of orthopaedic procedures, such as spinal fusion surgery.

8

BIBLIOGRAPHY

[1] *ACL Reamers – Lenkbar*. en-US. (Visited on 08/10/2022).

[2] Kamran Aghayev et al. "Transdiscal screw". U.S. pat. 10314631B2. H Lee Moffitt Cancer Ct & Res. June 11, 2019.

[3] Ahmad Nazmi Bin Ahmad Fuad et al. "On the development of a new flexible drill for orthopedic surgery and the forces experienced on drilling bovine bone". en. In: *Proceedings of the Institution of Mechanical Engineers, Part H: Journal of Engineering in Medicine* 232.5 (May 2018), pp. 502–507. (Visited on 06/12/2023).

[4] Farshid Alambeigi et al. "A Curved-Drilling Approach in Core Decompression of the Femoral Head Osteonecrosis Using a Continuum Manipulator". In: *IEEE Robotics and Automation Letters* 2.3 (July 2017). Conference Name: IEEE Robotics and Automation Letters, pp. 1480–1487.

[5] Peter M. Bonutti. "Surgical instrument positioning system". US2003009172A1. Jan. 2003.

[6] Daniel J. Burval et al. "Primary Pedicle Screw Augmentation in Osteoporotic Lumbar Vertebrae: Biomechanical Analysis of Pedicle Fixation Strength". In: *Spine* 32.10 (May 1, 2007), pp. 1077–1083. (Visited on 06/04/2021).

[7] Uroš Cerkvenik et al. "Functional principles of steerable multi-element probes in insects". en. In: *Biological Reviews* 94.2 (2019), pp. 555–574. (Visited on 06/12/2023).

[8] Luc P. Cloutier, Carl-Eric Aubin, and Guy Grimard. "Biomechanical study of anterior spinal instrumentation configurations". en. In: *European Spine Journal* 16.7 (July 2007), pp. 1039–1045. (Visited on 06/12/2023).

[9] Senthil K Eswaran et al. "Cortical and trabecular load sharing in the human vertebral body". In: *Journal of Bone and Mineral Research* 21.2 (2006), pp. 307–314.

[10] Brian Forsythe et al. "Optimization of Anteromedial Portal Femoral Tunnel Drilling With Flexible and Straight Reamers in Anterior Cruciate Ligament Reconstruction: A Cadaveric 3-Dimensional Computed Tomography Analysis". en. In: *Arthroscopy: The Journal of Arthroscopic & Related Surgery* 33.5 (May 2017), pp. 1036–1043. (Visited on 06/12/2023).

[11] Chad Glerum et al. "Pedicle-Based Intradiscal Fixation Devices and Methods". U.S. pat. 2021307924A1. Globus Medical Inc. Oct. 7, 2021.

[12] Patrick E. Greis et al. "The Influence of Tendon Length and Fit on the Strength of a Tendon-Bone Tunnel Complex: A Biomechanical and Histologic Study in the Dog". en. In: *The American Journal of Sports Medicine* 29.4 (July 2001), pp. 493–497. (Visited on 06/12/2023).

8

[13] Muhammad Jamil et al. "Comprehensive analysis on orthopedic drilling: A state-of-the-art review". en. In: *Proceedings of the Institution of Mechanical Engineers, Part H: Journal of Engineering in Medicine* 234.6 (June 2020), pp. 537–561. (Visited on 06/12/2023).

[14] B. Jobling. "A Revision of the Structure of the Head, Mouth-part and Salivary Glands of Glossina palpalis Rob.-Desv." en. In: *Parasitology* 24.4 (Jan. 1933). Publisher: Cambridge University Press, pp. 449–490. (Visited on 06/12/2023).

[15] F. Karaca, B. Aksakal, and M. Kom. "Influence of orthopaedic drilling parameters on temperature and histopathology of bovine tibia: An in vitro study". en. In: *Medical Engineering & Physics* 33.10 (Dec. 2011), pp. 1221–1227. (Visited on 06/12/2023).

[16] Esther P. de Kater et al. "A Toggling Resistant In-Pedicle Expandable Anchor: A Preliminary Study". In: *2022 44th Annual International Conference of the IEEE Engineering in Medicine & Biology Society (EMBC)*. 2022 44th Annual International Conference of the IEEE Engineering in Medicine & Biology Society (EMBC). ISSN: 2694-0604. July 2022, pp. 3313–3317.

[17] W. R. Krause. "Orthogonal Bone Cutting: Saw Design and Operating Characteristics". In: *Journal of Biomechanical Engineering* 109.3 (Aug. 1987), pp. 263–271. (Visited on 06/12/2023).

[18] Harald W. Krenn and Horst Aspöck. "Form, function and evolution of the mouthparts of blood-feeding Arthropoda". en. In: *Arthropod Structure & Development* 41.2 (Mar. 2012), pp. 101–118. (Visited on 06/12/2023).

[19] Justin H. Ma et al. "An Active Steering Hand-Held Robotic System for Minimally Invasive Orthopaedic Surgery Using a Continuum Manipulator". In: *IEEE Robotics and Automation Letters* 6.2 (Apr. 2021). Conference Name: IEEE Robotics and Automation Letters, pp. 1622–1629.

[20] Kimberly W. McDermott and Lan Liang. "Overview of Operating Room Procedures During Inpatient Stays in U.S. Hospitals, 2018: Statistical Brief #28". eng. In: (2006). (Visited on 09/09/2022).

[21] *Medial Portal ACL Reconstruction*. en-US. (Visited on 08/10/2022).

[22] *MicroFX OCD - Osteochondral Drilling System*. en-US. (Visited on 08/10/2022).

[23] Srinidhi Nagaraja and Vivek Palepu. "Comparisons of Anterior Plate Screw Pullout Strength Between Polyurethane Foams and Thoracolumbar Cadaveric Vertebrae". In: *Journal of Biomechanical Engineering* 138.10 (Oct. 1, 2016), p. 104505. (Visited on 01/04/2022).

[24] Chandana Samarasinghe et al. "Temperature and force generation in surgical bone drilling". In: *AIP Conference Proceedings* 2324.1 (Feb. 2021). Publisher: American Institute of Physics, p. 060007. (Visited on 03/10/2023).

[25] Alexander Sendrowicz et al. "Surgical drilling of curved holes in bone–a patent review". In: *Expert review of medical devices* 16.4 (2019). Publisher: Taylor & Francis, pp. 287–298.

8

[26] S. Sezek, B. Aksakal, and F. Karaca. "Influence of drill parameters on bone temperature and necrosis: A FEM modelling and in vitro experiments". en. In: *Computational Materials Science* 60 (July 2012), pp. 13–18. (Visited on 05/15/2023).

[27] *VersiTomic flexible ACL/PCL reaming system.* en-US. (Visited on 08/10/2022).

[28] Yan Wang et al. "A Handheld Steerable Surgical Drill With a Novel Miniaturized Articulated Joint Module for Dexterous Confined-Space Bone Work". In: *IEEE Transactions on Biomedical Engineering* (2022). Conference Name: IEEE Transactions on Biomedical Engineering, pp. 1–1.

[29] Hiroki Watanabe et al. "Development of a "steerable drill" for acl reconstruction to create the arbitrary trajectory of a bone tunnel". In: *2011 IEEE/RSJ International Conference on Intelligent Robots and Systems.* ISSN: 2153-0866. Sept. 2011, pp. 955–960.

[30] Jau-Ching Wu et al. "Pedicle screw loosening in dynamic stabilization: incidence, risk, and outcome in 126 patients". In: *Neurosurgical Focus* 31.4 (Oct. 2011), E9.

[31] R. Zebaze et al. "A new method of segmentation of compact-appearing, transitional and trabecular compartments and quantification of cortical porosity from high resolution peripheral quantitative computed tomographic images". en. In: *Bone* 54.1 (May 2013), pp. 8–20. (Visited on 09/13/2022).

[32] M R Zindrick et al. "A biomechanical study of intrapeduncular screw fixation in the lumbosacral spine". In: *Clinical orthopaedics and related research* 203 (Feb. 1, 1986), pp. 99–112.

[33] Michael R. Zindrick et al. "Analysis of the Morphometric Characteristics of the Thoracic and Lumbar Pedicles". en-US. In: *Spine* 12.2 (Mar. 1987), pp. 160–166. (Visited on 09/27/2022).

8

9

DESIGN OF A STEERABLE AND SENSING BONE DRILL

Bone drilling plays an essential role in various medical procedures, enabling access to challenging intervention sites within bone tissue and facilitating the creation of tunnels for placement of implants such as spinal bone anchors. Conventional rigid and straight bone drills often lack the manoeuvrability required in intricate procedures. Furthermore, the straight tunnels created with conventional drills for bone anchors may result in loosening of the anchor as the path is not optimised for the shape of, for instance, the vertebra. Especially in patients with compromise bone strength, such as osteoporosis, loosening of bone anchors has a high prevalence. This study proposes a novel steerable bone drill design ($\varnothing$ 2.75 mm, length: 130 mm) featuring a central lumen for interchangeable precurved nitinol cores, enabling controlled steering of the drill trajectory. This design enables the creation of multi-curved tunnels, enhancing manoeuvrability during drilling. Furthermore, the drill tip is designed to incorporate Diffuse Reflectance Spectroscopy (DRS) technology that is able to provide tissue feedback to alert the user for the risk of cortical breach during the drilling procedure. The developed proof-of-concept prototype successfully demonstrated the drilling of a multi-curve tunnel including a straight and a subsequent curved section, marking a significant advancement compared to conventional bone drills. This innovative steerable bone drill could enable the access to difficult-to-reach locations deep within the bone and may enhance the fixation strength of bone anchors through the utilisation of multi-curved tunnels.

9

9.1. Introduction

9.1.1. Bone Drilling

Bone drilling is essential in a wide range of medical procedures, facilitating access to specific intervention sites, enabling implant placement and aiding fracture fixation. However, conventional bone drills have a straight and rigid design, limiting drilling to straight tunnels. This lack of manoeuvrability restricts the range of accessible locations, as well as the inability to adjust the drill path during procedures, potentially resulting in significant damage to surrounding healthy tissue. The development of a steerable bone drill capable of drilling curved tunnels could offer access to more challenging locations, while minimising the risk of harm to surrounding anatomical structures.

Steerable bone drills could also aid the fixation strength of implants. In spinal fusion surgery, for instance, adjacent vertebrae are fused using screws and rods to restore spinal stability. The success of this procedure heavily relies on the fixation strength of the pedicle screws within the vertebra [20]. Pedicle screws are primarily surrounded by porous cancellous bone, with only a small section within the pedicle in contact with the dense cortical bone layer, yet this section contributes the most to the overall fixation strength of the screw [20, 19]. Especially in patients suffering from osteoporosis, where the bone density is compromised, pedicle screw fixation may be insufficient, potentially resulting in screw loosening [20]. Exploring alternative anchor paths along the cortical bone layer, as presented in Figure 9.1, could potentially enhance the fixation strength and the success rate of spinal fusion surgery by increasing the contact with the cortical bone layer. However, drilling such multi-curved paths necessitates a steerable bone drill.

9.1.2. Steerable Bone Drilling

Despite various designs of steerable bone drills presented in patent literature, commercially available bone drills are scarce [16]. Existing drills, such as the Carevature Dreal [6] and the *Stryker MicroFX OCD* [14], feature a flexible drive shaft to actuate a axially rotating drill tip, which is guided through a rigid tubular guide. While this design allows for accessing challenging entry points without damaging surrounding tissue, using a rigid guide restricts its ability to drill curved tunnels through bone. The *Lenkbar FlexMetric*® [1] and the *Zimmer Biomet Precision Flexible Reaming system* [13] employ a drill tip with a central lumen and a flexible tubular drive shaft, allowing advancement of the drill over a pre-placed guide wire. Despite enabling drilling of curved tunnels, these drills rely on the placement of a guide wire and are thus limited to gentle curves.

Currently available steerable bone drills fall short in enabling the drilling of multi-curved tunnels that are adaptable during procedures. The patent by Bonutti [2] proposes a steerable bone drill design allowing path adjustment during drilling, using multiple inflatable elements to steer the drill in the desired direction. However, to our knowledge, this design has yet to undergo practical validation, and therefore, the question remains if inflatable segments would allow for drilling the desired adaptable multi-curved tunnels. The challenge of developing a steerable bone drill lies in achieving sufficient axial rigidity required for bone penetration, whilst maintaining low bending stiffness for creating curved tunnels. Conventional axially rotating drills face bending challenges, necessitating flexibility in two orthogonal planes, hindering the required axial rigidity. Alternative
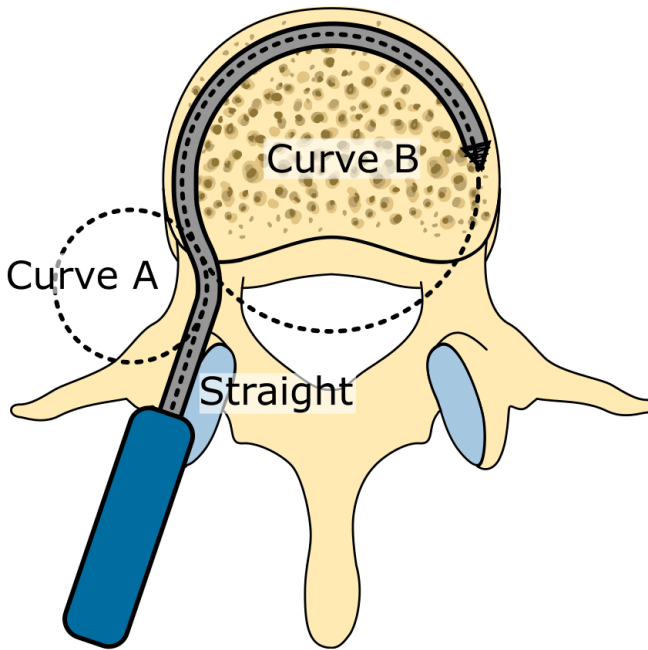
Figure 9.1: Alternative anchoring path aimed at increasing contact with the cortical bone layer to enhance the fixation strength of spinal bone anchors.

drilling methods such as milling, hammering, or pushing may offer viable solutions for the development of a steerable bone drill.

In order to create a multi-curved tunnel, the drill must manoeuvre through the bone in a snake-like manner, with the drill tip defining the path while the remainder of the drill follows the exact path of the drill tip. This can be achieved through complex mechanics such as Follow-The-Leader (FTL) mechanisms, wherein the pose of the tip is stored and conveyed to the following segments, ensuring the segments replicate the trajectory [4, 5]. FTL mechanisms are designed for minimally invasive procedures in soft tissues and generally do not rely on interaction with the tissue to navigate. However, in bone drilling, the surrounding bone tissue can in theory serve as a medium to retain the drill tip's path, enabling the drill to track the created tunnel effectively, resulting in the desired snake-like navigation without the need for a complex FTL mechanism.

9.1.3. DRILLING SAFETY

To enable multi-curved drilling in a safe manner, the location of the drill inside the vertebra needs to be precisely controlled and monitored. Vertebrae are surrounded by delicate anatomy, including nerves, blood vessels, muscles and ligaments and possess intricate contours, characterised by curved surfaces that provide protection to the spinal cord and allow for ligament attachment. Drilling through the vertebra, especially when creating curved tunnels, carries a risk of breaching the cortical bone layer, potentially

resulting in damage to the surrounding anatomy. Conventional safety measures such as 2D fluoroscopy or 3D navigation offer guidance, but expose both patients and surgical staff to radiation [9].

Alternatively, integrating sensors into a steerable drill can enhance safety. Electro-Magnetic Tracking (EMT) [8], Fiber Braggs Grating (FBG) sensors [10], and Diffuse Reflectance Spectroscopy (DRS) sensors [17] may provide viable options. The tracking accuracy with EMT quickly degrades when electric and metallic instruments are present, and the tracking volume is limited [8], making this undesirable for integration in a steerable drill. Optical fibers that are required for both FBG and DRS are compact and easily integrated into medical devices, making both techniques promising for enhanced safety in steerable drilling procedures [7]. FBG sensors utilise a grating structure within optical fibers to detect strain which can be used to determine the bending of the fiber and this the instrument's path [10]. Similarly DRS sensors employ optical fibers, that allows for the differentiation between cortical and cancellous bone, alerting the user before breaching the cortical bone layer [17, 3, 12].

9.1.4. GOAL OF THIS STUDY

The aim of this study is to explore a novel bone drill design engineered for the creation of multi-curved tunnels through bone, with the ability to modify the drill path during the procedure. The bone drill is designed to accommodate the integration of optical fibers to enhance drilling safety through tissue differentiation and path determination.

9.2. DESIGN

9.2.1. WORKING PRINCIPLE

Creating multi-curved tunnels through the vertebra will enable alternative fixation methods that can be explored, including macro-shape locks. A potential multi-curved path that could be utilised is presented in Figure 9.2a, comprising a straight section followed by a curved section (Curve A) and an oppositely curved section (Curve B). To drill along this path, the procedure using the novel drill (Figure 9.2b) design unfolds as follows: Step 1 initiates with drilling a straight tunnel; Step 2 progresses by extending this tunnel into Curve A; and Step 3 concludes with drilling Curve B (Figure 9.2c).

To achieve this multi-curved tunnel, we propose a system in which the path of the drill tip is stored in the surrounding bone. The proposed design consists of interchangeable super elastic nitinol pre-curved cores confined within a flexible sleeve. The precurved cores are manufactured from super-elastic nitinol rods, providing them with ability to endure large deformations without resulting in plastic deformation of the rod. This allows the cores to take on the shape of the multi-curved path drilled. The flexible sleeve, comprising a sharp tip at its distal end, is designed to penetrate the cancellous bone and create a tunnel by a pushing motion.

Upon introduction of a pre-curved nitinol core into the flexible sleeve, the sleeve molds and conforms to the curve of the core. In Step 1, a straight nitinol core is inserted into the flexible sleeve, resulting in a straight shape of the drill. As the sleeve and core advance into the cancellous bone, a straight tunnel is created. At the end of the straight tunnel, the core is withdrawn from the cancellous bone, while the sleeve remains within

the bone.

In Step 2, a pre-curved core is introduced into the sleeve. The elastic properties of the nitinol core, combined with the resistance of the cancellous bone surrounding the flexible sleeve, cause the core to deflect and conform to the pre-drilled straight tunnel when the core is introduced into the sleeve. As the core and sleeve are advanced further into the cancellous bone, a curved tunnel (Curve A) is formed, facilitated by the pre-curve of the nitinol core and the resulting force of the cancellous bone. After drilling Curve A, the core is removed.

In Step 3, the previous step is repeated by introducing an oppositely pre-curved nitinol core into the flexible sleeve. Upon insertion of the core into the sleeve, the core elastically conforms to the sleeve within the previously drilled tunnel. Advancement of the core and sleeve through the bone drills the second curve (Curve B). By employing cores with differently curved radii, the drilling of multi-curved tunnels with varying radii in three-dimensional space is achievable.

9.2.2. CONCEPT DRILL DESIGN

The concept drill design comprises a flexible sleeve connected to a drill tip that facilitates the integration of DRS technology and a lumen enabling the introduction of a variety of pre-curved nitinol cores for drilling multi-curved tunnels. To prevent any bias in drilling direction, a conical drill tip shape was chosen. Furthermore, to drill curved tunnels, the drill tip must apply sufficient force to penetrate through cancellous bone. A sharp drill tip offers advantages, as it minimises the required pushing force to advance the drill. However, the drill tip must also allow for the integration of DRS technology. The drill tip was designed to accommodate two optical fibers ($\varnothing$: 200 µm) with a fiber distance of 1.6 mm [12, 11]. This fiber distance is one to the determinants for the probing depth, the depth at which the cortical bone layer can be detected using the DRS sensor. Another determinant for the probing depth and the signal-to-noise ratio is the drill tip shape, as investigate by Losch *et al.* [12]. A sharp conical tip significantly reduces the sensitivity of the DRS sensor, but this effect is limited using a slight conical drill tip [12]. Therefore, a conical tip with an angle of 120° was selected which will reduce the probing depth compared to a blunt tip by 50%, but allows for penetration of cancellous bone (Figure 9.3) [12].

The sleeve that connects to the drill tip requires flexibility to conform to the shape of the introduced nitinol core, combined with a smooth inner surface for introducing the nitinol cores. Additionally, to safeguard the optical fibers integrated in the drill tip, a double-walled sleeve is required with the optical fibers in between the two layers. This also allows for the integration of additional optical fibers with fiber Bragg gratings to allow for determination of the drill path real time. The inner sleeve, a highly flexible Bowden cable sheath, offers a smooth inner surface. The outer sleeve, a heat-shrinking tube, provides a smooth surface for the sleeve's advancement into the cancellous bone.

The super elastic property of nitinol enables large deformations without risking plastic deformation. To create multi-curved tunnels, the pre-curved cores must be able to bend in the opposite direction to their initial pre-bend curve. The minimal radius (r) [mm] for achieving this without risking plastic deformation can be calculated using Equation 9.1, where d [m] represents the core diameter and ϵ [-] represents the allowable

(a)

Straight

Curve A

Curve B

(b)

Flexible
sleeve

Pre-curved
cores

(c)

Step 1:
Drill Straight

Step 2:
Drill Curve A

Step 3:
Drill Curve B

9
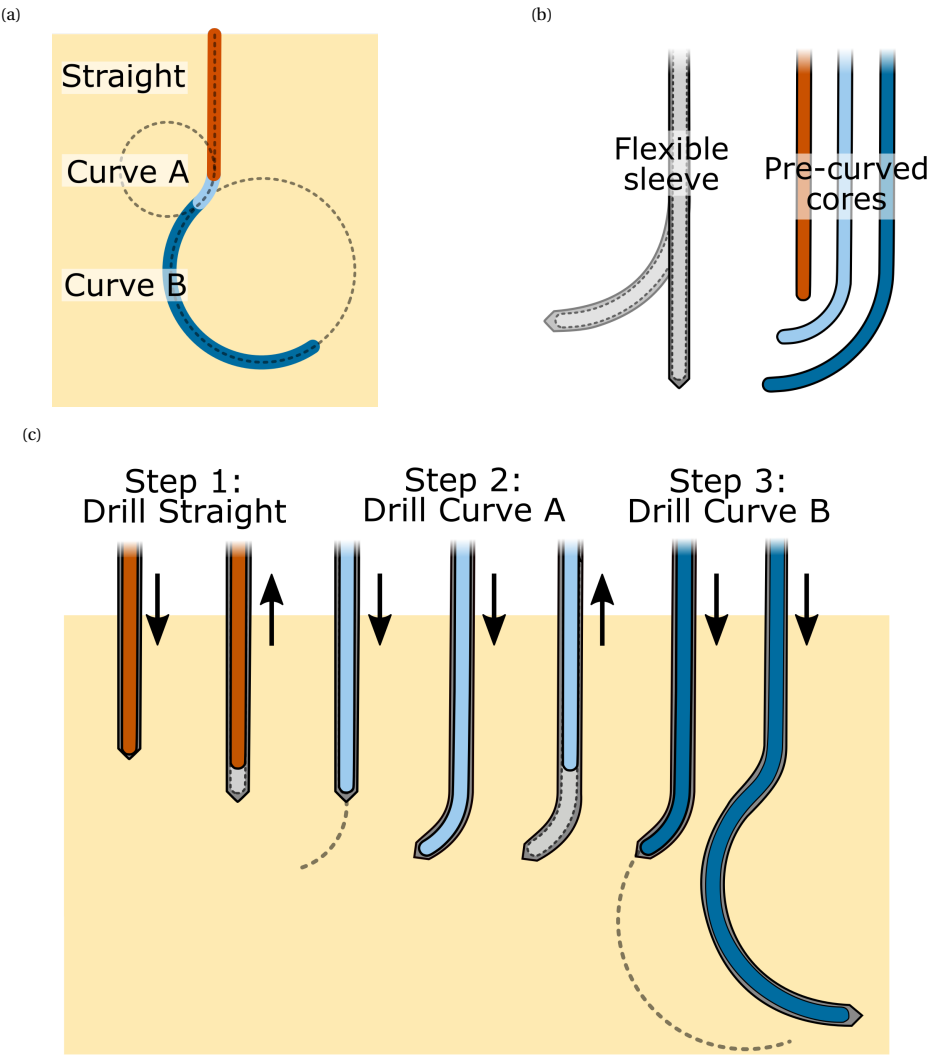
Figure 9.2: Working principle of the proposed steerable drill design. (a) Desired multi-curved drill path, (b) Components of the drill, including a flexible sleeve and multiple super elastic nitinol cores to guide the drill in the desired direction. (c) Working principle to drill the desired drill path.
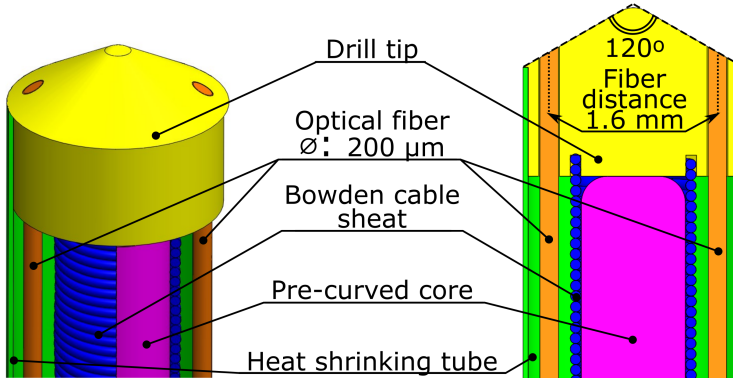
Figure 9.3: Schematic representation of the drill design, featuring a conical drill tip (yellow) with two optical fibers (orange) running through the flexible sleeve consisting of a Bowden cable (blue) and a heatshrinking tube (green), along with a nitinol curve (pink)

strain which is equal to 0.08 for super elastic nitinol [18].

$$r = \frac{d}{\epsilon} + \frac{d}{2} \tag{9.1}$$

From Equation 9.1 can be deducted that smaller core diameters allow for a smaller allowable minimum radii. However, cores with a smaller diameter may not have sufficient axial stiffness to effectively transmit the pushing force required to advance the drill through the cancellous bone. Therefore, nitinol cores with diameters of 0.5 mm, 0.8 mm and 1.0 mm were tested. These cores should theoretically allow for curvatures of r = 6.5 mm, 10.4 mm and 13 mm respectively.

PROOF-OF-CONCEPT PROTOTYPE

A proof-of-concept prototype was developed to validate the drilling and steering functionality of the proposed steerable bone drill design. Since the DRS technology has already been validated [12] and the addition of the optical fibers is not expected to influence drilling performance, the proof-of-concept prototype was developed excluding the optical fibers necessary for detecting cortical breach.

The developed proof-of-concept prototype consists of a stainless-steel drill tip manufactured using conventional machining techniques, glued to a flexible shaft comprising an inner sleeve made from an outer sheath of a Bowden cable (Schweizer Federtechnik GmbH & Co., $\varnothing_{inner}$ = 1.0 mm , $\varnothing_{outer}$ = 1.2 mm), and an outer sleeve comprising a heatshrinking tube (CellPack, $\varnothing$ = 2.40 mm, shrink ratio = 2:1) (Figure 9.4a). The straight and pre-curved cores utilised for steering the drill were fabricated from super elastic nitinol rods (Titanium Shop: $\varnothing$= 0.5 mm, $\varnothing$ = 0.8 mm & NDC: $\varnothing$ = 1.0 mm), which were curved in the desired curvature by placing them in a mould and heating them for at least 20 minutes at 500^oC. The manufactured proof-of-concept drill has an outer diameter of 2.75 mm and a length of 130 mm (Figure 9.4b).

9

(a)

(b)
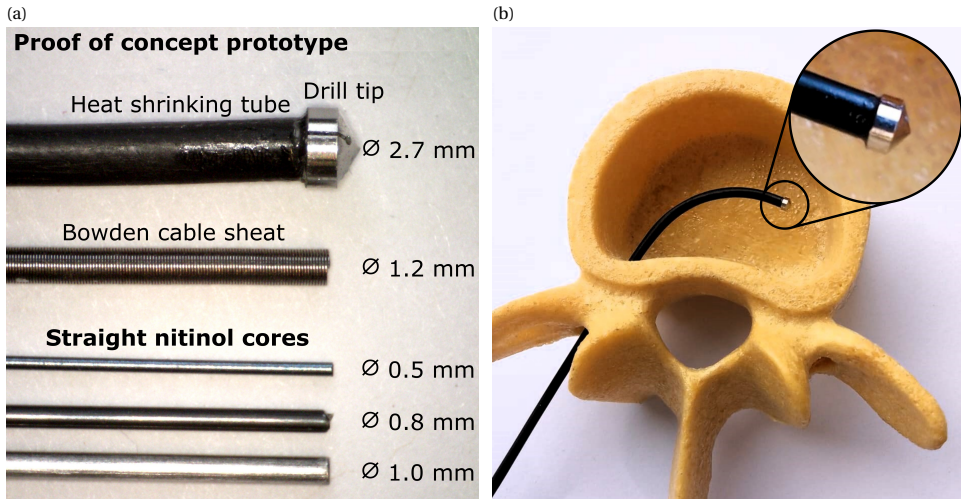
Figure 9.4: Proof-of-concept steerable drill prototype. (a) Close-up of the proof-of-concept prototype showing the fully assembled prototype including the drill tip and the outer heat shrinking tube, as well as the Bowden cable sheath forming the internal layer of the flexible sleeve and various straight nitinol cores. (b) Proof-of-concept prototype within a hollow vertebra model with a close-up of the drill tip.

9.3. Test

The proof-of-concept prototype drill was tested by drilling the first two steps of creating a multi-curved path, starting with a straight section followed by a curved section, into bone phantom material (SawBones Solid Foam Block, 5 PCF), which possesses mechanical properties similar to female osteoporotic bone [15]. To enable visual inspection of the drill path during the test, a clear PolyMethylMethAcrylaat (PMMA) plate was affixed on top of the bone phantom material, allowing the drill to penetrate through the bone phantom material along the PMMA plate. Both the bone phantom material and the PMMA plate were secured with a vice (Figure 9.5).

In the initial step of the test (Step 1), the straight section of the tunnel was drilled using a straight core, pushing the drill into the bone phantom material at a constant speed of 0.5 mm/s over a length of 3 cm using a linear stage. Subsequently (Step 2), the straight core was replaced with the curved core (radius curved section: 25 mm) to drill the curved section of the tunnel. Replacing just the core while the sleeve remained within the cancellous bone proved challenging, therefore, the drill and core were removed after drilling the initial straight section of the tunnel. At the start of Step 2 the drill housing the curved core was placed into the previously drilled tunnel by hand. Subsequently, the drill, housing the curved core, was advanced over a length of 3 cm into the bone phantom, drilling the curved section of the path.

The proof-of-concept prototype was tested using 0.5 mm, 0.8 mm and 1.0 mm diameter super elastic (pre-curved) nitinol cores. Straight drilling with the 0.5 mm core proved unsuccessful, as the pushing force required to advance the drill reached the limit of the
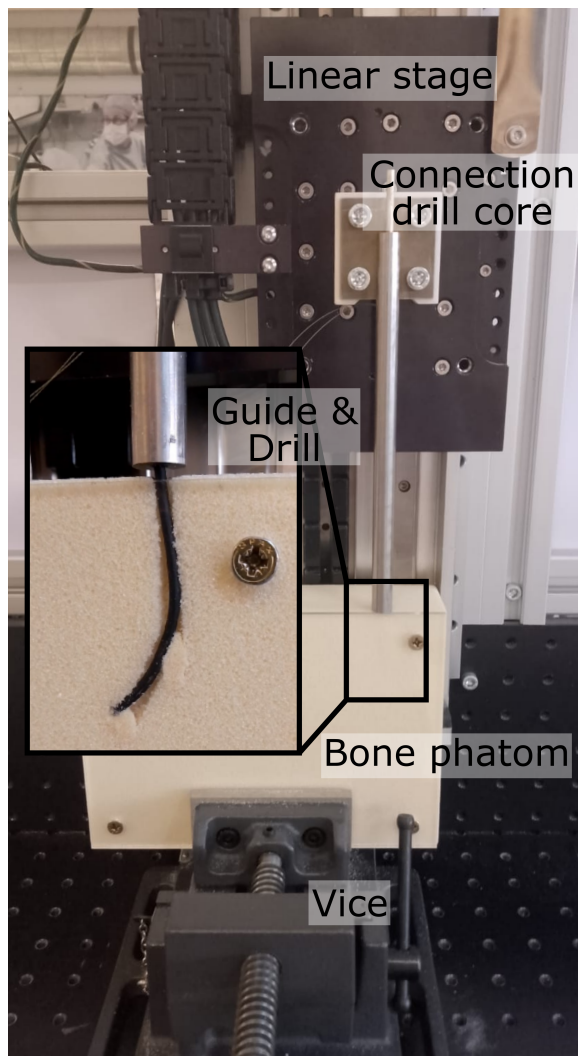
Figure 9.5: Experimental setup used in testing of the proof-of-concept prototype drill, featuring a linear stage utilised to advance the drill through the guide into the bone phantom material for drilling a multi-curved tunnel, starting with an initial straight tunnel followed by a curved tunnel.
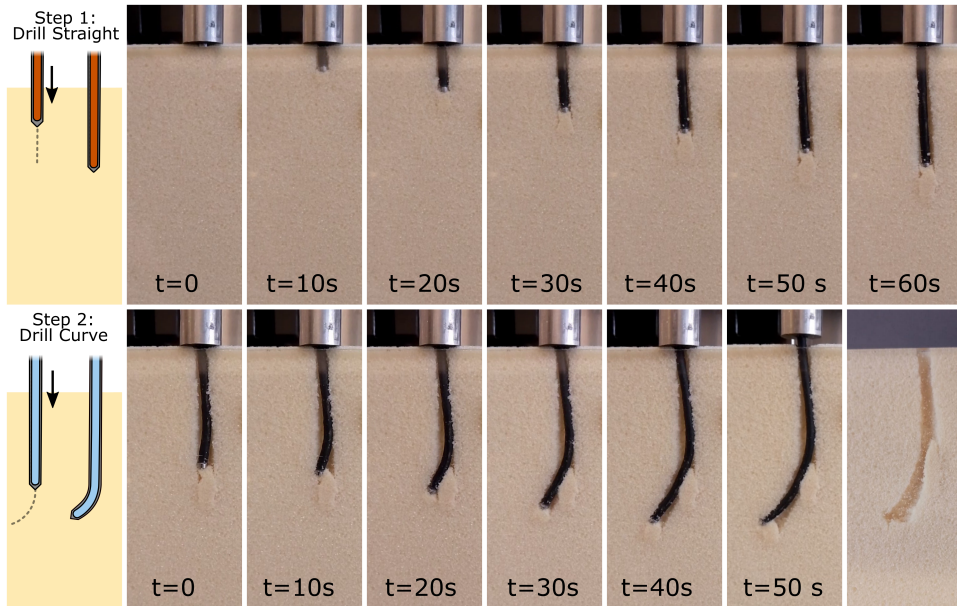
Figure 9.6: Testing of the drilling and steering performance of the proof-of-concept prototype drill. Step 1: Drilling of the curved section of the multi-curved tunnel by advancing the drill housing a straight core. Step 2: Drilling of the curved section of the multi-curved tunnel by advancing the drill housing a curved core.

linear stage, resulting in no progress through the bone phantom material. The 1.0 mm core successfully drilled the straight section. However, subsequent drilling of the curved section with a curved 1.0 mm core was unsuccessful due to the inability to deflect and advance the nitinol core within the previously drilled straight tunnel. The 0.8 mm core, on the other hand, combined the best of both worlds and successfully drilled both the straight and the curved section of the tunnel, as depicted in Figure 9.6. Drilling of the second opposed curved section (Step 3), however, proved challenging due to the difficulty introducing the pre-curved nitinol core into the curved tunnel in the opposite direction. The curved core tended to axially rotate in the same direction as the pre-drilled curved tunnel, hindering the drilling of the third opposed curved section. Throughout the drilling process of both the straight and curved tunnel, accumulation of bone phantom material at the drill tip was observed, making it increasingly difficult to advance the drill. After completing the drilling of the tunnel, the drill was removed, revealing the drilled tunnel, which included a straight section followed by a curved section.

9.4. DISCUSSION

9.4.1. MAIN FINDINGS

The proposed steerable bone drill design, along with the manufactured proof-of-concept prototype ($\varnothing$: 2.75 mm, length: 130 mm), demonstrated successful drilling through osteoporotic bone phantom material, creating a tunnel comprising a straight

and curved section. The prototype drill features a stainless-steel conical drill tip designed for integrating DRS technology to enable cortical breach detection. This drill tip is connected to a double-walled flexible sleeve which allows for incorporation of optical fibers with FBG to determine the path of the drill real-time. Various pre-curved cores manufactured from super elastic nitinol could be inserted into the flexible sleeve to guide the drill in the desired direction while advancing through bone.

The drilling and steering performance of the proof-of-concept drill prototype was tested in combination with different the super elastic nitinol cores ($\varnothing$ 0.5 mm, $\varnothing$ 0.8 mm and $\varnothing$ 1.0 mm). The 0.5 mm nitinol core was not able to advance the drill through the bone phantom material, possibly due to buckling within the flexible sleeve of the proof-of-concept prototype, caused by the space between the core and the interior of the flexible sleeve and creating high friction. While the nitinol core with a 1.0 mm diameter was able to successfully drill a straight tunnel through the bone phantom material, it was observed that upon introducing the curved core, its stiffness hindered compliance with the previously drilled straight tunnel. Consequently, drilling the curved section of the tunnel after successfully drilling the straight section was not possible. The 0.8 mm diameter nitinol core achieved successful drilling of both the straight and the subsequently curved section of the tunnel. Throughout the drilling process, accumulation of bone at the drill tip was noticed, potentially increasing drilling resistance posing a risk to the drilling of longer tunnels.

9.4.2. LIMITATIONS AND FUTURE RESEARCH

The presented proof-of-concept prototype successfully drilled a tunnel comprising a straight section followed by a curved section, utilising a pre-curved super elastic nitinol core. The impact of the core diameter on drilling performance was evident. Employing a core with a small diameter (0.5 mm) or a large diameter (1.0 mm) did not yield in successful drilling of multi-curved tunnels, either due to buckling in the case of the 0.5 mm core or the inability to adapt to the pre-drilled path in case of the 1.0 mm core, hindering successful drilling of a subsequent section of a multi-curved tunnel. Drilling of a multi-curved tunnel including a straight section followed by two opposed curved sections as presented in Figure 9.2a was not possible with the current design. Possibly a thinner, more flexible core would allow for this, however, this would require redesign of the flexible sleeve of the drill to eliminate the space between the core and the sleeve to minimise buckling.

The core diameter also significantly influenced the minimum achievable curve radius, thereby determining the diameter of the curved path that can be drilled. The 0.8 mm core, with a curve radius of 25 mm, proved effective in drilling a curved tunnel. Further research into the effects of core diameter, length, and radius of the curved section of the cores is desired. The drilling path may vary depending on the properties of the bone through which the tunnel is created. While the test of the proof-of-concept prototype was conducted in bone phantom material designed to mimic osteoporotic cancellous bone, future *ex-vivo* and *in-vivo* experiments are required to understand the dependency of inhomogeneous bone properties on the drilling and steering performance of the designed steerable bone drill. Furthermore, the effect of pushing or hammering the drill through bone could be investigated.

9
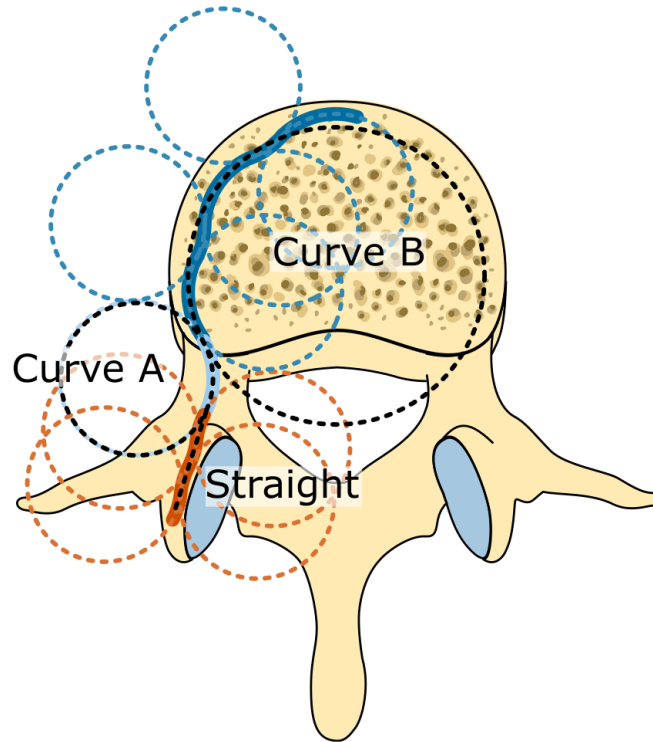
Figure 9.7: Schematic representation of the multi-curved drill path using a single curved core that is axially rotated 180° at certain intervals to drill straight and curved paths with varying radii. The coloured dotted lines indicate the path along which the drill is advanced.

The current drill design requires multiple pre-curved cores with different radii to facilitate drilling of curved tunnels of varying radii. However, in a clinical setting, the utilisation of multiple cores may be considered cumbersome and complex. To address this issue, exploring the feasibility of employing a single curved core to drill multi-curved tunnels could be of interest. By rotating the core axially by 180° each time the drill is advanced, it becomes feasible to drill a relatively straight path using a curved core (Figure 9.7, Straight path). While the curve of the core determines the smallest curve radius that can be drilled (Figure 9.7, Curve A), it is possible to drill a curved section with a larger diameter by periodically axially rotating the core 180° at specified intervals (Figure 9.7, Curve B).

The drill tip of the presented proof-of-concept prototype was designed to include DRS technology for cortical breach detection. However, the functionality of the DRS technology was not validated in this study, and the interaction between the DRS technology and the user, and subsequently between the user and the drill, was beyond the scope of this research.

9.5. CONCLUSION

This study introduces a novel steerable bone drill design and steering principle aimed at drilling multi-curved tunnels through cancellous bone. The drill comprises a flexible sleeve housing and a stainless-steel conical drill tip designed to incorporate DRS technology to provide cortical breach detection. Various super elastic nitinol cores can be inserted into the flexible sleeve to guide the drill in the desired direction during the procedure. A proof-of-concept prototype was tested using bone phantom material. Advancing the proof-of-concept prototype with a $\varnothing$ 0.8 mm super elastic nitinol core enabled drilling of a multi-curved tunnel comprising a straight section followed by a curved section. This innovative drill design represents a first step in the development of multi-curved steerable bone drilling, potentially expanding surgical capabilities in various medical procedures including orthopaedic surgery.

9

BIBLIOGRAPHY

[1]   *ACL Reamers – Lenkbar*. en-US. (Visited on 08/10/2022).

[2]   Peter M. Bonutti. "Surgical instrument positioning system". US2003009172A1. Jan. 2003.

[3]   Gustav Burström et al. "Diffuse reflectance spectroscopy accurately identifies the pre-cortical zone to avoid impending pedicle screw breach in spinal fixation surgery". In: *Biomedical Optics Express* 10.11 (Oct. 24, 2019), pp. 5905–5920. (Visited on 09/16/2021).

[4]   Howie Choset and Wade Henning. "A Follow-the-Leader Approach to Serpentine Robot Motion Planning". EN. In: *Journal of Aerospace Engineering* 12.2 (Apr. 1999). Publisher: American Society of Civil Engineers, pp. 65–73. (Visited on 03/29/2024).

[5]   Costanza Culmone et al. "Follow-The-Leader Mechanisms in Medical Devices: A Review on Scientific and Patent Literature". In: *IEEE Reviews in Biomedical Engineering* 16 (2023). Conference Name: IEEE Reviews in Biomedical Engineering, pp. 439–455. (Visited on 03/29/2024).

[6]   *Dreal*. en-US. (Visited on 01/11/2024).

[7]   Carl Fisher et al. "Perspective on the integration of optical sensing into orthopedic surgical devices". In: *Journal of Biomedical Optics* 27.1 (Jan. 2022). Publisher: SPIE, p. 010601. (Visited on 03/29/2024).

[8]   Alfred M Franz et al. "Electromagnetic Tracking in Medicine—A Review of Technology, Validation, and Applications". en. In: *IEEE TRANSACTIONS ON MEDICAL IMAGING* 33.8 (2014).

[9]   Ibrahim Hussain et al. "Evolving Navigation, Robotics, and Augmented Reality in Minimally Invasive Spine Surgery". In: *Global Spine Journal* 10.2 (Apr. 1, 2020), 22S–33S. (Visited on 12/01/2021).

[10] Fouzia Khan, Abdulhamit Donder, and Stefano Galvan. "Pose Measurement of Flexible Medical Instruments Using Fiber Bragg Gratings in Multi-Core Fiber". en. In: *IEEE SENSORS JOURNAL* 20.18 (2020).

[11] Merle S. Losch et al. "Diffuse reflectance spectroscopy of the spine: improved breach detection with angulated fibers". EN. In: *Biomedical Optics Express* 14.2 (Feb. 2023). Publisher: Optica Publishing Group, pp. 739–750. (Visited on 03/27/2023).

[12] Merle S. Losch et al. "Fiber-Optic Pedicle Probes to Advance Spine Surgery through Diffuse Reflectance Spectroscopy". en. In: *Bioengineering* 11.1 (Jan. 2024). Number: 1 Publisher: Multidisciplinary Digital Publishing Institute, p. 61. (Visited on 03/29/2024).

[13]   *Medial Portal ACL Reconstruction.* en-US. (Visited on 08/10/2022).

[14]   *MicroFX OCD - Osteochondral Drilling System.* en-US. (Visited on 08/10/2022).

[15]   Srinidhi Nagaraja and Vivek Palepu. "Comparisons of Anterior Plate Screw Pull-out Strength Between Polyurethane Foams and Thoracolumbar Cadaveric Verte-brae". In: *Journal of Biomechanical Engineering* 138.10 (Oct. 1, 2016), p. 104505. (Visited on 01/04/2022).

[16]   Alexander Sendrowicz et al. "Surgical drilling of curved holes in bone–a patent re-view". In: *Expert review of medical devices* 16.4 (2019). Publisher: Taylor & Francis, pp. 287–298.

[17]   Akash Swamy et al. "Diffuse reflectance spectroscopy, a potential optical sensing technology for the detection of cortical breaches during spinal screw placement". In: *Journal of biomedical optics* 24.1 (2019). Publisher: International Society for Optics and Photonics, p. 017002.

[18]   Robert J Webster, Allison M Okamura, and Nah J Cowan. "Toward active cannulas: Miniature snake-like surgical robots". In: *2006 IEEE/RSJ international conference on intelligent robots and systems.* IEEE. 2006, pp. 2857–2863.

[19]   James N. Weinstein, Bjorn L. Rydevik, and Wolfgang Rauschning. "Anatomic and Technical Considerations of Pedicle Screw Fixation:" in: *Clinical Orthopaedics and Related Research* &NA;284 (Nov. 1992), pp. 34–46. (Visited on 12/17/2021).

[20]   M R Zindrick et al. "A biomechanical study of intrapeduncular screw fixation in the lumbosacral spine". In: *Clinical orthopaedics and related research* 203 (Feb. 1, 1986), pp. 99–112.

9

III

ADDITIONAL FUNCTIONALITIES
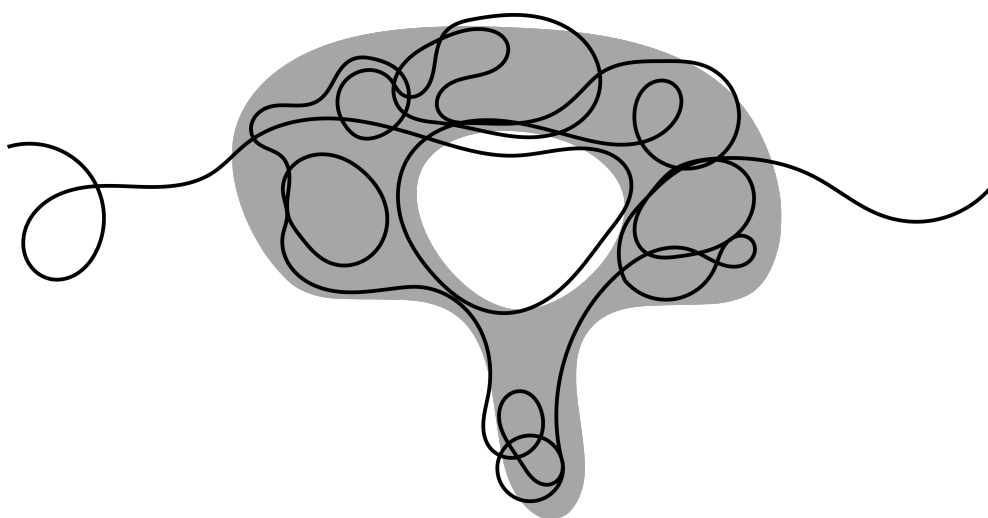
10

STATE-OF-THE-ART IN BONE BIOPSY NEEDLES

Bone biopsies have great value for the diagnosis of, amongst others, haematologic diseases. Although the bone biopsy procedure is mostly performed minimally invasive with the use of a slender cannula, the patient may still experience discomfort, especially when the procedure has to be repeated due to an unsuccessful biopsy. This review presents a comprehensive overview of bone biopsy devices presented in the patent literature. The patents were obtained using a classification search combined with keywords in the Espacenet patent database and were subsequently verified using pre-set eligibility criteria. This resulted in 62 unique patents included in this review. The included patents were categorised based on the used strategies for the three steps that can be identified during a bone biopsy (1) biopsy sampling, (2) biopsy severing and (3) biopsy harvesting. Most patents described strategies for multiple steps. Insight into the used strategies and the comprehensive overview may serve as a source of inspiration for the design of novel bone biopsy devices.

10

10.1. Introduction

10.1.1. Bone Biopsies

Bone biopsies and bone marrow aspirations have great diagnostic value and may be performed in combination to diagnose and evaluate of haematologic diseases such as leukaemia [51]. Bone biopsies are furthermore performed for the diagnosis of benign and malignant bone tumours, including metastatic bone diseases, lymphoma, and myeloma [45]. The bone biopsy procedure can be performed during open surgery in which a relatively large incision is made to reach the bone but mostly the biopsy procedure is performed minimally invasive. Bones have a hard outer shell of cortical bone which surrounds the porous cancellous bone. The pores of the cancellous bone are filled with bone marrow, a semi-solid spongy tissue that is responsible for the production of blood cells and plays a crucial role in the immune system. During a bone marrow aspiration, only a sample of the bone marrow is aspirated for investigation. During a bone biopsy, also called trephine or core biopsy, a section of the cancellous bone and the encapsulated bone marrow is taken from the patient. Where a bone marrow aspiration is solely used to investigate the bone marrow cells, bone biopsies allow the investigation of the structure of the bone marrow within the cancellous bone. Furthermore, a bone biopsy may be performed to investigate a bone lesion. Bone biopsies and bone marrow aspirations may be performed in the same intervention. In these cases, the bone marrow aspiration is usually performed first, after which, the bone biopsy is performed through the same skin incision. It is advised to enter the bone at least 1 cm away from the aspiration location to guarantee that the obtained bone biopsy is not affected by the bone marrow aspiration [7]. This review focuses on technology specifically developed for bone biopsy procedures, since performing a bone biopsy is more complex than a bone marrow aspiration and is considered more painful for the patient [7].

A bone biopsy can be performed in different areas of the human body depending on clinical requirements, but for suspected haematologic diseases often an area where bone can be reached with minimal damage to surrounding soft tissues is chosen, for example, the iliac crest (Figure 10.1) [51]. The bone biopsy procedure begins by creating an entry hole through the skin. Subsequently, a hollow needle between 10 gauge (3.2 mm) and 8 gauge (4.1 mm), referred to as a cannula is introduced through the skin incision with a twisting motion to create the entry hole to the target location within the cancellous bone [51]. During this step, a stylet is placed inside the cannula to prevent soft tissue and bone chips from entering the cannula and to avoid contamination of the biopsy [12]. Furthermore, the sharp point of the stylet aids the penetration of the strong cortical bone layer. Once the distal tip of the cannula has reached the target location, the stylet is removed from the cannula and the cannula is advanced further into the cancellous bone while applying slight pressure combined with a twisting motion [51]. During this process, part of the cancellous bone and encapsulated bone marrow, the biopsy, will enter the lumen of the cannula. When a biopsy sample of 1–3 cm long has been captured in the cannula, the cannula is turned and tilted to sever the biopsy from the surrounding bone [51] Subsequently, the cannula with bone biopsy sample is carefully retrieved from the patient to harvest the biopsy. A slight suction might be used to prevent the biopsy from slipping out of the cannula [51]. After the cannula is successfully retrieved, the biopsy is removed from the cannula using a blunt-tipped stylet that is inserted via the

10
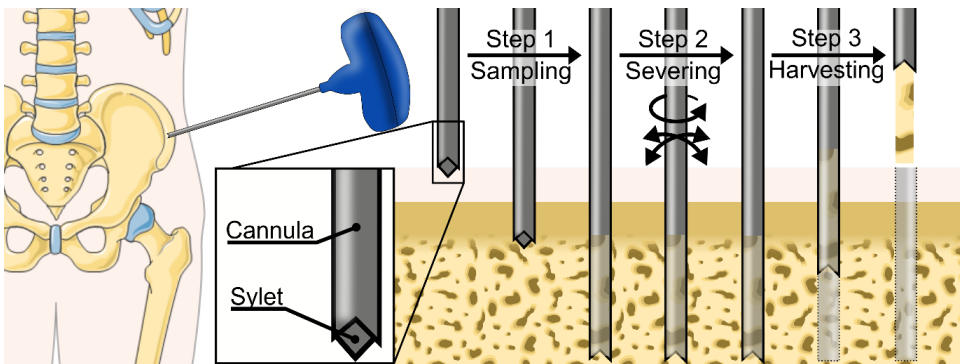
Figure 10.1: Schematic representation of a bone biopsy procedure. Illustration adapted from Servier Medical Art by Servier, licensed under a Creative Commons Attribution 3.0 Unported License.

distal end of the cannula as to push the biopsy out of the cannula.

10.1.2. CHALLENGES IN BONE BIOPSY

Bone biopsies are generally safe procedures with very low complication rates [61]. Breaking of the needle is rare with an estimated occurrence of 0.01% found in a study by Bain [8] but may have serious implications as the needle fragments might need to be removed surgically resulting in a longer hospital stay. Haemorrhage is the most common complication but only accounts for an incident rate of 0.02% [7]. Nevertheless, a bone biopsy procedure can cause significant pain and discomfort to patients [28]. The discomfort may be caused by the heat generated by the friction between the cannula and the bone during the insertion [1]. Furthermore, tilting the cannula to sever the biopsy can cause discomfort due to the creation of micro-fractures and trauma to the surrounding bone [6].

Although reports on serious long-term complications for bone biopsy procedures are low, the number of unsuccessful biopsies is much higher. Cervi [13] states that often two or three biopsies are performed to obtain a single useful biopsy sample. Multiple trials may be necessary due to unsuccessful severing of the biopsy, which makes it impossible to harvest the biopsy with the clinically available biopsy cannulas [51]. Furthermore, the biopsy can slip out of the cannula during retrieval of the cannula [51, 68]. Additionally, when the biopsy is successfully obtained, the biopsy might not be suitable for further investigation due to insufficient size of the biopsy or crushing artefacts in the biopsy that could be introduced during sampling or severing of the biopsy. The need to perform multiple biopsies not only results in more discomfort to the patient but also increases in costs, due to an increased procedure time and additional lab work [11].

10.1.3. GOAL OF THIS REVIEW

The goal of this review is to provide a comprehensive over-view of bone biopsy devices in patent literature, as patent literature provides insights in the latest technical developments in this field. The bone biopsy devices described in the patent literature are categorised based on the methods used in each of three steps that are performed in a

10

bone biopsy procedure, namely (1) biopsy sampling, (2) biopsy severing, and (3) biopsy harvesting (Figure 10.1).

10.2. Method

10.2.1. Patent Search Method

A classification search was conducted in the Espacenet patent database. For this search, only patents with the Cooperative Patent Classification (CPC) of A61B10/025 or a subcategory of this class were included as this class contains patents that describe biopsy devices for bone, bone marrow, or cartilage biopsies. Patents that also had the CPC of A61B10/0283 were excluded as this class includes devices that use vacuum aspiration which is suitable for bone marrow biopsies but not for bone biopsies. Only WORLD patents (WO*), European Patents (EP*), and United States patents (US*) were included in this study.

10.2.2. Eligibility Criteria

The scope of this review is to create an overview of devices that can be used to obtain a bone biopsy. Patents do not always specify the clinical application, hence the following eligibility criteria were used to exclude non-relevant patents. Only patents that describe a design for a device that is able to extract solid tissue such as bone, cartilage and/or tumour tissue, neoplastic or pathological tissue within the bone, were included. Devices that merely focus on bone marrow aspiration were excluded, as strategies used for bone marrow aspiration are not applicable for bone biopsies due to substantial differences between the procedures. Furthermore, the patent was required to describe the method used to obtain the biopsy. Patents solely focusing on, for instance, handle designs were excluded. Lastly, only patents that focus on the extraction of an intact piece of tissue without damaging it were included. This means that devices that focus on the extraction of fragmented bone, for instance to acquire bone grafts, were excluded as this would make the device unfitting for the extraction of bone biopsies for diagnostic purposes.

10.2.3. General Results

The search query resulted in the identification of 297 patents (January 2023). The patents were screened for eligibility by inspecting the title, abstract, and drawings. The description of the patent was screened for eligibility for all patents that were not excluded based on the inspection of the title, abstract and drawings. This resulted in a total of 62 patents being included in this review. Patents that had the same authors and described similar devices were regarded as duplicates although they might not be considered duplicates in the legal sense. In the case of 'duplicates', only the most recent patent was included in this review.

10.2.4. Classification

The patents were classified based on the method used for (1) biopsy sampling, (2) biopsy severing and (3) biopsy harvesting (Figure 10.2). In the methods used to sample the biopsy, a clear distinction was made between (1.a) devices designed for use in a premade hole, such that new bone is cultivated in the device over time, and (1.b) devices

that create a self-made hole through the cancellous bone to sample a biopsy. The hole is in those cases made by solely pushing the cannula into the bone, or by combining the pushing with a twisting motion in one or both directions. Severing of the biopsy sample from the surrounding bone can be achieved by (2.a) inducing shear forces by tilting or rotating the cannula. Severing of the biopsy sample from the surrounding bone can also be achieved by (2.b) tension forces or by (2.c) cutting the biopsy sample from the surrounding bone. The biopsy must be harvested from the patient's body when the cannula is retrieved without the risk of the biopsy slipping out the cannula. This can be achieved by (3.a) creating a shape lock between the biopsy and the cannula by either using a threaded section or a gripper, by (3.b) inducing friction between the biopsy and the cannula by a friction-inducing surface or by compressive forces on the biopsy or (3.c) by using suction.

10.3. RESULTS

10.3.1. BIOPSY SAMPLING

To sample the biopsy, the first step is to penetrate the cortical bone. There are two bone conditions in which bone biopsies are performed: 1) intact cortical bone and 2) weakened or non-existent cortical bone. After penetrating the cortical bone layer, the bone biopsy device is advanced into the cancellous bone sampling the targeted tissue such as pathological, tumorous, or neoplastic tissue.

PRE-MADE HOLE

Two patents describe a bone biopsy device that is intended to be placed into a pre-made hole in the bone [3, 21]. Over time the bone will grow within the hollow section of the biopsy device and subsequently the newly cultivated bone can be removed to obtain the bone biopsy. The process of the bone growing in the implant can span multiple weeks, and over this time the device should remain fixated in the surrounding bone.

Fox [21] describes an implant comprising an outer collar that is secured in the surrounding bone in which an inner structure with multiple slots is placed (Figure 10.3a). These slots allow bone in growth into the device. Furthermore, the sloths have sharpened edges that aid the severing of the biopsy during the removal of the inner structure. The collar may remain within the bone during harvesting of the biopsy sample. Afterwards, the inner structure can be placed back into the collar to obtain another bone biopsy if required.

The devices that use a pre-made hole are mainly intended for use in a research setting, for instance to investigate the effects on bone growth while biopsy devices that create a self-made hole are generally used for diagnostic purposes. This difference in application area results in significantly different designs, therefore, the patents of Albrektsson [3] and Fox [21], that describe a biopsy device using a pre-made hole will not be considered in the categorisation (2) biopsy severing and (3) biopsy harvesting.

SELF-MADE HOLE

Push   The remaining patents all describe the use of a self-made hole to sample the biopsy. All devices use an outer cannula that is advanced through the cancellous bone to sample the bone biopsy. This cannula is often used in combination with a stylet to
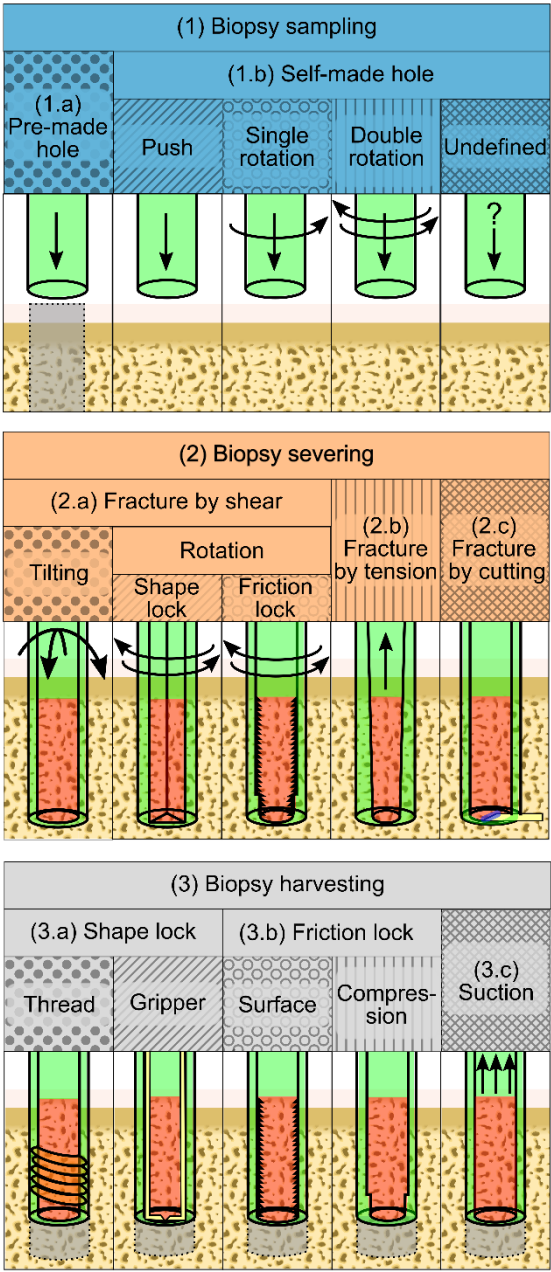
Figure 10.2: Overview of the methods used for (1) sampling the biopsy (2) severing the biopsy and (3) harvesting the biopsy in patent literature. The cannula is indicated in green, the biopsy in red and additional structures in yellow. The arrows indicate the motions of the cannula.

10
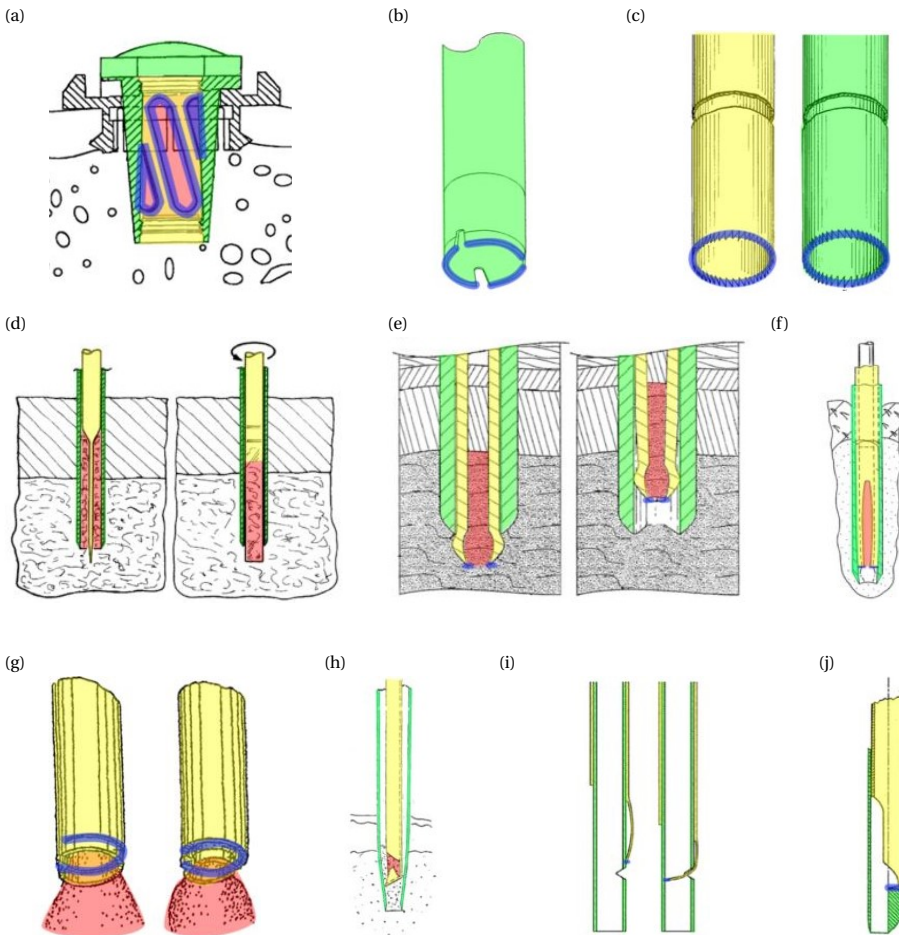
Figure 10.3: Bone biopsy devices comprising an outer cannula (green) an additional (inner) structure (yellow) and a sharp edge (blue) for biopsy (red) sampling and severing. (a) A bone biopsy device intended for implantation in a pre-made hole, figure adapted from [21]. (b) A biopsy device with a wider cutting edge compared to the cannula wall, figure adapted from [58]. (c) A bone biopsy device comprising two concentrically counter rotating cannulas, figure adapted from [44]. (d) A bone biopsy device that severs the biopsy by rotating the inner structure, figure adapted from [5]. (e) A bone biopsy device that severs the bone biopsy by pulling the bulbous inner structure upwards, figure adapted from [9]. (f) A bone biopsy device that compresses the biopsy and severs the biopsy by the sharp cutting edge, figure adapted from [47]. (g) A bone biopsy device with an inner needle with a snare that severs the biopsy, figure adapted from [25]. (h) A bone biopsy device that cuts the biopsy by plastic deformation of the inner structure, figure adapted from [46]. (i) A bone biopsy device that cuts the the biopsy by advancement of the additional outer structure, figure adapted from [50]. (j) A bone biopsy device that cuts the biopsy by rotating the inner structure, figure adapted from [57].

10

penetrate the soft tissue surrounding the bone and the strong cortical bone layer. After reaching the target location within the softer cancellous bone, the stylet is removed and the outer cannula is advanced through the cancellous bone. During this step, the bone biopsy material enters the lumen of the cannula.

Five patents describe the use of a linear pushing motion to advance the outer cannula through the cancellous bone [46, 37, 41, 55, 34]. The outer cannula of the devices described in these patents have a sharpened edge to cut through the bone. Malagoli [41] describes an outer cannula with a non-circular lumen and a sharpened distal end with teeth to help push the cannula through the bone. The sampled biopsy will have a non-cylindrical cross-section. Laughlin *et al.* [37] describe the use of an impact force instead of continuous pushing force to advance the cannula through the cancellous bone.

Single Rotation   Fourteen (14) patents describe the use of a single-sided rotation in combination with linear advancement of the cannula into the cancellous bone [58, 10, 15, 17, 18, 19, 27, 30, 38, 40, 43, 63, 64, 70]. A rotation in a single direction may be preferred when there is a thread-cutting section at the distal end of the cannula, or because the introduction of the cannula is motorised. Spranza [58] describes an outer cannula with a cutting edge that is slightly wider than the wall thickness of the cannula wall, resulting in a clearance between the outer cannula and the surrounding bone. This clearance eliminates friction and thus the generation of heat between the rotating cannula and bone (Figure 10.3b). Furthermore, the cutting edge has sections for the accumulation of bone chips. Aakerfeldt *et al.* [1] also describe the use of a thicker cutting edge to reduce heath generation, however the cannula is not introduced with a single rotation but with an oscillating rotation.

Double Rotation   Twenty-five (25) patents describe linear advancement of the cannula combined with a rotational movement in both directions (oscillatory rotation) [12, 1, 6, 13, 68, 44, 5, 9, 50, 4, 14, 22, 26, 29, 31, 33, 32, 42, 48, 49, 59, 60, 65, 67, 69]. Marino and Elbanna [42] describe the design of a cannula with a castellated teeth pattern at its distal end to reduce the accumulation of bone particles between the teeth as this would diminish the cutting ability. Matthews [44] describes a cannula that consists of two concentric tubes with saw teeth (Figure 10.3c). These saw teeth are directionally oriented such that the inner cannula should be rotated in the opposite direction of the outer cannula.

Undefined   Sixteen (16) patents describe a biopsy device that is able to create a self-made hole to sample the biopsy, however the cannula motion that is used to advance through the cortical bone is not defined [47, 25, 57, 2, 16, 20, 23, 24, 24, 25, 36, 35, 52, 53, 54, 56, 62, 66].

10.3.2. BIOPSY SEVERING

Once the biopsy is sampled by the cannula, the biopsy must be severed from the surrounding bone such that the biopsy can be harvested from the patient.

FRACTURE BY SHEAR

Tilting   Severing of the biopsy can be achieved by inducing shear forces. Thirteen (13) patents describe the use of a primarily tilting motion of the cannula to sever the biopsy [12, 13, 37, 15, 17, 19, 30, 40, 64, 48, 49, 67, 16]. Tilting of the cannula induces shear forces in the contact plane between the biopsy and the surrounding bone. The tilting of the cannula in different directions may be combined with rotating the cannula to sever the biopsy.

Shape Lock   Fourteen (14) patents describe the use of a rotational movement of the cannula to sever the biopsy from the surrounding bone [6, 68, 5, 41, 55, 34, 10, 4, 31, 33, 32, 42, 36, 35]. This eliminates the need to tilt the cannula. Severing by rotating the cannula can only be successful if the biopsy rotates together with the cannula to induce shear forces in the contact plane between the biopsy and the surrounding bone. Four patents provide designs that avoid the biopsy from rotating within the cannula by using a non-circular lumen [5, 41, 55, 34]. Malagoli [41], and Sachse and Sachse [55] both describe a cannula with a non-circular lumen to allow the severing of the sample by rotating the cannula. Joish [34] describes a cannula with an off-centre lumen in which the biopsy is captured. Rotation of the cannula around its central axis will result in the severing of the sample. Avaltroni [5] has a different approach as not the cannula itself is rotated but rather a blade that is introduced into the cannula after sampling the biopsy (Figure 10.3d). The blade cuts the biopsy in two halves and rotating the blade will sever the biopsy.

Friction Lock   Rotation of the biopsy with respect to the needle can also be avoided by increasing the friction between the biopsy sample and the inner surface of the cannula [6, 68, 10, 4, 31, 33, 32, 42, 36, 35]. For example, the use of a structure on the inside of the cannula such as barbs or grooves may increase the friction between the biopsy and the cannula [4, 35]. Another way to increase the friction between the biopsy and the inside of the cannula is by compressing the biopsy against the cannula wall, for instance by using a tapered tip [10], or a ridge at the distal end [6, 68, 31, 33, 32]. Due to the narrowing of the lumen at the distal end of the cannula, the biopsy will be slightly compressed as it enters the lumen due to the elasticity of the bone tissue. The increased friction induced by compression prevents the rotation of the sample with respect to the cannula and eases the severing. Krueger and Clark [36] and Marino and Elbanna [42] use the introduction of an inner needle in the cannula to compress the biopsy such that the friction is increased.

FRACTURE BY TENSION

Four patents describe a biopsy severing method by inducing tensional forces on the bone [9, 38, 63, 22]. Tensioning is only possible if the biopsy is well connected to the cannula by a shape lock, for instance, due to a threaded section at the distal end of the cannula [38, 63, 22]. Pulling the cannula, and thus the enclosed biopsy, out of the patient as to retrieve the cannula results in tensioning and finally fracturing of the biopsy from the surrounding bone. Baldridge [9] does not use a threaded section but rather proposes the use of an inner needle that has a bulbous end that extends from the outer cannula and is slightly larger than the cannula lumen (Figure 10.3e). Once the target area

10

is reached, the cannula with the inner needle is advanced through the cancellous bone such that the lumen of the inner needle fills with the cancellous bone. After obtaining a biopsy with the correct length, the inner needle is pulled into the outer cannula. Slits in the bulbous end allow for radial compression such that the inner needle fits within the outer cannula. This results in tensioning of the bone, and combined with the sharp edge of the bulbous end, in severing of the bone biopsy.

FRACTURE BY CUTTING

Sixteen (16) patents describe a cannula that can sever the biopsy from the surrounding bone by means of cutting [47, 24, 46, 50, 57, 27, 70, 60, 69, 2, 20, 24, 52, 53, 54, 66]. Five patents describe the use of an inner needle that consists of two or more semi-circular cutting blades that form a tweezers-like structure [47, 52, 53, 54, 66]. The inner needle is located within the cannula during insertion into the bone. After the biopsy is enclosed, the inner needle is moved deeper into the cannula, such that the tweezers is at the distal end of the cannula. Since the cannula is slightly tapered, this will result in compression of the distal tips of the tweezers and thus the cutting of the biopsy from the surrounding bone (Figure 10.3f). Rubinstein [54] describes a slightly different approach to compress the distal tips of the tweezers using a cannula with an oval lumen. In this design, the tweezers tips can be compressed even further by rotating the tweezers with respect to the oval lumen of outer cannula.

Goldenberg [24, 25] describes two cannula designs with a snare at the distal end that can be constricted once the bone biopsy is enclosed such that the biopsy is cut loose from the surrounding bone (Figure 10.3g). Zambelli [70, 69] and Miller and Ireland [46] describe the use of an inner needle that plastically deforms such that the biopsy is cut loose due to the tapered tip of the outer cannula (Figure 10.3h). Peliks *et al.* [50] describe the use of a pre-bend cutting blade that is located at the outside of the cannula (Figure 10.3i). During the insertion of the cannula, the cutting blade is forced in a straight position such that the cutting blade does not harm the advancement of the cannula through the cancellous bone. Once a biopsy with the right length is obtained, the pre-bend cutting blade is advanced through a slit at the distal end of the cannula such that the biopsy is severed from the surrounding bone. Furthermore, two patents describe the rotation of an inner needle as a means to cut the biopsy from the surrounding bone [57, 60] (Figure 10.3j).

10.3.3. BIOPSY HARVESTING

After the biopsy is sampled by the cannula and severed from the surrounding bone, the cannula must be retrieved from the patient to harvest the biopsy. Harvesting the biopsy may fail as the biopsy is not always well secured within the cannula and may slip out when retrieving the cannula.

SHAPE LOCK

Thread   Of the included patents, nineteen (19) describe the use of a shape lock to prevent the biopsy from exiting the cannula such that the biopsy can successfully be harvested. Four (4) patents describe a cannula with a threaded section at the distal end [30, 38, 63, 22], (Figure 10.4a). The cannula is advanced with a single rotation and as a result,
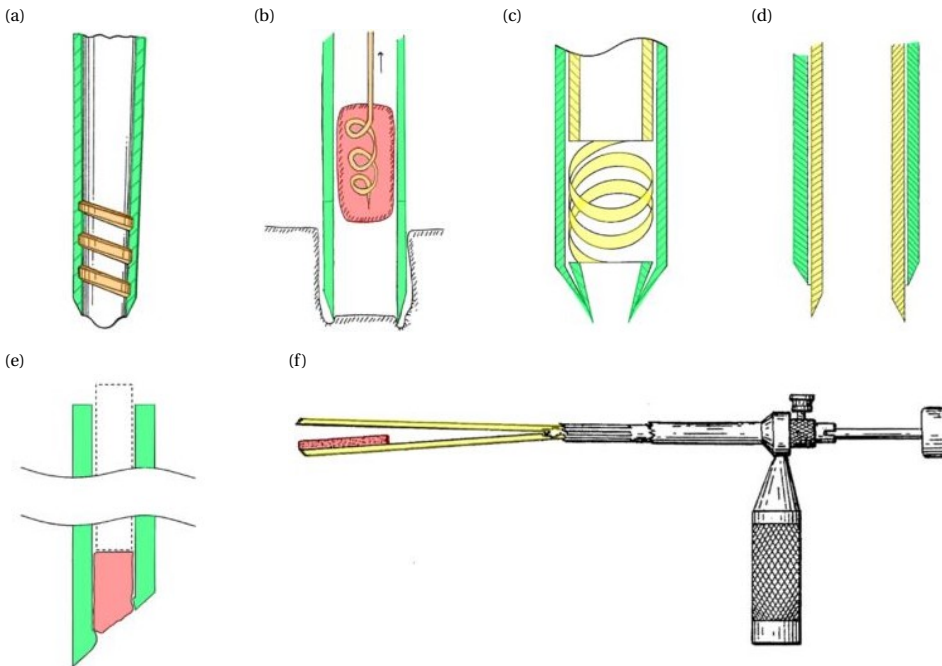
Figure 10.4: Bone biopsy devices comprising an outer cannula (green) an additional (inner) structure (yellow) and additional characteristics (orange) to retain the biopsy. (a) A bone biopsy device with a threaded section to create a shape lock between the biopsy and the cannula, figure adapted from [63]. (b) A biopsy device with a corkscrew inner structure to create a shape lock to retain the biopsy, figure adapted from [22]. (c) A bone biopsy device with a spring that can compress the biopsy to retain it figure adapted from [24]. (d) A bone biopsy device with a tapered inner structure to compress the biopsy for successful retainment, figure adapted from [29]. (e) A bone biopsy device that retains the biopsy by a sudden change in lumen diameter, figure adapted from [37]. (f) A bone biopsy device that compresses the biopsy and allows for easy removal from the inner structure, figure adapted from [17].

threads are cut in the bone biopsy. This creates a shape lock between the biopsy and the threaded section such that the biopsy is securely fixated. Gillespie *et al.* [22] also describe the use of a threaded section, but in the proposed design, an inner needle with a corkscrew at the distal end is used to create a shape lock (Figure 10.4b). The biopsy can be harvested by retrieving the cannula together with the inner needle without the risk of losing the biopsy.

Gripper The other fifteen (15) patents describe the use of a gripper to create a shape lock to secure the biopsy within the cannula when retrieving the cannula [25, 57, 27, 70, 60, 69, 2, 20, 24, 52, 53, 54, 66]. Goldenberg [24] describes an inner needle that is connected to the distal end of the cannula with a spring (Figure 10.4c). Rotation of the inner needle with respect to the cannula results in further coiling of the spring causing a decrease in the inner diameter of the spring. This secures the biopsy within the cannula.

10

Friction lock

Surface   Friction between the biopsy and the inner wall of the cannula can be used to prevent the biopsy from slipping out of the cannula during retrieval. Three patents use a friction-inducing surface on the inside of the cannula to prevent the biopsy from slipping out [13, 4, 36]. The inside of the lumen has groves or barbs to increase the friction between the cannula and the biopsy. The same friction-inducing surface can be used to sever the biopsy as described in Section 10.3.2.

Compression   Eighteen (18) patents describe the use of compression of the biopsy to increase the friction between the biopsy and the cannula via an increase in normal force to prevent the biopsy sample from slipping out of the cannula during retrieval [1, 6, 68, 5, 9, 47, 57, 10, 17, 40, 29, 31, 33, 42, 49, 36]. An increase in friction by using compression can be achieved by a tapered tip of the cannula [1, 10, 40, 48, 49]. The cannula lumen is narrower at the distal end and as a result, the biopsy is slightly compressed at the distal end which increases the normal force and thus the friction between the biopsy and the cannula and secures the biopsy during retrieving of the cannula. Hirsch *et al.* [29] describe a tapered tip with a slightly wider cutting edge at the distal end as compared to the rest of the lumen (Figure 10.4d). The compression of the biopsy when it is pushed into the lumen increases the friction between the cannula wall and the biopsy and thus prevents the biopsy from slipping out.

Five patents describe a sudden change in lumen diameter at the distal end of the cannula [68, 37, 31, 33, 32]. Although the working principle is similar to the cannulas with a tapered tip, these patents do not have a gradual change in lumen diameter but a sudden narrowing of the lumen at the distal end (Figure 10.4e). The tissue is cut and compressed through the narrow section of the lumen, which increases the friction to retain the biopsy. Furthermore, the biopsy can expand once it reaches the wider section of the lumen, resulting in an additional shape lock to retain the biopsy.

Seven patents describe the use of an additional structure to increase the friction between the biopsy and the cannula [6, 5, 9, 47, 17, 42, 36]. Examples are inner needles that are introduced within the cannula to compress the obtained biopsy. An example is the inner needle which consists of two semi-circular structures that together form a tweezers-like device described by Doppelt [17] (Figure 10.4f). Advancement of the inner needle through the cannula results in compression of the two tweezers halves due to the narrowing lumen at the distal end of the cannula. Compression of the tweezers tips compresses the biopsy and prevents it from slipping out of the cannula. A similar method is proposed by Mittermeier and Halbe [47].

10

Suction

Only one patent of Wiksell *et al.* [67] describes the use of suction to harvest the biopsy. In this device a negative pressure differential (suction) is created within the cannula, which prevents the biopsy from slipping out. Suction may also be used in combination with the earlier-mentioned strategies to harvest the biopsy.

After the removal of the cannula from the patient, the biopsy material must be removed from the cannula. Often a plunger with a blunt tip is used to push the biopsy out of the lumen. The pushing force that is used to achieve this could also harm the biopsy.

As an alternative to using a plunger to remove the bone biopsy from the cannula Doppelt [17] proposes a design that captures the biopsy between two semi-cylindrical structures. This would not only help to retain the biopsy during the removal of the needle. It also makes it possible to easily remove the bone biopsy from the needle while maintaining the structural integrity of the biopsy.

10.4. CONCLUSION

This review provides a comprehensive overview of the different bone biopsy devices described in patent literature. The search query used in the Espacenet database returned 297 patents of which 62 were deemed eligible for inclusion in this review. The patents were categorised based on the strategies used for the three major steps that are followed during a bone biopsy procedure (1) biopsy sampling, (2) biopsy severing, and (3) biopsy harvesting. The sampling of the biopsy may be achieved by creating a hole through the bone or by cultivating new bone in a pre-made hole. The severing of the biopsy can be achieved by tension forces, shear forces, or cutting. Harvesting the biopsy can be achieved by using a shape lock, friction between the biopsy and the device, or suction. It must be noted that the strategies used in one step of the biopsy procedure influences the possible strategies that may be used in the other steps of the biopsy. The provided overview may serve as a source of inspiration for the design of novel bone biopsy devices.

10.5. EXPERT OPINION

10.5.1. COMPARATIVE ANALYSIS

The goal of this review was to create a comprehensive overview of bone biopsy devices in patent literature. The different designs were categorised based on the strategies used for each of the three steps that are followed during a bone biopsy procedure (1) biopsy sampling, (2) biopsy severing and (3) biopsy harvesting. Figure 10.5 shows the distribution of the filed patents over the years for each of these identified steps. Between 1970 and 2010 there has been a steady increase in filed patents however, this growth dropped suddenly between 2010 and 2020. It seems plausible that the growth in filed patents will recover after 2020 based on the current amount of filed patents between 2020 and January 2023.

Sixty-six percent (66%) of the included patents described a method for both sampling, severing and harvesting of the bone biopsy sample. Seventy-four percent (74%) of the included patents clearly describe the introduction method of the cannula and thus the sampling of the biopsy. However, for the remaining 26% only mention that the cannula was able to cut through the bone without specifying the specific sampling method (e.g. push possibly combined with a rotating motion). Seventy-six percent (76%) of the included patents describe a method for severing the biopsy and 66% of the patents describe a method to retain the biopsy when the cannula is retrieved.

The overview with the different methods to sample, sever and harvest the bone biopsy indicated that certain methods are more frequently combined. For instance, the biopsy devices that employ a shape lock to sever the biopsy sampled the biopsy by pushing the cannula through the cancellous bone. The shape lock was often created by a non-rotational symmetric cross section of the cannula. Rotating the cannula during sampling would results in a rotational symmetric biopsy, making the use of a shape-lock to sever

10

the biopsy more challenging. Furthermore, biopsy devices that use a threaded section are always introduced by a single rotating motion such that screw thread cuts in the biopsy to achieve the desired shape lock. Devices that severe the biopsy by tensioning or cutting use an additional structure, such as an inner needle, that is subsequently used to create a shape lock in order to retain the biopsy when the cannula is retrieved from the patient. Lastly, when friction is used to retain the biopsy during severing, the same friction inducing strategy is also used to retain the biopsy when the cannula is removed.

All patents reviewed in this study describe innovative ideas for sampling, severing and harvesting bone biopsies. While the suitability for clinical practice is often not discussed in depth in patent literature, we can evaluate the proposed biopsy device designs' suitability for clinical practice based on the included information and current clinical practice. First of all, biopsy devices should have a small outer diameter to minimise trauma to the patient, while harvesting an as large as possible bone biopsy. It is, therefore, preferred that bone biopsy devices have a small wall thickness and thus a large lumen. The bone biopsy devices described in Group 2.c 'Fracture by cutting' and Group 3.a 'Shape lock' require an additional structure to sever and harvest the biopsy. This additional structure requires space and may increase the wall thickness and decrease the obtained biopsy which would make these devices less desirable for clinical practice. Furthermore, these structures might lack structural rigidity due to their small size, which can result in mechanical failure and inability to downsize these devices in future. The use of a friction lock, especially a friction inducing surface could, however, ease severing and harvesting of the bone biopsy without requiring an increase in wall thickness. This could increase the success-rate of bone biopsy procedures without adverse effect such as a larger outer diameter of the biopsy device.

Besides striving for a biopsy device with a small outer diameter, the usability of the biopsy device is of great importance for clinical application. Additional actions required by the user to obtain the biopsy compared to conventional biopsy needles are undesired as this will increase the procedure time and thus the associated costs [11]. Furthermore, a more complex device that requires more actions might increase the workload of the user, which is associated with a higher chance of complications [39]. Biopsy devices in Group 2.c 'Fracture by cutting' and biopsy devices in Group 3.a 'Shape lock' that use a gripper are expected to require an additional action to sever the biopsy with the inner needle and are, therefore, less desirable. Other solutions presented in Group 2.a 'Fracture by shear' do not require an addition action as compared to the current procedure and are therefore easier to implement in the current workflow. Finally, bone biopsy devices requiring implantation for bone ingrowth are only feasible if obtaining multiple samples over a longer time frame is required. These devices could be of use in specific applications but are not a substitute for the currently used biopsy needles.

10.5.2. Limitations and Future Research

This patent review focuses on the different mechanical solutions for the sampling, severing and harvesting of bone biopsies. Often a bone biopsy is combined with a bone marrow aspiration during one intervention with similar instrumentation. Even so, patents focusing on bone marrow aspiration were excluded as this is a different procedure with different challenges. Furthermore, this review only included patent literature and ex-

10
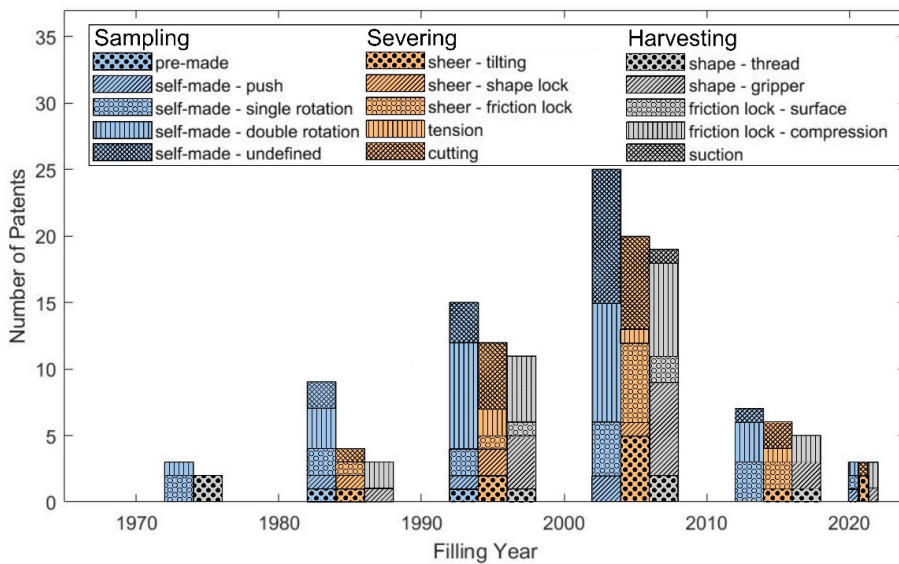
Figure 10.5: Temporal distribution of the methods presented in the included patents for biopsy sampling, severing and harvesting until January 2023.

cluded scientific literature, as patents are generally a good way to gain insight into the future development of devices. It could be of interest for future research to extend this patent review with a review of the scientific literature to emphasise the suitability for clinical practice of different bone biopsy designs more extensively.

This review provides a comprehensive overview of bone biopsy devices which can provide insights into the future development of the devices. The overview may also serve as a source of inspiration for the development of novel bone biopsy devices.

10.5.3. FIVE-YEAR VIEW

Over the years there has been an increasing focus on the severing and harvesting of bone biopsies. The successful severing of the biopsy and subsequently the harvesting will increase the success rate of the biopsy procedure. Fewer trials are needed to obtain one useful biopsy which will significantly decrease the discomfort to the patient. We expect that this trend will continue in the coming years. Attention should be directed to the discomfort that patients will experience with the use of these new devices that can sever and harvest the biopsies successfully. The use of an additional inner needle or structure in the cannula may result in a larger outer diameter of the cannula which may increase the discomfort of the patient. Furthermore, the use of the bone biopsy devices in the clinical workflow should not be forgotten. Ease of operation with a limited number of steps is a necessity to ensure usability of newly designed bone biopsy devices in practice. It is expected that in the next five years more focus will be on easily obtaining bone biopsies of high quality with as little discomfort to the patient as possible.

10

BIBLIOGRAPHY

[1] Dan Aakerfeldt, Gunnar Aastroem, and Haakan Ahlstroem. "Device for Biopsy Sampling". WO9517126A1. June 1995.

[2] Robert K. Ackroyd. "Dual Needle Core Biopsy Instrument". US2016074020A1. Mar. 2016.

[3] Thomas Albrektsson and Per Aspenberg. "A bone ingrowth chamber." EP0269175A2. June 1988.

[4] John B. Andelin and Martin T. White. "Bone marrow biopsy needle and method for using the same". US6110128A. Aug. 2000.

[5] Paolo Avaltroni. "Biopsy device". EP0992218A1. Apr. 2000.

[6] Paolo Avaltroni. "Improved needle instrument for taking osteomedullary bioptical samples". EP1396230A1. Mar. 2004.

[7] B. J. Bain. "Bone marrow trephine biopsy". en. In: *Journal of Clinical Pathology* 54.10 (Oct. 2001). Publisher: BMJ Publishing Group, pp. 737–742. (Visited on 01/13/2023).

[8] Barbara J. Bain. "Bone marrow biopsy morbidity and mortality: Short Report". en. In: *British Journal of Haematology* 121.6 (June 2003), pp. 949–951. (Visited on 01/13/2023).

[9] Danny J. Baldridge. "Bone marrow biopsy instrument". US5357974A. Oct. 1994.

[10] Carlo Bianchini. "Device for Bone Marrow Biopsy". WO2004082484A1. Sept. 2004.

[11] P. W. Bishop, K. McNally, and M. Harris. "Audit of bone marrow trephines." en. In: *Journal of Clinical Pathology* 45.12 (Dec. 1992). Publisher: BMJ Publishing Group Section: Research Article, pp. 1105–1108. (Visited on 01/13/2023).

[12] John R. Byrne et al. "Biopsy Needle Assembly". WO9603081A1. Feb. 1996.

[13] Paul Cervi. "Biopsy Needle". WO0056220A1. Sept. 2000.

[14] Guerrero De Stavropo Contreras and Stamatios M. Stavropoulos. "Apparatus for extracting bone marrow specimens". US4142517A. Mar. 1979.

[15] Joshua Cook. "Apparatus and method for harvesting bone". US10485558B1. Nov. 2019.

[16] Ramirez Jorge Armando Cortes et al. "Bone biopsy and bone marrow aspiration device". US8992442B2. Mar. 2015.

[17] Samuel H. Doppelt. "Bone biopsy apparatus". US4798213A. Jan. 1989.

[18] Thomas a Einhorn, Andrew Valenti, and Matthew Alves. "Bone boring instrument". US4782833A. Nov. 1988.

10

[19]   E. Elias and Y. Elias. "Bone Biopsy Instrument and Method". US3850158A. Nov. 1974.

[20]   Dean Allen Entrekin et al. "Bone Harvest System". WO2007149302A2. Dec. 2007.

[21]   William Casey Fox. "Bone Biopsy Implant". WO9624309A1. Aug. 1996.

[22]   Walter D. Gillespie et al. "Bone graft harvester". US6764452B1. July 2004.

[23]   Oren Globerman and Mordechay Beyar. "Integrated Bone Biopsy and Therapy Apparatus". WO2008001385A2. Jan. 2008.

[24]   Alec S. Goldenberg. "Bone Marrow Biopsy Needle". WO2009085389A2. July 2009.

[25]   Alec S. Goldenberg. "Bone Marrow Biopsy Needle-1". US2009082697A1. Mar. 2009.

[26]   Charles R. Gordon, James E. Deaton, and Corey Harbold. "Apparatus and Method for Bone Harvesting". US2015025534A1. Jan. 2015.

[27]   Norman Gray. "Bone biopsy needle". US5040542A. Aug. 1991.

[28]   Stephen Hibbs. "This Is Going to Hurt: Revisiting the Patient Experience of Bone Marrow Biopsies". In: *HemaSphere* 6.4 (Mar. 2022), e710. (Visited on 01/13/2023).

[29]   Joshua a Hirsch, Scott H. Mcintyre, and Yves P. Arramon. "Cannula for extracting and implanting material". US2004073139A1. Apr. 2004.

[30]   Hans-Rainer Hoffmann and Rudolf Matusch. "Biopsy Needle For The Histological Examination Of Body Tissue". US2008146964A1. June 2008.

[31]   Abul B. M. a Islam and David R. Bevan. "Biopsy needle". US4543966A. Oct. 1985.

[32]   Abul Bashar Mohammad Anwarul Islam. "Biopsy needle". US10307142B2. June 2019.

[33]   Abul Bashar Mohammed Anw Islam. "Bone marrow biopsy needle". US2004249306A1. Dec. 2004.

[34]   Suresh K. Joishy. "Two in one bone marrow surgical needle". US5012818A. May 1991.

[35]   John Krueger. "Bone biopsy instrument having improved sample retention". US2003050574A1. Mar. 2003.

[36]   John a Krueger and Grant A. Clark. "Bone marrow biopsy needle". US6443910B1. Sept. 2002.

[37]   Trevor Laughlin et al. "Tissue Coring Device". WO2020185961A1. Sept. 2020.

[38]   Choon Kee Lee. "Tissue sampling apparatus". US2014213931A1. July 2014.

[39]   Qing-Lian Lin et al. "Human reliability assessment for medical devices based on failure mode and effects analysis and fuzzy linguistic theory". en. In: *Safety Science* 62 (Feb. 2014), pp. 248–256. (Visited on 03/17/2023).

[40]   Rao Madhumathi, Clay Larkin, and Florence Lima. "Bone Biopsy System and Method". WO2021003335A1. Jan. 2021.

[41]   Enrico Malagoli. "Needle Instrument for Transcutaneous Biopsy of Bone Marrow Tissues". WO2005009246A1. Feb. 2005.

10

[42] James F. Marino and Jamil Elbanna. "Removable bone penetrating device and methods". US10292688B2. May 2019.

[43] Thierry Masseglia and Laurent Fumex. "Perforating trocar". US2008306405A1. Dec. 2008.

[44] Larry S. Matthews. "Counter rotating biopsy needle". US4306570A. Dec. 1981.

[45] Andreas F. Mavrogenis et al. "How Should Musculoskeletal Biopsies Be Performed?" In: *Orthopedics* 37.9 (Sept. 2014). Publisher: SLACK Incorporated, pp. 585–588. (Visited on 07/26/2023).

[46] Michael E. Miller and Dan Ireland. "Biopsy extractor". EP1136039A2. Sept. 2001.

[47] Manfred Mittermeier and Alan M. Hable. "Bone Marrow Biopsy Needle". WO0010465A1. Mar. 2000.

[48] Carlos Negroni. "Biopsy assembly". US2004127814A1. July 2004.

[49] Michael J. O'neill. "Bone harvesting method and apparatus". US5954671A. Sept. 1999.

[50] Robert Bilgor Peliks, Jeremy Snow, and Jade Ollerenshaw. "Bone Biopsy Device and Related Methods". WO2021178490A1. Sept. 2021.

[51] Roger S. Riley et al. "A pathologist's perspective on bone marrow aspiration and biopsy: I. performing a bone marrow examination". en. In: *Journal of Clinical Laboratory Analysis* 18.2 (2004). _eprint: https://onlinelibrary.wiley.com/doi/pdf/10.1002/jcla.20008, pp. 70–90. (Visited on 01/05/2023).

[52] Alan Rubinstein, Andrew M. Olah, and Emery Olah. "Bone Marrow Biopsy Needle". WO9627330A1. Sept. 1996.

[53] Alan I. Rubinstein. "Bone Marrow Biopsy Needle". WO0200109A1. Jan. 2002.

[54] Daniel B. Rubinstein and Alan I. Rubinstein. "Bone Marrow Biopsy Needle with Cutting and/or Retaining Device at Distal End". WO9319675A1. Oct. 1993.

[55] Hans Sachse and Rainer Sachse. "Oscillating bone harvesting device". US6179853B1. Jan. 2001.

[56] Eric Schofield, Roy K. Lim, and Michael C. Sherman. "Dual Outside Diameter Cannula for Insertion into Bone". WO2004000127A1. Dec. 2003.

[57] Borhane Slama and Hacene Zerazhi. "Osteomedullar Biopsy Trocar". US2008139961A1. June 2008.

[58] Joseph John Spranza. "Hardware for cutting bone cores". US2003199879A1. Oct. 2003.

[59] Robert K. Strasser and Robert L. Netsch. "Bone biopsy needle assembly". US4838282A. June 1989.

[60] William R. Swaim. "Biopsy Hand Tool for Capturing Tissue Sample". WO9722299A1. June 1997.

10

[61]   Anderanik Tomasian and Jack W. Jennings. "Bone marrow aspiration and biopsy: techniques and practice implications". en. In: *Skeletal Radiology* 51.1 (Jan. 2022), pp. 81–88. (Visited on 01/05/2023).

[62]   Carl W. Tretinyak. "Biopsy needle". US4403617A. Sept. 1983.

[63]   David H. Turkel. "Coaxial Bone Marrow Biopsy and Aspirating Needle". WO9405210A1. Mar. 1994.

[64]   Miklos I. Vilaghy and Gabor Zellerman. "Bone biopsy instrument kit". US4010737A. Mar. 1977.

[65]   Suresh Wadhwani and Greg Smith. "Bone marrow biopsy, aspiration and transplant needles". US5331972A. July 1994.

[66]   John L. Ward. "Biopsy instrument". US4785826A. Nov. 1988.

[67]   Hans Wiksell et al. "Arrangement for Taking a Sample of Bone Marrow and/or Evacuating the Sinuses". US2007270712A1. Nov. 2007.

[68]   Flavio Augusto Zambelli. "Bone biopsy device and process for making the same". EP1277440A1. Jan. 2003.

[69]   Roberto Zambelli. "Bone biopsy device". EP2215971A1. Aug. 2010.

[70]   Roberto Zambelli. "Improved Bone Biospy Device". EP3326540A1. May 2018.

10

11

DESIGN OF A SOFT TISSUE TRANSPORTER

Tissue transport is a challenge during Minimally Invasive Surgery (MIS) with the current suction-based instruments as the increasing length and miniaturisation of the outer diameter requires a higher pressure. Inspired by the wasp ovipositor, a slender and bendable organ through which eggs can be transported, a flexible transport mechanism for tissue was developed that does not require a pressure gradient. The flexible shaft of the mechanism consists of ring magnets and cables that can translate in a similar manner as the valves in the wasp ovipositor. The designed transport mechanism was able to transport 10 wt% gelatin tissue phantoms with the shaft in straight and curved positions and in vertical orientation against gravity. The transport rate can be increased by increasing the rotational velocity of the cam. A rotational velocity of 25 RPM resulted in a transport rate of 0.8 mm/s and increasing the rotation velocity of the cam to 80 RPM increased the transport rate to 2.3 mm/s though the stroke efficiency decreased by increasing the rotational velocity of the cam. The transport performance of the flexible transport mechanism is promising. This means of transportation could in the future be an alternative for tissue transport during MIS.

11.1. INTRODUCTION

11.1.1. TISSUE TRANSPORTATION DURING SURGERY

The transportation of gasses, liquids and solids in the human body is a key function that needs to be fulfilled to support life. Disturbances to these processes can cause serious symptoms and often require surgical treatment to resolve the issue. Treatment often involves the removal and, therefore, transportation, of the disturbance, such as thrombus, cancerous or infectious tissue, from the intervention site to outside the patient's body [25, 20]. The removal, and thus transportation, of liquids and solids from the body is also of vital importance for diagnostic purposes [10]. Vice versa, the transportation of substances, such as medicine [7] or radioactive particles [17], from outside the patients' body towards a target area inside the body is essential for treatment purposes.

Whereas the removal of tissues is generally a relatively straightforward procedure in open surgery, it is more challenging in Minimally Invasive Surgery (MIS). During open surgery a relatively large incision is made, allowing for easier removal of the obstruction, as the distance between the surgical opening and the intervention site is short and the path is wide. Nowadays, more and more surgeries are performed minimally invasive, in which one or multiple small (5–15 mm) incisions are made through which entry to the body is obtained. MIS is associated with positive primary and secondary outcomes, such as shorter hospital stays and less postoperative pain [12]. One major downside of MIS is, however, that the transportation and subsequent removal of tissues is more challenging due to the small incision size and a longer, sometimes curved, pathway between the intervention site and the incision.

11.1.2. SUCTION-BASED INSTRUMENTS

Suction-based instruments are the current standard in MIS to transport a variety of substances from the operation area to outside the patient's body. Transportation is achieved by creating a pressure gradient in a tubular structure, such that substances in front of the tube tip are sucked in and can, subsequently, be removed.

Although suction-based instruments function generally well, they become less effective with the ongoing trend of miniaturisation. Restrictions to the outer dimensions pose a problem for suction-based instruments, as a smaller lumen diameter and a longer tube require a higher pressure difference to achieve adequate transportation [11]. Another often occurring problem during suction-based transport is clogging. Clogging is mainly the result of friction between the transported tissue and the instrument's wall [21] (Figure 11.1). Clogging makes further transportation impossible and requires removal of the clogged tissue part, with an increase in the procedure time as a result. Therefore, a reliable alternative for suction-based transport that is not prone to clogging is needed.

11.1.3. BIOLOGICAL INSPIRATION: WASP OVIPOSITOR

An interesting biological example of reliable transport through a very slender tube can be found in parasitic wasps. Parasitic wasps possess an ovipositor: a thin and flexible tubular organ with which they can drill in a living host, to deposit their eggs inside this host (Figure 11.2a). The egg transport through the ovipositor is not achieved by a pressure gradient, such as in suction-based instruments, but by an oscillatory motion of the

11
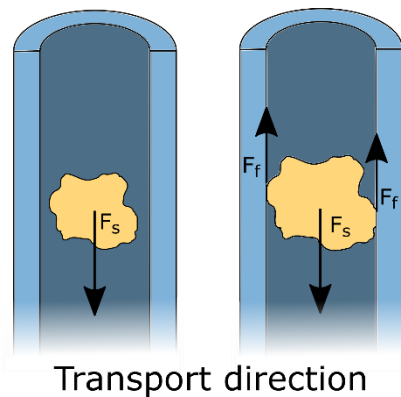
Figure 11.1: Schematic representation of suction-based transport. A suction force F_s acts on the tissue, resulting in transportation of the tissue. Clogging occurs when the piece of tissue is in contact with the walls of the tube and the resulting friction forces F_f. Clogging prevents any further transportation of the tissue part. are larger than the suction force F_s

ovipositor valves that together form the tubular ovipositor [4, 6, 19].

The ovipositor generally consists of three independently translating valves: one dorsal valve and two ventral valves. The valves are enclosed by the ovipositor sheath and can slide axially with respect to each other while being kept in place radially by a tongue-and-groove connection, called olistheter [1]. The chitinous flaps of the ventral valves are thought to provide a seal that prevents the egg from escaping the egg channel during oviposition [1].

It is hypothesised that the egg transport relies on the friction between the egg and the valves [4, 1]. The exact motion sequence that results in the transportation of the eggs is, however, not fully known. One hypothesis is that the transportation of the egg and the drilling occurs simultaneously. The sequence of valve movements would result in drilling the ovipositor deeper into the substrate and simultaneously transport and deposition of the eggs. A second hypothesis is that the wasp can transport eggs through the ovipositor without drilling the ovipositor deeper into the substrate. In this scenario, the transportation is thought to be achieved by small translations of the ovipositor valves in a repeating sequence, see Figure 11.2b.

Following the second hypothesis, the egg transport sequence starts with all three valves translating in the desired transport direction (Figure 11.2b, Step 1). The egg will move along with the valves due to the friction between the egg and the valves. Subsequently one of the valves retracts while the other two valves remain stationary (Figure 11.2b, Step 2). It is important to note that the wasp's eggs are somewhat flexible resulting in the friction force being dependent on the contact surface between the egg and the valve. Therefore, the egg will remain stationary, as the combined friction with the two stationary valves exceeds the friction with the single retracting valve, assuming that all valves have the same contact surface with the egg. After the retraction of the first valve, the second valve retracts, while the other two valves remain stationary (Figure 11.2b, Step 3). Again, the egg will remain stationary. The final step in the sequence is the re-

11

(a)

(b)
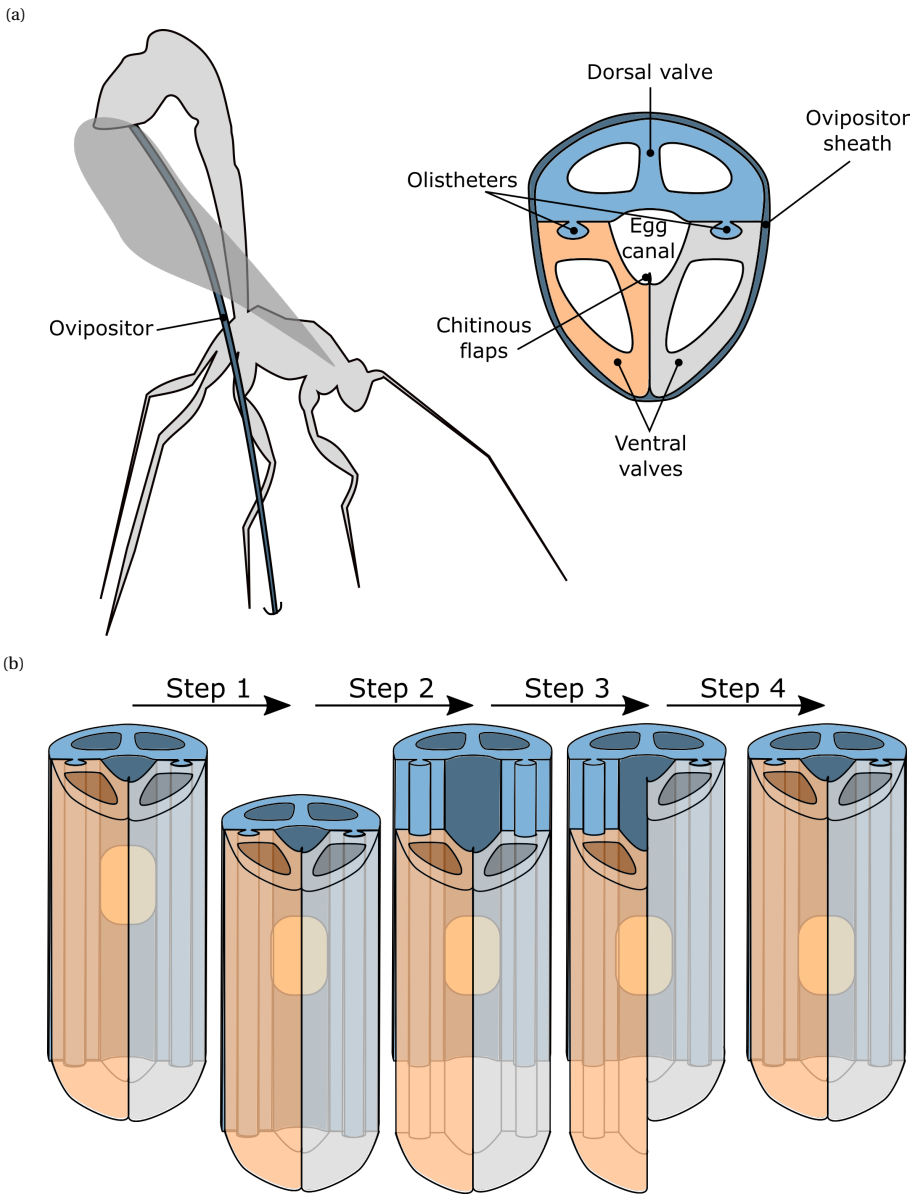
Figure 11.2: Schematic representation of a parasitic wasp that uses a needle-like organ called an ovipositor to transport eggs into host material [4, 6, 19]. (a) The ovipositor generally consists of one dorsal valve and two ventral valves that are held together by tongue-and-groove connections, called olistheters, that allow the valves to slide with respect to each other. The chitinous flaps prevent the egg from escaping the egg channel and the ovipositor is covered by the ovipositor sheath. (b) A possible motion sequence of the valves that results in transport of the eggs along the ovipositor.
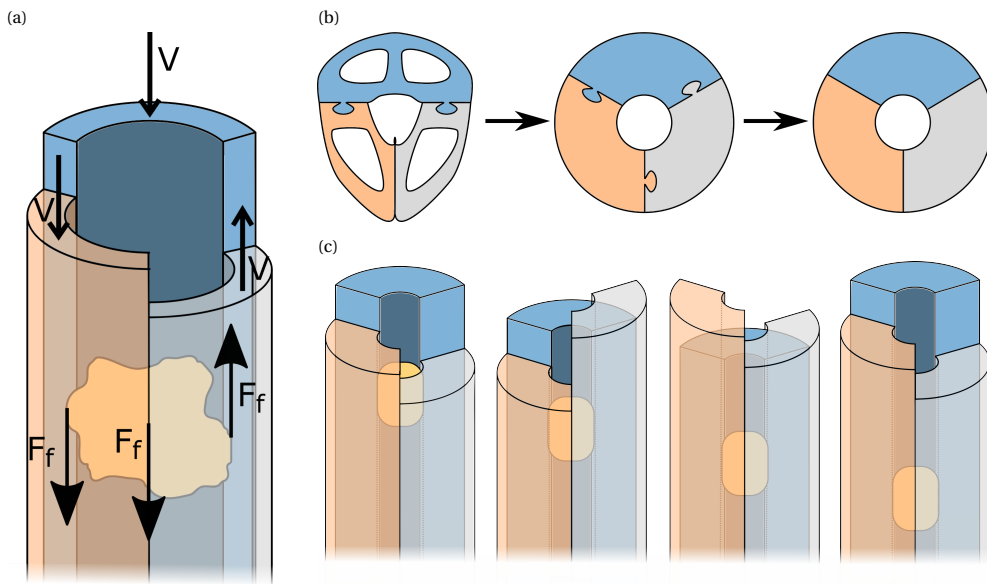
Figure 11.3: Simplification of the wasp ovipositor to three semi-circular blades that form a tube. (a) Forces acting during friction-based transport. (b) Simplification process of the ovipositor. (c) Friction-based transport, for explanation see text.

traction of the third valve while the others remain stationary (Figure 11.2b, Step 4). After this step, all the valves are back in their initial position, while the egg has moved one stroke length in the transport direction.

This cycle is repeated until the egg has been transported along the entire length of the ovipositor. This transport method is called friction-based transport, as the friction between the egg and the valve is what effectuates the transportation.

11.1.4. FRICTION-BASED TRANSPORT

In suction-based instruments, the friction between the transported tissue and the walls of the instrument is a major cause of clogging. This problem does not occur in the wasp's ovipositor, as the friction between the transported egg and the valves is what effectuates the transportation (Figure 11.3a). Friction-based transport could, therefore, be an interesting alternative for suction-based transport.

To better understand how to apply the working principle of egg transport in the design of a tissue transport mechanism, the shape of the ovipositor was simplified as a cylinder held together by the olistheters. Further simplification of the ovipositor valves results in three semi-circular blades that form a circular lumen through which the tissue can be transported (Figure 11.3b).

Transportation of the tissue is achieved once the resultant friction force on the tissue is larger in the transport direction than in the opposite direction. The resultant friction

force $\overrightarrow{F}_{friction}$ [N] is the sum of the friction forces induced by each of the blades and can be written as illustrated in Equation 11.1. Assuming that with relatively small pieces of tissue the effect of gravity can be neglected, that the tissue is flexible such that the generated friction is dependent on the contact surface, that the inner surface properties and material of the blades are identical, and that the tissue has full contact with each of the three blades, each blade results in the same absolute value of friction force (Equation 11.2). A possible motion sequence for the blades is depicted in Figure 11.3c. In this motion sequence, two valves advance in the transport direction, while one valve simultaneously retracts. This results in a resultant friction force in the transport direction that is twice as large as in the opposite direction (Equation 11.3). A system comprising of more than three blades will also be able to transport the tissue in the desired direction as long as Equation 11.3 holds.

$$\overrightarrow{F}_{friction} = \overrightarrow{F}_{friction\,1} + \overrightarrow{F}_{friction\,2} + \overrightarrow{F}_{friction\,3} \tag{11.1}$$

$$|\overrightarrow{F}_{friction\,1}| = |\overrightarrow{F}_{friction\,2}| = |\overrightarrow{F}_{friction\,3}| \tag{11.2}$$

$$\sum \overrightarrow{F}_{friction\,advancing\,valves} > \sum \overrightarrow{F}_{friction\,retracting\,valves} \tag{11.3}$$

11.1.5. OVIPOSITOR INSPIRED INSTRUMENTS

The ovipositor has been a source of inspiration for a number of designs. Multiple self-propelling needles have been developed [9, 15, 26], of which some are even steerable [23, 24]. Furthermore, friction-based transport has been used in the development of a rigid tissue transport mechanism described by Sakes *et al.* [22]. This mechanism can transport tissue phantoms with a variety of material characteristics without the need for a pressure differential. The instrument consists of six reciprocating semi-cylindrical blades that mimic the valves of the ovipositor, similar to the system shown in Figure 11.3c.

11.1.6. GOAL OF THIS STUDY

Friction-based transport could be a viable alternative for the currently used suction-based tissue transport mechanisms, but has till now only been used in rigid form. The use of a flexible friction-based tissue transport mechanism increases the area that can be reached as the instrument can bend to follow the patient's anatomy, which could be interesting for a wide variety of medical procedures, such as the removal of tissue in gastro-intestinal interventions, Ear Nose Throat (ENT) or endo-nasal skull base surgery, or in cardiovascular procedures, e.g., for the removal of occluded tissue from blood vessels. The goal of this study is, therefore, to explore a novel design for a flexible friction-based tissue transporter and to evaluate its use for future surgical applications.

11

11.2. PROPOSED DESIGN

11.2.1. FLEXIBLE VALVES

Following the ovipositor mechanism, the basis of the proposed design are valves that, through small oscillatory translations, transport the tissue. In the design of Sakes *et al.*
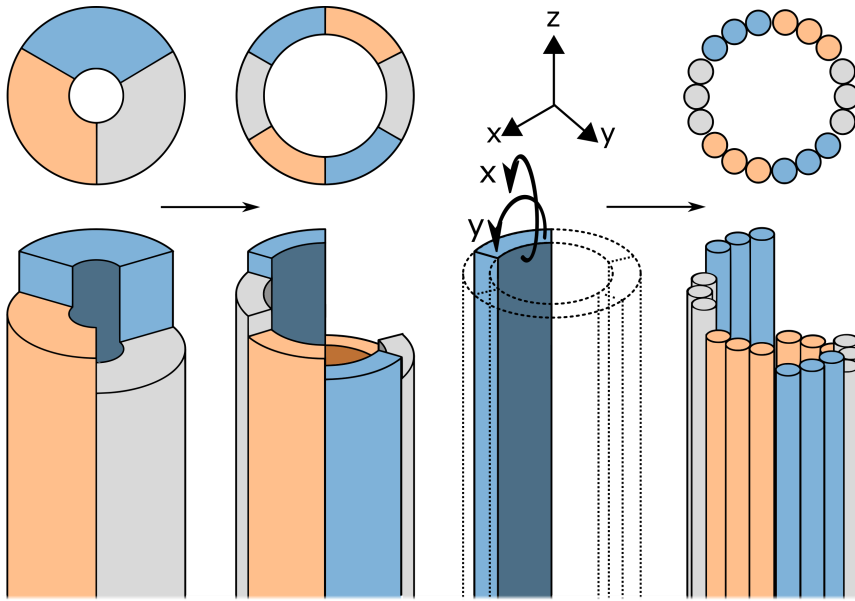
Figure 11.4: Schematic representation of the design process from the rigid transport mechanism described by Sakes *et al.* to the flexible blades. For explanation, see text.

[22], the complex-shaped valves of the wasp are simplified to rigid semi-circular blades, see Figure 11.4. These semi-circular blades are rigid but could be made out of flexible material in order to create a flexible transport mechanism. However, semi-circular blades have a preferred axis of bending, allowing relatively easy bending around the x-axis, see in Figure 11.4, but a strong resistance to bending around the y-axis. Together, the blades form a tubular structure and bending this tube would always require multiple blades to bend in their unpreferred direction. Therefore, an alternative must be found for these semi-circular blades. Structures with a round cross-section do not have a preferred axis of bending, ensuring equal flexibility in both bending planes. It was therefore chosen to use cylindrical blades that exhibit high flexibility, such as cables.

11.2.2. Lumen Formation

The cables that mimic the ovipositor valves need to form a tubular structure with a constant lumen diameter through which the tissue can be transported. It was decided to create the shaft using eighteen 0.6 mm cables such that the tubular structure would have an inner diameter of approximately 3.8 mm. The tongue-and-groove interlocking mechanism in wasp ovipositors is nearly impossible to manufacture in combination with cables. A number of alternative solutions that prevent radial movement of the cables while allowing the cables to translate in the longitudinal direction are presented in Figure 11.5. To ensure uninterrupted contact between the cables and the to be transported tissues, the solution should not contain elements that protrude inside the lumen. Using rings

11

(a)

(b)

(c)
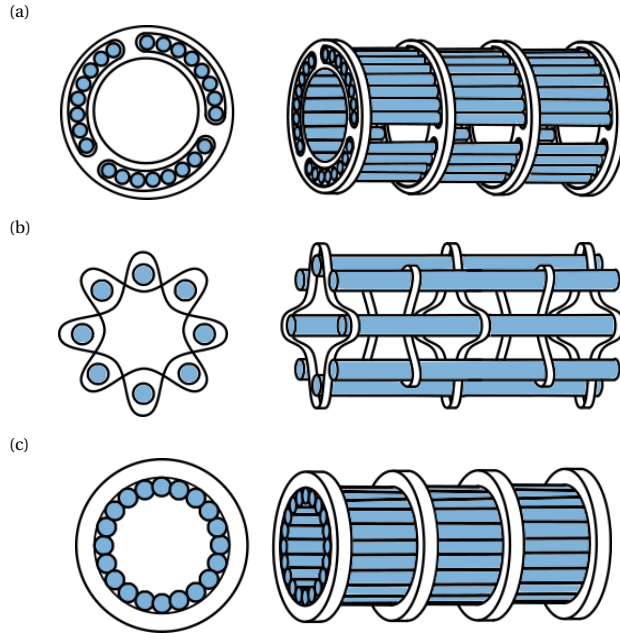
Figure 11.5: Different options to create an open lumen while still allowing the cables to translate. (a) rings with holes, (b) woven structures, (c) ring magnets.

with holes (Figure 11.5a) or thin structures that are woven through the cables (Figure 11.5b) are, therefore, undesired. After careful consideration, it was chosen to use external ring magnets to prevent radial movement of the cables. Ring magnets that surround the cables, will attract the cables and thus create a tubular structure and lumen without protruding structures at the inside, providing that the cables are made of a ferromagnetic material, such as steel (Figure 11.5c).

The ring magnets must be located at a certain distance from each other. A large distance will increase the risk of collapse of the cable structure during bending of the tube. There is, however, a trade-off, as more magnets will increase the magnetic normal force acting on the cables, increasing the friction between the cables and the ring magnets, which in turn will increase the force needed to translate the cables. The maximum distance between the ring magnets that would still avoid lumen collapse even in a curved position was determined empirically. To keep the magnets at a certain distance while also allowing flexibility, we decided to use compression springs as distance holders. The entire shaft was covered by a heat shrink tube in order to prevent tissue escaping from the shaft during transportation.

11.2.3. ACTUATION

The handle must allow for easy actuation of the transport mechanism and thus the cables. It was decided to design the handle such that the system can be actuated manually, as this limits the number of required parts for this prototype. In a future version, the use

of motorised actuation might be desired as it could result in faster and a more constant transport rate. In the study of Sakes *et al.* [22], reliable tissue transport was achieved with the sequence of five blades moving in the desired transport direction, with the remaining 6th blade moving in the opposite direction (5:1). Following this design, it was chosen to divide the eighteen cables in six groups of three cables each.

Each cable group is glued to an aluminium slider, such that the entire cable group can be actuated simultaneously by translating the slider. In the previously developed prototype by Sakes *et al.* [22], a barrel cam, consisting of a cylindrical part with a groove in which the pin of a slider fits, was used to actuate the blades (Figure 11.6a). The groove was designed in such a way that five sliders are moving in the desired direction while one slider moves in the opposite direction, resulting in the 5:1 sequence with a stroke length of 5.2 mm. A similar design was used for cable actuation in the flexible prototype, with one major difference: in the flexible prototype, translational movements of the sliders in the desired sequence (5:1) are achieved by a new inside-out barrel cam design. The inside-out barrel cam is hollow and surrounds the sliders, allowing the tissue to be transported through the cam and handle such that it can easily be removed (Figure 11.6b). In the prototype, the outside of the barrel cam has a star-shaped knob to allow for precise manual actuation of the transport mechanism (Figure 11.6c). Furthermore, a crank was connected to the cam to allow for faster and easier actuation of the cam. Depending on the clockwise or counter clockwise rotation of the cam, the transport direction will reverse, making the same system usable to transport substances from and to the target location.

Figure 11.7 shows the final prototype. The flexible tissue transport mechanism consists of eighteen galvanised steel cables (Engelmann, 1×7, $\varnothing$ 0.6 mm) arranged in six groups of three cables, that form a tubular structure due to the eight neodymium ring magnets (Conrad Components Permanent magnet Ring N35M, $\varnothing_{outer}$ 10mm, $\varnothing_{inner}$ 5 mm, length 2 mm) that are placed around the cables. In between two ring magnets, a compression spring ($\varnothing_{inner}$ 6.5 mm, $\varnothing$ wire 0.6 mm, free length 12 mm) is placed. The shaft with a length of 115 mm was partly covered by a heat shrink tube ($\varnothing$ 9.5 mm) leaving 15 mm of cables uncovered at the tip. The cables can translate in the longitudinal direction by sliding through the ring magnets. Three cables are glued to each of the sliders (manufactured using electrical discharge machining). These three cables will thus be simultaneously actuated by the inside-out cam (manufactured using a Perfactory 4 Standard 3D-printer by EnvisionTec).

A photo of the prototype is shown in Figure 11.8. After the fabrication and assembly of the prototype, the transport mechanism was tested. Tissue phantoms were placed inside the lumen at the tip of the transport mechanism. By manually actuating the system, the phantoms were transported through the flexible shaft and the handle. Figure 11.9 shows one of the tissue phantoms exiting the handle after being transported through the mechanism. A video showing the working principle of the flexible wasp-inspired tissue transport mechanism can be found in the research data supporting the findings described in this thesis available at:https://doi.org/10.4121/e718db33-3cf4-4738-adbe-1209a130d0c7.v1.

11
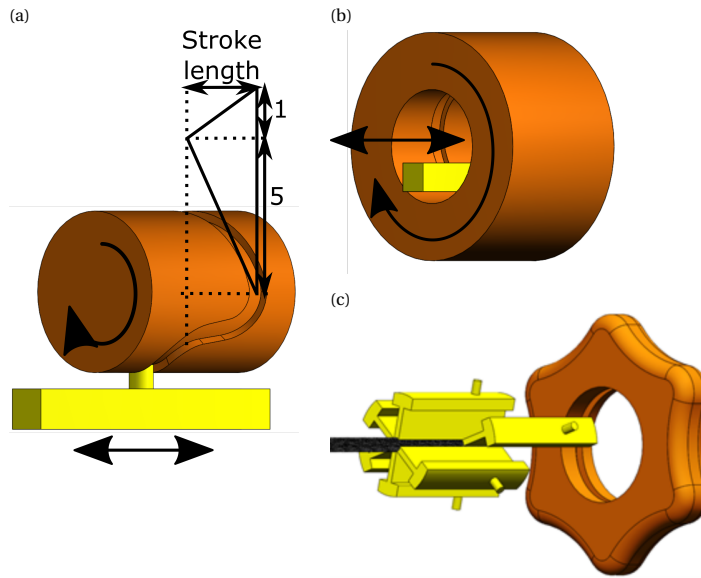
Figure 11.6: Representation of the cam design. (a) The effect of the groove on the motion sequence of the sliders. (b) Schematic drawing of the inside-out barrel cam. (c) The cam (orange) and sliders (yellow) of the transport mechanism prototype.

11.3. PROOF-OF-PRINCIPLE EXPERIMENT

11.3.1. EXPERIMENT GOAL

The performance of the transport mechanism was evaluated during a proof-of-principle experiment. The goal of this proof-of-principle experiment was threefold: 1) to determine the effect of the shaft curvature on the performance of the friction-based transport mechanism, 2) to evaluate the effect of shaft orientation (horizontal vs vertical) on the transport performance, and 3) to determine the effect of the rotational velocity of the cam on the transport performance.

11.3.2. EXPERIMENTAL FACILITY

EXPERIMENT SET-UP

Figure 11.10 shows the experimental set-up. The transport mechanism was initially designed as a handheld manually-actuated prototype. However, for testing purposes, an electric motor (Igarashi 33GN2738-132-GV-5 12.0V with a 75:1 gearbox) and a voltage source were connected to the mechanism, such that the rotational velocity of the cam could be precisely controlled and adjusted. The transport mechanism was mounted in an aluminium experimental base to ensure correct shaft orientation. When testing the transport mechanism in the vertical position, the standard was rotated 90°, such that the shaft was in vertical orientation. 3D-printed straight and curved tubes that could
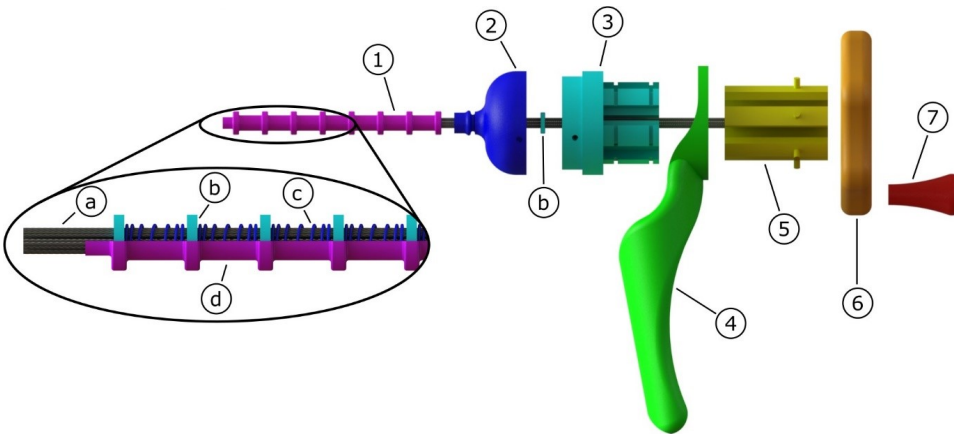
Figure 11.7: Schematic representation of the flexible transport mechanism consisting of 1) flexible shaft, 2) tip, 3) slider house, 4) hand grip, 5) sliders, 6) cam, 7) crank. The flexible shaft consists of a) cables that form a lumen due to their attraction to the b) ring magnets. The ring magnets are kept in place by c) compression springs, and all is enclosed by a d) heat shrink tube.

be placed in a base plate were used to ensure correct curvature of the shaft. A camera (Nikon Coolpix P500) was used to film the experiment and to later identify the number of cam rotations needed to transport the gelatin through the transport mechanism.

GELATIN TISSUE PHANTOMS

The transport performance was tested by transporting gelatin tissue phantoms. gelatin is a widely used substance for soft tissue phantoms, as it is easy to handle and can produce phantoms with similar Young's moduli as real tissue [8, 18]. A phantom with 10 wt% of dry gelatin powder results in a phantom with a Young's modulus around 70 KPa [14]. This corresponds to the Young's modulus of tendons [3], glandular breast tissue and prostate tissue [16]. The gelatin tissue phantoms were made by mixing dry gelatin powder (dr. Oetker) with tap water of approximately 90^oC. The mixture was stirred until the gelatin was completely dissolved. Subsequently, the gelatin mixture was poured into a gelatin tray (Figure 11.10) to create a gelatin layer with a thickness of 20 mm and was left to cool for 24 h at approximately 7^oC. The gelatin tray was removed from the fridge an hour before the experiments, to allow the tissue samples to reach room temperature. A 3D-printed gelatin cutter was used to cut gelatin cylinders with a 5 mm diameter and 20 mm height. The cutter was, subsequently, used to place the tissue sample into the lumen of the transport mechanism.

11.3.3. EXPERIMENT VARIABLES

INDEPENDENT VARIABLES

The following variables were manipulated during the experiment:

- Shaft curvature: The shaft was tested in straight position, as well as in two circular curves: Curve 1 with an angle of 30° over a length of 8 cm and Curve 2 with an angle of 60° over a length of 8 cm.

11
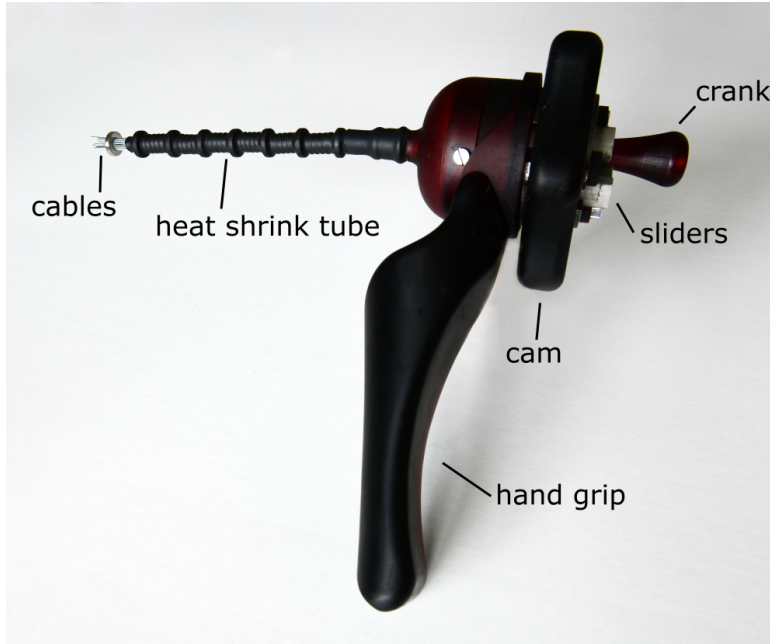
Figure 11.8: Photo of the flexible ovipositor-inspired tissue transport mechanism with an extra ring magnet around the tip of the shaft to elucidate the working principle.

- Shaft orientation: During MIS, the transport mechanism will be used in different orientations relative to gravity. The transport mechanism was therefore tested in two extreme scenarios: 1) in a horizontal orientation in which the gravity is perpendicular to the transport direction and 2) in a vertical orientation in which gravity is opposite to the transport direction.

- Rotational velocity: To determine the effect of the rotational velocity of the cam on the transport performance, the experiments were carried out with three rotational velocities: 25, 53, and 80 RPM.

DEPENDENT VARIABLES

The following variables were measured during the experiment:

- Transport rate: Visual analysis of video recordings were used to determine the transport time. The transport rate [mm/s] was calculated by subdividing the distance over which the tissue phantom was transported $d_{transport}$ [mm] by the transport time $t_{transport}$ [s] needed to achieve this, see Equation 11.4. The transport distance $d_{transport}$ is 163 mm, which is equal to the length of the shaft surrounded by heat shrink tube plus the length of the handle, minus the length of the tissue phantom.

$$transport\,rate = \frac{d_{transport}}{t_{transport}} \tag{11.4}$$
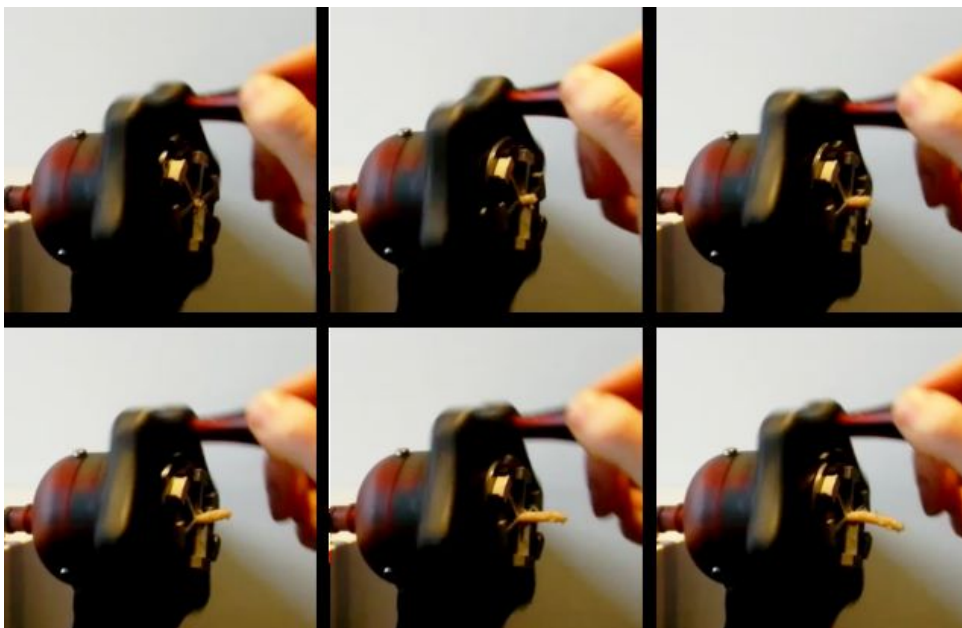
Figure 11.9: Photo of the tissue leaving at the end of the tissue transport mechanism using manual actuation. The photos were taken one actuation cycle apart.
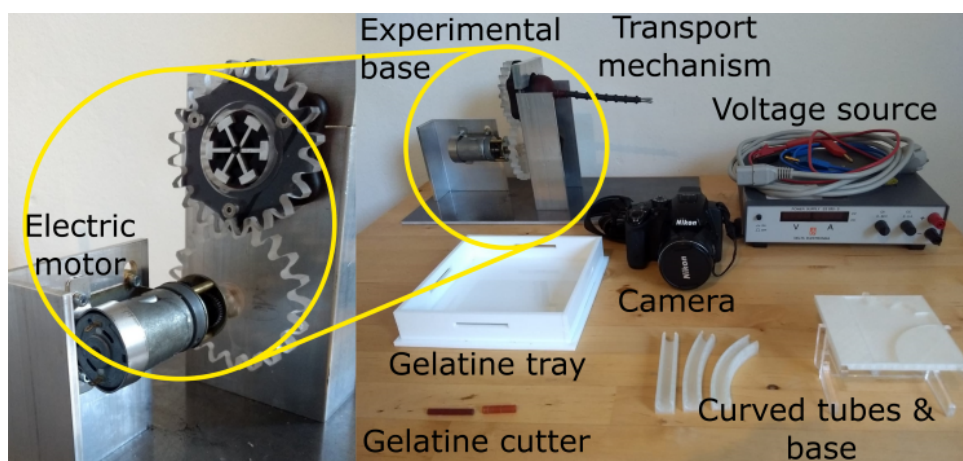
Figure 11.10: Experimental facility. The experimental facility consisted of an electromotor connected to a voltage source and the handle of the transport mechanism through a gear mechanism, the transport mechanisms placed inside an aluminium frame, a camera to record the experiments, a based plate containing 3D-printed tubes for the shaft curvature experiment, and a gelatin tray with cutter for the manufacturing of the tissue phantoms.

11
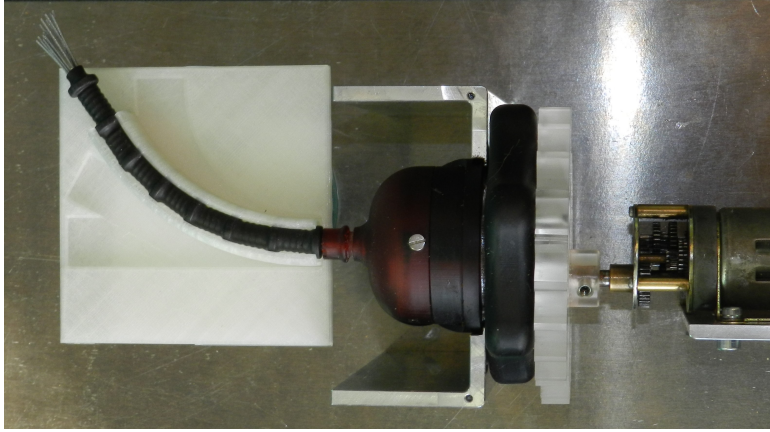
Figure 11.11: Photo showing the flexible shaft of the transport mechanism placed inside the 10° curved tube.

- Stroke efficiency: In order to determine the efficiency of the tissue transport, the amount of slip between the cables and the tissue phantom was measured. The stroke efficiency stroke [%] was calculated by dividing the measured transport distance per stroke $d_{measured}$ [mm/stroke], by the theoretical maximum transport distance per stroke $d_{theoretical}$ [mm/stroke], multiplied by 100% (Equation 11.5). The measured transport distance per stroke $d_{measured}$ can be found by dividing the total transport distance $d_{transport}$ [mm] by the required number of strokes, $n_{strokes}$ [-], which is equal to the number of cam rotations. The number of cam rotations was determined by visual analysis of the video recordings. The theoretical maximum transport distance $d_{theoretical}$ depends on the motion sequence (5:1) and the stroke length of the sliders (5.2 mm). The theoretical transport distance per stroke is equal to $65 \cdot 5.2$ mm = 6.24 mm in this prototype.

$$storke\ efficiency = \frac{d_{measured}}{d_{theoretical}} \cdot 100\% \qquad (11.5)$$

11.3.4. EXPERIMENT PROTOCOL
The proof-of-principle experiment was divided in three sub-experiments.

1. Curvature Test: In order to test the effect of the shaft curve on the transport performance, the mechanism was tested with the shaft in the straight position and in the two curved positions. Figure 11.11 shows the flexible shaft in the curved position.

2. Orientation Test: In order to test the effect of the shaft orientation on the transport performance, the mechanism was tested in the horizontal and the vertical orientation with the transport direction opposing gravity.

3. Rotational Velocity Test: In order to test the effect of the rotational velocity on the transport performance, both the Curvature Test and the Orientation Test were performed at the three rotational velocities.

Table 11.1: Overview of the transport rate [mm/s] of the friction-based transport mechanism for different shaft orientations, curvatures and rotational velocities.

Transport rate [mm/s]	Test condition			
rotational velocity	straight horizontal	30° curved	60° curved	straight vertical
25 RPM	0.83±0.08	0.81±0.09	0.77±0.08	0.78±0.08
53 RPM	1.61±0.15	1.50±0.19	1.37±0.25	1.78±0.20
80 RPM	2.27±0.32	2.20±0.14	1.96±0.19	2.26±0.23

Each test condition was repeated six times. The tests started with placing the gelatin tissue phantoms inside the lumen at the tip of the transport mechanism. In order to ensure proper contact between the cables and the gelatin, the gelatin was transported manually by rotating the cam until the gelatin sample was entirely inside the lumen surrounded by the heat shrinking tube. The test ended once the tip of the gelatin cylinder reached the proximal end of the transport mechanism, which was determined by eye. This way the gelatin cylinder was completely surrounded by cables for the duration of the test.

11.3.5. DATA ANALYSIS

For each condition, the mean and the standard deviation were determined for both the transport rate and the stroke efficiency. The statistical analysis was conducted by performing ANOVA analyses and t-tests on the data. All data analysis was performed with MATLAB R2019B.

11.4. RESULTS PROOF-OF-PRINCIPLE EXPERIMENT

11.4.1. CURVATURE TEST

The boxplots in Figure 11.12 summarise the results of the experiment. The mean transport rate for the shaft in the straight, 30° curved and 60° curved position can be found in Table 11.1. Transport rates of 0.83 ± 0.08, 0.81 ± 0.09, and 0.77 ± 0.08 mm/s were found for the straight, 30° curved and 60° curved positions at a rotational velocity of 25 RPM, respectively. For a rotational velocity of 53 RPM, higher transport rates of 1.61 ± 0.15, 1.50 ± 0.19, and 1.37 ± 0.25 mm/s for the straight, 30° curved and 60° curved position were found, respectively. Finally, as expected, the highest transport rates of 2.27 ± 0.32, 2.20 ± 0.14, and 1.96 ± 0.19 mm/s for the straight, 30° curved and 60° curved position were found for a rotational velocity of 80 RPM, respectively. There was no statistical effect of the shaft curvature on the transport rate.

11.4.2. ORIENTATION TEST

The effect of the shaft orientation of the transport mechanism on the transport rate was investigated by performing a two-tailed t-test. This showed that there was no statistical effect of shaft orientation on the transport rate at the 25, 53 and 80 RPM rotational velocities of the cam (p = 0.284, p = 0.143, and p = 0.928, respectively).

11

(a)   (b)
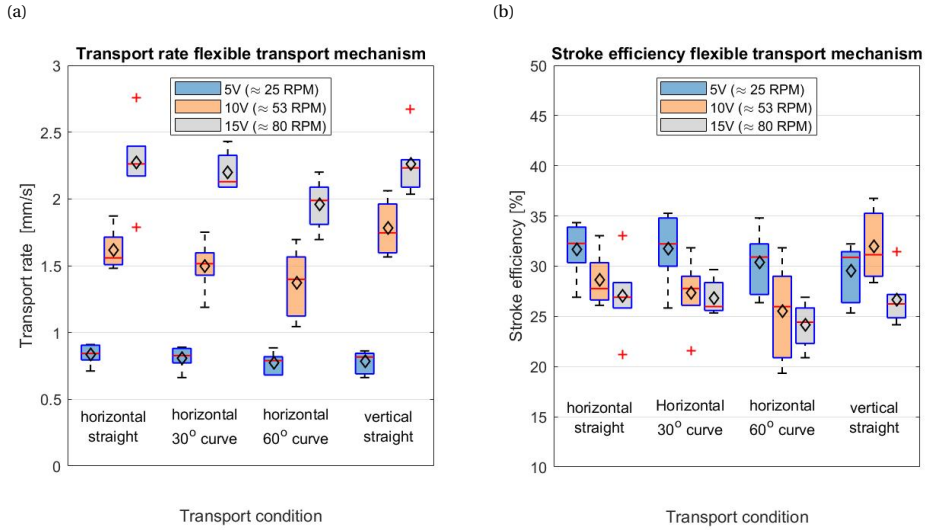
Figure 11.12: Boxplot displaying (a) the transport rate [mm/s] and (b) the stroke efficiency [%] for different test conditions; the shaft in horizontal orientation while being straight, in 30° and 60° curved position and with the shaft in vertical orientation. The maximum and minimum values are indicated by the outermost horizontal solid lines on each of the boxplots. The median is indicated by the horizontal red line in each boxplot, while the mean is indicated by the black diamond.

11.4.3. ROTATIONAL VELOCITY TEST

Based on the one-way ANOVA, a statistically significant difference was found in the transport rate at different rotational velocities of the cam. The average stroke efficiency for the test conditions: straight horizontal, 30° curved, 60° curved and vertical straight, can be found in Table 11.2. The one-way ANOVA test showed that there is a statistically significant effect of the rotational velocity of the cam on the stroke efficiency for the horizontal 30° curved ($p = 2.39 \cdot 10^{-2}$), horizontal 60° curved ($p = 1.99 \cdot 10^{-2}$) and the vertical straight condition ($p = 2.89 \cdot 10^{-2}$). There was no statistical significance found on the rotational velocity on the stroke efficiency in the horizontal straight transport condition ($p = 6.17 \cdot 10^{-2}$).

11.5. DISCUSSION

11.5.1. MAIN FINDINGS

The proof-of-principle experiments show that the shaft curvature and shaft orientation (horizontal vs vertical) do not influence the transport rate significantly. The rotational velocity of the cam did have a significant effect on the transport rate of the tissue. The transport rates for the shaft in straight position were 0.83 ± 0.08 mm/s, 1.61 ± 0.15 mm/s and 2.27 ± 0.32 mm/s with a rotational velocity of the cam of 25, 53 and 80 RPM, respectively. An increase of the rotational velocity of the cam resulted in an increase of

Table 11.2: Overview of the stroke efficiency [%] of the friction-based transport mechanism for different shaft orientations, curvatures and rotational velocities.

Stroke efficiency [%]	Test condition			
rotational velocity	straight horizontal	30° curved	60° curved	straight vertical
25 RPM	32±3	32±3	30±3	30±3
53 RPM	29±3	27±3	26±5	32±4
80 RPM	27±4	27±2	24±2	27±3

the transport rate. The prototype has been designed for manual actuation, but in future designs motorised actuation might be desirable to further increase the transport rate. Although increasing the rotational velocity of the cam resulted in an increase of the tissue transport rate, the stroke efficiency showed a decrease when increasing the rotational cam velocity in the horizontal test conditions. This decrease in stroke efficiency could indicate that there is a limit to the tissue transport rate that can be achieved by increasing the rotational velocity of the cam.

The rigid tissue transport mechanism, which also uses friction-based transport, has a comparable transport rate of 1.49 mm/s when used with similar circumstances (9 wt% gelatin tissue phantoms, rotational velocity cam = 46 RPM) [22]. This transport rate is 50–165 times lower than the clinically used morcellators that use suction-based transport. However, during interventions that are performed in close proximity to delicate structures and in which the transport rate is of secondary interest, the use of friction-based transport could still be beneficial [22].

One of the main disadvantages of the currently used suction-based instruments is that miniaturisation is challenging as this would require a larger pressure difference than what is achievable. This problem does not arise when miniaturising the proposed friction-based transport mechanism. In the current design, miniaturisation of the outer diameter of the shaft is limited by the size of the used ring magnets. Using smaller ring magnets could allow for a smaller outer diameter, however, the magnetic force acting on the cables is dependent on the volume of the magnet. This means that at some point the magnets will not be able to generate the required magnetic force to ensure the lumen formation of the cables. Down scaling of the cables would lower the required magnetic force and could thus allow for further miniaturisation of the prototype. Besides this, alternative methods to form a lumen of the cables could be investigated. For instance, braiding the cables to the springs with a thin and smooth wire. These methods might be more space-efficient and could therefore be beneficial for minimally invasive surgery.

Elongation of the flexible shaft would increase the number of magnets required to ensure the open lumen over the entire length of the shaft. This could pose a challenge, as more magnets will increase the friction force between the cables and the magnets during the translating motion of the cables. Research is needed to get more insight in the effects of elongating the shaft.

11

11.5.2. Limitations and Future Research
The performance of the transport mechanism was tested by using gelatin tissue phantoms. Although gelatin is commonly used as a tissue phantom, the homogeneous struc-

ture of gelatin could influence the transport rate. Furthermore, in the research of Sakes *et al.* [22], it was found that there is a statistically significant effect of the gelatin density and thus the tissue elasticity on the transport rate. Therefore, it would be valuable to repeat these tests with real tissue in clinical *ex-vivo* and *in-vivo* settings. *In-vivo* testing would require the prototype to be biocompatible hence, alternatives must be found for the materials now used in the prototype, such as the galvanised cables and the heat shrink tube. Furthermore, as this transport mechanism is expected to be used in combination with a tissue separating instrument, it would be valuable to test this transport mechanism in combination with such an instrument or look into the possibilities of adding a tissue separating grasper at the tip of the instrument.

The ovipositor on which the flexible transport mechanism is based is steerable. With slight adjustments, the prototype could also be made steerable. For instance, by adding steering cables that are connected to the tip of the flexible shaft and run along the shaft. Pulling on one of these cables would result in bending of the flexible shaft allowing the surgeon to actively steer the tip of the transport mechanism to the target location. Similar principles have been used before to create steerable catheters [2], endoscopes [5] and laparoscopic instruments [13].

The proposed prototype shows that friction-based transport can be used in a flexible system which allows the flexible transport mechanism to transport tissue without the adverse effects, such as clogging, that are linked to suction-based instruments. In the future, this design might serve as an alternative for the currently used flexible suction-based instruments and can be used in a wide variety of minimally invasive interventions.

11.6. CONCLUSION

This paper presents the design of a novel flexible tissue transport mechanism that uses a wasp-ovipositor-inspired transport method. This method allows for continuous tissue transport while eliminating clogging as a sub-optimal behaviour mode of the currently used suction-based transportation mechanisms. The prototype could transport 10 wt% gelatin tissue phantoms with no significant difference depending on the shaft curvature and orientation. The transport performance of the flexible transport mechanism is promising and could in future be used in a wide variety of medical interventions, such as tissue removal during minimally invasive procedures.

11

BIBLIOGRAPHY

[1]   T. Ahmed et al. "Sense organs on the ovipositor of Macrocentrus cingulum Brischke (Hymenoptera: Braconidae): their probable role in stinging, oviposition and host selection process". In: *Journal of Asia-Pacific Entomology* 16.3 (Sept. 1, 2013), pp. 343–348. (Visited on 07/20/2021).

[2]   Awaz Ali et al. "Catheter steering in interventional cardiology: Mechanical analysis and novel solution". In: *Proceedings of the Institution of Mechanical Engineers, Part H: Journal of Engineering in Medicine* 233.12 (Dec. 1, 2019). Publisher: IMECHE, pp. 1207–1218. (Visited on 09/20/2021).

[3]   K. Arda et al. "Quantitative assessment of normal soft-tissue elasticity using shear-wave ultrasound elastography". In: *American Journal of Roentgenology* 197.3 (2011). Publisher: Am Roentgen Ray Soc, pp. 532–536.

[4]   A. D. Austin and T. O. Browning. "A mechanism for movement of eggs along insect ovipositors". In: *International Journal of Insect Morphology and Embryology* 10.2 (Jan. 1, 1981), pp. 93–108. (Visited on 04/12/2021).

[5]   P. Breedveld et al. "A new, easily miniaturized steerable endoscope". In: *IEEE Engineering in Medicine and Biology Magazine* 24.6 (Nov. 2005). Conference Name: IEEE Engineering in Medicine and Biology Magazine, pp. 40–47.

[6]   U. Cerkvenik et al. "Mechanisms of ovipositor insertion and steering of a parasitic wasp". In: *Proceedings of the National Academy of Sciences* 114.37 (2017). Publisher: National Acad Sciences, E7822–E7831.

[7]   T. Y. P. Chin et al. "Accuracy of Intramuscular Injection of Botulinum Toxin A in Juvenile Cerebral Palsy: A Comparison Between Manual Needle Placement and Placement Guided by Electrical Stimulation". In: *Journal of Pediatric Orthopaedics* 25.3 (June 2005), pp. 286–291. (Visited on 07/20/2021).

[8]   S. Cournane, A. J. Fagan, and J. E. Browne. "Review of ultrasound elastography quality control and training test phantoms". In: *Ultrasound* 20.1 (2012). Publisher: SAGE Publications Sage UK: London, England, pp. 16–23.

[9]   L. Frasson et al. "STING: a soft-tissue intervention and neurosurgical guide to access deep brain lesions through curved trajectories". In: *Proceedings of the Institution of Mechanical Engineers, Part H: Journal of Engineering in Medicine* 224.6 (2010). Publisher: Sage Publications Sage UK: London, England, pp. 775–788.

[10] G. Hong et al. "Usefulness of Endobronchial Ultrasound-Guided Transbronchial Needle Aspiration for Diagnosis of Sarcoidosis". In: *Yonsei Medical Journal* 54.6 (Oct. 1, 2013). Publisher: Yonsei University College of Medicine, pp. 1416–1421. (Visited on 07/20/2021).

11

[11]   Yin C. Hu and Michael F. Stiefel. "Force and aspiration analysis of the ADAPT technique in acute ischemic stroke treatment". In: *Journal of Neurointerventional Surgery* 8.3 (Mar. 2016), pp. 244–246.

[12]   T. Jaschinski et al. "Laparoscopic versus open appendectomy in patients with suspected appendicitis: a systematic review of meta-analyses of randomised controlled trials". In: *BMC Gastroenterology* 15.1 (Apr. 15, 2015), p. 48. (Visited on 07/20/2021).

[13]   Filip Jelínek, Rob Pessers, and Paul Breedveld. "DragonFlex Smart Steerable Laparoscopic Instrument". In: *Journal of Medical Devices* 8.1 (Jan. 7, 2014). (Visited on 09/20/2021).

[14]   A. Karimi and M. Navidbakhsh. "Material properties in unconfined compression of gelatin hydrogel for skin tissue engineering applications". In: *Biomedical Engineering/Biomedizinische Technik* 59.6 (2014). Publisher: De Gruyter, pp. 479–486.

[15]   S. Y. Ko, B. L. Davies, and F. R. y Baena. "Two-dimensional needle steering with a "programmable bevel" inspired by nature: Modeling preliminaries". In: *2010 IEEE/RSJ International Conference on Intelligent Robots and Systems*. IEEE, 2010, pp. 2319–2324.

[16]   T. A. Krouskop et al. "Elastic moduli of breast and prostate tissues under compression". In: *Ultrasonic imaging* 20.4 (1998). Publisher: SAGE Publications Sage CA: Los Angeles, CA, pp. 260–274.

[17]   E .D. Kwon, S. A. Loening, and C. E. Hawtrey. "Radical prostatectomy and adjuvant radioactive gold seed placement: results of treatment at 5 and 10 years for clinical stages A2, B1 and B2 cancer of the prostate". In: *The Journal of urology* 145.3 (1991). Publisher: Elsevier, pp. 524–531.

[18]   A. Leibinger et al. "Soft Tissue Phantoms for Realistic Needle Insertion: A Comparative Study". In: *Annals of Biomedical Engineering* 44.8 (Aug. 1, 2016), pp. 2442–2452. (Visited on 07/20/2021).

[19]   N. M. M. E. van Meer et al. "The ovipositor actuation mechanism of a parasitic wasp and its functional implications". In: *Journal of anatomy* 237.4 (2020). Publisher: Wiley Online Library, pp. 689–703.

[20]   M. H. Meissner. "Rationale and indications for aggressive early thrombus removal". In: *Phlebology* 27.1 (2012). Publisher: SAGE Publications Sage UK: London, England, pp. 78–84.

[21]   G. Rioufol et al. "Large tube section is the key to successful coronary thrombus aspiration: findings of a standardized bench test". In: *Catheterization and cardiovascular interventions* 67.2 (2006). Publisher: Wiley Online Library, pp. 254–257.

[22]   A. Sakes et al. "Development of a Novel Wasp-Inspired Friction-Based Tissue Transportation Device". In: *Frontiers in Bioengineering and Biotechnology* 0 (2020). Publisher: Frontiers. (Visited on 07/20/2021).

[23]   M. Scali et al. "Design and evaluation of a wasp-inspired steerable needle". In: *Bioinspiration, Biomimetics, and Bioreplication 2017*. Vol. 10162. International Society for Optics and Photonics, 2017, p. 1016207.

11

[24] M. Scali et al. "Ovipositor-inspired steerable needle: design and preliminary experimental evaluation". In: *Bioinspiration & Biomimetics* 13.1 (Dec. 5, 2017). Publisher: IOP Publishing, p. 016006. (Visited on 02/02/2021).

[25] M. Spear. "The Necessity of Wound Debridement". In: *Plastic Surgical Nursing* 30.1 (Mar. 2010), pp. 54–56. (Visited on 07/20/2021).

[26] T. Sprang, P. Breedveld, and D. Dodou. "Wasp-inspired needle insertion with low net push force". In: *Conference on Biomimetic and Biohybrid Systems*. Springer, 2016, pp. 307–318.

11

12

DESIGN OF A SOFT TISSUE GRIPPER

Tissue removal is critical for restoring bodily balance, enhancing tissue regeneration, and diagnosing pathological conditions like cancer. While superficial tissue excision is straightforward, challenges arise in accessing deeper anatomical sites, especially in minimally invasive procedures. Various devices, including aspiration tools, flexible grippers (i.e., bioptomes), and basket-shaped devices, have been developed to facilitate tissue transport but face issues such as clogging and limited continuous tissue removal capabilities. In recent years, a novel tissue transport mechanism has been proposed inspired by the ovipositors of parasitic wasps that overcomes current limitations of tissue transportation devices by using a reciprocating motion for tissue transport. Building on this mechanism, this study proposes a novel compliant tissue gripper that can be used in conjunction with the ovipositor-inspired transportation mechanism comprising the same wire ropes that are used for tissue transport. The gripper comprises six blades made up of three wire ropes. Actuation of the gripper is achieved through a voluntary opening mechanism in which the outer shaft is pulled back to enable the compliant gripper to open. Experimental testing evaluated the prototype's ability to grip and transport gelatin tissue phantoms of different sizes (3, 4, and 5 mm), shapes (spherical and cylindrical), and orientations (concentric and orthogonal). It was found that the gripper was able to successfully grip and transport tissue phantoms with different shapes and sizes, although the concentric cylindrical tissue phantom illustrated the fastest transfer into the lumen with an average of 4.8 cam rotations until tissue transport. Furthermore, experiments demonstrated the prototype's effectiveness in gripping and transporting tissues in curved configurations, though deformation of the gripper occurred at extreme angles, resulting in the inability to transport one sample in the 60° configuration. This novel tissue transport mechanism shows promise in addressing current limitations in tissue removal, offering continuous transport without clogging and adaptability to various surgical scenarios. Further refinement and testing are necessary to validate its efficacy in clinical settings.

12.1. Introduction

Tissue removal constitutes a vital intervention to restore balance to the body, enhance the regenerative potential of healthy tissues, and diagnose various pathological conditions, including cancer. While the excision of superficial tissues is a straightforward procedure, the challenge intensifies when dealing with deeper, more inaccessible anatomical sites, particularly when employing minimally invasive approaches. In minimal invasive approaches, longer pathways between the target and collection size, restricted instrument size of between 5-10 mm in diameter, and limited functionalities of the transportation tools complicate tissue removal from the body.

To allow for fast and efficient tissue transport during minimally invasive surgery, aspiration devices, flexible grippers (i.e., bioptomes), and basket-shaped devices have been developed. In aspiration-based devices, a pressure difference between the distal and proximal end of the instrument is used to transport tissues. This is, for example, used in fine needle aspiration to take biopsies [13], morcellators to remove large tissue masses from the stomach area [12], and aspiration catheters to remove thrombus for the vasculature [7]. In flexible grippers and basket-shaped devices, such as bioptomes and biopsy baskets, a shape grip is used to grab, resect, and remove the tissue from the body. These devices do not allow for continuous tissue removal and thus need to be reinserted several times during the procedure or be used in combination with a tissue pouch.

The movement of catheters and bioptomes inside the vasculature is linked to increased vascular damage [1, 5]. With sheaths and catheters being rotated inside the vasculature or being exchanged for catheters of varied sizes or functions, arrhythmias, and damage to vessels or sensitive structures are some of the most frequently occurring complications [14]. Unfortunately, reinsertion is a common procedure in both bioptomes and aspiration catheters, albeit for different reasons. Whereas in bioptomes and biopsy baskets, reinsertion is a necessity to obtain multiple samples, aspiration catheters are plagued with loss of functionality due to clogging, requiring retraction and reinsertion. Furthermore, the efficacy of aspiration catheters is highly dependent on thrombus composition, with a severe increase in the risk of clogging with more dense and coherent tissues [7]. The inability to reliably transport tissues is a recurring problem in a variety of medical applications, including cardiology [7, 9] and gynaecology [4].

There is a need for a new type of tissue transport mechanism that allows for continuous tissue transportation, is not affected by tissue composition, and is not plagued by clogging. An interesting transport example found in nature that has the potential to solve current challenges in tissue transport can be found in the ovipositors of parasitic wasps. The female parasitic wasp can transport her eggs through her ovipositor, a long and thin tubular organ, using a reciprocating movement of its valves [3]. Using this transport method is advantageous over aspiration, as it minimises the chances of clogging by using the friction between the tissues and the transport mechanism for transportation. Furthermore, using a friction differential for tissue transport also minimises the effect of the diameter and length of the transport mechanism on transport efficiency, allowing for ultra long and slender shafts in the future.

Research in mimicking the parasitic wasp ovipositor has resulted in a range of novel transport mechanisms [10, 6] using friction as its primary means of transportation. The transport mechanism by de Kater *et al.* [6] consists of 18 wire ropes ($\varnothing$0.6 mm) arranged

12

in a cylindrical shape by five ring magnets ($\varnothing_{inner}$ 5 mm, $\varnothing_{outer}$ 10 mm, and a thickness of 2 mm) spaced 20 mm apart. Compression springs were placed between the ring magnets to ensure distancing while maintaining flexibility. Finally, a heat shrink tube was used to close off the system and keep both the ring magnets and compression springs in place. Transportation is accomplished by sequentially moving the majority of the wire ropes toward the handle. Provided that each wire rope maintains identical contact with the tissue, the collective friction force exerted by the retracting wire ropes on the tissue is greater than the friction force of the advancing wire ropes. Continuous tissue transport is facilitated by an internal cam mechanism. A similar principle was used in the design of a rigid friction-based transport system [10].

The wasp-inspired flexible transport mechanism has shown merit in transporting tissue phantoms with varying stiffnesses and heterogeneities [6]. However, so far, no system has been implemented to grasp the target tissue smoothly [6]. In the current prototypes, the tissue sample was placed inside the lumen, after which the system was actuated. To allow for direct tissue transport without the need for additional tools, a mechanism needs to be incorporated that transfers tissue into the transport mechanism. Therefore, this study aims to design a mechanism that grasps and transfers tissue into the lumen of the transport mechanism. In the upcoming section, the design of the proposed solution is described, followed by a description of the proof-of-principle experiment and its results.

12.2. DESIGN PROCESS

12.2.1. COMPLIANT GRIPPER DESIGN

Following the design by de Kater *et al.* [6], the basis of the proposed design is the use of wire ropes that transport the tissue using small oscillatory translations. We suggest using these wire ropes to both grasp and transport the target tissue to minimise device complexity while adding extra functionality.

To allow for tissue gripping, the wire ropes were shaped into a compliant gripper configuration and were given an initial outward bend followed by an inward bend, see Figure 12.1. To get the wire rope in the desired flower-like shape, we plastically deformed the wires using a mold that contained predefined paths. To allow for a broad range of tissue sizes that could potentially be grasped, a 10 mm opening diameter was chosen, resulting in a 35° outward wire curvature over a radius of 35 mm and an overall tip length of 35 mm.

Although compliant grippers are commonly used in medical devices and offer a flexible and gentle approach to grasping and manipulating tissues during minimally invasive procedures, our design offers distinct advantages. First, the compliant gripper is manufactured out of compliant cables, which allows for easy integration with the transportation mechanism without adding additional components to the system. Secondly, the compliant gripper comprises separate elements that remain unconnected to each other, which enables individual movement of the gripper blades, increasing versatility and allowing for transportation.

The device consists of 18 wire ropes, each potentially being able to form one gripper blade, resulting in a maximum total of 18 gripper blades. Using individual wires as grip-

12
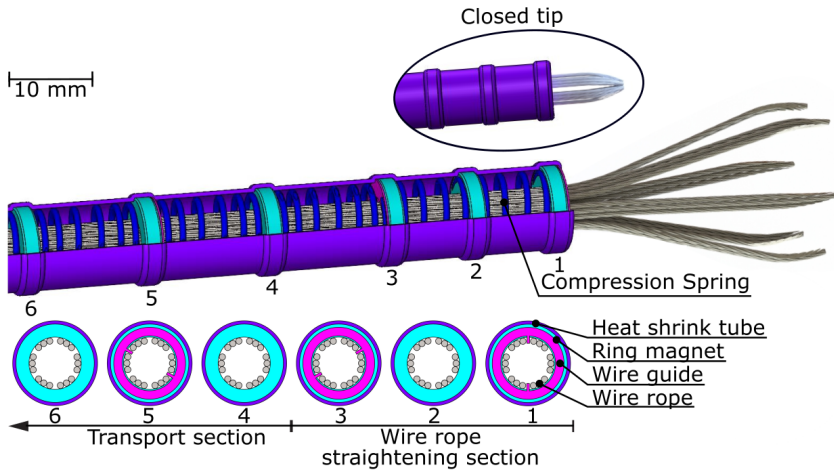
Figure 12.1: Schematic representation of the compliant gripper design. The gripper consists of wire ropes that form a lumen due to their attraction to the ring magnets, which are kept in place by compression springs. Unwanted tangential movement of the wire ropes over the magnet surface is prevented by the wire guides. The shaft is enclosed by a heat shrink tube.

per blades improves the versatility of the gripper. However, single wire ropes are very sensitive to twisting motions when opening and closing the gripper. To add stability to the gripper, a six-blade gripper configuration was selected, with each blade consisting of three wire ropes. In this configuration, it is impossible for all wires to converge to the centre. Therefore, the wire ropes were soldered together after which they were ground down to a point such that the blade tips converge towards the centre when closing the gripper.

The wire ropes are kept in position using an outer concentric shaft containing ring magnets, similar to the device developed by de Kater *et al.* [6]. During each gripping operation, the wire ropes bend inwards to create a shape grip with the tissue. The inwards bending motion might cause the lumen to collapse if the elastic forces in the wire ropes exceed the magnet force the ring magnets apply. Therefore, two extra ring magnets ($\varnothing$ 10 mm) were added to the distal end of the shaft to prevent lumen collapse. Furthermore, the gripper's bending motion, combined with the reciprocating motion of the transport mechanism, could cause tangential movement of the wire ropes after multiple actuation cycles, which can deform the gripper. To ensure proper functioning of the gripper and transport mechanism, 3D-printed wire guides were attached to the ring magnets. The wire guides contain two small pins, dividing the wire ropes into two groups of nine wires and preventing unwanted tangential movement of the wire ropes over the magnet surface. To maintain a predetermined separation between the magnets while ensuring flexibility, we opted for compression springs as distance holders. The complete shaft was enveloped with a heat shrink tube to mitigate the risk of tissue escaping during transportation.

12

12.2.2. ACTUATION UNIT GRIPPER

To create the grasping motion, the wire ropes need to translate relative to the concentric shaft. This motion can be achieved by moving the wire ropes backward toward the housing or moving the shaft toward the gripper. Moving the wire ropes, and thus the gripper, backwards is unwanted as this will shift the position of the tip. Therefore, it was chosen to translate the shaft over the wire ropes.

The manual operation of the gripper, achieved by translating the shaft, can be implemented through various methods, both passive and active. In a passive sliding mechanism, the shaft can smoothly move back and forth to any desired position, where it will then remain fixed. Additional options include voluntary closing, voluntary opening, and bi-stable mechanisms. However, both the passive sliding and bi-stable mechanisms were disregarded due to the risk of inadvertent gripper opening. Consequently, only the voluntary opening and voluntary closing mechanisms remained under consideration, prompting an analysis of the application scenarios.

The application scenarios revealed that during insertion, navigation, tissue transport, and retraction of the instrument, the gripper should be maintained in a closed configuration, whereas an open gripper configuration is only needed during tissue gripping. A voluntary closing mechanism would require active actuation of the device during the majority of the operation, which can be taxing on the operator. Hence, the decision was made to adopt a voluntary opening configuration for gripper actuation.

The voluntary opening mechanism is manually actuated using two handles, see Figure 12.2a. Between the handles and the housing, a compression spring keeps the gripper in the closed position during insertion, navigation, and retraction. The compression spring can be pre-tensioned using a nut-bolt mechanism to aid in closing the gripper. When opening is desired, the shaft is slid back from the tip by manually moving the handles towards the housing. An extra magnet with a wire guide is placed between the handles and the housing to prevent buckling of the wire ropes at this location.

12.2.3. ACTUATION UNIT TRANSPORT MECHANISM

The working principle of the transport mechanism is based on the creation of a friction differential between the wire ropes and the environment. To maximise the friction differential between the tissue and the blades, the majority of blades should move in the desired transport direction. Since the gripper consists of six gripper blades, the maximum obtainable friction differential is 1-5, in which five gripper blades move in the desired transport direction and one gripper blade moves in the opposite direction.

The 1-5 motion sequence is created using a cam mechanism in the handle. The cam translates a rotary motion into the 1-5 reciprocating motion of the gripper blades. Inside the cam grooves, sliders run. To each slider, three wire ropes are fixed using a set screw. In the handle, the wire ropes fan outwards towards a larger diameter to allow for sufficient space for wire rope fixation, as well as the ability to retrieve the tissue samples.

12.2.4. FINAL DESIGN

In Figure 12.2b, the final design is illustrated. The gripper consists of 18 wire ropes ($\varnothing$ 0.6 mm) arranged in groups of three. The distal tips of these three wire ropes were soldered together to form one of the six blades of the gripper. The gripper is actively

12
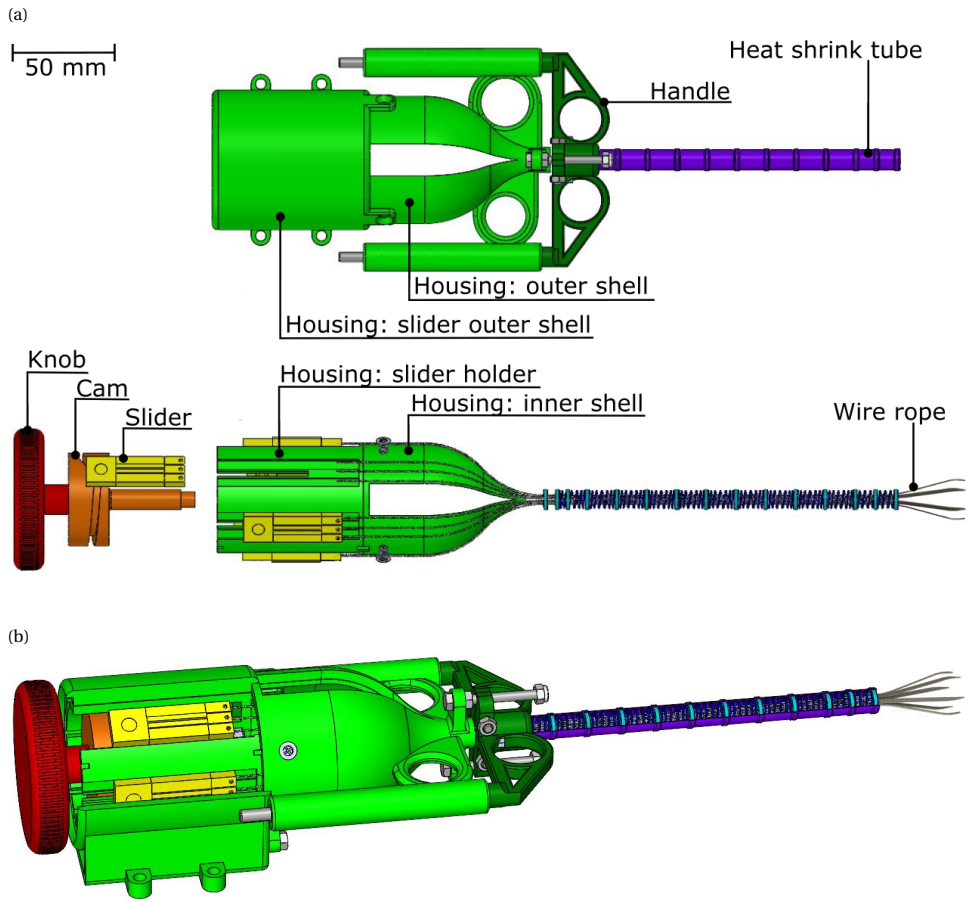
Figure 12.2: Exploded view (a) and assembly (b) of the actuation units of the gripper and the transport mechanism. The actuation unit consists of a rotary knob for actuation of the transport mechanism, cam, six sliders connected to the wire ropes of the gripper using a set screw, housing, and handle for voluntary opening of the gripper.

Figure 12.3: Photo of the ovipositor-inspired tissue gripper and transporter.

opened by manually pulling the handles towards the housing. To open the gripper, the magnets within the shaft slide away from the tip, allowing the gripper blades to bend outwards. In the closed state, three magnets straighten the wire ropes resulting in an 11-mm outer diameter of the shaft. The instrument is designed to be hand-operated, with the option to add an electromotor to actuate the tissue transport mechanism. For this purpose, a knob was added to the cam to allow for manual actuation of the transport mechanism.

12.2.5. PROTOTYPE DEVELOPMENT
The final prototype is illustrated in Figure 12.3. The handles, housing, and cam were manufactured using Stereo-lithography (SLA, Formlabs 3B, Formlabs, USA). The sliders were manufactured from aluminium through manual milling processes. For the shaft, commercially available compression springs (C0360-029-0500M, Amatec, the Netherlands), ring magnets (N35M 1.24T, Conrad, the Netherlands), and heat shrink tubes (1572512, Conrad, the Netherlands) were used. Furthermore, commercially available galvanised steel wire ropes (Engelmann, Germany) were used for the gripper and transport mechanism. The prototype was assembled using off-the-shelf available screws and bolts.

12.3. PROOF-OF-PRINCIPLE EXPERIMENT
12.3.1. EXPERIMENTAL GOAL AND VARIABLES
The goal of the experiment was to determine the ability of the prototype to effectively grip and subsequently transport different tissue diameters, geometries, and orientations both in the straight and curved configuration. The prototype was tested on its:

- Ability to grip the tissue: the ability of the prototype to grip and contain the tissue phantoms in the gripper blades [Y/N].

12

- Ability to transport the gripped tissue: the ability of the prototype to transport the successfully gripped tissue through the shaft towards the handle [Y/N].
- The number of cam rotations before tissue transportation: the number of cam rotations required before the gripped tissue sample was fully inside the tissue transportation lumen [#].

In order to test the prototype's ability to grip and transport different types and shapes of tissues, the following independent variables were tested:

- Tissue diameter: spherical tissue phantoms with a diameter of 3 mm, 4 mm, and 5 mm were tested to determine the prototype's ability to grasp and transport tissues of different diameters.
- Tissue geometry. The prototype's ability to grip different tissue geometries was tested using spherical ($\varnothing$ 3, 4, and 5 mm) and cylindrical-shaped ($\varnothing$ 4 mm with a length of 6.5 mm) tissue phantoms.
- Tissue orientation: the cylindrical-shaped tissue phantoms were gripped in two different orientations: 1) concentric to the transport system and 2) orthogonal to the transport system.
- Shaft curvature: to test the effectiveness of the gripper when the flexible transport mechanism was curved, the performance of the gripper was evaluated with the flexible transport mechanism in different curved positions with a radius r = 60 mm and angles of 20°, 40°, and 60°. The straight position was used as the control configuration.

The effect of tissue elasticity and shaft orientation on tissue transport was not tested, as this was previously tested in a study by de Kater *et al.* [6]. Each measurement was repeated six times.

12.3.2. EXPERIMENTAL FACILITY AND PROTOCOL

The experimental set-up consisted of the prototype fixed to an experimental rig, the tissue phantom placed on a thin needle, and a camera, see Figure 12.4. The tissue phantoms were manufactured out of 10 wt% gelatin (Dr. Oetker, gelatin powder) in water, which, after setting, has a similar Young's modulus as muscle and liver tissue [8, 11]. A syringe and a 3D-printed mold were used to obtain the spherical and cylindrical tissue phantoms.

To grip the tissue phantoms from the needle, the gripper was opened, slid forward over the phantom tissue sample, closed, and then slid back. To determine if the grasped tissue was constrained, the gripper was rotated 360° around its longitudinal axis and held with the tip fully pointing down at a 90° angle for 10 seconds. When the tissue did not fall out of the grasp, the tissue was considered constrained. The ability of the prototype to transport the successfully gripped tissue was, subsequently, determined by rotating the actuation knob until the tissue sample was successfully transferred from the gripper to the lumen of the transport mechanism, which was determined by eye.

Using this approach, the ability of the prototype to grip and transport different diameter spherical tissue phantoms was determined in the straight configuration. The same experiment was repeated for the cylindrical tissue phantoms orientated in line with the

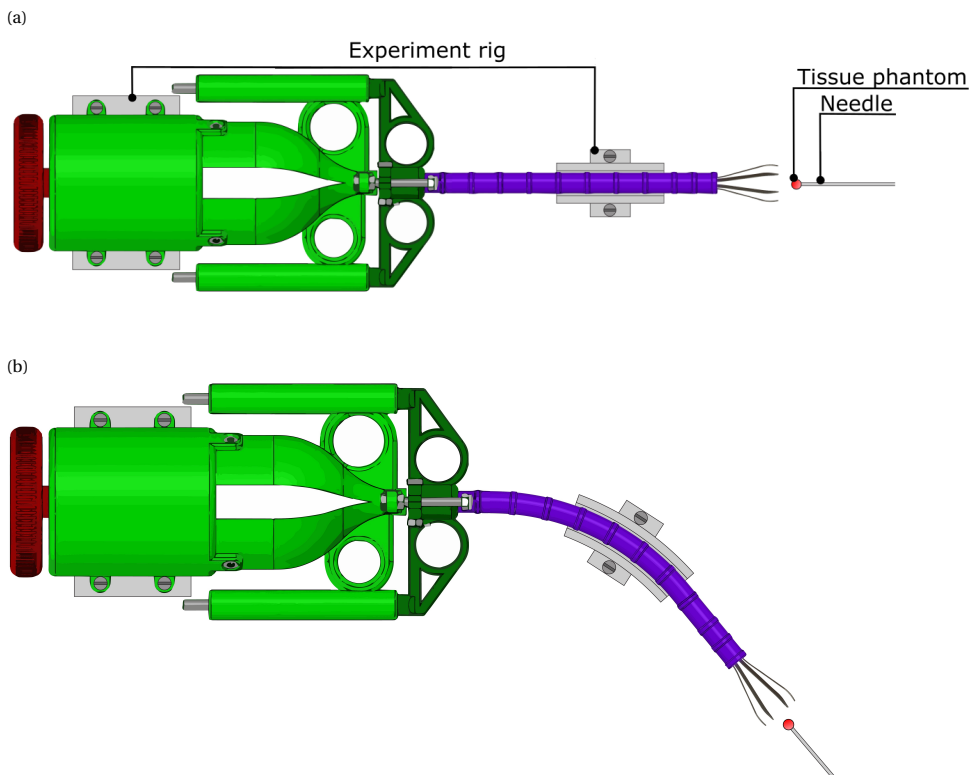**12**

(a)

Experiment rig

Tissue phantom
Needle

(b)

Figure 12.4: Experimental facility. The experimental facility consisted of an experiment rig to which the proto-type was connected, and a tissue phantom placed on a thin needle. (a) Straight shaft configuration. (b) Curved shaft configuration.

12

Table 12.1: Overview of the results of the ability to grip and transport the tissue in the straight configuration for different tissue phantom shapes.

Tissue Phantom Shape	Ability to grip the tissue [Y/N]	Ability to transport the gripped tissue [Y/N]	Number of cam rotations before transportation [#]
⌀3 mm spherical	Y, 6/6	Y, 6/6	20.7 ± 19.1
⌀4 mm spherical	Y, 6/6	Y, 6/6	8.5 ± 2.4
⌀5 mm spherical	Y, 6/6	Y, 6/6	6.0 ± 0.6
⌀4 mm, 6.5 mm cylindrical -Concentric	Y, 6/6	Y, 6/6	4.8 ± 2.0
⌀4 mm, 6.5 mm cylindrical -Orthogonal	Y, 6/6	Y, 3/6	8.8 ± 4.8

tissue transport direction and orientated orthogonal to the transport direction, both in the straight configuration. Finally, the ability of the gripper to grip the 5 mm spherical tissue samples was determined in the curved configuration.

12.4. Results

12.4.1. Effects of Tissue Phantom Shape

Table 12.1 indicates an overview of the results of the tissue phantom shape experiment. All samples were successfully gripped and constrained by the gripper, though not all samples were constrained by shape. Three samples (50%) of the orthogonally oriented cylinders (⌀ 4 mm) did not get transported due to the way they were grasped. After closing the gripper, the cylinders were clamped by friction between two blades and did not contact any of the other blades. Because of this, the cylindrical tissue sample did not reorient to align with the lumen of the transport mechanism but was rolled back and forth between the two wire rope groups. The orthogonal cylindrical tissue phantoms that were in contact with four (or more) wire rope groups did reorient and were transferred into the lumen quickly. Out of the 3 mm, 4 mm, and 5 mm diameter spherical tissue phantoms, the 5-mm diameter tissue phantom illustrated the fastest and most constant transfer into the lumen, with an average of 6.0 ± 0.6 cam rotations until transport, despite the tissue being 1.2 mm larger than the lumen diameter. However, the concentric cylindrical tissue phantom was the fastest in entering the lumen overall, with an average of 4.8 ± 2.0 cam rotation until tissue transport. The highest dispersion was found in the 3-mm diameter spherical tissue phantoms, with a standard deviation of 19.1 cam rotations. It was observed that in the tests, the 3 mm diameter spherical tissue phantoms were not in contact with all six blades, possibly substantiating the high standard deviation observed with these samples.

12

Table 12.2: Overview of the results of the instrument's configuration on the ability to grip and transport the ⌀5 mm spherical tissue phantoms.

Shaft configuration	Ability to grip the tissue [Y/N]	Ability to transport the gripped tissue [Y/N]
0° (Control)	Y, 6/6 (100%)	Y, 6/6 (100%)
20°	Y, 6/6 (100%)	Y, 6/6 (100%)
40°	Y, 6/6 (100%)	Y, 6/6 (100%)
60°	Y, 6/6 (100%)	Y, 5/6 (83.3%)

12.4.2. EFFECT OF INSTRUMENT CONFIGURATION

The 5 mm diameter spherical tissue phantoms were all successfully grasped for all curvatures, see Table 12.2. Furthermore, all phantoms successfully entered the transportation lumen for the 20° and 40° shaft angles (100%). However, when the transport mechanism was bent over an angle of 60°, one out of six samples (16.7%) did not enter the lumen of the transport mechanism. It was observed that in the 60° bend, the gripper was severely deformed.

12.5. DISCUSSION

12.5.1. SUMMARY OF MAIN FINDINGS

In this study, we have developed a novel grasping system for use in conjunction with the wasp-inspired transport mechanism [6]. The developed prototype was tested on its ability to grip and transport tissue phantoms of different shapes and sizes. From this experiment, it was found that the prototype was able to successfully grip and transfer tissue phantoms into the lumen of the transport mechanism.

The device is intended for use during minimally invasive surgery. For this purpose, the device needs to perform six steps, as illustrated in Figure 12.5. In Step 1, the device is inserted into the human body, either through a natural orifice or an incision. Subsequently, the device is guided towards the target area while circumnavigating delicate structures. Once arrived at the target location, in Step 2 and 3, the gripper is opened and positioned around the tissue. In Step 4, the gripper is closed to constrain the tissue. At this point, the tissue should not be able to leave the gripper. The tissue is transferred into the lumen of the transport mechanism in Step 5. When tissue transfer into the lumen has been accomplished, the gripper can be reopened to grasp another tissue sample, repeating Steps 2-5. Once all target tissue has been removed, the gripper can be extracted, as illustrated in Step 6.

12.5.2. LIMITATIONS OF THIS STUDY

The initial prototype underwent testing to assess its proficiency in grasping and transporting gelatin tissue phantoms. These evaluations were conducted within a controlled environment rather than a clinical setting and only a restricted number of experiment repetitions were performed, reducing the statistical reliability of the results. To enhance

12

Step 1
Insert gripper through natural orifice
or surgical incision

Step 2
Open gripper

Step 3
Position gripper
around tissue

Step 6
Extract gripper

Step 5
Transfer tissue
into lumen
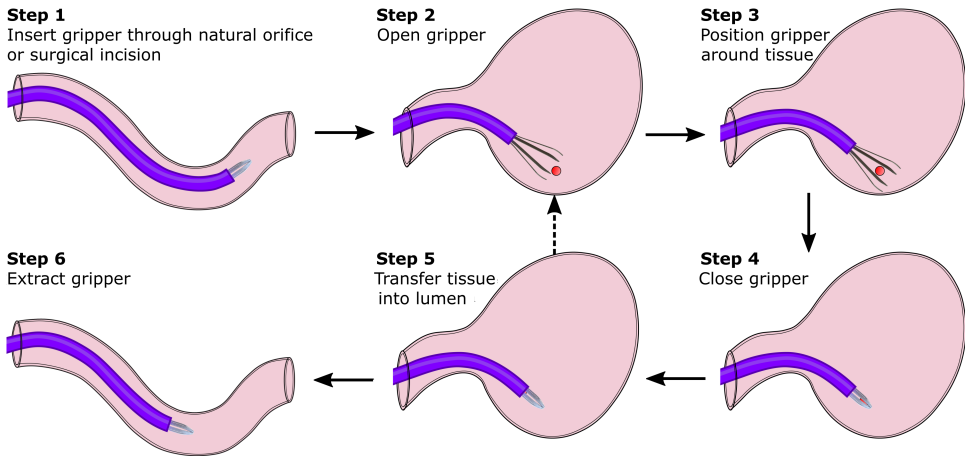
Step 4
Close gripper

Figure 12.5: Intended use of the instrument. Step 1: Instrument insertion in the human body through a natural orifice or surgical incision. Step 2: Manual opening of the gripper. Step 3: Positioning of the gripper around the target tissue (in red). Step 4: Grasping of the target tissue through closing of the gripper around the target tissue. Step 5: Tissue transport through manual actuation of the internal cam. Step 6: Instrument extraction. Steps 2-4 can be repeated to extract multiple pieces of tissue without the need for extraction.

the validity of the assessments, it is recommended that the gelatin tissue phantoms be replaced with actual tissue in *ex-vivo* and *in-vivo* settings. This adjustment aims to ensure that the gripper can consistently and effectively grasp and transfer real tissue into the lumen.

Engaging surgeons in the testing process is advised for a more comprehensive evaluation of the prototype. This involvement will facilitate gathering feedback regarding any functional or practical issues that may arise during the operation of the device. This future investigation should involve a larger sample size and take place in a clinical setting to ensure the reliability and relevance of the results. Furthermore, biocompatible materials should be used for future use in a clinical setting. Therefore, alternative materials must be found to replace those currently used in the prototype, such as the galvanised cables and the heat shrink tube.

12.5.3. RECOMMENDATIONS FOR FUTURE RESEARCH

With a future clinical instrument in mind, the developed prototype should be redesigned based on the intended application and tested in a clinical setting. The handle should allow for easy single handed control of the gripper and tissue removal system. Presently, the gripper requires considerable force to operate, requiring two-handed operation. Furthermore, in order to use the device during minimally invasive procedures and even increase the application area of the device to, for example, cardiovascular interventions, further miniaturization should be explored. Miniaturization could be enabled by incorporating smaller diameter cables and ring magnets and thin-walled heat shrink tubing or exploring alternative methods to keep the cables together, such as using heat shrink tubing instead of ring magnets, similar to the design of our sub-millimetre wasp-inspired

12

needles [11, 2].

With a future clinical instrument in mind, the developed prototype should be re-designed based on the intended application and tested in a clinical setting. The handle should allow for easy single-handed control of the gripper and tissue removal system. Presently, the gripper requires considerable force to operate, requiring two-handed operation.

In the future, the developed prototype can be made steerable to allow for easy gripping of tissues in front of the device tip. For this purpose, the blades should be individually actuated to prevent gripper deformation, as was observed in the current prototype. Another design direction to explore is adding a cutting edge to the blades to enable tissue resection in front of the device tip. Furthermore, adding an electric motor to actuate the transport mechanism would eliminate the need for the user to switch between actuating the gripper and the transport mechanism, which eases operation.

12.6. CONCLUSION

A wire rope-based gripper was incorporated into the friction-based transport mechanism inspired by the wasp ovipositor. The design incorporated plastically deformed wire ropes to create a compliant section for opening and closing of the gripper. A cam, handles, and a shaft, including magnets, were employed for the controlled manipulation of the wire ropes, ensuring consistent gripper shape while allowing for the actuation of the transport mechanism. The two handles with springs enabled a voluntary opening operation during tests, demonstrating successful single-person operation. The gripper effectively grasped and transferred gelatin tissue phantoms of different shapes, sizes, and orientations into the transport mechanism. Future research can include introducing steerability to enhance the gripper's orientation capabilities. In conclusion, the wire rope-based gripper represents a promising development for a new surgical instrument, marking a significant step forward in this innovative approach.

12

BIBLIOGRAPHY

[1] Jean Bismuth et al. "Feasibility and Safety of Remote Endovascular Catheter Navigation in a Porcine Model". en. In: *Journal of Endovascular Therapy* 18.2 (Apr. 2011). Publisher: SAGE Publications Inc, pp. 243–249. (Visited on 04/25/2024).

[2] Jette Bloemberg et al. "Design and evaluation of an MRI-ready, self-propelled needle for prostate interventions". In: *Plos one* 17.9 (2022), e0274063.

[3] U. Cerkvenik et al. "Mechanisms of ovipositor insertion and steering of a parasitic wasp". In: *Proceedings of the National Academy of Sciences* 114.37 (2017). Publisher: National Acad Sciences, E7822–E7831.

[4] Sarah Cohen and James A Greenberg. "Hysteroscopic Morcellation for Treating Intrauterine Pathology". In: *Reviews in Obstetrics and Gynecology* 4.2 (2011), pp. 73–80. (Visited on 04/25/2024).

[5] Philippe Généreux et al. "Vascular Complications After Transcatheter Aortic Valve Replacement". In: *Journal of the American College of Cardiology* 60.12 (Sept. 2012). Publisher: American College of Cardiology Foundation, pp. 1043–1052. (Visited on 04/25/2024).

[6] Esther P. de Kater et al. "Design of a Flexible Wasp-Inspired Tissue Transport Mechanism". In: *Frontiers in Bioengineering and Biotechnology* 9 (2021). (Visited on 12/19/2022).

[7] Jawid Madjidyar et al. "Influence of Thrombus Composition on Thrombectomy: ADAPT vs. Balloon Guide Catheter and Stent Retriever in a Flow Model". en. In: *RöFo - Fortschritte auf dem Gebiet der Röntgenstrahlen und der bildgebenden Verfahren* 192.3 (Mar. 2020), pp. 257–263. (Visited on 04/25/2024).

[8] Yohan Payan, ed. *Soft tissue biomechanical modeling for computer assisted surgery*. en. Studies in mechanobiology, tissue engineering and biomaterials 11. OCLC: ocn781681911. Heidelberg ; New York: Springer, 2012. ISBN: 978-3-642-29013-8 978-3-642-29014-5.

[9] Suwatchai Pornratanarangsi et al. "Extraction of challenging intracoronary thrombi: multi-device strategies using guide catheters, distal vascular protection devices and aspiration catheters". eng. In: *The Journal of invasive cardiology* 20.9 (Sept. 2008), pp. 455–462.

[10] A. Sakes et al. "Development of a Novel Wasp-Inspired Friction-Based Tissue Transportation Device". In: *Frontiers in Bioengineering and Biotechnology* 0 (2020). Publisher: Frontiers. (Visited on 07/20/2021).

[11]   Marta Scali et al. "Design of an ultra-thin steerable probe for percutaneous in-
       terventions and preliminary evaluation in a gelatine phantom". en. In: *PLOS
       ONE* 14.9 (Sept. 2019). Publisher: Public Library of Science, e0221165. (Visited
       on 04/25/2024).

[12]   Gregory P. Schmitz et al. "Minimally invasive micro tissue debriders having tar-
       geted rotor positions". US20140114336A1. Apr. 2014. (Visited on 04/25/2024).

[13]   Erhard E Starck et al. "Percutaneous aspiration thromboembolectomy." In: *Radi-
       ology* 156.1 (1985), pp. 61–66.

[14]   R. West, G. Ellis, and N. Brooks. "Complications of diagnostic cardiac catheteri-
       sation: results from a confidential inquiry into cardiac catheter complications".
       en. In: *Heart* 92.6 (June 2006). Publisher: BMJ Publishing Group Ltd Section: In-
       terventional cardiology and surgery, pp. 810–814. (Visited on 04/25/2024).

12

13

DISCUSSION

13.1. FINDINGS OF THIS THESIS

13.1.1. THESIS AIM

The primary objective of the research described in this thesis was to enhance the fixation strength of bone anchors utilised in spinal fusion surgery. The fixation strength of spinal bone anchors is crucial, as low pedicle screw fixation strength can lead to issues such as screw loosening, potentially necessitating revision surgery [12]. This concern is particularly pronounced in patients suffering from osteoporosis, where decreased bone density compromises the fixation strength of spinal bone anchors, thereby contributing to screw loosening and resulting in a lower success rate for spinal fusion surgery overall [12, 3].

In this thesis a number of alternative spinal bone anchor designs intended for spinal fusion surgery were explored, whilst also investigating various steerable bone drill designs to aid anchor placement. Based on this research, this thesis presents three innovative anchor designs (Part I) and three novel steerable drill designs (Part II) that hold promise to improve the fixation strength during spinal fusion surgery. To further aid spinal fusion surgery and other fields of surgery, for example in biopsy procedures, additional functionalities to aid tissue removal and transport of biopsies were explored (Part III).

13.1.2. PART I: ANCHOR DESIGN

The first chapter of this part, Chapter 2, describes an exploration of alternative designs for spinal bone anchors in patent literature. This revealed five potential anchoring techniques that could potentially improve fixation strength: 1) anchors utilising threaded sections, 2) anchors employing a curved path through the vertebra, 3) anchor that (partly) expand, 4) anchors utilising bone cement, and 5) anchors aiming to stimulate bone ingrowth. In the development of novel spinal bone anchors, key considerations include not only the potential increase in fixation strength but also aspects of placement safety and anchor removal potential. This latter aspect poses particular challenges for cement-augmented and bone ingrowth-inducing spinal bone anchors. To enable easy removal whilst simultaneously improving fixation strength, three novel spinal bone anchors were presented that aim to enhance the fixation strength of the conventional pedicle screw by employing a curved path using a curved compliant anchors, as well as the

use of expandable sections to conform to the pedicle and the use of a macro-shape lock with the cortical bone layer.

Chapter 3 described a spinal bone anchor design that enhances the fixation strength of a cannulated pedicle screw by introducing a curved nitinol rod that is advanced through the pedicle screw into the vertebral body. This curved rod enhances the pull-out resistance by 14% through a macro-shape lock within the vertebral body, providing an additional means of fixation along the micro-shape lock of the screw thread with the surrounding bone tissue. The use of a macro-shape lock was further investigated in Chapter 5 where the design of an L-shaped anchor was introduced. This L-shaped anchor allows for the establishment of a macro-shape lock with the cortical bone of the vertebral body to enhance the fixation strength on top of the present micro-shape lock established by the screw thread. The pull-out force increased from 23 N when surrounded by cancellous bone to 123 N when in contact with the cortical bone.

Although pull-out strength is the gold-standard to compare pedicle screw fixation strength, screw loosening is often caused by toggling of the pedicle screw. Chapter 4 described the design of an expandable section of a pedicle screw that can deform to the hourglass-shape of the pedicle to increase the contact area of the screw with the cortical bone layer and as such could increase the toggling resistance of the anchor.

13.1.3. Part II: Anchor placement

The second part of this thesis was dedicated to exploring bone drills capable of following alternative trajectories trough the vertebra to allow for the placement of alternative bone anchors. These drills allow the surgeon to reach specific entry points, drill curved tunnels or navigate along the cortical bone layer. Chapter 6 presented a review of steerable bone drills in scientific and patent literature which revealed that steerable drills can create curved tunnels through three steering methods: 1) device-defined steering, creating a predetermined path defined by the drill itself; 2) environment-defined steering, where the tunnel is shaped by tissue interaction forces during the drilling procedure; and 3) user-defined steering, allowing the user to dictate the drill path during the procedure. Chapter 7 described the design of a flexible drill ($\varnothing_{outer}$ 4 mm) utilising a hydraulic pressure wave to hammer through bone. This flexible drill can successfully transfer the hydraulic pressure wave in various shaft orientations (straight, 45° curve and 90° curve) and can be used in combination with a guide, resulting in device-defined steering. The majority of the bone drills including device-defined steerable bone drill only allow for drilling predetermined paths through the bone, which does not allow for real-time adjustment of the drill path or difference in the anatomy of patients. Both environment-defined and user-defined steering allows for adjustment to the patient's anatomy, increasing safety.

An environment-defined bone drill is presented in Chapter 8. The tsetse fly inspired bone drill is able to deflect upon contact with the cortical bone layer with an insertion angle up to 15°, enabling drilling along the cortical bone layer. This can potentially increase the contact with the cortical bone layer when placing an alternative pedicle screw in the future. Interestingly, in the current design the drill produces a rectangular tunnel due to the oscillating drilling method. Alternative tunnel cross sections would be achievable with minor alteration to the drill tip shape. This could be beneficial for alternative

anchor designs, such as the spinal bone anchor presented in Chapter 4 which conforms to the oval hour-glass shape of the pedicle.

Chapter 9 described the design and early testing of an user-defined steerable bone drill ($\varnothing_{outer}$ 2.75 mm, length 130 mm) capable of drilling multi-curved tunnels. The design utilises a flexible tubular sleeve and multiple replaceable pre-curved nitinol cores. The cores originate from the anchor presented in Chapter 3, which showed that pre-curved nitinol rods can create curved tunnels through cancellous bone. The replaceable cores allow the user to steer the drill along the desired path by simply replacing the curved core by another core with a different curve. The drill was designed to incorporate Diffuse Reflectance Spectroscopy (DRS) technology to enhance safety by detecting and preventing cortical breach.

13.1.4. PART III: ADDITIONAL FUNCTIONALITIES

In the final part of this thesis, various enhancements to aid tissue transport, either during bone surgery or other medical application areas, were explored. Spinal fusion may be a necessity following tumour removal, which initially requires a bone biopsy procedure to confirm the diagnosis. Chapter 10 presented a comprehensive review of bone biopsy needles presented in patent literature, in which three challenging phases during a biopsy procedure were distinguished: 1) sampling of the biopsy, 2) severing of the biopsy, and 3) harvesting of the biopsy, each presenting numerous possible solutions.

Beyond the challenges of harvesting bone biopsies, acquiring soft tissue biopsies, or the removal of soft tissue, presents their own difficulties, as described in Chapter 11, primarily due to clogging of the currently-used suction devices. Drawing inspiration from the parasitic wasp, a flexible transportation device was developed and proven suitable for successful transportation of gelatin tissue phantoms. A rotational velocity of the cam of 25 RPM resulted in a transport rate of 0.8 mm/s of the gelatine tissue phantom, and by increasing the cam velocity to 80 RPM a transport rate of 2.3 mm/s could be achieved. Before soft tissue biopsies can be transported with this device, the tissue needs to be gripped. In Chapter 12, the wasp-inspired tissue transportation device was enhanced with a gripper at the tip to aid tissue removal. The instrument was able to successfully grip and subsequently transport gelatin tissue samples with different shapes (spherical and cylindrical), sizes ($\varnothing$ 3 mm, $\varnothing$ 4 mm and $\varnothing$ 5 mm) and orientations (concentric and orthogonal).

13.2. FUTURE PERSPECTIVES

13.2.1. TOWARDS CLINICAL USE

This thesis presents an explorative study into alternative anchoring and anchor placement methods for use in spinal fusion surgery. Although various alternative designs for spinal bone anchors and steerable bone drills are presented, it is important to note that these designs were primarily designed for research purposes rather than immediate clinical application. The focus of the development process was primarily on the technical capabilities of the instrument, with other factors such as ease of use for clinicians, manufacturability on a large scale, and cleanability not being the main focus points. Redesigning the presented prototypes is a necessity to enable clinical use, starting with *ex-vivo*

and *in-vivo* experiments. Additionally, adherence to regulations, such as the European regulations for medical devices (Medical Device Regulation, MDR) is crucial to ensure quality, safety and performance of clinical tests of medical devices within the European Union.

Considering the risks posed by climate change to future health, sustainability should be a key consideration in all new medical developments [10]. The substantial waste generated in healthcare, especially in orthopaedic wards, underscores the importance of environmental impact assessment in medical product design [2]. This can be achieved through the use of environmentally-friendly materials, recycling or reusing implants, and ensuring that instruments meet requirements for cleanability and sterilisation to allow safe reuse of products [6]. The presented steerable bone drill designs in Part II, compose of multiple parts which cannot easily be disassembled, making the designs difficult to sterilise and reuse. However, improving the fixation strength of bone anchors could reduce the need for revision surgery, making complex single-use instruments potentially more sustainable compared to current methods.

While validation experiments of the developed prototypes were conducted primarily in bone phantom material to investigate initial fixation strength with different anchoring techniques, long-term effects such as screw loosening due to toggling requires further investigation. Being a living tissue, bone adapts to applied loads (Wolff's law), which necessitates *in-vivo* experiments to assess the long-term fixation strength of spinal bone anchors [4]. This especially holds for the spinal bone anchor designs presented in Part I. These bone anchors are intended to be implanted within the vertebra for a long term, meaning that the bone will adapt to the applied loads. This might result in bone growth around the wedges of the expandable spinal bone anchor presented in Chapter 4, which could make the removal of the anchor challenging.

13.2.2. OTHER APPLICATION AREAS

The primary application area of this thesis is spinal fusion surgery, however, the alternative bone anchors and steerable bone drills developed herein have potential applications across various orthopaedic procedures. For instance, Kirschner wires (K-wires), commonly used to fixate bone fragments, bear resemblance to the curved nitinol anchors presented in Chapter 3. Flexible pre-curved anchors could potentially offer higher fixation forces as compared to straight K-wires and enable alternative pathways that conform better to the shape of different bones. Additionally, the anchors presented in Part I, may be applicable in a variety of orthopaedic procedures, for instance to enhance the fixation of plates and hip implants. The flexible and steerable drills presented in Part II could also benefit a wide range of orthopaedic procedures, including implant placement, arthroplasty, and the removal of lesion areas, as presented in Chapter 6.

13.2.3. NON-FUSION CORRECTION

In this thesis, a range of alternative anchoring and placement methods are investigated to enhance the fixation strength of bone anchors used in spinal fusion surgery. Spinal fusion surgery is employed to correct severe scoliosis, often necessitating invasive open surgery with large incisions [5]. This procedure involves correcting the deformity all at once by applying high corrective forces, and eliminating all motion between the adja-

cent vertebrae to establish the desired fusion. Spinal fusion inhibits spine growth, posing a challenge in treating conditions like early onset scoliosis where patient growth is expected, potentially leading to a shortened trunk that may hinder lung development [8].

A promising direction for future research lies in exploring non-fusion correction methods, which correct spine deformities without relying on rigid fusion of adjacent vertebrae. For instance, telescopic growing rods allows spine lengthening during growth but come with risks such as increased infection susceptibility and higher corrective forces on the pedicle screws which results in a higher chance of screw loosening [1, 11]. To bypass the high infection risk, magnetically controlled growing rods can be used, as these rods can be lengthened remotely without requiring surgery. Although these magnetically growing rods hold a smaller infection risks, they are associated with hardware problems such as screw loosening and rod breakage [9].

As part of the research described in this thesis, an alternative non-fusion correction design was developed utilising buckled posteriorly placed leaf flexures to generate a small, nearly constant corrective force that gradually corrects spinal deformities over time (Figure 13.1) [7]. Since the correction occurs gradually over an extended period, it is thought that applying a gentle yet consistent corrective force is sufficient for successful treatment of the spinal deformity. Furthermore, this less invasive procedure would reduce the pain, and allows for earlier intervention when the deformity is less severe. Additionally, this non-fusion technique not only reduces the severity of the procedure but also preserves more vertebral motion, maintaining patient mobility, and promoting growth. While non-fusion correction methods differ from conventional spinal fusion, they still require firm fixation to the vertebrae. Unlike spinal fusion, where anchors become redundant after successful fusion of the vertebrae, non-fusion techniques necessitate long-term fixation of the spinal bone anchors. The alternative anchoring methods and steerable bone drill designs presented in this thesis hold potential for successful implementation in both spinal fusion and non-fusion correction procedures.

13.3. CONCLUSION

The primary objective of this thesis was to enhance the effectiveness of spinal fusion surgery by introducing alternative designs for bone anchors and steerable bone drills. A thorough review of patent literature offered a comprehensive understanding of the state-of-the-art in spinal bone anchors. This review, as well as an analysis of the commercially available instruments, served as a foundation for the development of a range of prototypes for spinal bone anchors. These prototypes employ various techniques aimed at enhancing the fixation strength, including curved pathways, expandable sections and implementing a macro-shape lock with the cortical bone layer.

Expanding beyond the advancement of spinal bone anchor designs, this thesis also delves into the development of novel flexible bone drills. It begins by exploring the state-of-the-art in steerable bone drills by a review of patent and scientific literature. The identified steering techniques resulted in the development of a number of steerable bone drill prototypes. These drills can be steered using a guiding mechanism, using tissue interaction forces, or by the user.

This thesis finally investigates additional functionalities for biopsy procedures. This
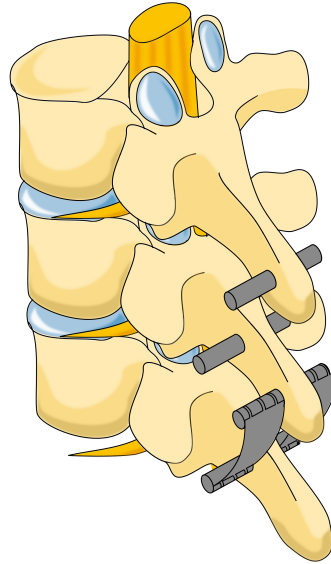
Figure 13.1: Schematic representation of the proposed non-fusion correction technique, utilising posteriorly placed buckled leaf springs to correct for early onset scoliosis.

exploration begins with an examination of the existing state-of-the-art in bone biopsy needles. Subsequently the design of a flexible tissue transported is introduced, which is later enhanced with a gripper. This thesis shows the potential of novel spinal bone anchor designs, alternative anchor pathways through the utilisation of steerable bone drills and possible additional functionalities to enhance spinal bone anchor fixation in spinal fusion surgery.

13

BIBLIOGRAPHY

[1] Behrooz A Akbarnia et al. "Dual growing rod technique for the treatment of progressive early-onset scoliosis: a multicenter study". In: *Spine* 30.17S (2005), S46–S57.

[2] Md Maksud Alam et al. "Report: healthcare waste characterization in chittagong medical college hospital, Bangladesh". In: *Waste Management & Research* 26.3 (2008), pp. 291–296.

[3] Daniel J. Burval et al. "Primary Pedicle Screw Augmentation in Osteoporotic Lumbar Vertebrae: Biomechanical Analysis of Pedicle Fixation Strength". In: *Spine* 32.10 (May 1, 2007), pp. 1077–1083. (Visited on 06/04/2021).

[4] Jan-Hung Chen et al. "Boning up on Wolff's Law: mechanical regulation of the cells that make and maintain bone". In: *Journal of biomechanics* 43.1 (2010), pp. 108–118.

[5] Asad M Lak et al. "Minimally invasive versus open surgery for the correction of adult degenerative scoliosis: a systematic review". In: *Neurosurgical Review* 44 (2021), pp. 659–668.

[6] Timothy McAleese et al. "Sustainable orthopaedic surgery: initiatives to improve our environmental, social and economic impact". In: *The Surgeon* (2023).

[7] Anton Meiring. "Correction of Scoliosis: Design and Validation of a Constant Force Mechanism". In: (2023).

[8] Karsten Ridderbusch et al. "Strategies for treating scoliosis in early childhood". In: *Deutsches Ärzteblatt International* 115.22 (2018), p. 371.

[9] Kar H Teoh et al. "Do magnetic growing rods have lower complication rates compared with conventional growing rods?" In: *The Spine Journal* 16.4 (2016), S40–S44.

[10] Nick Watts et al. "The 2018 report of the Lancet Countdown on health and climate change: shaping the health of nations for centuries to come". In: *The Lancet* 392.10163 (2018), pp. 2479–2514.

[11] Yan-Bin Zhang and Jian-Guo Zhang. "Treatment of early-onset scoliosis: techniques, indications, and complications". In: *Chinese medical journal* 133.3 (2020), pp. 351–357.

[12] M R Zindrick et al. "A biomechanical study of intrapeduncular screw fixation in the lumbosacral spine". In: *Clinical orthopaedics and related research* 203 (Feb. 1, 1986), pp. 99–112.

ACKNOWLEDGEMENTS

Many know that I am always in for outdoor adventures, whether it is hiking through the Balkan mountains, participating in a multi-day adventure race in France, or cross-country skiing and snow camping in Norway. While this PhD wasn't exactly an outdoor adventure, it was an adventure nonetheless. As with most adventures, there were though days where everything seemed to go wrong. On these days the paths were longer and steeper than anticipated, and all the detours would make me go astray. Yet, upon reaching the first peak, the breathtaking views made every challenge worthwhile. Another similarity between my outdoor activities and pursuing my PhD is that I was never alone. Thus, I would like to thank everyone who helped make this PhD journey possible.

First of all, my appreciation goes to my promotors, Paul and Aimée, who acted as my tour guides throughout this PhD. Whenever I found myself lost or unsure of the path ahead, they steered me back on track, or more often charted an new route. I am also thankful to everyone member of this project's user committee. Their knowledge provided valuable insights. During this PhD project, I had the pleasure of collaborating with many bachelor and master students. Thank you for your hard work and contributions to this thesis. Furthermore, special acknowledgement goes to David Jager and Remi van Starkenburg. This thesis would be reduced to only theoretical thoughts where it not for the amazing prototypes you manufactured.

To Fabian, Indra, Merle, Mostafa, Jette, Karin, Kirsten, and Vera – your presence always made it a pleasure to come to the office. Fabian, your knowledge on 3D printers in truly admirable. Kirsten, as the 'senior PhD' of the office you have been a great example and mentor, providing valuable advice at the COVID stained start of my PhD and beyond. Indra, though we only shared the same office for the last two months of my PhD, I can not imagine it without you. Mostafa, I really enjoyed our discussion on the academic world and how it could be improved. Karin, thank you for sharing you experiences, the great conversations and the tour at the HU. Jette, you are holding this office together and your laser focus is commendable. I'll miss your presence at the desk next to me, although as you know, 'I need my space' ;). Vera, your enthusiasm and creativity are infectious. You make every project seem like the coolest project possible. And to Merle, I am grateful for our collaboration on this spine project. Knowing that we were going to tackle this project together made it all the more enjoyable. Beyond our time in the office, I would to thank Jette, Vera and Merle, for the countless coffee breaks, sport lessons, conference trips, movie nights and sport lessons outside office hours. Who said that colleagues can not be friends.

In addition to my office mates, I have had the pleasure of meeting numerous great colleagues during my PhD project, be it during lunch breaks, conferences, or one of the many other events. While I can not name everyone, I must mention Anneke, Bob, Nianlei and Robin, thank you!

My 'stoer' and 'cool' housemates (I still struggle with the difference) deserve special

recognition for their invaluable advice and for celebrate every success with me. I would like to especially thank Konstanze, for the last year of my PhD you have been like third promotor, mainly focusing on the 'life' side of the work-life balance.

I feel incredibly lucky to have such wonderful friends. I would not have been able to enjoy my PhD as much as I did without our shared moments, whether on holiday, during an adventure race, a day trip, or simply having tea together. Special acknowledgement goes to Sanne my fellow 'muurbloempje'. I admire your strength and your ability to see the good side in every situation. I am so grateful for our conversations about anything and everything. And to Lydia, thank you for inviting me to join you on your 'Norge på langs' trip. It was amazing and definitely 'de reis van mijn leven'.

Last but certainly not least, I want to express my gratitude to my parents and big little brother. Thank you for your unwavering support, assistance, and understanding. I feel immense grateful for knowing that you are always there to have my back.

Once again, to all who have played a part in this journey, thank you!

Curriculum Vitae

Esther Paula DE KATER

28-09-1994	Born in Rotterdam, the Netherlands.

WORK EXPERIENCE

2020-2024	PhD. Mechanical Engineering Delft University of Technology, Delft, the Netherlands *Thesis:* Fix(at)ing the Spine *Promotor:* Prof. dr. ir. P. Breedveld *Promotor:* Dr. ir. A. Sakes
2019	Internship Department of Electrical and Electronic Engineering University College Cork, Cork, Ireland
2015-2016	Internship mathematics teacher secondary school Melanchton Bergschenhoek, Bergschenhoek, the Netherlands

EDUCATION

2017-2020	Master in Mechanical Engineering Delft University of Technology, Delft, the Netherlands
2017-2020	Master in Biomedical Engineering Delft University of Technology, Delft, the Netherlands
2013-2017	Bachelor in Mechanical Engineering Delft University of Technology, Delft, the Netherlands
2007-2013	Secondary school Wolfert Dalton Hillergersberg, Rotterdam, the Netherlands

AWARDS

2022	Best Poster Award, iSMIT Conference, Oslo, Norway

LIST OF PUBLICATIONS

PUBLICATIONS PART OF THIS THESIS

- **de Kater E. P.**, Blom, M. N., van Doorn, T. C., Tieu, Q. H., Jager, D. J., Sakes, A., Breedveld, P. (2024). Enhancing spinal bone anchor pull-out resistance with an L-shaped anchor. Plos one, 19(5), e0302996.

- **de Kater E. P.**, Boetzkes, J. A., Sakes, A., Breedveld, P. (2023). Bone biopsy devices-a patent review. Expert Review of Medical Devices, 20(11), 919-928.

- **de Kater E. P.**, Müller, R., Sakes, A., Breedveld, P. (2023). Tsetse fly inspired steerable bone drill—a proof of concept. Frontiers in Bioengineering and Biotechnology, 11, 1197940.

- **de Kater E. P.**, Weststeijn C., Sakes A., Breedveld P. (2022). A toggling resistant in-pedicle expandable anchor: a preliminary study, in 2022 44th Annual Conference of the IEEE Engineering in Medicine & Biology Conference (EMBC), (pp. 3313-3317). IEEE.

- **de Kater E. P.**, Sakes A., Edström E., Elmi-Terander A., Kraan G., Breedveld P. (2022). Beyond the pedicle screw–a patent review. European Spine Journal, 31(6), 1553–1565.

- **de Kater E.P.**, Sakes A., Bloemberg J., Jager D.J., Breedveld P. (2021). Design of a flexible wasp-inspired tissue transport mechanism. Frontiers in Bioengineering and Biotechnology, 9, 782037.

OTHER PUBLICATIONS

- Meiring A.R., **de Kater E.P.**, Stadhouder A., van Royen B.J., Breedveld P., Smit T.H. (2023). Current models to understand the onset and progression of scoliotic deformities in adolescent idiopathic scoliosis: a systematic review. Spine Deformity, 11(3), 545-558.

- Sakes A., van de Steeg I., **de Kater, E.P.**, Posthoorn P., Scali M., Breedveld P. (2020). Development of a novel wasp-inspired friction-based tissue transportation device. Frontiers in Bioengineering and Biotechnology, 8, 575007.

(INTER)NATIONAL CONFERENCES

- **de Kater E.P.**, Müller, R., Sakes, A., Breedveld, P. (2023). The design of a tsetse fly inspired bone drill. NEV Entomology Day 2023, December 15, Ede, The Netherlands, (Oral presentation).

- **de Kater E.P.**, Müller, R., Sakes, A., Breedveld, P. (2023). The design of a tsetse fly inspired bone drill. 34th Conference of International Society for Medical Innovation and Technology (iSMIT), October 19-21, Lukang, Taiwan, (Oral presentation).

- **de Kater E. P.**, Kaptijn, T.G., Sakes A., Breedveld P. (2023). Design of a Flexible Bone Drill Using a Hydraulic Pressure Wave. The Hamlyn Symposium on Medical Robotics, June 26-29, London, United Kingdom (Poster presentation).

- **de Kater E. P.**, Weststeijn C., Sakes A., Breedveld P. (2023). Increasing the fixation of spinal bone anchors by increasing cortical bone contact 9th Dutch Conference of Bio-Medical Engineering, January 26-27, Egmond aan Zee, The Netherlands (Poster presentation).

- **de Kater E. P.**, Weststeijn C., Sakes A., Breedveld P. (2022). A toggling resistant in-pedicle expandable anchor: a preliminary study. 44th International Engineering in Medicine and Biology Conference (EMBC), July 11-15, Glasgow, United Kingdom (Oral presentation)

- **de Kater E. P.**, Sakes A., Breedveld P. (2022). Flexible wasp-inspired tissue transport mechanism. 33rd Conference of International Society for Medical Innovation and Technology (iSMIT), May 30-31, Oslo, Norway (Poster presentation).

- **de Kater E.P.**, Sakes A., Breedveld P. (2022). Anchor trajectory optimization for spinal fusion surgery. 33rd Conference of International Society for Medical Innovation and Technology (iSMIT), May 30-31, Oslo, Norway (Oral presentaion).

- **de Kater E.P.** , Sakes A., Breedveld P. (2021). Design of a flexible ovipositor inspired tissue-transporting mechanism. 8th Dutch Conference of Bio-medical Engineering, January 28-29, Online (Oral Presentation).

PhD Portfolio

Courses and Workshops

Discipline-Related Skills

- Data Management Plan Training
- Freehand Sketching of Products and Mechanisms
- Summer school Computational Design for Additive Manufacturing
- 3Me PhD Video competition 2021
- Structuring your Design Oriented PhD project

Research Skills

- Speed reading and Mind mapping
- The Informed Researcher: Information and Data Skills
- Basic Problem Solving & Decision-making for Researchers
- Software carpentry Workshop

Transferable skills

- PhD start-up module A,B&C
- Online Self-Presentation
- Creative Thinking: Techniques and Tools or Success
- Teamwork, Leadership and Group Dynamics
- English for Academic Purposes (EAP-4)
- Managing the Academic Publication Review Process
- Mental Fitness Intervention Program
- Career Shaping Event 2022
- Career Development - Exploring a research career outside Academia
- Career Development - Career Strategies for Women in Science
- Writing a Dissertation (Prom 3)
- Designing Scientific Posters and Covers for Thesis with Adobe InDesign

Organisation and Popular Science Events

- **Nacht van de Ontdekkingen 2023**, Hortus Botanicus, Leiden, The Netherlands
Art and Science festival to inspire and explain about the field of bio-inspired design.

- **Soft Robotics Summer School 2022**, RoboHouse, Delft, The Netherlands
  Co-organise the Dutch Soft Robotics Summer School for PhD students and junior employees to learn more about the field of soft robotics during this two-week summer school.

- **Girls day 2022, 2023 & 2024**, TU Delft Faculty of Mechanical Engineering, Delft, The Netherlands
  Co-organise a workshop about biomedical engineering to inspire high school girls to consider studying mechanical engineering at the TU Delft.

Eᴅᴜᴄᴀᴛɪᴏɴ

Cᴏᴜʀsᴇs

- **Bio-Inspired Design 2020-2021, 2021-2022 & 2022-2023**
  Coach several group projects and grade the final reports and prototypes.

Sᴜᴘᴇʀᴠɪsɪɴɢ Iɴᴛᴇʀɴsʜɪᴘ Sᴛᴜᴅᴇɴᴛs

- **Stefan Scholtes**
  Internship: *Bio-Inspired Development of an Anchoring Device as Part of a Steerable Bone Drill for Lumbar Vertebrae*

Sᴜᴘᴇʀᴠɪsɪɴɢ Bᴀᴄʜᴇʟᴏʀ Sᴛᴜᴅᴇɴᴛs

- **Huy Tieu, Michiel Blom and Ton van Doorn**
  Bachelor Project Mechanical Engineering: *Experimental Investigation of a Novel Bone Anchor for Spinal Fixation: Pull-Out Tests on Synthetic Bone Models*

- **Bastiaan Blank, Gyaan Ramsoekh and Mischa van Bavel**
  Bachelor Project Mechanical Engineering: *Development of a Bone Tissue-simulating Phantom for testing a DRS-enhanced Steerable Drill*

Sᴜᴘᴇʀᴠɪsɪɴɢ Mᴀsᴛᴇʀ Sᴛᴜᴅᴇɴᴛs

- **Suzet Giltay**
  Literature Report: *Concentric Tube Robots for Medical Applications: a Review*
  Master Project Mechanical Engineering: *Design of a Steerable Needle for Prostate Interventions*

- **Jos Boetzkes**
  Literature Report: *Minimally Invasive Cancellous Bone Biopsy Instruments: A Patent Review*
  Master Project Mechanical Engineering: *Design of a Novel Mechanism for Use in a Cancellous Bone Biopsy Instrument*

- **Anton Meiring**
  Literature Report: *Modelling of Adolescent Idiopathic Scoliosis - A Systematic Review*
  Master Project Mechanical Engineering: *Correction of Scoliosis: Design and Validation of a Constant Force Mechanism*

- **Güven Aydin**

  Literature Report: *Puncturing of Internal Organs Enclosed with a Capsule during Surgical Interventions - A Patent Review in the Medical Domain*

  Master Project Mechanical Engineering: *The ProSTATIC – A Suction based Stabilisation Instrument for the Prostate*

- **Robin Blok**

  Literature Report: *Steering Techniques for Tunnel Drilling Machines - A Patent Review*

  Master Project Mechanical Engineering: *The Development of an Oscillating Steerable Bone Drill*

- **Cornel Weststeijn**

  Literature Report: *Expandable Dental Implants using a Threaded Component*

  Master Project Mechanical Engineering: *Design of an Expandable In-Pedicle Anchor for Spinal Fusion Surgery*

- **Guy Kaptijn**

  Literature Report: *Handheld Ultrasonic Surgical Instruments' End Effectors used for Bone Machining- A Patent Review*

  Master Project Mechanical Engineering: *Hydraulic pressure wave bone drilling: A Step towards Trajectory Controlled Drilling in the Vertebra*

- **Rob Müller**

  Literature Report: *Piercing Mouth parts, Ovipositors and Stinger of Insects*

  Master Project Mechanical Engineering: *Bio-Inspired Flexible Vertebral Drill: The Design, Manufacturing and Evaluation of a Prototype*

- **Hugo Kooiman**

  Master Project Mechanical Engineering: *Design of a Grasping Mechanism for a Friction-Based Transport Mechanism*

- **Sanne Treep**

  Master Project Mechanical Engineering: *A Double-Walled Flexible Friction-Based Locomotion and Transport Mechanism*

- **Olivier Hiemstra**

  Master Project Mechanical Engineering: *Design of an external patient specific guide for drilling a tunnel through the scaphoid*